

CRANFIELD UNIVERSITY

MEIKE HEURICH

**DEVELOPMENT OF AN AFFINITY  
SENSOR FOR OCHRATOXIN A**

CRANFIELD HEALTH

PhD thesis

January 2008

**CRANFIELD UNIVERSITY**

**CRANFIELD HEALTH**

**PhD Thesis**

**ACADEMIC YEARS 2004 - 2007**

**MEIKE HEURICH**

**DEVELOPMENT OF AN AFFINITY SENSOR  
FOR OCHRATOXIN A**

**Supervisor: Dr. I. E. Tothill**

**January 2008**

This thesis is submitted in partial fulfilment of the requirements  
for the degree of Doctor of Philosophy

© Cranfield University, 2008. All rights reserved. No part of this publication may be  
reproduced without the written permission of the copyright owner.

## ABSTRACT

Ochratoxin A is a contaminant in wine and known to be immunosuppressive and possibly carcinogenic. Therefore, the development of a rapid and sensitive method for field analysis is required for risk assessment and management. The work presented in this thesis reports the construction of a sensor platform capable of fulfilling these requirements. As a sensor platform, screen-printed thick film electrodes and microelectrodes on a silicone support were investigated for sensor development. As biological recognition elements, an antibody specifically binding ochratoxin A and a peptide receptor that was designed using computational modelling were examined.

A disposable immunosensor for ochratoxin A was developed based on screen-printing technology. An indirect competitive immunoassay format was used on bare screen printed gold electrode (SPGE). The performance of this sensor was compared to carboxymethylated dextran (CMD) modified SPGE. Detection was performed by chronoamperometry monitoring the reaction of tetramethylbenzidine and hydrogen peroxide catalysed by horseradish peroxidase. The SPGE-based immunosensor achieved a detection limit of  $100 \text{ ng L}^{-1}$  and the CMD-modified SPGE immunosensor  $10 \text{ ng L}^{-1}$ . The latter has been used for ochratoxin A determination in wine samples and was validated against standard HPLC and a commercial immunoassay test kit. Wine sample analysis involved the sample pre-treatment using immunoaffinity chromatography, electrochemical wine component characterisation and interference control. The immunosensor format was transferred to a gold microelectrode array based on a silicone support for the purpose of signal sensitivity enhancement and miniaturisation in the prospect of field analysis. Preliminary data showed the characterisation of the microelectrode array immunosensor construction and characterisation. Further optimisation is needed to establish a calibration curve with the required sensitivity.

The second part of the work comprised the design of a peptide receptor for ochratoxin A using computational methods by screening *de novo* designed peptide libraries. An octapeptide (CSIVEDGL) and a 13-peptide (GPAGIDGPAGIRC) were selected for

synthesis and affinity characterised for ochratoxin A recognition using a surface plasmon resonance biosensor (Biacore<sup>TM</sup>). The peptide receptors showed good sensitivity for ochratoxin A of 10  $\mu\text{g L}^{-1}$ . Preliminary affinity characterisation resulted in  $K_A = 63 \text{ mM}^{-1}$  for the 13-mer peptide and  $K_A = 84 \text{ mM}^{-1}$  for the octapeptide, which appears to be binding with higher strength to ochratoxin A. The affinity values correspond to the binding score (binding energy) calculated by computational modelling. This work shows the potential of designing peptide receptors for small molecules (e.g. ochratoxin A) and suggests their application in affinity sensors for detecting ochratoxin A contamination.

## ACKNOWLEDGEMENTS

First of all, I would like to express my gratitude to my supervisor Dr. I.E. Tothill for accepting me as a student and for giving me guidance, independence and support.

I am also very grateful to Bengt Danielsson for allowing me back into my old ‘biosensor group’ in Lund for a while to use their Biacore instrument. I also would like to thank everyone at Cranfield Health and the School of Water Sciences who have offered their support and friendship over the years. With special thanks to my ‘accomplices’ Charlie Parker and Gudrun Winkler for sharing the Cranfield experience. I also would like to thank the Cranfield Student Association and its staff for a great working atmosphere over the two years I worked ‘at the bar’.

I specifically want to thank my parents, Sigrun and Wolfgang Heurich, who have inspired and supported my scientific interest for over a decade now, for never questioning my career choices and the freedom they gave me throughout my life. I am especially proud of my younger sister, Bianca, who studies to become a biochemist and consequently a PhD as well.

I would like to dedicate this work to the fond memories of Otto and Anneliese Heurich, for being nothing but proud of the achievements of their granddaughters and whom I would have truly wished to witness the completion of this work.

Finally, I would like to thank my partner Yura, for your enormous patience, never ending care and love and whose determination had an immense impact on this work. I also dedicate this thesis to you.

“..

*And all I ask is a tall ship and a star to steer her by,*

...”

Sea-Fever by John Masefield (1878 – 1967)

# CONTENTS

<b>ABSTRACT</b>	<b>I</b>
<b>ACKNOWLEDGEMENTS</b>	<b>III</b>
<b>CONTENTS</b>	<b>IV</b>
<b>LIST OF TABLES</b>	<b>XI</b>
<b>LIST OF PLATES</b>	<b>XIII</b>
<b>LIST OF FIGURES</b>	<b>XIV</b>
<b>NOTATION</b>	<b>XIV</b>
<b>CHAPTER 1 : LITERATURE REVIEW</b>	<b>1</b>
<b>1.1 Background</b>	1
<b>1.2 Mycotoxins</b>	3
1.2.1 Legislation	6
<b>1.3 Ochratoxin A</b>	7
1.3.1 Toxicity	9
1.3.2 Regulations of daily intake and permissible limits in food	11
<b>1.4 Sample extraction and clean-up</b>	11
<b>1.4.1 Sampling</b>	12
1.4.2 Extraction from wine and clean-up	13
1.5 Antibodies as Immunochemical Reagents	15
1.5.1 Antibody structure and function	15
1.5.2 The principle of antibody recognition	16
1.5.3 The difference between affinity and avidity	17
1.6 Immunoassays	18
1.6.1 How to develop an immunoassay	18
1.6.1.1 Immobilisation (coating)	19
1.6.1.2 Blocking reagents and detergents	21
1.6.1.3 Enzyme labels in immunoassays	21
1.6.2 Competitive enzyme linked immunoassays	23
1.7 Chromatography based techniques	25
1.7.1 High Performance Liquid Chromatography	25
1.7.2 Thin layer chromatography and Gas chromatography	26

---

<b>1.7.3 Immunoaffinity Chromatography (IAC)</b>	29
1.7.4 Current Research using Immunoassays	29
1.8 Electroanalytical methods and applications	33
1.8.1 Cyclic voltammetry	33
1.8.2 Chronoamperometry	33
1.8.3 Hydrogen peroxide detection	35
1.8.4 Redox mediators	36
1.8.5 The classic three-electrode system	38
1.8.6 Miniaturization and electrode arrays	40
1.8.7 Electrode modification	41
1.8.8 Wine electrochemistry	44
1.9 Biosensors	45
1.9.1 Electrochemical biosensors	47
1.9.2 Surface plasmon resonance-based optical biosensors	50
1.10 Biomimetics	51
1.10.1 Peptide structure and synthesis	53
1.11 Computational chemistry	56
1.11.1 Force Fields	56
1.11.2 Minimisation	59
1.11.3 Simulated annealing	61
1.11.4 Introduction to SYBYL and the Tripos force field	62
1.11.5 Introduction to Leapfrog	62
1.11.6 Docking with FlexiDock	64
1.11.7 Current research in peptide modelling	66
1.12 Aims and Objectives	68
<b>CHAPTER 2 : IMMUNOASSAY DEVELOPMENT FOR OCHRATOXIN A</b>	<b>72</b>
2.1 Introduction	72
2.2 Materials	73
2.2.1 Chemicals and Immunoreagents	73
2.2.2 Equipment	74
2.2.3 Buffer solutions	74
2.3 Methods	75

---

2.3.1 Immunoaffinity purification of antibody with BSA	75
2.3.2 Ochratoxin A-BSA coating procedure	75
2.3.3 Temperature, antibody concentration and blocking reagent addition to the coating buffer	77
2.3.4 Indirect non-competitive ochratoxin A immunoassay	78
2.3.5 Indirect competitive ochratoxin A (-BSA) immunoassay	79
2.3.6 Production of ochratoxin A-HRP conjugate	80
2.3.7 Activity characterisation of ochratoxin A-HRP conjugate	80
2.3.8 Direct non-competitive ochratoxin A-HRP immunoassay	80
2.3.9 Wine sample analysis	81
2.3.9.1 Indirect competitive immunoassay for wine analysis	81
2.3.9.2 Wine analysis using an immunoassay test kit (Ridascreen)	82
2.3.9.3 Wine analysis using HPLC	82
2.4 Results and Discussion	84
2.4.1 Ochratoxin A-BSA coating concentration	84
2.4.2 Increased dynamic range of the assay	87
2.4.3 Ochratoxin A-BSA coating incubation time	88
2.4.4 Antibody incubation time, temperature and blocking reagent	90
2.4.5 Calculation of the functional affinity constant	96
2.4.6 Ochratoxin A coating to solid phase support	98
2.4.7 Indirect competitive immunoassay using ochratoxin A (- BSA)	100
2.4.8 Direct non-competitive ochratoxin A-HRP immunoassay	102
2.4.9 Analysis of wine samples using an indirect enzyme immunoassay	104
2.5 Concluding remarks	106
<b>CHAPTER 3 : SURFACE PLASMON RESONANCE ANALYSIS OF OCHRATOXIN A ANTIBODIES</b>	<b>110</b>
3.1 Introduction	110
3.2 Experimental	111
3.3 Methods	111
3.3.1 Amine coupling of ochratoxin A-BSA to the CM5 sensor chip	111
3.3.2 Amine coupling of ochratoxin A antibody to the CM5 sensor chip	112
3.3.2.1 Production of Ochratoxin A-HRP conjugate	113
3.3.2.2 Wine sample preparation	113



---

3.3.2.3 Control experiments	114
3.4 Results and Discussion	116
3.4.1 Immobilisation of Ligands	116
3.4.2 Binding interaction analysis of ochratoxin A antibodies	117
3.4.3 Immobilised ochratoxin A-BSA-conjugate	117
3.4.3.1 Ochratoxin A-BSA ligand with antibody B analyte	117
3.4.3.2 Ochratoxin A-BSA ligand with antibody A	120
3.4.4 Immobilised antibody	123
3.4.4.1 Antibody B ligand with ochratoxin A-BSA analyte	123
3.4.4.2 Antibody A ligand with ochratoxin A-BSA analyte	125
3.4.4.3 Antibody A ligand with ochratoxin A-HRP analyte	126
3.4.5 Immobilised ochratoxin A-BSA with ochratoxin A competitor	129
3.4.5.1 Ochratoxin A-BSA ligand with antibody B and ochratoxin A competitor	129
3.4.5.2 Ochratoxin A-BSA ligand with antibody A and ochratoxin A competitor	131
3.4.6 Wine sample analysis	132
3.4.7 Control experiments	136
3.4.7.1 Multi-valance of the binding interaction	136
3.4.7.2 Mass transfer control experiment	137
3.4.7.3 BSA cross-reactivity	139
3.5 Concluding remarks	141
<b>CHAPTER 4 : SCREEN PRINTED ELECTRODE BASED IMMUNOSENSOR FOR OCHRATOXIN A</b>	<b>143</b>
4.1 Introduction	143
4.2 Experimental	146
4.3 Methods	147
4.3.1 Fabrication of screen printed electrodes	147
4.3.2 Electrochemical noise of screen printed electrodes	149
4.3.3 Voltammetric studies	150
4.3.3.1 Cyclic voltammetry	150
4.3.3.2 Cyclic voltammetric studies of TMB	150
4.3.3.3 Redox peak characterisation	151
4.3.3.4 Redox peak (interference) investigation	151

---

4.3.3.5 Voltammetric studies of ochratoxin A–BSA adsorption	151
4.3.3.6 Voltammetric studies of wine samples	152
4.3.4 Amperometry	152
4.3.4.1 Amperometric studies of TMB/H <sub>2</sub> O <sub>2</sub> (HRP)	152
4.3.4.2 Chronoamperometric characterisation of ochratoxin A-BSA	154
4.3.4.3 Chronoamperometric characterisation of anti-ochratoxin A antibody	155
4.3.4.4 Ochratoxin A biosensor development	155
4.3.4.5 Surface modification of SPGE	156
4.3.4.6 Sample preparation and analysis	157
4.3.4.7 Microelectrode arrays –preliminary characterisation-	159
4.3.4.8 Preliminary direct immunosensor	160
4.4 Results and discussion	161
4.4.1 Electrode fabrication and configuration	161
4.4.2 Economical aspects of screen printed electrode-based sensor	162
4.4.3 Electrochemical noise of screen printed electrodes	163
4.4.4 Choice of electroactive species 3,3',5,5'-tetramethylbenzidine	165
4.4.5 Cyclic voltammetric studies of TMB	167
4.4.6 Identification and characterisation of KCl peak	170
4.4.7 Interference control	172
4.4.8 Potential selection for amperometric studies with TMB	176
4.4.9 Cyclic voltammetry of ochratoxin A –BSA adsorption	177
4.4.10 Electrochemical characterisation of wine	181
4.4.11 Wine interference study on SPGE	182
4.4.12 Chronoamperometric studies of TMB/ H <sub>2</sub> O <sub>2</sub> /HRP system	184
4.4.13 Optimal ochratoxin A-BSA concentration	187
4.4.14 Optimal antibody concentration	189
4.4.15 Indirect competitive ochratoxin A immunosensor	190
4.4.16 Biosensor optimisation through surface modification	192
4.4.17 Analysis of ochratoxin A in wine samples	194
4.4.18 Microelectrode immunosensor	196
4.4.19 Preliminary direct competitive ochratoxin A immunosensor	202

---

4.5 Conclusions	203
<b>CHAPTER 5 : COMPUTATIONAL MODELLING OF PEPTIDE RECEPTORS</b>	<b>208</b>
5.1 Introduction	208
5.2 Experimental	210
5.3 Methods	210
5.3.1 Drawing tools	210
5.3.2 Energy minimisation	210
5.3.3 Simulated annealing	212
5.3.4 Ligand design using LeapFrog	213
5.3.5 Receptor-ligand docking using FlexiDock	216
5.4 Results and Discussion	218
5.4.1 Minimisation and annealing	218
5.4.2 Leapfrog assisted design using ochratoxin A	219
5.4.3 <i>De novo</i> designed peptides	221
5.4.4 <i>De novo</i> peptide design using a starting molecule	223
5.4.5 Screening the peptide receptor library	226
5.4.6 Docking simulation for lead sequence selection	226
5.5 Concluding Remarks	230
<b>CHAPTER 6 : SURFACE PLASMON RESONANCE ANALYSIS OF PEPTIDE RECEPTORS</b>	<b>233</b>
6.1 Introduction	233
6.2 Experimental	233
6.3 Methods	234
6.3.1 Solid phase binding assay of peptide-ochratoxin A interaction	234
6.3.2 Bioanalysis of peptide-ochratoxin A interaction using Biacore	235
6.4 Results and Discussion	237
6.4.1 Solid phase binding assay of peptide-ochratoxin A interaction	237
6.4.2 Peptide immobilisation level on CM5	239
6.4.3 Immobilised peptide interaction with ochratoxin A-BSA	239
6.4.4 Immobilised ochratoxin A-BSA interaction with peptides	243
6.5 Concluding remarks	245
<b>CHAPTER 7 : CONCLUSIONS</b>	<b>249</b>
<b>CHAPTER 8 : FUTURE WORK AND ALTERNATIVE APPROACHES</b>	<b>254</b>

<b>REFERENCES &amp; BIBLIOGRAPHY</b>	<b>260</b>
<b>PUBLICATIONS</b>	<b>299</b>
<b>APPENDICES</b>	<b>301</b>

## LIST OF TABLES

Table 1.1: The molecular family of ochratoxins.	8
Table 1.2: Immobilisation techniques for biomolecules.	20
Table 1.3: Summary of fluorescing mycotoxins using a RP-C18 column (Mycotox™) in a mobile phase of acetonitrile/methanol/phosphate buffer (pH 3.3) [Pickering <i>et al.</i> , 2004].	26
Table 1.4: Chromatography based techniques for ochratoxin A determination.	28
Table 1.5: List of Immunoassay-based commercially available test kits for Ochratoxin A.	31
Table 1.6: Examples of 1 e <sup>-</sup> and 2 e <sup>-</sup> acceptor/donors.	36
Table 1.7: Types of intermolecular forces [Selassie <i>et al.</i> , 2003].	53
Table 1.8: Research on peptide receptors and synthetic peptides [Tripos™].	66
Table 2.1: List of chemicals and supplier.	73
Table 2.2: Ochratoxin A-BSA coating concentrations.	76
Table 2.3: Antibody dilutions for indirect immunoassay.	77
Table 2.4: Ochratoxin A concentrations adsorbed onto a polystyrene surface.	78
Table 2.5: Competitor concentrations pre-mixed with ochratoxin A-antibody.	79
Table 2.6: Wine samples pre-mixed with ochratoxin A-antibody	81
Table 2.7: Wine samples analysed with indirect competitive assay and commercial immunoassay kit (Ridascreen) compared to HPLC data as verification method.	105
Table 3.1: Immobilisation levels of ligands immobilised on carboxymethylated gold surface via amine coupling.	116
Table 4.1: Screen printer DEK 248 parameters for screen printing electrodes onto a polyester substrate using imaged screens.	147
Table 4.2: End-user prices of screen printed gold electrodes per piece (valid 2007).	162
Table 4.3: Effect of applied potential on the current response on SPGE with TMB.	177
Table 4.4: Comparison of sensor and standard immunoassay test kit results for measurement of ochratoxin A in wine samples.	195
Table 5.1: Parameters used for energy minimization.	211
Table 5.2: Parameters used for simulated annealing.	213
Table 5.3: Parameters used for LeapFrog.	214
Table 5.4: LeapFrog electrostatic screening box dimensions.	214
Table 5.5: Summary of relative move frequencies.	216

Table 5.6: Minimisation of ochratoxin A structure.	218
Table 5.7: Binding energies for all 21 amino acids with ochratoxin A.	220
Table 5.8: Binding energy and corresponding H-bonds highest scoring peptide sequences interacting with ochratoxin A generated from LeapFrog.	221
Table 5.9: Binding energy and corresponding H-bonds of lead peptide sequences interacting with ochratoxin A generated from LeapFrog using starting ligands.	224
Table 5.10: Binding energies for the highest scoring peptide sequences.	226
Table 5.11: List of 11 highest ranking peptides screened with FlexiDock shown in descending order	227
Table 6.1: Ligands immobilised to CM5 chips and their immobilisation response.	239

## LIST OF PLATES

Plate 4.1: Illustration of the screen printed gold electrode (SPGE) with working electrode (WE), counter electrode (CE) and reference electrode (RE) connected via a 1-outlet edge connector (insert) with ribbon data cable to a potentiostat (Autolab). Three electrodes can be fitted into the 3-outlet edge connector for simultaneous multiple measurements. ....	161
--	-----

## LIST OF FIGURES

Figure 1.1: The ochratoxin structure.	8
Figure 1.2: Procedure for determination of mycotoxins in solid samples (left) and liquid samples (right) Visconti <i>et al.</i> [1999].	12
Figure 1.3: Immunoaffinity column design containing solid extraction phase made from antibody-modified support beads binding ochratoxin A.	14
Figure 1.4: Direct competitive enzyme immunoassay format.	23
Figure 1.5: Indirect competitive enzyme immunoassay format.	24
Figure 1.6: Chemical structures of 3,3',5,5'-tetramethylbenzidine (TMB) and its oxidation states according to Josephy <i>et al.</i> [1982].	38
Figure 1.7: Micro square electrode arrays (single nanopore electrodes displayed as 5x5 array) developed by Tyndall National Institute, Cork, Ireland.	41
Figure 1.8: Biacore detection utilising surface plasmon resonance [Biacore™].	50
Figure 1.9: Peptide bond formation from amino acid monomers.	54
Figure 1.10: A molecule is viewed as a collection of points (atoms) connected by rods (bonds) with different elasticity (force constants) [Steinbach, 1996].	58
Figure 1.11: The energy minimisation principle [Steinbach, 1996]. $P$ (●) is the initial point on the energy surface. The energy minimum (●) can be characterized by a small change in energy and/or a zero gradient between steps towards a minimum. At a minimum of the potential energy surface, the net force on each atom vanishes, therefore the stable configuration [Tsai, 2002].	60
Figure 1.12: Leapfrog electrostatic screening displaying all possible site points for the interactions of a molecular template with suitable monomers [Chianella <i>et al.</i> , 2002].	63
Figure 1.13 : Flowchart outlining the consecutive milestones carried out in this thesis.	71
Figure 2.1: Serial dilution curve of adsorbed ochratoxin A-BSA. The ochratoxin A-antibody is binding at three distinct dilutions (■ 1/2000; ● 1/4000, and ▲ 1/6000) diluted from stock solution of 1 mg ml <sup>-1</sup> . Absorbance was at 492 nm by monitoring the catalysis of OPD with H <sub>2</sub> O <sub>2</sub> by HRP. Each error bar represents standard deviation of three replicates. The curves were fitted using a 4-parameter fit.	85



- Figure 2.2: Logarithmic scale of the dynamic working range showing three anti-ochratoxin A-antibody dilutions (■ 1/2000; ● 1/4000, and ▲ 1/6000) made from stock solution of 1 mg ml<sup>-1</sup>. Absorbance was at 492 nm by monitoring the catalysis of OPD with H<sub>2</sub>O<sub>2</sub> by HRP. Each error bar represents standard deviation of three replicates. Linear regression depicts corresponding equations and R-squared values. 86
- Figure 2.3: Serial dilution curve of ochratoxin A-BSA adsorbed to the wells of a microtitre plate. The anti-ochratoxin-antibody is shown binding at four distinct dilutions (■ 1/1000; ● 1/2000, ▲ 1/5000, and ◇ 1/10,000) from stock solution 1 mg ml<sup>-1</sup>. The highest antibody concentration 1/1000 achieved saturation which indicates its molecular excess on the microtitre plate. Absorbance was determined at 492 nm by monitoring the catalysis of OPD with H<sub>2</sub>O<sub>2</sub>. Each error bar represents standard deviation of two replicates. The curves were fitted using a 4-parameter fit. 87
- Figure 2.4: Different concentrations of adsorbed ochratoxin A-BSA is shown as a function of coating time. Ochratoxin A-BSA was adsorbed to the wells of a microtitre plate at coating concentrations (■ 750 µg L<sup>-1</sup>; ● 100 µg L<sup>-1</sup>; ▲ 10 µg L<sup>-1</sup> and ◇ 1 µg L<sup>-1</sup>). The anti-ochratoxin-antibody was added at 1/200 dilution made from stock solution 1 mg L<sup>-1</sup> and incubated overnight at 4°C. Absorbance was determined at 492 nm monitoring the catalysis of OPD with H<sub>2</sub>O<sub>2</sub>. Each error bar represents standard deviation of two replicates. 89
- Figure 2.5: Serial dilution curve of ochratoxin A-BSA at 4°C incubation temperature versus incubation time (■ 0.5, ● 2; ▲ 4, ◇ 16, and ○ 24 hours) of anti-ochratoxin A-antibody. The anti-ochratoxin-antibody was added at 1/200 dilution made from stock solution 1 mg L<sup>-1</sup> and incubated overnight at 4°C. Blocking reagent was bovine serum albumin (A) and casein (B). Absorbance was determined at 492 nm monitoring the catalysis of OPD with H<sub>2</sub>O<sub>2</sub>. Double measurements were performed and the standard deviation is depicted as error bars. 91
- Figure 2.6: Serial dilution curve of ochratoxin A-BSA at room temperature versus incubation time (■ 0.5, ● 2; ▲ 4, ◇ 16, and ○ 24 hours) of anti-ochratoxin A-antibody. The anti-ochratoxin-antibody was added at 1/200 dilution made from stock solution 1 mg L<sup>-1</sup>. Blocking reagent was bovine serum albumin (A) and casein (B). Absorbance was determined at 492 nm monitoring the catalysis of OPD with H<sub>2</sub>O<sub>2</sub>. Double measurements were performed and the standard deviation is depicted as error bars. 93
- Figure 2.7: Serial dilution curve of ochratoxin A-BSA at 37°C incubation temperature versus incubation time (■ 0.5, ● 2; ▲ 4, ◇ 16, and ○ 24 hours) of anti-ochratoxin A-antibody. The anti-ochratoxin-antibody was added at 1/200 dilution made from stock solution 1 mg L<sup>-1</sup>. Blocking reagent was bovine serum albumin (A) and casein (B). Absorbance was determined at 492 nm monitoring the catalysis of OPD with H<sub>2</sub>O<sub>2</sub>. Double measurements were performed and the standard deviation is depicted as error bars. 95

- Figure 2.8: Experimental signal curve for anti-ochratoxin A antibody at 7 different ochratoxin A-BSA coating concentrations (■ 0, ● 0.1, ▲ 1, □ 10, ○ 100, △ 1000, ◆ 10.000, and ◇ 100.000  $\mu\text{g L}^{-1}$ ). Absorbance was determined at 492 nm monitoring the catalysis of OPD with  $\text{H}_2\text{O}_2$ . The curves were fitted using a 4-parameter fit. 97
- Figure 2.9: Signal curve of increasing ochratoxin A coating concentration (■). The signal curve depicts signal – background (blank reference). Absorbance is measured at 492 nm monitoring the catalysis of OPD with  $\text{H}_2\text{O}_2$ . Double measurements were performed and the standard deviation is depicted as error bars. 99
- Figure 2.10: Signal curve (blank corrected) shows increasing concentrations of ochratoxin A-BSA competitor (■). Absorbance is measured at 492 nm monitoring the catalysis of OPD with  $\text{H}_2\text{O}_2$ . Standard deviation is depicted as error bars. 100
- Figure 2.11: Signal curve (blank corrected) shows increasing concentrations of ochratoxin competitor (●). Absorbance is measured at 492 nm monitoring the catalysis of OPD with  $\text{H}_2\text{O}_2$ . Standard deviation is depicted as error bars. 101
- Figure 2.12: Spectrophotometric investigation of ochratoxin A-HRP activity upon substrate addition [■]. Absorbance was determined at 450 nm monitoring the catalysis of TMB with  $\text{H}_2\text{O}_2$  and plotted against ochratoxin A-HRP dilution factor. 102
- Figure 2.13: Signal curve of immobilised ochratoxin A-antibody ( $2.5 \mu\text{g L}^{-1}$ ) via protein A (■) and passive adsorption (●) interacting directly with increasing ochratoxin A-HRP concentration. Absorbance was determined at 450 nm monitoring the catalysis of TMB with  $\text{H}_2\text{O}_2$ . 103
- Figure 2.14: Standard curve of ochratoxin A using the indirect competitive assay for wine sample analysis. Ochratoxin A standard concentrations (0, 25, 75, 225, 675 and 2025  $\text{ng L}^{-1}$ ) were obtained from the Ridascreen test kit. Absorbance was monitored at 450 nm using TMB/ $\text{H}_2\text{O}_2$ . 104
- Figure 3.1: Covalently immobilised ochratoxin A-BSA is linked to the sensor chip surface through a carbodiimide linker. The illustration represents amine coupling. The ochratoxin A antibody is passed over the surface at a set flow rate displaying association and dissociation from the immobilised ochratoxin A-BSA ligand. 117
- Figure 3.2: Sensorgram of response unit versus time illustrating the binding of ochratoxin A-antibody (Biogenesis) to immobilized ochratoxin A-BSA. A medium concentration ( $10 \mu\text{g ml}^{-1}$ ) antibody was measured in duplicate to assess the reproducibility of the method. The ochratoxin A-antibody concentrations as displayed from top to bottom ranged from 100, 50, 10, 5, 2, 1 and 0  $\text{mg L}^{-1}$ . The zero concentration is equivalent to the same volume of buffer injected over the surface. All curves were subtracted by a blank reference surface (ethanolamine blocked). 118

- Figure 3.3: Sensorgram of response unit versus time illustrating the binding of ochratoxin A-antibody (Biogenesis) to immobilized ochratoxin A-BSA. A medium concentration ( $10 \mu\text{g ml}^{-1}$ ) antibody was measured in duplicate to assess the reproducibility of the method. The ochratoxin A-antibody concentrations as displayed from top to bottom ranged from 100, 50, 20, 10, 5, 2, 1, 0.5, 0.2, 0.1, 0.05 and  $0 \text{ mg L}^{-1}$ . The zero concentration is equivalent to the same volume of buffer injected over the surface. All curves were subtracted by a blank reference surface (BSA blocked). 119
- Figure 3.4: Sensorgram of response unit versus time illustrating the binding of ochratoxin A-antibody (Acris) to immobilized ochratoxin A-BSA. All curves are reference subtracted. The ochratoxin A-antibody concentrations as displayed from top to bottom ranged from 10, 5, 2, 1,  $0.5 \text{ mg L}^{-1}$  and zero injection (PBS). The zero concentration is equivalent to the same volume of buffer injected over the surface. All curves were subtracted by a blank reference surface (ethanolamine blocked). 120
- Figure 3.5: Sensorgram of response unit versus time illustrating the binding of ochratoxin A-antibody (Acris) to immobilized ochratoxin A-BSA. All curves are BSA reference subtracted. The ochratoxin A-antibody concentrations as displayed from top to bottom ranged from 100, 50, 20, 10, 5, 2, 1, 0.5, 0.2, 0.1, 0.05 and  $0 \text{ mg L}^{-1}$ . The zero concentration is equivalent to the same volume of buffer injected over the surface. All curves were subtracted by a blank reference surface (BSA blocked). 121
- Figure 3.6: Covalently immobilised ochratoxin A antibody is linked to the sensor chip surface through a carbodiimide linker. The illustration represents amine coupling. The ochratoxin A-BSA analyte is passed over the surface at a set flow rate displaying association and dissociation from the immobilised ochratoxin A antibody ligand. 123
- Figure 3.7: Sensorgram of response unit versus time illustrating varying ochratoxin A-BSA concentrations (top to bottom: 100, 10, 1, 0.1 and  $0.01 \text{ mg L}^{-1}$ ) binding immobilized anti-ochratoxin A antibody (Biogenesis). All curves are reference subtracted with non-specific IgG used as blank. 124
- Figure 3.8: Sensorgram of response unit versus time illustrating the binding of ochratoxin A-BSA to immobilized ochratoxin A-antibody (Acris). All curves are reference subtracted with non-specific IgG used as blank. All conjugate concentrations were measured in duplicate to assess the reproducibility of the method. The ochratoxin A-BSA concentrations as displayed from top to bottom ranged from 100, 50, 20, 10, 5, 2, 1, 0.5, 0.2, 0.1 and  $0 \text{ mg L}^{-1}$ . 125

- Figure 3.9: Sensorgram of response unit versus time illustrating the binding of ochratoxin A-HRP (Horseradish peroxidase) to immobilized ochratoxin A-antibody (Acris; amine coupling). All curves are reference subtracted with non-specific IgG used as blank. All conjugate concentrations were measured in duplicate to assess the reproducibility of the method. The ochratoxin A-BSA concentrations as displayed from top to bottom ranged from 100, 50, 20, 10, 5, 2, 1, 0.5, 0.2, 0.1 and 0 mg L<sup>-1</sup>. 127
- Figure 3.10: Covalently immobilised ochratoxin A-BSA is linked to the sensor chip surface via amine coupling. The ochratoxin A antibody is premixed with varying ochratoxin A concentrations and the solution is then passed over the sensor surface at a set flow rate illustrating the competitive reaction of premixed ochratoxin A and immobilised ochratoxin A-BSA ligand for antibody binding sites. 129
- Figure 3.11: Sensorgram of response unit versus time illustrating the binding of ochratoxin A-antibody (Biogenesis) to ochratoxin A in solution competing with immobilized ochratoxin A-BSA. The measurement was performed in duplicate and the ochratoxin A concentrations in solution with the antibody are displayed in duplicate from top to bottom: 0, 0.0001; 0.001; 0.01; 0.1; 1; 10 and 100 mg L<sup>-1</sup> ochratoxin A standard. 130
- Figure 3.12: Sensorgram of response unit versus time illustrating the binding of ochratoxin A-antibody (Acris) to ochratoxin A in solution competing with immobilized ochratoxin A-BSA. The measurement was performed in duplicate and the ochratoxin A concentrations in solution with the antibody are displayed in duplicate from top to bottom: 0, 0.0001; 0.001; 0.01; 0.1; 1; 10 and 100 mg L<sup>-1</sup> ochratoxin A standard. 131
- Figure 3.13: Sensorgram of response unit versus time illustrating the binding of ochratoxin A-antibody (Acris) to ochratoxin A in solution competing with immobilized ochratoxin A-BSA. The reference surface is blocked with BSA and used as blank. The measurement was performed in duplicate and the ochratoxin A concentrations in solution with the antibody are displayed in duplicate from top to bottom: 0, 0.0001; 0.001; 0.01; 0.1; 1; and 10 mg L<sup>-1</sup> ochratoxin A standard (in HEPES buffer pH 7.4). 132
- Figure 3.14: Standard curve displaying response signal [RU] versus ochratoxin A standard concentration: 0; 0.0001; 0.001; 0.1 and 10 mg L<sup>-1</sup> in HBS, pH 7.4. 133
- Figure 3.15: Normalised response signal [RU] times 100 versus ochratoxin A standard concentration: 0; 0.0001; 0.001; 0.1 and 10 mg L<sup>-1</sup>. 134
- Figure 3.16: Sensorgram of response unit versus time illustrating wine samples premixed with ochratoxin A antibody A passed over the sensor surface. Any ochratoxin A present in a wine sample binds the antibody and is competing with immobilized ochratoxin A-BSA. Signal spikes result from interfering substances present in wine. 135

- Figure 3.17: Sensorgrams of response unit versus time showing a fixed concentration of ochratoxin A-BSA ( $10 \text{ mg L}^{-1}$ ) analyte binding to immobilized ochratoxin A-antibody at two distinct flow rates:  $1 \text{ } \mu\text{l min}^{-1}$  (blue) and  $5 \text{ } \mu\text{l min}^{-1}$  (red). 136
- Figure 3.18: Association rate constant  $k_a$  versus increasing flow rate. Ochratoxin A antibodies (antibody A (■) and antibody B (●)) are passed over a sensor surface with immobilised ochratoxin A-BSA. The binding interaction is observed at increasing flow rates ( $5, 15$  and  $75 \text{ } \mu\text{l min}^{-1}$ ) and the increasing association constant ( $k_a$ ) is related to mass transfer. 137
- Figure 3.19: Dissociation rate constant  $k_d$  versus increasing flow rate. Ochratoxin A antibodies (antibody A (■) and antibody B (●)) are passed over a sensor surface with immobilised ochratoxin A-BSA. The binding interaction is observed at increasing flow rates ( $5, 15$  and  $75 \text{ } \mu\text{l min}^{-1}$ ) and the increasing dissociation constant ( $k_d$ ) is related to mass transfer. 138
- Figure 3.20: Sensorgram of response unit versus time illustrating the binding of antibody B to immobilized BSA (bovine serum albumin). All antibody concentrations are displayed from top to bottom ranged from  $100, 50, 20, 10, 5, 2, 1, 0.5, 0.2, 0.1, 0.05$  and  $0 \text{ mg L}^{-1}$ . 139
- Figure 3.21: Sensorgram of response unit versus time illustrating the binding of antibody A to immobilized BSA (bovine serum albumin). All antibody concentrations are displayed from top to bottom ranged from  $100, 50, 20, 10, 5, 2, 1, 0.5, 0.2, 0.1, 0.05$  and  $0 \text{ mg L}^{-1}$ . 140
- Figure 4.1: The immunosensor procedure proposed for ochratoxin A analysis using immunoaffinity purification of wine samples, transfer of the sample extract to the immunoassay-modified screen-printed gold electrode and measurement using chronoamperometry. 145
- Figure 4.2: Three-electrode design of screen printed gold electrodes fabricated in-house at Cranfield University, 2006. 148
- Figure 4.3: Immunoassay layer on SPGE showing HRP catalysed reaction of  $\text{H}_2\text{O}_2$  and TMB at a gold working electrode with a set potential. 154
- Figure 4.4: Electrochemical potential [mV] illustrated versus time [seconds]. Curves display the potential noise of the cell potential [mV] for SPGE (black), SPCE (green), SPCE-Dupont (blue) and gold microelectrode AuME (red). 163
- Figure 4.5: Electrochemical current [ $\mu\text{A}$ ] depicted as columns comparing the current noise for screen-printed gold (SPGE), carbon (SPCE), carbon (SPCE-Dupont) and gold (Au) microelectrodes. The current noise was determined as an average value of an alternating current signal over 600 seconds. 164
- Figure 4.6: Current versus electrochemical potential shows the cyclic voltammograms of TMB (black) and hydroquinone (red) on bare screen-printed gold electrodes (SPGE). The cyclic voltammograms were monitored separately upon addition of  $20 \text{ } \mu\text{l}$  TMB and hydroquinone at a scan rate of  $50 \text{ mV s}^{-1}$ . 166

- Figure 4.7: Current versus electrochemical potential shows the cyclic voltammograms (CV) of 20  $\mu\text{l}$  TMB solution on SPGE at different scan rates [ $v$ ]. From inner to outer cyclic voltammogram the scan rate is 25; 50; 75; 100; 150; 200; and 400  $\text{mV s}^{-1}$ . 167
- Figure 4.8: Anodic peak currents [ $\mu\text{A}$ ] versus square root of scan rate  $\sqrt{v}$  [ $\sqrt{(\text{V s}^{-1})}$ ] obtained from cyclic voltammograms on bare SPGE with increasing scan rate. Linear relationship of anodic peak current  $pa_{,1}$  ( $\square$ ) and  $pa_{,2}$  ( $\blacksquare$ ) as well as the cathodic peak current  $pc$  ( $\bullet$ ) of TMB with the scan rate  $v$ . 168
- Figure 4.9: Linear relationship of peak separation [ $\text{mV}$ ] versus scan rate  $v$  obtained from cyclic voltammograms for anodic peaks  $pa_{,1}$  [ $\blacksquare$ ] and  $pa_{,2}$  [ $\bullet$ ] of TMB on a bare SPGE. 169
- Figure 4.10: Cyclic voltammograms of  $\text{H}_2\text{O}$  (blue); 0.1 M PBS, pH7.4, containing 0.1M KCl (red); and TMB solution (black) on bare SPGE recorded at a scan rate of 50  $\text{mV s}^{-1}$ . 170
- Figure 4.11: Cyclic voltammograms of 0.1 M KCl on bare SPGE (red) compared to bare SPCE (black) and of 0.1 M KCl on SPCE (red). Scan rate is 50  $\text{mV s}^{-1}$ . 171
- Figure 4.12: Cyclic voltammograms of Nafion-modified bare SPGE. Nafion-modified reference electrode is shown in black; whole (3-electrode) modified SPGE is shown in red. The cyclic voltammogram was recorded in 0.1 M PBS, pH7.4, containing 0.1 M KCl at a scan rate of 50  $\text{mV s}^{-1}$ . 173
- Figure 4.13: Cyclic voltammograms of Nafion-modified reference electrode on bare SPGE with 20  $\mu\text{l}$  added TMB solution compared to 0.1 M PBS, pH7.4, containing 0.1M KCl. Nafion-modified reference electrode in 0.1 M PBS is shown in black and with TMB is shown in red. 174
- Figure 4.14: Current [ $\mu\text{A}$ ] versus step potential [ $\text{mV}$ ] illustrates step-amperometry of 20  $\mu\text{l}$  TMB solution on bare SPGE. The current was recorded over a hundred seconds for each step potential (-600 to +600  $\text{mV}$ ). 176
- Figure 4.15: Cyclic voltammogram of ochratoxin A-BSA (0.1  $\text{mg L}^{-1}$ ) on SPGE at a scan rate of 50  $\text{mV s}^{-1}$ . Addition of 20  $\mu\text{l}$  ochratoxin A-BSA solution (red) added prior to measurement and after overnight adsorption of ochratoxin A-BSA (black). 178
- Figure 4.16: Cyclic voltammograms of 20  $\mu\text{l}$  TMB solution (red) and the control 50 mM PBS, pH 7.4, 0.1 M KCl (black) on SPGE at a scan rate of 50  $\text{mV s}^{-1}$ . 179
- Figure 4.17: Plot of scan rate versus peak separation for anodic peak [ $\blacksquare$ ] and cathodic peak [ $\bullet$ ] of ochratoxin A-BSA (50 mM PBS, pH 7.4 in 0.1 M KCl adsorbed on SPGE at a scan rate of 50  $\text{mV s}^{-1}$ ). 180
- Figure 4.18: Cyclic voltammograms of 20  $\mu\text{l}$  red wine sample diluted in 0.1 M PBS, pH 7.4 containing 0.1 M KCl (red) compared to synthetic wine (black) and monitored on a bare SPGE at a scan rate of 50  $\text{mV s}^{-1}$ . 181

- Figure 4.19: Cyclic voltammograms of a red wine sample (black), 1:10 diluted red wine sample (red) and 1:10 diluted red wine sample treated with PVPP (blue) on SPGE at a scan rate of  $50 \text{ mV s}^{-1}$ . Dilution buffer was 5%  $\text{Na}_2\text{CO}_3$ , 1% PEG, pH 8.3. 182
- Figure 4.20: Chronoamperometry of current [ $\mu\text{A}$ ] versus time [sec] illustrates the current response upon the addition of  $\text{H}_2\text{O}_2$  and then TMB when applying zero potential (black) compared to applying a potential at -150 mV (red). 184
- Figure 4.21: Chronoamperometry of current [ $\mu\text{A}$ ] versus time [sec] illustrates the current response upon the addition of TMB and  $\text{H}_2\text{O}_2$  (black) in comparison to the addition of TMB/ $\text{H}_2\text{O}_2$ /HRP (red) at an applied potential of -150 mV. 186
- Figure 4.22: Chronoamperometry of current [ $\mu\text{A}$ ] versus time [sec] illustrates the current response upon the addition of TMB and  $\text{H}_2\text{O}_2$  to the immunosensor surface (non-competitive immunoassay-modified SPGE). The change in current at an applied potential of -150 mV was monitored over time. The grey arrow depicts increasing adsorbed ochratoxin A-BSA concentration (black) [0.1; 0.5; 1; 2; 5; 10; and 100  $\text{mg L}^{-1}$  ochratoxin A-BSA] with decreasing current compared to the negative control BSA (red). 187
- Figure 4.23: Current -[ $\mu\text{A}$ ] versus immobilised ochratoxin A-BSA (■) concentration illustrates the current response with increasing ochratoxin A-BSA adsorbed to the SPGE. 188
- Figure 4.24: Current -[ $\mu\text{A}$ ] versus immobilised anti-ochratoxin A antibody (■) concentration illustrates the current response with increasing antibody concentration bound to a fixed concentration of adsorbed ochratoxin A-BSA. 189
- Figure 4.25: Chronoamperometry of current [ $\mu\text{A}$ ] versus time [sec] illustrates the current response upon the addition of TMB and  $\text{H}_2\text{O}_2$  to the immunosensor surface (indirect competitive immunoassay-modified SPGE). The change in current at an applied potential of -150 mV was monitored over time. The grey arrow depicts the increasing ochratoxin A competitor concentration (black) [0.00001; 0.0001; 0.001; 0.01; 0.1; 1; and 10  $\text{mg L}^{-1}$  ochratoxin A] inversely proportional to the current response. The negative control is 0.1 M PBS, pH 7.4 (red). 190
- Figure 4.26: Competitive response curve of current -[ $\mu\text{A}$ ] versus ochratoxin A (■) competitor concentration illustrating the current response with increasing ochratoxin A [ $\mu\text{g L}^{-1}$ ] applied with fixed antibody and immobilised ochratoxin A-BSA concentration on SPGE monitored using the Autolab potentiostat. Standards are prepared in PBS, pH 7.4. 191
- Figure 4.27: Cyclic voltammograms of current [ $\mu\text{A}$ ] versus potential [V] of CMD-modified SPGE illustrating adsorbed carboxymethylated dextran (CMD) (red) compared to bare SPGE in 0.1 M PBS, pH 7.4 containing 0.1 M KCl at a scan rate of  $50 \text{ mV s}^{-1}$ . 192

- Figure 4.28: Competitive response curve of current  $[-\mu\text{A}]$  versus ochratoxin A (■) concentration illustrating the current response with increasing ochratoxin A competitor  $[\mu\text{g L}^{-1}]$  concentration on CMD-modified SPGE monitored using the Autolab potentiostat. Standards are prepared in PBS, pH 7.4. The curve was fitted using a four parameter fit. 193
- Figure 4.29: Current versus electrochemical potential shows the cyclic voltammograms (CV) of 10  $\mu\text{l}$  TMB solution on SPGE at different scan rates  $[\text{V}]$ . From inner to outer cyclic voltammogram the scan rate is 25; 50; 75; 100; 150; 200; and 400  $\text{mV s}^{-1}$ . 197
- Figure 4.30: Anodic peak currents  $[\mu\text{A}]$  versus square root of scan rate  $\sqrt{v}$   $[\sqrt{(\text{V s}^{-1})}]$  obtained from cyclic voltammograms on bare gold microelectrodes with increasing scan rate. 198
- Figure 4.31: Cyclic voltammograms of  $\text{H}_2\text{O}$  (blue); 0.1 M PBS, pH7.4, containing 0.1M KCl (red); and TMB solution (black and seen as insert) on bare gold microelectrodes recorded at a scan rate of 50  $\text{mV s}^{-1}$ . 199
- Figure 4.32: Current  $[\mu\text{A}]$  versus step potential  $[\text{mV}]$  illustrates step-amperometry of 20  $\mu\text{l}$  TMB solution on bare gold microelectrodes. The current was recorded for each step potential (-600 to +600 mV) over a hundred seconds. 200
- Figure 4.33: Chronoamperometry of current  $[\mu\text{A}]$  versus time  $[\text{sec}]$  illustrates the current response upon the addition of TMB and  $\text{H}_2\text{O}_2$  to the immunosensor surface (indirect competitive immunoassay-modified gold microelectrode). The change in current at an applied potential of +150 mV was monitored over time. Increasing ochratoxin A competitor concentrations [6; 12; and 50  $\text{mg L}^{-1}$  ochratoxin A] are shown in black and negative control is 0.1 M PBS, pH 7.4 (red). 201
- Figure 4.34: Competitive response curve of current  $[-\mu\text{A}]$  versus ochratoxin A (■) concentration illustrating the current response with increasing ochratoxin A competitor  $[\mu\text{g L}^{-1}]$  concentration on SPGE modified with protein A bound antibody. Standards are prepared in PBS, pH 7.4. The curve was fitted using a four parameter fit. 202
- Figure 5.1: Setup of minimization via the SYBYL menu bar. 211
- Figure 5.2: Setup of annealing via the SYBYL menu bar. 213
- Figure 5.3: Minimised and annealed structure of the ochratoxin A template (shown in stick and ball). 218
- Figure 5.4: Electrostatic screening of the ochratoxin A template (seen in purple). Coloured dots are depicting the sites of interaction tried by the LeapFrog tool. 219
- Figure 5.5: Ochratoxin A template (seen in purple) interacting with distinct amino acids (from left to right: isoleucine, valine, glycine, methionine, lysine and tryptophan). 221



- Figure 5.6: Left: Ochratoxin A with tripeptide (from left to right: Ile-Gly-Ala) linked via 4 H-bonds. Binding energy:  $-44.55 \text{ kcal mol}^{-1}$ . Right: ochratoxin A with tetrapeptide (from top to bottom: Ile-Gly-Ala-Pro) linked via 3 H-bonds Binding energy:  $-44.54 \text{ kcal mol}^{-1}$ . 222
- Figure 5.7: Peptide interaction with ochratoxin A, applying a starting ligand. Left: Ochratoxin A with tripeptide (from left to right: Pro-Ser-Ile) linked via 4 H-bonds. Binding energy:  $-38.34 \text{ kcal mol}^{-1}$ . Right: Ochratoxin A with tripeptide (from left to right: Gly-Ser-Ile) linked via 4 H-bonds. Binding energy:  $-35.56 \text{ kcal mol}^{-1}$ . 225
- Figure 5.8: Final result of de novo designed peptide sequences shown interacting with ochratoxin A. The 13-mer peptide (A, left) and the octapeptide (B, right) sequence are seen as space-filled, ochratoxin A as stick & ball structures. 228
- Figure 6.1: Plot of absorbance at 450 nm versus ochratoxin A–HRP conjugate (stock concentration of  $1.9 \text{ mg ml}^{-1}$ ) using immobilised octapeptide CSIVEDGL via amine coupling (■) and site-directed thiol coupling (●). Standard deviation of the multiple measurements is depicted as error bars. The curves are fitted with a four parameter fit. 237
- Figure 6.2: Plot of absorbance at 450 nm versus ochratoxin A–HRP conjugate (stock concentration of  $1.9 \text{ mg ml}^{-1}$ ) using immobilised 13-mer GPAGIDGPAGIRC via amine coupling (■) and site-directed thiol coupling (●). Standard deviation of the multiple measurements is depicted as error bars. The curves are fitted with a four parameter fit. 238
- Figure 6.3: Sensorgrams displaying  $100 \text{ mg L}^{-1}$  ochratoxin A-BSA binding to immobilised peptides a) 13-mer GPAGIDGPAGIRC in blue and b) CSIVEDGL is shown in red; and  $100 \text{ mg L}^{-1}$  BSA binding to c) 13-mer in dark grey and d) octapeptide in light grey. 240
- Figure 6.4: Sensorgrams show the binding interaction of immobilised synthetic octamer CSIVEDGL (A) and 13-mer GPAGIDGPAGIRC (B) peptide with decreasing ochratoxin A-BSA analyte concentration (from top to bottom: 100, 1, 0.1, 0.01  $\text{mg L}^{-1}$ ). The zero reference is shown in grey. The sensorgrams were trimmed by removing the signal spikes occurring at injection start and stop. 241
- Figure 6.5: Sensorgram (resonance units versus time) showing the octapeptide CSIVEDGL (red) binding immobilised ochratoxin A-BSA and the reference BSA (blue). 243
- Figure 6.6: Sensorgram (resonance units versus time) showing the 13-mer peptide GPAGIDGPAGIRC (green) binding immobilised ochratoxin A-BSA and the reference BSA (blue). 244

## NOTATION

### Symbols (units):

A	Ampere
C	Concentration (mol L <sup>-1</sup> , M)
D	Diffusion coefficient (cm <sup>2</sup> s <sup>-1</sup> )
E	Electrochemical potential (volts, V)
F	Faraday constant (96,485 C)
I	Current (Ampere, A)
mg	Milligram
RU	Refractive index change (Resonance units)
t	Time (second, s)
μ	Micro
μL	Microlitre
μg L <sup>-1</sup>	Microgram per Litre
μA	Micro ampere
μg	Microgram
ng	Nanogram
nm	Nanometer
V	Volts

### Abbreviations:

AOAC	Association of Official Agricultural Chemists
A <sub>50</sub>	50 % of maximum absorbance
aa	Amino acid
Ab	Antibody
Ag	Antigen
Ag/AgCl	Silver/Silver chloride
Au	Gold
AuME	Gold Microelectrode
BIA	Biospecific interaction analysis
BSA	Bovine serum albumin
CE	Counter electrode
CM5	Carboxymethylated gold chip
CMD	Carboxymethylated dextran
CV	Cyclic voltammetry
EC	European Commission

---

EU	European Union
$E_p$	Peak potential (V)
EDAC	<i>N</i> -Ethyl- <i>N'</i> -(3dimethylaminopropyl) carbodiimide hydrochloride
EIA	Enzyme immunoassay
ELISA	Enzyme-linked immunosorbent assay
EMAN	European Mycotoxin Awareness Network
FAO	Food and Agricultural Organisation
FDA	Food and Drug Association
FTIR	Fourier Transform Infrared Spectroscopy
H <sub>2</sub> O <sub>2</sub>	Hydrogen peroxide
HPLC	High Performance Liquid Chromatography
HRP	Horse Radish Peroxidase
$I_p$	Peak current (A)
IA	Immunoassay
IAC	Immunoaffinity Chromatography
JECFA	Joint Expert Committee on Food Additives of the United Nations
$k_a$	Association rate constant [ $M^{-1}s^{-1}$ ]
$k_d$	Dissociation rate constant [ $s^{-1}$ ]
$K_A$	Equilibrium affinity constant [ $M^{-1}$ ]
$K_D$	Equilibrium dissociation constant [M]
kDa	kilo Dalton
KCl	Potassium chloride
LC	Liquid Chromatography
LOD	Limit of detection
ME	Microelectrode
MTP	Micro titre plate
$M_w$	Molecular weight
MS	Mass Spectroscopy
NHS	<i>N</i> -Hydroxysulfosuccinimide sodium
NMR	Nuclear magnetic resonance spectroscopy
OTA	Ochratoxin A
PEG	Polyethylene glycol
PVA	Polyvinyl alcohol
PVPP	Polyvinylpyrrolidone
RE	Reference electrode
$R_{max}$	Maximum binding capacity
RT	Room temperature
SPR	Surface plasmon resonance

SPCE	Screen-printed carbon electrode
SPDP	<i>N</i> -Succinimidyl 3-(2-pyridyldithio)-propionate
SPGE	Screen-printed gold electrode
TMB	3,3',5,5'-tetramethylbenzidine
TLC	Thin layer chromatography
UV	Ultraviolet
WE	Working electrode
w/v	Weight per volume
WHO	World Health Organisation
ZRA	Zero resistance ammeter

## CHAPTER 1 : LITERATURE REVIEW

### 1.1 Background

Wine as a beverage has been known since 5000-6500 B.C., when the ancient Greeks made wine in their numerous colonies in Italy, southern France, and Spain. As of today, these countries are leading the world's largest wine production and export. Wine has been praised by poets like Homer and Ovid and philosophers such as Plato and Socrates for its ability to induce relaxation, inspiring thoughts, new hopes and creativity.

The roman encyclopedist and natural philosopher Pliny the Elder quoted "*in vino sanitas*", which means "in wine there is health". But is this really true?

For some, wine is purely an alcoholic drink; others, however, regard wine not only as a beverage, but a uniquely complex beverage that is complex in terms of taste and also in environmental, historical and cultural factors influencing its production. From a scientist's point of view, wine is very complex indeed, not only because it is made up of many different components, but also due to its controversy as health benefit and health hazard. The health benefit is known; moderate wine consumption, especially red wine, can reduce the risk of acute myocardial infarction or cancer by up to 34% [Gronbeck *et al.*, 2000]; thanks to the generous amount of polyphenols in wine. Phenolic compounds favourably influence multiple biochemical systems, such as increased high-density lipoprotein cholesterol, antioxidant activity, decreased platelet aggregation and endothelial adhesion, or suppression of cancer cell growth [Lorimier, 2000]. With all things, there is a drawback, as wine also has negative health effects that do not have to be entirely related to alcohol, but to contaminants such as heavy metals, pesticides or carcinogens. The benefits and disadvantages of wine consumption in humans have been extensively reviewed by Tomera [1999]. One substance was not described in that review even though its toxicity has been known since 1965 [van der Merwe *et al.*, 1965] and it has been related to wine contamination since 1996 [Zimmerli & Dick, 1996]. This contaminant is ochratoxin A.

Ochratoxin A is a mycotoxin, which is a group of molecules produced by certain fungi such as *Aspergillus* or *Penicillium*. These fungi can grow on grapes, which are processed predominantly into red wine and, due to the stable nature of ochratoxin A, it is processed alongside. As for every toxin, the dose is crucial and above a certain level of consumption, ochratoxin A can become a serious health risk, since it is immunosuppressive and genotoxic [Walker, 1999], but above all it has been classified as possibly carcinogenic. The International Agency for Research on Cancer (IARC) categorises it as a possibly carcinogenic substance into category ‘group 2B’, which is used for substances when there is inadequate evidence of carcinogenicity in humans, but there is sufficient evidence of carcinogenicity in animal experiments [IARC, 1993]. Just recently, the EU has established the maximum acceptable level of ochratoxin A contamination in wine that is  $2 \mu\text{g L}^{-1}$  (Commission Regulation – EC No. 123/2005). It was found that wine consumption can contribute up to 10–13% of total ochratoxin A intake (whereas the main intake of 40–50% is due to cereals) [Jorgensen, 2005].

A study conducted by Altieri *et al.* [2004] related alcohol and particularly wine consumption to cancer occurrence. The authors concluded that alcohol concentration per se, rather than specific contaminants, is a major risk factor for oral cancer, but also admitted that this conclusion remains speculative. The study indicated that in populations with frequent wine consumption, wine can strongly increase the risk of e.g. oral cancer.

In Britain the wine consumption has risen 60 % in the last decade and currently an average of 20 litres of wine is consumed per capita each year. In comparison, the average per capita consumption in France and Italy is close to 60 litres a year [IWSR, 2007]. The IWSR (International Wine and Spirit Record) also predicts that world wine consumption will grow by 4.8% between 2005 and 2010 to a total volume of 238,825 million hectolitres.

One could argue that many people do not drink alcohol or wine and thus are not affected. However, ochratoxin A is also present in grapes and grape juice, cereals and

coffee, to mention a few sources [Adams, 1995]. Ochratoxin A basically contaminates every food commodity where ochratoxin A producing fungi grow.

The thesis reports the development of an affinity sensor for ochratoxin A for determination in wine samples. Comprising the required elements of specificity, sensitivity, time and cost-effectiveness, the biosensor has to be carefully assembled. Two kinds of recognition element were investigated; one was an antibody specifically binding ochratoxin A and the other a peptide receptor for ochratoxin A that is designed using computational modelling. Peptides have various advantages in terms of molecular stability and availability, compared to antibodies, which are being more commonly used in immunosensors. Also, the production of antibodies for a specific molecule can be time and cost-consuming and generally requires animal resources.

The first stage of the biosensor development involved the parallel execution of computational design of peptide receptors for ochratoxin A and the consecutive characterisation of both the antibody and peptide recognition elements using binding assays.

The second stage comprised the construction of the transducer component of the biosensor for both types of recognition elements. The transducer relates the biological signal (as a result of a binding interaction) via a detector towards an electronic data output. Electrochemical detection was chosen using an electrode as transducer. Complexity of wine plays a significant role as the components of wine have to be considered for achieving interference-free and sensitive detection.

## **1.2 Mycotoxins**

Fungi are everywhere and come in many forms: as mushrooms, yeasts and filamentous moulds, to name a few. Moulds grow naturally in many agricultural crops. This occurs both in the field, after harvest and during storage, and later when processed into food and animal feed. Moulds are microscopic, filamentous fungi that grow as multi-cellular filaments called hyphae forming a mycelium [Adams, 1995]. These species of fungi

produce mycotoxins as secondary metabolites, whose specific function is yet undetermined, but who, together with hydrolytic enzymes, inhibit the growth of competing microorganisms. Mycotoxins are considered secondary metabolites as they not required for the growth of the producing fungus and therefore. The major difference of toxic metabolites associated with food poisoning from fungi versus the toxins produced by bacteria is that mycotoxins are generally small in molecular weight (300-400 Daltons), whereas bacterial toxins are often macromolecules such as polypeptides, proteins or lipopolysaccharides [Adams, 1995].

Mycotoxins are produced by several biosynthesis pathways in fungi:

- polyketide route (e.g. patulin; ochratoxin<sup>1</sup>),
- terpene route (e.g. trichothecenes),
- amino acid route (e.g. aflatoxins), and
- tricarboxylic route (e.g. rubratoxin).

In relation to their pathway, mycotoxins show significant diversity in their chemical structures and biological activity [Bhatnagar *et al.*, 2001]. The three genera *Aspergillus*, *Penicillium* and *Fusarium* comprise the largest number of mycotoxin-producing species, but not all species within these genera produce toxins. Production is often depended on temperature and water activity. Different genera grow under distinct conditions. For example, *Aspergillus* prefers high humidity and temperature found in tropical and subtropical climates [EMAN, 2004] whereas *Penicillium verrucosum* grows only at temperatures below 30°C and at a lower water activity, but can be also found at temperatures as low as 5°C [WHO, 1990]. Generally, fungal growth can occur over a wide range of these environmental factors [Bhatnagar *et al.*, 2001].

Mycotoxicoses (poisoning resulting from exposure to fungal toxins) occurs when fungal toxins are ingested by animals or humans, and affects various organs, most commonly liver, kidney and lungs and the nervous, endocrine and immune system. The effect of a

---

<sup>1</sup> Biosynthesis pathway for ochratoxin A has not yet been established, but there are indications it derives from the shikimate pathway (phenylalanine moiety) and the pentaketide pathway (dihydroisocoumarin) [Ringot *et al.*, 2006].



mycotoxin depends on the affected species and intra-species susceptibility, which is age, sex, nutritional status and the condition of the immune system [Bhatnagar *et al.*, 2001].

The liver and kidney have a high capacity to bind many mycotoxins while other mycotoxins are highly lipophilic and can accumulate in body fat. A toxic response will be critically influenced by the rate of adsorption (gastrointestinal tract, lungs, and skin), distribution through the blood stream, enzymatic degradation (hydroxylation of ochratoxin A by e.g. proteases results in ochratoxin  $\alpha$ ) or excretion [Smith, 1991].

Because of their diversity of chemical structures and differing physical properties, mycotoxins exhibit a wide array of biological effects on mammalian systems. Hence, they can be genotoxic, mutagenic, carcinogenic (e.g. Aflatoxin), potent renal carcinogenic, nephrotoxic (e.g. Ochratoxin), or embryogenic, teratogenic or oestrogenic (e.g. Zearalenone) [Smith, 1991]. Furthermore, some of the mycotoxins show immunosuppressive activity by inhibiting protein biosynthesis, which can occur in different ways such as: (1) inhibition of transcription (e.g. aflatoxin), (2) inhibition of the phenylalanine tRNA synthetase (e.g. ochratoxin) or (3) inhibition of the translation through binding to the eukaryote ribosome (e.g. T-2 toxin) [Adams, 1995]. Selected mycotoxins are described briefly in the following paragraph.

Aflatoxin is the best known and one of the most potent carcinogens and has been linked to a wide variety of human health problems. Primarily, *Aspergillus flavus*, *Aspergillus parasiticus*, and *Aspergillus nomius* produce aflatoxins. The Food and Drug Administration (FDA) has established maximum allowable levels of total aflatoxin in most food commodities at 20  $\mu\text{g kg}^{-1}$ . The maximum level for milk products is even lower at 0.5  $\mu\text{g L}^{-1}$ .

T-2 Toxin is a trichothecene produced by *Fusarium* species and can cause permanent damage to the digestive tract. In 2000 the European Commission (EC) proposed maximum levels for trichothecenes in food at 500  $\mu\text{g kg}^{-1}$  on an advisory base.

Vomitoxin, chemically known as Deoxynivalenol, is produced by several species of *Fusarium*. Vomitoxin has been associated with outbreaks of acute gastrointestinal illness in humans. The FDA advisory level for vomitoxin for human consumption is 1 mg kg<sup>-1</sup>.

Zearalenone is also a mycotoxin produced by *Fusarium* species. Zearalenone toxin is similar in chemical structure to the female sex hormone estrogen and targets the reproductive organs. Maximum levels for zearalenone in e.g. cereals have not yet been set by the EC, although maximum tolerable levels in food (mainly cereals) is about 1 mg kg<sup>-1</sup> are advised by the FDA.

### **1.2.1 Legislation**

Mycotoxin contamination in food, feeds and beverages has received much attention in the past decade based on their unfavourable impact on human health and economic effects. The food and feed industry encountered considerable losses in life stock animals such as poultry and swine due to contamination of animal feeds with mycotoxins such as aflatoxin, fumonisin and zearalenone. This resulted in the reduction of agricultural food export, which has resulted in considerable economic losses for the producing countries.

The EU has set limits for 40 mycotoxin–food combinations; according to the European Commission Regulation (EC) No 123/2005 of 26 January 2005 (amending Regulation (EC) No. 466/2001). The regulations involved are increasingly based on scientific opinions of regulatory authorities such as the Joint Expert Committee on Food Additives of the United Nations (JECFA) and the European Food Safety Authority (EFSA). This has a significant impact on mycotoxin regulations; regarding the rapid alert system for food and feed and the creation of an EU Community reference laboratory for mycotoxin analysis. Large European research and networking projects such as ‘BioCop’, ‘MoniQA’ or ‘GoodFood’ (funded by the EC’s 6<sup>th</sup> Framework Program) do also have an impact [Van Egmond *et al.*, 2007] on regulations.

To ensure that these regulations are followed, monitoring schemes have been introduced. It needs to be ensured that the results from food and feed monitoring fulfil the requirements of the legislation. Therefore, any analytical method that is used for monitoring must meet established and accepted performance criteria. This is important in terms of legal actions and trade specifications (e.g. rejection of imports due to contamination), as well as monitoring and risk assessment studies. Both rapid and reliable screening and confirmatory methods must be available to fulfil regulations in daily practice. Official methods in mycotoxin legislation comprise approximately 45 analytical methods for determination of mycotoxins in a few dozen countries [FAO, 2004; AOAC, 2005].

At a world wide level, international inquiries were held regularly in recent decades [1981, 1987, 1995, and 2003] and regulations published for mycotoxins in food and feed [Schuller *et al.*, 1983; Van Egmond, 1989; FAO, 1997 & 2004]. The most recent enquiry in 2003 was conducted by the National Institute for Public Health and the Environment, under contract to the Food and Agricultural Organization (FAO). At least 99 countries had mycotoxin regulations for food and/or feed in 2003, an increase of approximately 30% compared to 1995 [van Egmond *et al.*, 2007].

### **1.3 Ochratoxin A**

Ochratoxin (Figure 1.1) was discovered by van der Merwe *et al* in 1965. In cool and temperate regions, ochratoxin A is mainly produced by *Penicillium verrucosum*, which is a known contaminant of cereals like barley, wheat and rye. Ochratoxin can be also produced by *Aspergillus ochraceus* that contaminates mostly food from (sub)-tropical origin like maize, coffee beans, cocoa, soy beans, spices and dried fruits [Adams, 1995]. Ochratoxin is found in wine and grape-derived juices as well as in other beverages such as beer (malt barley) [Walker, 1999]. The wide variety of contamination is a result of fungal infection under favourable environmental conditions in the field during growth, at harvest, in storage or in shipment.

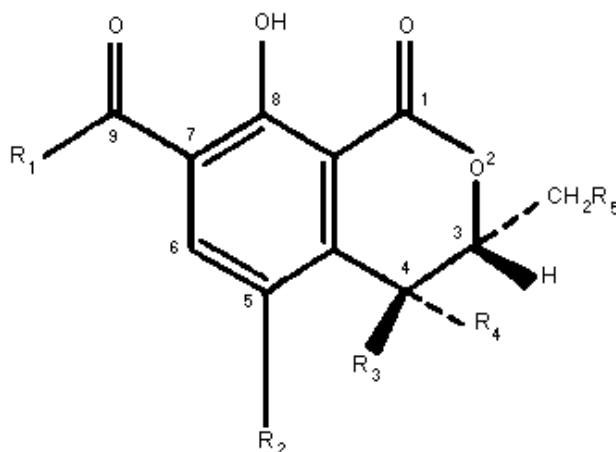


**Figure 1.1:** The ochratoxin structure.

The ochratoxin family consist of ochratoxin - A; - B; - C; - A-methyl ester; - B-methyl ester; - B-ethyl ester; -  $\alpha$ ; -  $\beta$ ; and - 4-Hydroxyochratoxin A [Chu, 1998] as listed in Table 1.1. Ochratoxin A and ochratoxin esters are the toxic members of the group [Betina, 1985].

**Table 1.1:** The molecular family of ochratoxins.

R1	R2	R3	R4	R5	Trivial name
Phenylalanyl	Cl	H	H	H	Ochratoxin A
Phenylalanyl	H	H	H	H	Ochratoxin B
Phenylalanyl ethyl ester	Cl	H	H	H	Ochratoxin C (ethyl ester)
Phenylalanyl methyl ester	Cl	H	H	H	Ochratoxin A methyl ester
Phenylalanyl methyl ester	H	H	H	H	Ochratoxin B methyl ester
Phenylalanyl ethyl ester	H	H	H	H	Ochratoxin B ethyl
OH	Cl	H	H	H	Ochratoxin $\alpha$
OH	H	H	H	H	Ochratoxin $\beta$
Phenylalanyl	Cl	H	OH	H	4R-Hydroxyochratoxin A
Phenylalanyl	Cl	OH	H	H	4S-Hydroxyochratoxin A
Phenylalanyl	Cl	H	H	OH	10-Hydroxyochratoxin A

The ochratoxin A structure is composed of a 3,4- dihydro-3-methyl-isocoumarin moiety linked via the 7-carboxy group to L- $\beta$ -phenylalanine by an amide bond. Its molecular weight is 403.8 Dalton. The molecular formula is  $C_{20}H_{18}ClNO_6$ .

Contributing to the understanding of the pathway of ochratoxin biosynthesis, Mantle and Harris [2001] suggested fermentation dynamics of the ochratoxin producing fungi *Aspergillus ochraceus* and found that ochratoxin A and B production is growth-

associated and that ochratoxin  $\alpha$  seems to be a precursor of ochratoxin A. Structure activity studies indicate that the toxicity of ochratoxin A is attributable to its isocoumarin moiety and that the lactone carbonyl group (in the lactone-opened form OP-ochratoxin A) may be involved [Xiao *et al.*, 1996]. Neither the dissociation of the phenolic hydroxyl group nor the iron-chelating properties of ochratoxin A were directly related to its toxicity [Xiao *et al.*, 1996]. The molecule is highly hydrophobic and anionic with metal-chelating properties. It shows non-specific protein interactions due to these and other properties. Therefore, acidic form of ochratoxin A is soluble in organic solvents (IARC, 1993), whereas the sodium salt is soluble in water. Ochratoxin A is generally a very stable compound that can only be completely hydrolyzed to ochratoxin  $\alpha$  by heating under reflux for 48 hours in 6 M hydrochloric acid [Van der Merwe *et al.*, 1965].

### **1.3.1 Toxicity**

Upon ingestion, ochratoxin A is absorbed from the stomach as a result of its acidic properties and the gastrointestinal tract. Accumulation occurs in blood and kidney and at lower concentrations in the liver, muscle and fat. Metabolism of ochratoxin A has not been elucidated in details and at present, data regarding biotransformation in kidney and liver are controversial as a significant proportion of ochratoxin A is excreted unchanged [Galtier, 1978; Ringot, 2006]. Elimination of ochratoxin A in humans is extremely slow, since the toxin is exhibiting unusual toxico-kinetics, with a half-life in blood of 840 hours (=35 days) after oral ingestion [Schlatter *et al.*, 1996]. This is partly explained, by the fact that 99 % ochratoxin A is bound to serum proteins, which facilitates its passive absorption [Chu, 1971 & 1974].

Effects of acute poisoning have been reported following single dose administration. Examples are haemorrhages in various organs and fibrin thrombi in the spleen, brain, liver, kidney and heart. Nephrosis, hepatic and lymphoid necrosis, and enteritis with villous atrophy have also been observed in the test species [Albassam *et al.*, 1987; JECFA, 2001]. Ochratoxin A toxicity tests in rat have shown LD<sub>50</sub> value (50% Lethal

Dose) of  $20 \mu\text{g kg}^{-1}$  [Pittet, 1998]. As of May 2006, there are no documented cases of acute toxicity reported in humans.

In humans, the subchronic and chronic effects of ochratoxin A are of greatest concern [FEHD, 2005]. Ochratoxin A has been shown to be mutagenic, nephrotoxic, genotoxic, teratogenic and immunotoxic to several species of animals. Ochratoxin A-mediated mutagenicity requires additional processing of cytochrome P<sub>450</sub>-derived metabolism [De Groene *et al.*, 1996]. The genotoxic effect remains rather unclear as most short-term assays for gene-mutations were negative and assays for unscheduled DNA synthesis (UDS), sister chromatid exchange (SCE) and chromosomal aberrations in CHO cells (cell line derived from chinese hamster ovary cells) were similarly negative or equivocal. However, ochratoxin A has been reported to cause DNA single strand breaks in mouse spleen cells *in vitro* and in kidney, liver and spleen cells *in vivo* [Walker, 1999]. Ochratoxin A is an immunosuppressive agent [Muller *et al.*, 1995 and 1999] and leads to inhibition of immune responses transmitted by B- and T-lymphocytes [Petzinger, 2002]. In relation to the humoral immunity, ochratoxin A induces a regression of IgG-, IgA-, and IgM- immunoglobulines [Muller *et al.*, 1995]. It is also a potent competitive inhibitor for the phenylalanine hydrolase, phenylalanine tRNA synthetase, and other enzymes that use phenylalanine as substrate. The inhibitory effect is based on its structural homology, since its chemical structure is composed of a phenylalanine group. The daily administration of a medium dose ( $50 \mu\text{g kg}^{-1}$  ochratoxin A) produces an inhibitory effect that could be diminished by competitive action of phenylalanine [Zanic-Grubisic *et al.*, 2000].

The main target site of ochratoxin A toxicity in human is the renal proximal tubule, where it exerts cytotoxic and carcinogenic effects. Dietary exposure to ochratoxin A in parts of Bulgaria, Romania and the former Yugoslavia may have association with 'Balkan Endemic Nephropathy', which is a chronic kidney disease that is characterised by progressive hypercreatinemia, uraemia, hypertension and oedema [JECFA, 2002].

Human exposure, as demonstrated by the occurrence of ochratoxin A in blood and human milk, has been observed in various countries in Europe. In central European countries, ochratoxin A is probably the most ubiquitous mycotoxin, which can be

detected at levels greater than  $0.1 \mu\text{g kg}^{-1}$  in more than 90% of human blood samples [Petzinger, 2002]. Ochratoxin A was found more frequently and at high concentrations in blood samples obtained from people living in regions where the disease ‘Balkan Endemic Nephropathy’ occurs [JECFA, 2002]. However, the Joint FAO/WHO Expert Committee on Food Additives (JECFA) concluded in 2001 that the epidemiological and clinical data available do not provide a basis for carcinogenic potency in human and that ‘Balkan Endemic Nephropathy’ may involve other nephrotoxic agents [Creppy *et al.*, 1984].

In 1993, the International Agency for Research on Cancer (IARC) classified ochratoxin A as possible human carcinogen (Group 2B) and concluded that there was sufficient evidence in animal experiments (causing tumours of the kidney and liver of mice and rats) for carcinogenicity of ochratoxin A but inadequate evidence in humans [IARC, 1993].

### **1.3.2 Regulations of daily intake and permissible limits in food**

During the past few years, levels of contamination in foods sampled in Europe ranged in wine from  $0.01\text{-}7.0 \mu\text{g L}^{-1}$  and in rye  $0.05\text{-}121 \mu\text{g kg}^{-1}$ . In 2006, the EFSA Panel on Contaminants in the Food Chain (CONTAM) of the European Food Safety Authority (EFSA) has published a tolerable daily intake of  $17 \text{ ng kg}^{-1}$  per body weight for ochratoxin A. Further reduction of the limits set may be required in the future, particularly in commodities such as dried wine fruit, wine and grape juice [EFSA, 2006]. Regarding the legal limits of ochratoxin A in food commodities such as cereals and cereal products, dried vine fruits, roasted and soluble coffee, wine, grape juice, and foods for infants and children, permissible limits have been set by the European Commission under EC regulation 466/2001 [2001] , 472/2002 [2002], and 123/2005 [2005]. The latter introduced the current permissible limit of ochratoxin A in wine and grape containing beverages of  $2 \mu\text{g L}^{-1}$ .

### **1.4 Sample extraction and clean-up**

Mycotoxin determination is a complex process. The mycotoxin concentration of a bulk lot is usually estimated by taking a sample of the whole and measuring the mycotoxin

concentration, inferring the bulk to contain as much as the sample [Whitaker, 2004]. The determination procedure involves sampling of possibly mycotoxin contaminated food or feed, preparing the sample (i.e. grinding and homogenisation, extraction, filtration, and dilution) for clean-up. Clean-up removes interfering substances such as lipids, carbohydrates and proteins. Figure 1.2 shows a typical procedure for processing mycotoxins in solid samples according to the European Mycotoxin Awareness Network (EMAN) compared to liquid sample treatment as described by Visconti *et al.* [1999].

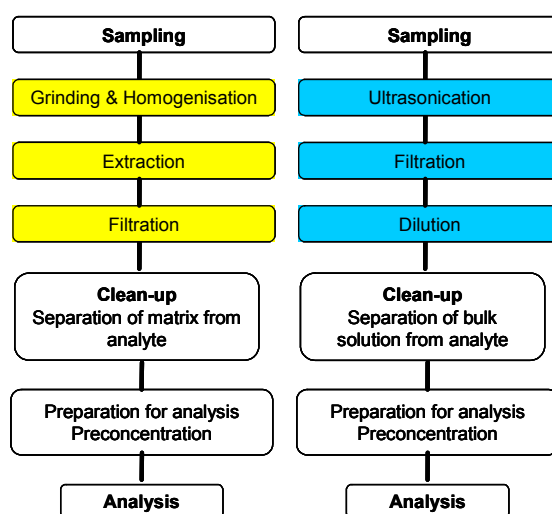


**Figure 1.2:** Procedure for determination of mycotoxins in solid samples (left) and liquid samples (right) Visconti *et al.* [1999].

Solid samples are grinded to get a uniform composition out of a coarse sample, then extracting the analyte of interest and filtering to remove unwanted particles. Liquid samples, such as fizzy drinks (e.g. beer or some wines), are ultrasonicated to remove bubbles, followed by filtration to remove interfering particles, which is also aided by dilution. Dilution is also used to set the pH and ionic strength of the sample solution. The following subchapters describe the main steps of the mycotoxin determination from sampling to analysis and will give a more detailed overview on liquid sample treatment.

### 1.4.1 Sampling

The sampling procedure specifies how the sample will be selected and how much will be taken from the bulk lot [Whitaker, 2004]. Sampling error can be the greatest source of variance in the analytical procedure due to uneven distribution of the contaminated



samples or physical characteristics of the sample (e.g. uneven particle size). It also occurs that the mycotoxin contamination is not related to the amount of mould present and it can come to further mould or mycotoxin development during lengthy transit to the laboratory and in storage [Ratcliff, 2002]. One method of sampling is to use a probe sampler on recently blended lots of grain, since mould growth usually occurs in spots in a bulk lot.

Another method is to collect small samples from a continuous stream of material [Woloshuk, 2001]. However, due to the variability associated with each step of such sampling procedures, the real mycotoxin concentration of a bulk lot cannot be determined with 100% certainty. Difficulties arise due to variation in coarse material particle size. The sample size to be taken should be related to size of the specific particles and level of homogeneity. Increasing sample size will result in more reliable analytical results, thus larger samples should be taken according to particle size, i.e. peanuts > corn > wheat > rice > milled products. Fluids and well-mixed process products such as wine, beer or milk and milk products do not normally present such sampling problems [Smith, 2001] due to their homogeneous nature. A review published by Coker *et al.* [1995] describes the complex design of efficient sampling procedures for mycotoxins.

#### **1.4.2 Extraction from wine and clean-up**

Clean-up procedures are performed to extract mycotoxins from contaminated material and remove possible interferences. The Association of Official Agricultural Chemists (AOAC) publishes official methods of extraction for mycotoxins in food and feeds [Scott, 1997]. However, a number of the official methods of analysis were adopted AOAC some 20–35 years ago and might be outdated as no performance parameters are given or only recoveries for the methods (by spiking) and coefficients of variation (CVs) are reported, which do not relate information on precision, systematic error, interference, or in-depth statistical analyses.

Such one method is based on liquid-liquid partitioning, which involves the separation of analyte between immiscible solvents until equilibrium. Since liquid-liquid partitioning

is a batch method and can not be automated, the method is now often replaced by less labour intensive and economical techniques such as Solid Phase Extraction (SPE). Furthermore, Ion Exchange Chromatography (IEC) can be applied if the mycotoxin is present in its ionic state [EMAN, 2004]. A frequently used method is immunoaffinity chromatography (IAC) (Figure 1.3), which is based on the binding interaction of mycotoxin-specific antibodies and thus depends on their availability [Dietrich *et al.*, 1995]. IAC has several advantages over other clean-up methods as it is more analyte-specific, uses less solvent, can be automated and columns reused [Scott, 1997]. Immunoaffinity columns can be both used for mycotoxin clean-up and detection when incorporated into a HPLC system. The clean-up procedure for ochratoxin A involves generally IAC, SPE or IEC [EMAN, 2004]. Immunoaffinity clean-up has been set as European Standard (prEN 14133) for ochratoxin A analysis in wine and beer according to the work published by Visconti *et al.* [1999].

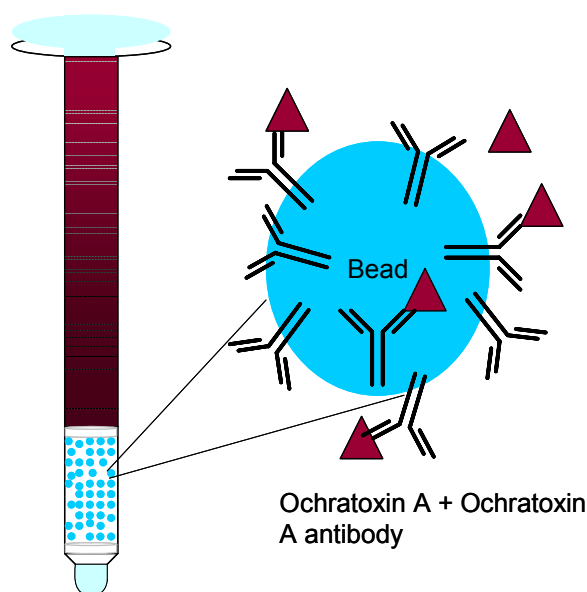


**Figure 1.3:** Immunoaffinity column design containing solid extraction phase made from antibody-modified support beads binding ochratoxin A.

With ochratoxin A clean-up in beverages such as wine or beer, the possible interferences of ethanol and sugars are of great importance since they are making up a large part of the sample. Ratola *et al.* [2004] observed that most studies on ochratoxin A contamination in beverages do not comprise records about the possible interference of ethanol or sugar content in the clean up process and established experimentally that

there seems to be no interference of such parameters in the process of ochratoxin A clean-up when using immunoaffinity chromatography.

## **1.5 Antibodies as Immunochemical Reagents**

Antibodies as immunological entities were not recognized in connection with chemistry until 1907, when Arrhenius published a series of his lectures entitled “Immunochemistry: The Application of the Principles of Physical Chemistry to the Study of Biological Antibodies”. The importance of this publication was in the mathematical approach with which (as established in physical chemistry) Arrhenius explained various *in vivo* and *in vitro* occurrences in relation to antibody-antigen complex formation. Hence, Arrhenius was the founder of the term ‘immunochemistry’ [Arrhenius, 1907].

### **1.5.1 Antibody structure and function**

Antibodies or immunoglobulines (Ig) are glycoproteins that are found in serum and tissue fluids. An antibody consists of two identical heavy polypeptide chains (50-65 kDa) and two identical light chains (25 kDa), which are connected via disulfide bridges and non-covalent interactions. There are five distinct antibody classes: IgG, IgM, IgA, IgE and IgD. The heavy chain of the antibody is built by four (IgG, IgA and IgD) or five (IgM and IgE) domains which are termed the variable domains ( $V_H$ ) and constant domains ( $C_{H1}$ ,  $C_{H2}$  and  $C_{H3}$ ). The light chain consists of two domains,  $V_L$  and  $C_L$ . Antibodies can be subdivided into two  $F_{ab}$ -fragments and one  $F_c$ -fragment. The  $F_{ab}$ -fragment (antigen binding site) consists of a light chain and two N-terminal domains of the heavy chain, connected via disulfide bridges. The  $F_c$ -fragment (crystallisable fraction) consists of the remaining C-terminal domains of the heavy chain. To obtain the fragments, it is possible to enzymatically digest the antibody molecule using the enzyme papain. Each antibody class can be further subdivided into five chain-classes regarding five different constant regions [Janeway & Travers, 2004]. In contrast to polyclonal antibodies, monoclonals are produced by one B lymphocyte clone only. To produce monoclonal antibodies, spleen cells producing specific antibodies and immortal myeloma cells are fused. The spleen cells are obtained by immunization of an animal

species (e.g. mouse), which in turn generates specific antibody-producing cells. Since those cells are mortal, they are fused with immortal myeloma cells using PEG (polyethylene glycol). The fusion produces a hybrid cell line that is named hybridoma. Those hybridoma cells, which are producing the desired antibody, are cloned from one single cell. This cell line is producing the same, monoclonal antibody molecule [Ducey, 1997].

### **1.5.2 The principle of antibody recognition**

Antibody recognition was further unravelled by Carl Landsteiner, who, in 1930, investigated many of the fundamental principles of this field using a molecular approach (immunoprecipitation). Landsteiner observed that small molecules (later termed haptens), in contrast to larger protein molecules, were not immunogenic; that is being capable of inducing an immune response by themselves. He also found that small molecules could be attached to a carrier protein to facilitate an immune response, called hapten-carrier conjugates. Antibody recognition is mediated by a versatile binding site (known as paratope) composed variable domains of the heavy ( $V_H$ ) and light chains ( $V_L$ ). Those domains contain highly variable loops called complementary determining region (CDR), which are capable of virtually recognizing any specific molecular structure [Day, 1990; Nezlin, 1994]. The paratopes of immunoglobulins recognize in the complementary antigen a 3-dimensional array of closely placed atoms, together known as the epitope [Van Regenmortel, 1998]. This explains antibodies are being capable of discriminating minor differences in molecular structures and exhibit region-selective properties with molecular isomers i.e. the ability of one antibody to bind one and not another member of a family of chemically related substances. In the immune system, specific signals lead to the elimination of pathogens, whereas noise occurs as a result of a non-specific input, where the immune system eliminates the host (autoimmunity). Effectively, the immune system has to differentiate between self and non-self; this is the basis of specific selection [Langman, 2000].

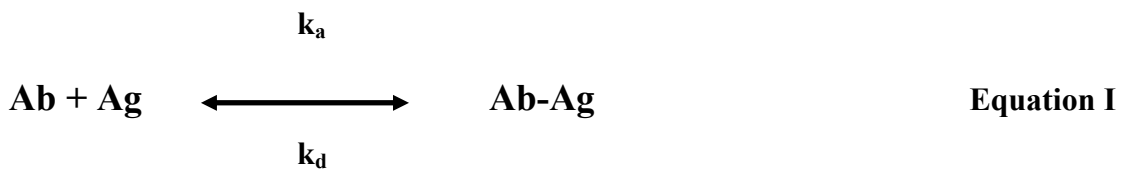
As pointed out by Berzofsky and Schechter [1981], the concept of specificity of antibodies is complementary to the concept of cross-reactivity. One type of cross-reactivity arises when a particular antibody recognizes the same epitope in two different

proteins. Another type when the antibody recognizes an epitope on a heterologous antigen (e.g. isomer) that is different but structurally related to the epitope of the antigen (antigen used to raise the antibody). Generally, the antibody's paratope will bind with higher affinity to the homologous epitope [Underwood, 1985].

### 1.5.3 The difference between affinity and avidity

Affinity describes the binding strength of a monovalent binding interaction of an antibody with an antigen (e.g. binding of a  $F_{ab}$ -fragment to one epitope on an antigen) [Karush, 1978] while avidity describes the total binding strength of a polyvalent binding interaction depending on the number of paratopes and epitopes [Goldblatt, 1997].

The binding interaction is described as equilibrium between association and dissociation of the antibody-antigen complex and is illustrated as follows:



$k_a$  = association rate constant

$k_d$  = dissociation rate constant

The equilibrium is described by the affinity constant  $K_A$ :

$$K_A = k_a / k_d \quad \text{Equation II}$$

The time taken to reach equilibrium is dependent on the rate of diffusion and the affinity of the antibody for the antigen, and can vary widely. The affinity constant for antibody-antigen binding can span a wide range, extending from below  $10^5 \text{ M}^{-1}$  to above  $10^{12} \text{ M}^{-1}$  and can be affected by temperature, pH and solvent. Affinity constants can be determined for monoclonal antibodies, but not for polyclonal antibodies, as multiple binding interactions take place between polyclonal antibodies and their antigens.

Increased specificity does not necessarily correlate with greater affinity of antibodies in terms of better stereochemical complementarity with their antigens. Antibodies with lower affinity may discriminate better between two heterologous antigens (isomers) [Underwood, 1985; van Regenmortel, 1998].

## **1.6 Immunoassays**

Immunoassays (IA) use antibodies for determination of sample components [Hage, 1999] mostly on solid state polystyrene microtitre plates (MTP). The method is based on the selective nature of an antibody which is binding specifically to its antigen. Some examples are the radioimmunoassay (RIA) that use radio-labelled analytes, fluorescence-immunoassay (FIA) using fluorescent labels such as o-phthalaldehyde [Jones, 1983], chemiluminescence immunoassay (CIA) with chemiluminescent labels such as luminol [Zhuang, 2000] and enzyme-immunoassay (EIA) with enzyme labels like horseradish peroxidase (HRP) [Al-Kaissi, 1983] or alkaline phosphatase. A common immunoassay technique is the enzyme-linked immunosorbent assay (ELISA) [Janeway & Travers, 1999]. Immunoassays are rapid, simple and portable. Both threshold (visually) and quantitative (spectrophotometric) determination is available. Immunoassays can be extremely specific and sensitive, often in the ng to  $\mu\text{g L}^{-1}$  range [Trucksess, 1997].

### **1.6.1 How to develop an immunoassay**

The goals in developing an immunoassay include (1) achieving the best signal/noise ratio for the sensitivity level desired; (2) to have a robust reproducible assay for the sample being tested; and (3) to be able to measure the antigen over a biological relevant assay range (dynamic range). Therefore, ideal concentrations of each assay reagent must be established empirically.

The signal generated by a sample containing analyte, relative to the signal of the same sample without analyte, is the signal/noise ratio. As the signal/noise ratio increases, the assay becomes better at measuring small amount of antigen. To establish the optimal

dilutions of reagent concentrations, a checkerboard titration is performed, which is a single experiment in which the concentration of two components is varied.

### **1.6.1.1 Immobilisation (coating)**

The amount of antibody or antigen bound to the microtitre well is critical to the assay sensitivity and has to be carefully controlled. Molecular orientation of the bound substance is random and may reduce the number of potential binding sites for the analyte through sterical hindrance [ThermoCorp, 2004].

When considering the binding capacity of adsorbent plastic surfaces for biomolecules, one must distinguish between the total amount of molecules that can be bound to the surface and the amount that can be bound and still remain biologically active. Both quantities are very much dependent on the properties of the biomolecules (concentration, size, and hydrophobicity), the character of the surface, coating time, temperature, pH, ionic strength of buffer). Coating stability is determining the sensitivity and precision of the assay and can be affected by the microtitre plate surface, size and hydrophobicity of the compound to be coated or long-term storage conditions [ThermoCorp, 2004]. Microtitre plates commonly used are MaxiSorb™ or PolySorb™ from Nuncbrand®. While PolySorb™ predominantly presents hydrophobic groups; MaxiSorb™ has in addition many hydrophilic groups, which results in a fine patchwork of hydrophobic and hydrophilic binding sites. On a MaxiSorb™ surface, adsorption of hydrophilic macromolecules will be greatly facilitated binding the macromolecules by hydrogen bonds [Esser, 1988].

There are several other points to consider when coating on a microtitre plate. It is important to ensure that the coating buffer is free of detergent, since they often compete for binding and cause low and uneven binding. Smaller molecules such as peptides require chemically-activated microtitre plates such as amine-functionalised plates to achieve covalent attachment to the plate surface [Piercenet, 2007]. Static supports and coupling methods for immunoassays are factors to be considered in immunoassay design.

Table 1.2 lists three selected methods for immobilisation [Hermanson *et al.*, 1992; Eggins, 2002].

**Table 1.2:** Immobilisation techniques for biomolecules.

<b>Immobilisation</b>	<b>Method description</b>	<b>Positive and Negative Features</b>
Physical adsorption	Weak electrostatic or van der Waals interaction or Hydrogen bonds (–OH, =O, –NH <sub>2</sub> , =NH, ≡N)	+ High coupling yields - Desorption, random orientation
Cross-linking	Chemically bondage using bifunctional reagents (e.g. Glutaraldehyde)	+ Stabilization of adsorbed material - Biomaterial might be inactive
Covalent bonding	Establishment of a chemical bond between a functional in the biomaterial and the support.	+ Stable bond + High coupling yield - Random orientation

For antibodies, proteins, and peptides different immobilisation techniques are recommended for different supports. Proteins can be immobilized using all mentioned techniques, depending on the particular application. Biomolecules may undergo conformational changes (e.g. denaturation) during passive adsorption on synthetic surfaces and thereby lose their biological activity [Butler *et al.*, 1992].

Enzymes in particular are to be immobilized covalently and the active site should be protected during the procedure to keep enzyme-activity. Peptides are recommended to be covalently immobilized via reactive amines-, thiol- or carboxyl-groups. Site-directed immobilisation techniques are considered to enhance the orientation of peptides [Hermanson, 1992] and antibodies [Kooyman & Lechuga, 1996]. With capture antibodies there is the risk of steric hindrance due to saturated surface adsorption [Esser, 1988]. Surface adsorption of molecules is non-specific; therefore it is a well known possibility that any substance can adsorb to the microtitre plate surface at any stage of the assay. It is important to block unoccupied sites on the plate surface to reduce the amount of non-specific binding of protein during subsequent steps of the assay.



### 1.6.1.2 Blocking reagents and detergents

A blocking interval step should improve the sensitivity of the assay by reducing background interference. The proper choice of blocking reagent depends on the antigen itself and on the type of enzyme conjugate to be used. Examples of blocking reagent include bovine serum albumin (BSA), non-fat milk powder, gelatine, casein or in recent years, polymers have been used as a new class of blocking agents in immunoassays. In this context, polymers such as polyvinyl alcohol (PVA) [Rodda & Yamaraki, 1994] have significant blocking abilities and do not interfere with specific binding. In addition, PVA has been shown to stabilize the immuno-reactive activities of proteins [Boyd, 1995; Raghuvanshi *et al.*, 1998]. Rodda and Yamazaki [1994] also demonstrated a significant improvement in the specificity of the secondary antibody reaction using PVA with enzyme-labelled rabbit IgG compared with the specificity obtained using traditional blocking agents. It has been shown that blocking agents can be added to the buffer solutions of all assay steps to enhance the effect.

A detergent is usually used in ELISA for washing off loosely or non-specifically bound reactants eliminating steric hindrance caused by reactant accumulation on the surface. It may also be used for blocking excess surface (e.g. polystyrene) after coating with one reactant to avoid unspecific immobilisation of subsequent reactants. Detergents are molecules consisting of a distinct hydrophobic and hydrophilic part (e.g. Tween, Triton). They disperse hydrophobic molecules in aqueous medium and the blocking effect is based on the ability to compete with other molecules for both hydrophobic and hydrophilic binding sites. If no other blocking agent is used, detergent must be present during incubation in all reaction steps to avoid unspecific adsorption [Esser, 1989].

### 1.6.1.3 Enzyme labels in immunoassays

Enzyme labels are used when the detecting molecule does not comprise any physicochemical properties that can be directly measured. In immunoassays, the primary antibody can be directly conjugated to an enzyme label, which is used for detection. An alternative to the direct method is the use of a peroxidase-labelled secondary antibody that recognises the primary antibody in its F<sub>c</sub> fragment according to

the species it was raised in (e.g. anti-rabbit antibody). The choice of method depends upon the availability of the primary antibody, its enzyme conjugate and the sensitivity level required. Enzyme labelled biomolecules can be used in a variety of detection methods such as colorimetry, fluorescence or chemiluminescence, depending on substrate and detection setup. In many applications, colorimetric substrates provide a sufficient level of sensitivity and dynamic range [Piercenet, 2007].

Colorimetric detection is highly depended on the enzyme label and the substrate used. Differences in stabilities of both enzyme and substrate as well as the turn-over rate of the enzyme are having an impact on the sensitivity of the assay. Peroxidases, such as the horseradish peroxidase (HRP), catalyse the reaction of hydrogenperoxide with a number of chromogenic substrates (e.g. ABTS (2,2'-azino-bis(3-ethylbenzthiazoline-6-sulphonic acid); OPD (o-phenylenediamine); and TMB (3,3',5,5'-tetramethylbenzidine)).



The reaction is resulting in a coloured or fluorescent product or with the release of light as a by-product (chemiluminescent). Peroxidases are found in multiple isoenzyme forms and show high sensitivity and for their substrates. The availability of a variety of substrates (colorimetric, fluorescent or chemiluminescent) and its high turnover rate makes horseradish peroxidase ( $M_w$  40 kDa) the enzyme of choice for many applications. HRP-antibody conjugates are superior to e.g. alkaline phosphatase and  $\beta$ -galactosidase-conjugates due to their higher specific enzyme activity (more HRP molecules/mole of antibody) and immunological reactivity (less steric hindrance because of the size of HRP) as well as molecular stability [Piercenet, 2007].

Alkaline phosphatase catalyses the conversion of phosphate esters and is widely distributed in a large number of species and tissues.



When used as a label, calf intestinal alkaline phosphatase (MW 140,000) offers several distinct advantages over other enzymes. Because reaction rates remain linear, sensitivity

can be improved by allowing the reaction to proceed for longer periods of time [Piercenet, 2004].

### 1.6.2 Competitive enzyme linked immunoassays

Non-competitive immunoassays involve the use of two antibodies for two different epitopes on the antigen such as the sandwich ELISA. However, small haptens do not usually comprise two distinct epitopes and thus competitive assays are generally used for small hapten determination. Direct competitive immunoassays (Figure 1.4) involve the immobilisation of specific antibody to a microtitre plate. Unlabelled sample antigen (e.g. ochratoxin A) and enzyme-labelled antigen (e.g. ochratoxin A-HRP) is competing for the antibody binding sites.

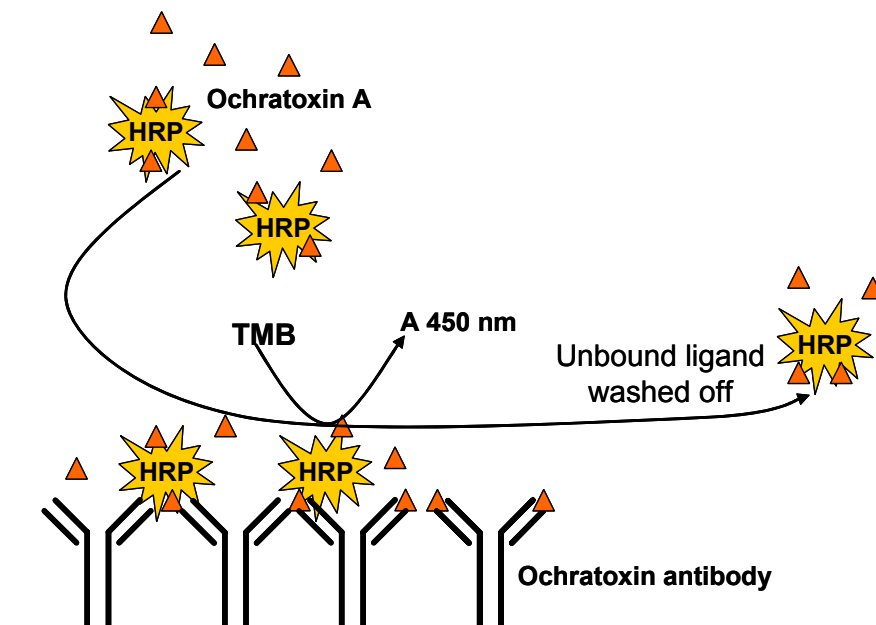


**Figure 1.4:** Direct competitive enzyme immunoassay format.

The amount of antibody-bound labelled antigen (e.g. ochratoxin A-HRP) is quantified colorimetrically, where the colour intensity is inversely proportional to the amount of free antigen (e.g. ochratoxin A) in the sample.

Alternatively, the indirect competitive immunoassay (Figure 1.5) involves immobilisation of e.g. ochratoxin A-BSA to the microtitre plate. Free antigen (e.g. ochratoxin A) sample is added to the microtitre well premixed with a known amount of

specific antibody. Immobilized ochratoxin A-BSA and the ochratoxin A-sample compete for antibody binding sites.

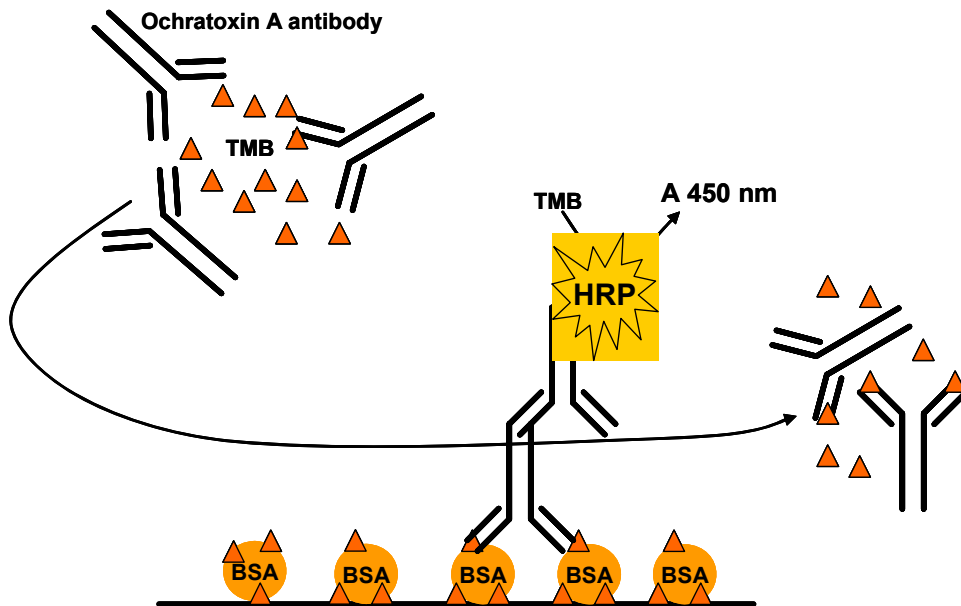


**Figure 1.5:** Indirect competitive enzyme immunoassay format.

The ochratoxin A-BSA-bound antibody is quantified indirectly by addition of an enzyme-labelled secondary antibody and determined colorimetrically. The colour intensity is inversely proportional to the amount of free antigen (e.g. ochratoxin A) in the sample [Wiley Encyclopaedia, 1999].

## **1.7 Chromatography based techniques**

Analysis of mycotoxins in food often requires trace analytical techniques because mycotoxins are typically present in agricultural commodities at levels ranging from ng kg<sup>-1</sup> to µg kg<sup>-1</sup>. Mycotoxins vary greatly in their structural, and thus also their physical properties. Consequently, it is impossible to develop methods that are applicable to all mycotoxins [Wiley Encyclopaedia, 1999]. Thus, the choice of analytical method used to separate, detect, and quantify mycotoxins depends on its physicochemical properties. Early studies used biological methods, such as microbial, animal, and plant toxicity assays, to detect the presence of mycotoxins. Antimicrobial properties of mycotoxins have been applied for the detection of aflatoxin-B<sub>1</sub>, patulin, and ochratoxin A. In animal toxicity, mice and rats have been successfully used to detect aflatoxins and chickens have been used for the detection of ochratoxin A. However, with the development of sophisticated instrumentation, chemical techniques became the methods of choice.

### **1.7.1 High Performance Liquid Chromatography**

High performance liquid chromatography (HPLC) offers improved resolution, increased sensitivity, improved accuracy and precision. The ability to automate also makes it useful for large-scale analysis. Reverse-phase (RP) liquid chromatography is being increasingly used for many mycotoxins [Bhatnagar *et al.*, 2001]. Columns used for mycotoxin separation are e.g. RP-C<sub>18</sub> used for detection of *Fusarium* mycotoxins such as deoxynivalenol (DON), or nivalenol (NIV), which can also be detected simultaneously. Fumonisin, aflatoxins and ochratoxins are also separated by RP-C<sub>18</sub> columns differing in the mobile phase composition. HPLC allows ultra-trace analysis at the ng or even the pg level. It allows for analysis of thermally labile, poorly volatile, polar, and ionic compounds.

Common HPLC detectors used in mycotoxin analysis are the diode array detector (DAD), the fluorescence detector (FD) or secondary detection via mass-spectrometry (MS) [Wiley Encyclopaedia, 1999]. However, disadvantages of HPLC are that samples are required to be highly processed regarding clean-up to achieve sensitive detection limits. HPLC also lacks a sensitive universal detector for all mycotoxins. Only one

sample can be analyzed at any given time, the running costs are high, trained personal is normally required to operate the equipment and interpret the results; and also measurements and washing intervals are time-consuming [Smith, 2001]. Most mycotoxins can be detected visually as they contain a chromophore and thus high molar absorbtivity and/or fluorescent properties such as for ochratoxin, aflatoxins, or zearalenone (Table 1.3) or by colour development after spraying with a chromatographic reagent such as Ninhydrin [Coker, 1997].

**Table 1.3:** Summary of fluorescing mycotoxins using a RP-C18 column (MycotoxTM) in a mobile phase of acetonitrile/methanol/phosphate buffer (pH 3.3) [Pickering *et al.*, 2004].

Mycotoxin	Extinction (nm)	Emission (nm)
Ochratoxin A	335nm	455nm
Aflatoxin	365nm	455nm
Zearalenone	275nm	455nm

Alternatively, non- absorbing/fluorescing mycotoxins can be analyzed directly by gas chromatography-mass spectrometry (GC-MS) or liquid-chromatography-mass spectrometry (LC-MS). However, interfering compounds can be present despite of clean-up procedures, which can have an effect on the outcome of the measurement. The two main techniques to confirm the identity of mycotoxins are chemical derivatisation (into e.g. ochratoxin  $\alpha$ ) and mass-spectrometry [Wiley Encyclopaedia, 1999].

### 1.7.2 Thin layer chromatography and Gas chromatography

Thin Layer Chromatography (TLC) is a semi-quantitative technique, which requires intense sample clean-up. Some mycotoxins naturally fluoresce or absorb in the far UV region, so TLC is easy to perform [Wiley Encyclopaedia, 1999]. Mycotoxins are quantified by comparing visually the intensity of the fluorescence/absorbance of the sample spot with a series of standards. More accurate quantification is achieved instrumentally with a densitometer. Detection limits for TLC on e.g. silica gel plates are in the range of  $\text{ng kg}^{-1}$  to  $\mu\text{g kg}^{-1}$ , depending on the analyte, source of contamination, and clean-up method [Lin *et al.*, 1998]. In contrast to HPLC, TLC allows greater

versatility and is more suitable for the analysis of complex organic materials such as cereals [Smith, 2001]. TLC is rapid and in most instances an inexpensive separation technique. Special applications of TLC deal with multi-mycotoxin analyses and of structurally related mycotoxins [Betina, 1985].

Gas chromatography (GC) is the method of choice for some mycotoxins that exhibit little or no UV absorption or fluorescence. Most mycotoxins are not volatile at GC temperatures (30 – 350 °C), and must be derivatised to a volatile form. GC's advantage, compared to HPLC, is that it has effective detectors for mycotoxin analysis, such as the flame ionization detector (FID), the electron capture detector (ECD), and also the mass spectrometer (MS) [Wiley Encyclopaedia, 1999].

More specialized and thus rare methods are supercritical fluid chromatography (SFC) or capillary electrophoresis (CE). SFC uses a mobile phase with the solvating properties of a liquid and the diffusivity and viscosity of a gas to separate non-volatile or thermally labile compounds, e.g. trichothecenes [Roach *et al.*, 1989]. CE is capable of separating several charged and water-soluble molecules in a single run and has been used to separate and quantify aflatoxins and ochratoxins [Wiley Encyclopaedia, 1999].

A selection of current research in ochratoxin analysis in various media using HPLC and other chromatographic techniques is summarized in Table 1.4.

**Table 1.4:** Chromatography based techniques for ochratoxin A determination.

<b>Method</b>	<b>Food</b>	<b>Sensitivity</b>	<b>Reference</b>
GC-MS using SPE/derivatisation	Variety of food samples	0.1 $\mu\text{g kg}^{-1}$	[Jiao <i>et al.</i> , 1992]
HPLC-FLD using IAC clean-up	Blood, serum and milk	5-10 $\text{ng L}^{-1}$	[Zimmerli <i>et al.</i> , 1995]
HPLC-FLD using solvent extraction and IAC clean-up	Wheat and oats	0.8 $\mu\text{g kg}^{-1}$	[Solfrizzo <i>et al.</i> , 1998]
HPLC-FLD using IAC clean-up	Wine	0.01 $\mu\text{g L}^{-1}$	[Visconti <i>et al.</i> 1999]
HPLC-FLD using IAC clean-up	Coffee	0.2 $\mu\text{g kg}^{-1}$	[Leoni <i>et al.</i> , 2000]
HPLC-FLD using IAC clean-up	Beer	0.01 $\mu\text{g L}^{-1}$	[Visconti <i>et al.</i> 2000]
GC-MS and electronic nose using no clean-up (collection of volatile compounds at increased temperature)	Barley grain	5 $\mu\text{g kg}^{-1}$	[Olsson <i>et al.</i> , 2001]
HPLC with ESI, MS-MS, and FLD detection and SPE clean-up	Wine	1 $\mu\text{g L}^{-1}$	[Leitner <i>et al.</i> , 2002]
TLC using IAC clean-up	Green coffee.	10 $\mu\text{g kg}^{-1}$	[Pittet <i>et al.</i> , 2002]
HPLC-MS using IAC clean-up	Raisins	0.5-1.4 $\mu\text{g kg}^{-1}$	[Lindenmeier <i>et al.</i> , 2004]
LC-FLD using solid-phase extraction (SPE)	Must, wine and beer	0.1-1.0 $\mu\text{g L}^{-1}$	[Saez <i>et al.</i> , 2004]
LC- FLD using liquid-phase microextraction (LPME)	Wine	0.2 $\mu\text{g L}^{-1}$	[Gonzalez-Penas <i>et al.</i> , 2004]



### 1.7.3 Immunoaffinity Chromatography (IAC)

Affinity chromatography is a type of chromatography where the separation of molecules is not based on chemico-physical properties but on a molecular binding interaction. Affinity chromatography is generally used to separate an antibody mixture (e.g. antiserum) using a specific antigen (e.g. protein A is specific for IgG) which is immobilized in the stationary phase of the affinity column. Unbound molecules are washed off the column whereas bound molecules are eluted using e.g. low pH solutions. The term immunoaffinity chromatography describes a type of affinity chromatography where the stationary phase contains antibodies or antibody-like molecules. It is possible to integrate an immunoaffinity column into an HPLC system. Both techniques have their distinctive strength and drawbacks. Immunoassays are fast, inexpensive and sensitive. Although a group of analytes can be determined, multi-analyte analysis is not possible with immunoassays. Standard chromatography however, shows very high performance for quantitative analysis. The drawbacks are high costs per sample and often sufficient sensitivity can only be obtained sample pre-concentration. Furthermore, setup, calibration, sample concentration and clean-up are time-inefficient. Combination of immunoassays with chromatographic techniques is highly complementary and effective as the data generally do not interfere [Weller, 2000].

### 1.7.4 Current Research using Immunoassays

Three kinds of immunoassays have been developed for mycotoxin analysis including the radioimmunoassay (RIA), and the enzyme linked immunosorbent assay (ELISA). The RIA and ELISA analyses are mainly based on the competition of unlabelled mycotoxin in the sample and labelled (either radio- or enzyme-label) mycotoxin standard, binding to its specific antibody. IAC involves the use of antibody columns that specifically bind the mycotoxin which is subsequently eluted and quantified [Wiley Encyclopaedia, 1999].

Initially, the radioimmunoassay was a common application [Aalund *et al.*, 1975; Rousseau *et al.*, 1985] for ochratoxin A analysis. One of the first reporting an enzyme-linked immunosorbent assay for ochratoxin A was Petska *et al.* [1981]. This was

followed by a report on ochratoxin A ELISA in barley [Morgan *et al.*, 1983] and wheat [Lee & Chu, 1984].

Since then, the ochratoxin A analysis has shifted more towards chromatography applications such as TLC and HPLC and more recent LC-MS combinations [Reinsch *et al.*, 2007]. Generally, the research focus is to develop more sensitive methods, to improve sample clean-up and detection. The method(s) that received the widest acceptance has been collaboratively studied by the Association of Official Analytical Chemists (AOAC) and subsequently adopted by that organization as an official method [Helrich, 1990].

Current research on ochratoxin A using immunoassays can be found [Thirumala-Devi *et al.*, 2000], however is often based around antibody production and characterisation [Chu *et al.*, 1976; Candlish *et al.*, 1986; Gyongyosi-Horvath *et al.*, 1996]. It is also common to use commercial available kits for antibody characterisation [de Saeger *et al.*, 2002; Koeller *et al.*, 2006] as a time-effective alternative. However, current interests in immunoassay research are in immunoaffinity column applications [Goryacheva *et al.*, 2006] or multi-analyte and multi-component analysis [Saha *et al.*, 2007].

Over the last years a number of immunochemical methods have been developed. These are very sensitive, specific and rapid. Some of these methods have been incorporated into test kits and are commercially available (Table 1.5).

**Table 1.5:** List of Immunoassay-based commercially available test kits for Ochratoxin A.

Company	Product	Reference	Format	Sensitivity [ $\mu\text{g L}^{-1}$ ]	Range [ $\mu\text{g L}^{-1}$ ]
R-Biopharm Rhône Ltd/UK	Ridascreen® Ochratoxin A	www.r-biopharmrhone.com	Direct Competitive EIA (OTA-HRP conjugate)	0.025-0.625	0.025 - 2
Eurodiagnostica/ NL	Ochratoxin-A EIA	www.eurodiagnostica.com	Direct Competitive EIA (OTA-HRP conjugate)	0.5	0.25 - 8
DiffChamb/ SWE	Transia® Plate Ochratoxin A	www.diffchamb.com/	Indirect competitive ELISA	3	-
TecnaLab/ Italy	Immunoscreen OCHRA®	www.tecnalab.com/home	Direct competitive EIA	0.1	0.1 - 10
Neogen/ USA	Veratox® for OT	www.neogen.com/	Direct competitive ELISA	1	2 - 25
Tepnel Biosystems/ UK	BioKits ®Ochratoxin A Assay Kit	www.tepnelbiosystems.com/	Indirect competitive ELISA (biotin-labelled OTA, avidin-HRP-conjugate)	<0.3	NA
Romer Labs/ Singapore	AgraQuant® Ochratoxin Assay	www.romerlabs.com	Direct competitive ELISA (OTA-HRP-conjugate)	2	2 - 40
Helica/ USA	MycoMonitor® Ochratoxin A Assay	www.accuratechemical.com	Competitive ELISA	2	NA
Vicam/ USA	OchraTest®-Affinity Columns	www.vicam.com/	Anti-OTA-antibody columns; detection of eluted OTA via HPLC or Fluorimeter	1 (FL) 0.25 (HPLC)	1 - 100 0.25 - 100
Toxi-Test/Belgium	Flow-trough ELISA Kit for OTA	www.toxi-test.com/	-Enzyme-linked immuno-filtration assay for rapid screening of OTA in cereals	4 (cereals) 8 (coffee)	NA

Though most accurate and reliable, sending mycotoxin samples for analysis is often cost and time consuming. Because of the need for fast determination of mycotoxin levels, a variety of mycotoxin tests are sold that are easy to use and relatively inexpensive. The information derived from these kits is basically of two types: quantification or threshold levels. The advantages of the immunochemical methods are their ease of use and the short time required for the analysis. For determining threshold levels of the toxin, immunochemical test kits are probably the method of choice [Woloshuk, 2001].

## **1.8 Electroanalytical methods and applications**

Electroanalytical chemistry is a group of quantitative and analytical methods based upon the electrical properties of an analyte solution as part of an electrochemical cell. Electrochemical methods comprise many advantages, such as being analyte specific and can give sensitive information about analyte activity and concentration [Bard & Faulkner, 1980; Kissinger & Heinman, 1996].

### **1.8.1 Cyclic voltammetry**

Cyclic voltammetry is the measurement of current response over a range of electrode potentials (potential window). The same potential window is scanned in the opposite direction (hence the term cyclic). By plotting the current versus the voltage of the electrode potential one obtains a cyclic voltammogram (CV). Electroactive species formed by oxidation on the first (forward) scan can be reduced on the second (reverse) scan, if the reaction is reversible. Cyclic voltammetry can be used to study the electrochemical properties of substances in solution as well as at the electrode/electrolyte interface. One can obtain information about the cathodic and anodic peak potential ( $E_{pc}$ ;  $E_{pa}$ ) and the cathodic and anodic peak current ( $I_{pc}$ ,  $I_{pa}$ ). It can also be used to determine the electrode potential required for the oxidation or reduction of different redox species (e.g. mediators). This involves cycling a dilute mediator solution between two fixed potentials versus Ag/AgCl at a desired scan rate. During oxidation and reduction, the mediator shows a peak on the cyclic voltammogram, depending on whether the redox reaction is reversible. The determined peak potential can be used as working potential during e.g. amperometric measurements [Evans *et al.*, 1983; Kissinger *et al.*, 1983].

### **1.8.2 Chronoamperometry**

By applying an analyte-specific electrochemical potential on a working electrode, submerged in analyte solution, a redox analyte is oxidised at the anode or reduced at the cathode. The measured current is a function of the concentration of this redox analyte.

Amperometric detection is based on the measurement of current between a working and a counter electrode with respect to the reference electrode (e.g. Ag/AgCl).

In all electrochemical methods, the rate of oxidation and reduction depend on:

- 1) redox reaction rate & mass transport
- 2) electrode kinetics (electron transfer at the electrode) which depend on:
  - a) characteristics of the reaction
  - b) characteristics of electrode surface
  - c) temperature

Mass transport or mass transfer can be described by diffusion, which is the movement of particles due to a concentration gradient. If an electrochemical reaction depletes (or produces) some species at the electrode surface, then a concentration gradient develops and the electroactive species will tend to diffuse from the bulk solution to the electrode (or from the electrode out into the bulk solution). In contrast, within a flow cell or environment where the solution around the electrode is stirred, a stable diffusion profile is observed at the electrode surface and hence the establishment of a steady unchanging current [Bird *et al.*, 2002].

In case of a planar electrode placed in an unstirred solution, which contains excess electrolyte and a small amount of electro-active material, one speaks of non-equilibrium conditions. Upon the application of a suitable potential (potential at which the electroactive component is electrolysed completely), at  $t = 0$ , the concentration ( $C$ ) of the electroactive component at the electrode surface is reduced to zero ( $[C] = 0$ ) instantly. Thus, a concentration gradient will be established; down which material will flow from solution to the electrode surface. With progressing time, the diffusion layer grows; stretching further into the bulk solution. Thus, the slope of the diffusion gradient will also change with time resulting in a non-steady state current. The flux of components to the electrode surface changes as a function of time. This is described appropriately by the Cottrell equation [Cottrell, 1902]:

$$I = nFACD^{1/2}\pi^{-1/2}t^{-1/2} \quad \text{or} \quad I = nFAC\sqrt{(D/\pi t)} \quad \text{Equation V}$$

I = Current [Ampere]

n = number of electrons transferred/molecule

F = Faraday's constant [96,500 C mol<sup>-1</sup>]

A = electrode area [cm<sup>2</sup>]

D = diffusion coefficient [cm<sup>2</sup> s<sup>-1</sup>]

C = concentration [mol cm<sup>-3</sup>]

Regarding the applied potentials in chronoamperometry, the current response to a positive potential is a current 'spike' towards more positive values followed by a time-dependent decay. At applied negative potentials, however, the current 'spikes' towards more negative values with a 'reverse' decay towards more positive values. Generally, one can state that the diffusion-controlled current 'decays' towards zero ampere. The integration of the Cottrell equation for determination of the electro-active surface area is described by Brett & Brett [1993]. The Cottrell equation is valid for linear diffusion models; in case of radial diffusion, which can occur with micro-or nano-electrode arrays, the establishment of the real geometry of the working electrode becomes more complex.

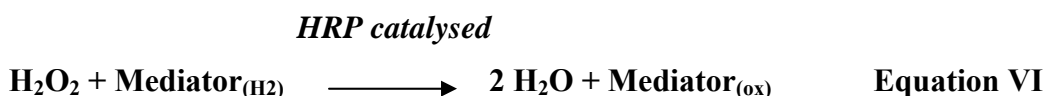
### 1.8.3 Hydrogen peroxide detection

Hydrogen peroxide (H<sub>2</sub>O<sub>2</sub>) is often utilised in biosensor detection since it is a substrate for the enzyme horseradish peroxidase (HRP), which catalyses the oxidation of a number of (chromogenic) hydrogen donors by H<sub>2</sub>O<sub>2</sub> [Pütter & Becker, 1983]. Horseradish peroxidase is widely used as enzyme label in immunological reactions enabling the reaction be monitored electrochemically or colorimetrically (section 1.6.1.2). Since H<sub>2</sub>O<sub>2</sub> can be detected by both oxidation and reduction, it is used to monitor reactions as either a consumed reactant or increasing product. However, direct electrochemical detection of H<sub>2</sub>O<sub>2</sub> requires high potentials (oxidation of H<sub>2</sub>O<sub>2</sub> occurs at + 650 mV vs Ag/AgCl) where interferences (from sample components) become more prominent and the signal response becomes unstable over time. This can be overcome

by deposition of noble metals (Pt, Pd, Au) on e.g. carbon electrodes to reduce interferences [Cass *et al.*, 1984].

#### 1.8.4 Redox mediators

Mediators are implemented in the sensor design to decrease interference effects from the sample matrix [Cagnini *et al.*, 1995; Ricci *et al.*, 2003]. The use of redox mediators or electrochemical substrates such as TMB [McKimm-Breschkin, 1990] is applied to shuttle electrons from H<sub>2</sub>O<sub>2</sub> to the electrode surface and thus decreases the high overpotential needed for H<sub>2</sub>O<sub>2</sub> oxidation [Thenmozhi *et al.*, 2007]. The catalytic mechanism of HRP in solution is based on the formation of several intermediates and was proposed by Chance [1949]. The hydrogen donor can be also referred to as mediator, which is generally a low molecular weight substance that acts as intermediate electron acceptor at low electrochemical potentials. The catalytic reaction of HRP with H<sub>2</sub>O<sub>2</sub> and the hydrogen donor are as follows.



By transferring the electrons from H<sub>2</sub>O<sub>2</sub> to the mediator, the latter is electrochemically oxidised by acting as electron acceptor and subsequently reduced by releasing the electrons at the electrode and thus producing a current.

Table 1.6 lists some examples of mediators that act as either one or two electron acceptors/donors.

**Table 1.6:** Examples of 1 e<sup>-</sup> and 2 e<sup>-</sup> acceptor/donors.

1 e <sup>-</sup> acceptor/donor	2 e <sup>-</sup> acceptor/donor
Hexacyanoferrate	Anthraquinone
Ferrocene	Hydroquinone
Methyl viologen	TMB



The characteristics of a 1 e<sup>-</sup> acceptor/donor are as follows:

- The potential [E] does not change with pH of the solution since H<sup>+</sup> does not participate
- No radical intermediates
- Moderate reaction rates with peroxidases

Whereas the characteristics of a 2 e<sup>-</sup> acceptor/donor are:

- The potential [E] varies with pH
- Radical intermediates can be present
- High reaction rates with peroxidases

The drawback of the use of mediators is that the mediator itself is not specific for any enzyme and therefore the reaction can be subject to non-specific interferences. The advantage is that this allows substitution of a variety of mediators.

One example is the use of TMB (3,3',5,5'-tetramethylbenzidine), which is used as a sensitive chromogen for horseradish peroxidase [Liem *et al.*, 1979] in enzyme-linked binding assays. Generally, benzidine-related compounds are well known substrates for HRP-catalysed H<sub>2</sub>O<sub>2</sub> reaction. The two step reaction forms initially a charge-transfer complex of the parent diamine and the diimine oxidation product (in equilibrium with its free radical). Addition of equimolar hydrogen peroxide to TMB yields the yellow diimine, which is stable at acid pH [Josephy *et al.*, 1982]. The overall reaction results in 2 electrons as depicted in Figure 1.6.

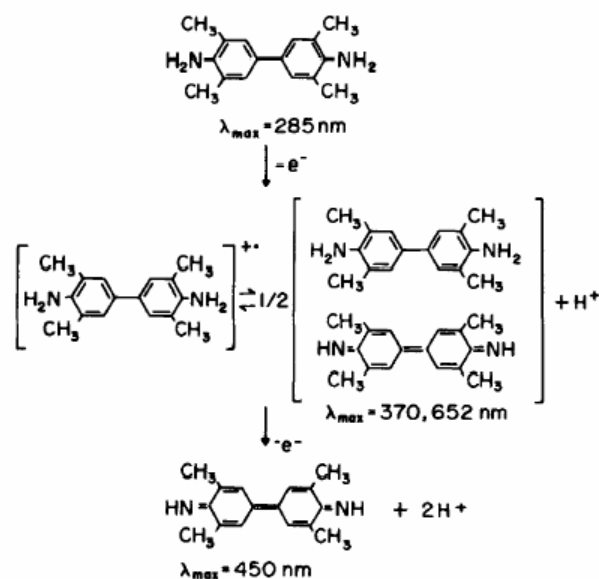


**Figure 1.6:** Chemical structures of 3,3',5,5'-tetramethylbenzidine (TMB) and its oxidation states according to Josephy *et al.* [1982].

The use of TMB as electrochemical mediator has been widely applied [He *et al.*, 1997a, 1997b; Compagnone *et al.*, 1998]. TMB was found to be a sensitive substrate for electrochemical detection using low levels of HRP, as compared to hydroquinone [Volpe *et al.*, 1998]. The most suitable electrochemical method of monitoring the oxidised TMB species is considered chronoamperometry, since only the signal from oxidised TMB is required and this should be readily achieved by applying a negative working potential. This is not feasible using cyclic voltammetry owing to the fact that any reduced TMB would be electrochemically oxidised at the initial potential, which would give an erroneous measurement for the resulting reduction peak [Crew *et al.*, 2007].

### 1.8.5 The classic three-electrode system

The construction of an electrochemical cell requires only two electrodes measuring the potential of the working electrode relative to a reference electrode, whose potential is constant. This is sufficient for potentiometric measurements, since there is no current flowing through the cell (potential difference at zero current). When monitoring the change of current, such as in amperometry, an external constant potential is applied, one requires the precise control over that potential. This is given by using a three-electrode

system, in which the potential of the working electrode (fixed) is controlled relative to the reference electrode. During the electrochemical reaction the current produced is measured between the working electrode and a counter electrode. A good reference electrode needs to have a potential that is stable with time and temperature, and that is not altered by passing a small current. An example is the silver/silver chloride (Ag/AgCl) electrode, which is immersed in an electrolyte solution containing Cl<sup>-</sup> ions [Bott, 1995]. Particularly, the choice of working electrode can be crucial for a specific measurement. Generally, a working electrode acts as a donor or acceptor of electrons in exchange with molecules in close proximity of the electrode surface. The electrode material must be conductive and electrochemically inert over a wide potential range. Commonly used working electrode materials for e.g. voltammetry include platinum, gold, mercury, and glassy carbon. The choice of material depends upon the potential window required as well as the rate of electron transfer, which can vary considerably from one material to another. Gold is more conductive than carbon [Barbalace, 2007] and thereby increases the rate of electron transfer ensuring reversible redox behaviour of the electrochemical system. Gold is also more chemically inert, belonging to the class of noble metals.

Screen printed electrodes (SPE) come as planar carbon, gold, or platinum working electrode including a Ag/AgCl reference electrode and a counter electrode, all of them printed subsequently on plastic, silicone or ceramic support. The three-electrode design of a screen printed electrode can be considered as a disposable electrochemical cell onto which the sample droplet is placed. Another advantage is the applied low reagent volume, which is in the micro-litre range. The great versatility presented by the screen printed electrodes lies in the wide range of ways in which the electrodes may be modified. The composition of the printing inks may be altered by the addition of very different substances such as metals, enzymes, polymers, complexing agents, etc. There is also the possibility of post-modifying the manufactured electrodes by means of depositing various substances on the surface of the electrodes such as metal films, polymers, or enzymes [Eggins, 2002].

In current applications, graphite materials are preferred for electrodes due to their simple technological processing and low-cost, although other materials such as gold and silver-based inks are also used for analysis and determination of various elements. Thus, Mascini and co-workers performed the determination of lead and other environmentally hazardous metals such as Cu, Hg and Cd on gold-based SPEs [2006]. Screen-printed gold electrodes have also been applied to the determination of lead in wastewater and soil extracts by Noh *et al.* [2006].

### **1.8.6 Miniaturization and electrode arrays**

Micro- and nano-technology allows for the production of microelectrodes and microelectrode arrays. Microelectrodes (1-20  $\mu\text{m}$ ) offer many advantages over conventional macroelectrodes in electroanalytical applications. These include high current density, high signal:noise ratio, dominance of radial diffusion, low ohmic drop, chemical concentration measurements in a microsecond time under appropriate conditions, and low dependence from hydrodynamics [Bond, 1994].

One of the benefits of miniaturization is that the current density (Ampere per area) increases with decreasing electrode size. This is substantial at electrode width below 20 micrometer and quasi-exponentially at below 10 micrometers. This has been explained through diffusion processes, which are the rate limiting factor in static systems. The smaller the electrode area the faster is the diffusion from solution to the electrode surface and the less mass transport limitations. Diffusion can be linear (1-D) or radial (3-D) depending on the ion transfer. Radial, or 3-D diffusion, is illustrated by a sigmoidal voltammogram, whereas linear (1-D) diffusion shows the characteristic peaks-shaped voltammograms [Sandison *et al.*, 2002].

Microelectrode arrays are an alternative to their macroelectrodes counterparts due to their ability to produce a voltammetric response of similar or raised magnitude [Beni *et al.*, 2006], showing less background current [Wightman and Wipf, 1989; Amatore *et al.*, 1995; Fletcher and Horne, 1999]. A microelectrode or ultra-microelectrode may be viewed as any electrode in which the electrode is smaller in magnitude than the diffusion layer [Arrigan, 2004]. Maximum current density is achieved when each

electrode in the array acts as an individual microelectrode with no overlapping diffusion layers. In this case, radial diffusion dominates the mass transport of the reactant, leading to larger mass transport coefficients compared to planar diffusion [Wightman and Wipf, 1989].

A series of different electrochemical cell designs have been fabricated in the Tyndall National Institute using photolithography (microelectrode arrays and cell-on-a-chip) and ion-beam lithography (has been investigated for the fabrication of nanopore electrode arrays). The microelectrodes used in this thesis were described by Lanyon *et al.* [2007] and a schematic view of a microelectrode arrays (used as working electrodes) is seen in Figure 1.7.

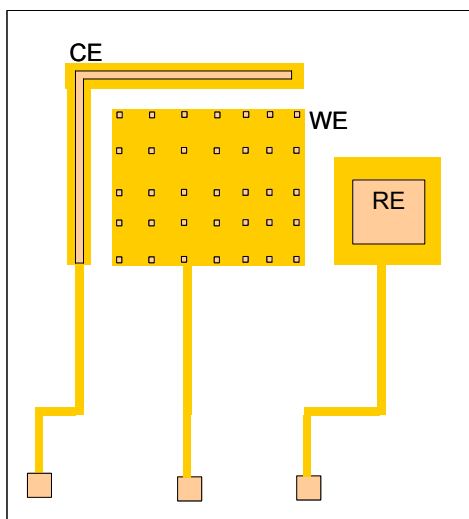


**Figure 1.7:** Micro square electrode arrays (single nanopore electrodes displayed as 5x5 array) developed by Tyndall National Institute, Cork, Ireland.

The microelectrodes shown here (Figure 1.7) have been characterized using cyclic voltammetry to determine the charging current or the electrode area; SEM images of a single nanopore electrode and nanopore electrode arrays were recently published [Lanyon *et al.*, 2007]. This array electrode setup allows for multi-sample and multi-component determination using sample volumes in the 1-10  $\mu\text{l}$  range.

### 1.8.7 Electrode modification

Modification of electrode surfaces provides an effective means of enhancing the power of voltammetric sensors [Murray *et al.*, 1987]. The terminology and definition of

chemically modified electrodes was updated by Durst *et al.* [1997] by reviewing the distinguishing features of a chemically modified electrode (CME) compared with other electrode concepts in electrochemistry. Electrodes can be modified using a number of biologically or chemically reagents that have desirable properties and thus the modified electrodes can display these properties [Arrigan, 1994].

Furthermore, electrodes can be modified by biological reagents such as proteins and thus referred to as biologically modified electrodes (BME). Methods of immobilisation include adsorption, entrapment or covalent binding to the electrode surface. Adsorption is experimentally simple and can be performed on numerous supports, from polystyrene over silica to gold. It is regarded a mild coupling method that preserves protein activity [Kennedy and Cabral, 1983]. However, it can be reversible; moreover, it does not provide as high surface loading of protein as covalent coupling [Ulbrich *et al.*, 1991]. Lower surface loading implies a decreased initial sensitivity relative to a sensor with covalent immobilisation; desorption would further reduce the sensitivity over time.

The use of chemically and biologically modified electrodes has been reviewed by Gilmartin *et al.* [1995]. Most of the biological components are either immobilised via a functional group or by physical adsorption. However, Moulton *et al.* [2003] found that the adsorbed protein layer had the effect of blocking the electron transfer. The degree of electron blocking correlated with the amount of adsorbed protein: the greater the adsorption, the larger the blocking effect. It has already been known that the adsorption of proteins onto electrode surfaces disturbs electrochemical analysis of clinical samples [Guo *et al.*, 1996]. Generally, the more distant the electron producing reaction from the surface the more the reaction is diffusion controlled and has to overcome several (protein)-barriers.

Carboxymethylated dextran (CMD) modification of gold surfaces is commonly known in Biacore<sup>TM</sup> technology [Loefas *et al.*, 1990; Johnsson *et al.*, 1991] where the CMD-modified gold chip is used for binding interaction analysis using the optical detection method surface plasmon resonance. The main concept of CMD modification is to control the amount of immobilised reagent and to reduce non-specific binding and also

in terms of reproducibility and durability of the coated layer. The CMD modified gold surfaces have been also applied in quartz crystal microbalance (QCM) [Rickert *et al.*, 1997; Storri *et al.*, 1998; Tombelli *et al.*, 2000]. To date, little work has been reported on the use of CMD-modified gold electrodes. Pallarola *et al.* [2006] reports the application of CMD to avoid non-specific adsorption of proteins on gold electrodes. The only electrochemical assay described using carboxymethylated gold electrodes has just recently been reported by Priano *et al.* [2007], which is based on a three-electrode system. This is used for monitoring a current that is generated by the addition of hydrogen peroxide and a redox mediator to determine lipopolysaccharides from *Salmonella minnesota* at concentrations as low as  $0.1 \mu\text{g L}^{-1}$  (0.1 ppb). Surprisingly, even though the technique of chemically modified electrodes (CME) has been long known, the use of carboxymethylated dextran is new.

### 1.8.8 Wine electrochemistry

Wine is a complex matrix containing redoxactive species including organic acids, polyphenols, and anthocyanins [Kilmartin *et al.*, 2001 and 2002, Zou *et al.*, 2002]. In electrochemical wine analysis electroactive species in the wine sample may react directly at the electrode surface [Zhao *et al.*, 2004]. Wines are generally containing up to  $3.5 \text{ g L}^{-1}$  phenolic compounds (commonly expressed as gallic acid). The ideal potential range for amperometric determination is considered to be from -150 to 0 mV versus SCE where electrochemical interferences are minimal. It was furthermore found that gallic acid can be oxidised at low potentials in the range of -100 mV versus SCE [Avramescu *et al.*, 2001]. The change in the applied potential to -150 mV versus pseudo-Ag/AgCl [Avramescu *et al.*, 2002] contributed not only to the decrease of electrochemical interferences, but also to a reduction in sensitivity as the coefficient of variation increased 5 fold.

Selecting a potential that results in low interference from wine components is one solution. Another is to reduce or remove the concentration of one or more undesirable components. This is known as ‘wine fining’. Fining agents are commonly adsorptive or reactive substances that can be grouped according to their chemical nature and mode of action:

- Bentonite (electrostatic; removes proteins)
- Proteins: gelatin, isinglass (collagen), casein, albumen (remove e.g. tannins)
- Carbons (non-specific adsorbtive agent, smaller polyphenols)
- Synthetic polymers: PVPP (polyphenols, phenols)
- Others, including chelators and enzymes (e.g. tyrosinase)

Since polyphenols are the main source of electrochemical interferences and electrode fouling [Siebert and Lynn, 1997], the polymer polyvinyl polypyrrolidone (PVPP) can be most successfully applied to remove polyphenols from wine samples [Zoecklein *et al.*, 1990; Morris and Main, 1995].



## 1.9 Biosensors

Above all, an ideal analytical method should be specific. This means it should be able to measure the amount of a specific substance accurately, no matter what other substances, and to what extent, present in the sample. In practice, only a few analytical methods achieve this aim, but many are selective, meaning they can detect a small group of molecules in a crude mixture. The need for an analytical method that is capable of specifically detecting a single substance was early recognised. It became clear that no chemical analysis could be ever as specific as nature itself. Biomolecules such as enzymes or antibodies were not only selective but also highly specific for a single biomolecular group in any crude mixture. The idea was to combine chemical analysis with biomolecules initiating the rise of bioanalysis and biosensors.

Entering the term ‘biosensor + definition’ into an internet search engine one stumbles upon more than a quarter of a million entries covering a broad range of terms to describe a biosensor. The simplest way of describing a biosensor to non-scientific persons is that ‘*a biosensor is an analytical device which converts a specific biological response into an electrical signal*’. However, reality is not as simple a matter.

Initially, Turner *et al.* [1987] defined a biosensor as ‘a compact analytical device incorporating a biological or biologically-derived sensing element either integrated within or intimately associated with a physicochemical transducer. The usual aim of a biosensor is to produce either discrete or continuous digital electronic signals which are proportional to a single analyte or a related group of analytes’.

In 1996, the following proposal for a biosensor definition was offered: ‘A biosensor is a self-contained integrated device, which is capable of providing specific quantitative or semi-quantitative analytical information using a biological recognition element (biochemical receptor) which is retained in direct spatial contact with a transduction element. Because of their ability to be repeatedly calibrated, we recommend that a biosensor should be clearly distinguished from a bioanalytical system, which requires additional processing steps, such as reagent addition’ [Thevenot *et al.*, 1996]. This proposal was later on accepted as official definition by the IUPAC published in 1999.

However, Scheller *et al.* [1997] had pointed out, that ‘owing to the rapid technological progress essential parts of it [...the definition...] appear ambiguous. Thus, in the light of the ability of miniaturized bioreactors to interact with transducers (without additional sample processing elements) on single chip the term, “direct spatial contact” of the elements is amenable to different interpretations. Furthermore, the borderline between recognition tools that are biological in nature and synthetic (organic) receptor molecules is no longer well definable; these two classes of recognition elements are merging. This is especially true for enzyme models, polymers imprinted by biomolecules, and, although to a lesser extent, (synthetic) oligonucleotides and ionophores, which mimic the function of channels. Although at present routine application of biosensor technology is more or less restricted to enzyme electrodes, optical immunosensors, and whole cell-based receptor assays, the forefront of biosensor research exploits results and principles of molecular biotechnology and nanotechnology for creating qualitatively new molecular sensors’.

So, where do we stand today? With the ever growing market in biosensors [Newman & Turner, 2005] and development of new applications in the field of biomimetic sensors such as molecular imprinted polymers [Haupt and Mosbach, 1998; Piletsky, 1999], aptamers [Tombelli, 2005], and synthetic receptors [Allender, 2006], it is hard to distinguish what is a biosensor by definition. For example what is ‘bio’ and what is not and should there not be a common nomenclature for a common concept?

Historically, the biosensor concept was initiated by Clark and Lyons in 1962 when they coupled the enzyme glucose oxidase to a platinum electrode [Clark and Lyons, 1962]. Further biosensors did arise due to the demand of functional characteristics such as sensitivity, cost, selectivity, versatility, range, availability, future adaptability and simplicity, which were/are not provided by conventional analytical methods. Electrochemical biosensors are favoured, often comprising all those characteristics; closely followed by optical sensors, which differ only in their costs and availability. Other sensors such as piezoelectric sensors are showing viewer functional characteristics (expensive, low availability) and are thus lower rated [Cunningham, 1998].

### 1.9.1 Electrochemical biosensors

Electrochemical biosensors can be divided into conductimetric, potentiometric and amperometric biosensors depending on the electrochemical property to be measured. Conductimetric biosensors monitor the changes in conductance/impedance using noble metal electrodes, whereas potentiometric biosensors measure the potential difference between the working electrode and a reference electrode at zero current. Amperometric biosensors measure the currents resulting from the electrochemical oxidation or reduction of an electroactive species at a constant potential.

Commercial biosensors are commonly amperometric biosensors, which have been divided into three generations. The first-generation biosensors were proposed by Clark and Lyons and implemented by Updike and Hicks, who coined the term enzyme electrode [Clark and Lyons, 1962; Updike and Hicks, 1967]. Typically, an oxidase (e.g. glucose oxidase) is immobilized behind a dialysis membrane at the surface of a platinum electrode. The enzyme's function is to selectively oxidize an analyte by the reduction of O<sub>2</sub> [Durst *et al.*, 1997]. Second-generation biosensors use mediators, which replace O<sub>2</sub> as the electron shuttle and use other redox enzymes in addition to oxidases as O<sub>2</sub> can result in high interferences. Third-generation sensors are co-immobilising enzyme and mediator (in contrast to free diffusion of O<sub>2</sub> or mediator) at an electrode surface, making the recognition element an integral part of the electrode transducer. Parallel immobilisation of enzyme and mediator can be accomplished by (1) mediator-labelling of the enzyme followed by enzyme immobilisation, (2) enzyme immobilisation entrapped in a redox polymer (redoxpolymer is the mediator), or (3) enzyme and mediator co-immobilisation in a conducting polymer. The most known amperometric biosensor is the glucose biosensor, which has been successfully commercialized for blood glucose monitoring [Newman & Turner, 2005].

Enzyme-based biosensors primarily rely on two mechanisms. The first involves the catalytic transformation of an analyte (substrate) into a detectable product or co-product. The second mechanism involves the detection of an analyte that inhibits or mediates the enzyme's activity. Although very selective and sensitive, inherent limitations for this type of biosensor are primarily those imposed by the nature of the enzyme itself and

include the limited number of analytes that happen to be substrates/inhibitors for the enzyme. The detection limits for these sensors are determined by the enzyme's catalytic properties and are defined by kinetic constants, such as the Michaelis Menten constant  $K_M$  and the  $V_{max}$  value [Rogers, 1998]. One of the first enzyme sensors on screen-printed carbon electrodes (SPCE) was developed by Newman *et al.* [1992] and further investigated in terms of catalytic materials and membranes [Newman *et al.*, 1995]. Enzymatic sensors constructed with SPEs present a great number of applications, such as the determination of hydrogen peroxide using SPEs with immobilized horseradish peroxidase [Ledru *et al.* 2006], the construction of a glucose biosensor with flow-injection analysis [White *et al.*, 1996] or monitoring microbial fermentation [Tothill *et al.*, 1997].

Instead of enzymes, antibodies can be used as recognition element. Bioaffinity-based biosensors primarily depend on the use of antibodies directed towards a wide range of analytes and the antibody's relative affinity and selectivity for a particular compound or closely related group of compounds [Rogers, 1998]. Interestingly, immunosensors do not fit the official definition of biosensors, which states that biosensors should operate reversibly and in real-time. The antigen-antibody reaction, which is the basis of immunosensors, can be irreversible and usually requires the addition of labelled compounds, which only allow the indirect determination of the concentration of antigen-antibody complexes. Consequently, immunoanalytical procedures, including immunosensor systems, are based on multi-step assays and deliver a signal some time after the introduction of the analyte [Bilitewski, 2000]. Most of the electrochemical immunosensors are based on the enzyme-linked immunosorbent assay (ELISA) principle, where either antibody or antigen is immobilised to the transducer. Electrochemical immunosensing requires labelling of either antigen or antibody, since their binding interaction is accompanied by only small physico-chemical changes [Warsinke *et al.*, 2000; Darain *et al.*, 2003], which can not be electrochemically detected. Peroxidases, phosphatases, ureases and glucose oxidases proved to be best-suited enzyme labels [Darain *et al.*, 2003; Moore *et al.*, 2003]. Several immunosensors have been reported for the detection of hormones, where Butler and Guilbault [2006] describe an amperometric immunosensor, based on disposable SPCE, for the

determination of 17- $\beta$  estradiol in water, or seafood toxins such as in the case of domoic acid [Micheli *et al.*, 2004]. The measurement principle of indirect competitive detection was employed by Lu *et al.* [2002] who fabricated immunosensors by immobilizing a boldenone-BSA conjugate on the surface of SPCEs, followed by the competition between the free boldenone for the corresponding antibody. A secondary anti-species IgG-HRP conjugate determines the degree of competition. The electrochemical technique chosen in this case was chronoamperometry. This technique was also employed for the determination of testosterone in bovine urine [Coneely *et al.*, 2007].

Immunochemical assays for food contaminant analysis [Tothill, 2003] and the application of biosensors in food analysis [Tothill *et al.*, 2001; Tothill and Turner, 2003] has been discussed. Electrochemical immunosensors for mycotoxins using differential pulse voltammetry (DVP) with SPCEs based on an indirect competitive assay format has been described [Ammida *et al.*, 2004 & 2006; Pemberton *et al.*, 2006]. Micheli *et al.* [2005] described an electrochemical immunosensors based on the immobilisation of antibodies on SPCEs and direct competition between free aflatoxin M1 and aflatoxin M1-HRP. An indirect competitive format was presented for simple and fast measurement of aflatoxin B1 in barley using DPV and SPCEs [Ammida *et al.*, 2004 & 2006]. Alarcon *et al.* described an indirect [2004] and direct [2006] competitive immunoassay for ochratoxin A using polyclonal antibodies on SPCEs. The immunosensor appears to be suitable for ochratoxin A screening in wheat. Electrochemical detection of mycotoxins can be either monitored by direct electrochemistry, or by following the binding interaction of a mycotoxin with an immobilized recognition element [Logrieco *et al.*, 2005]. Direct electrochemistry of mycotoxins has been reported by Calcutt *et al.* [2001] for the electrochemical oxidation of ochratoxin A. Electrochemical monitoring of mycotoxin interaction was also studied using a DNA based electrochemical biosensors capable of detecting compounds able to intercalate within the DNA chains [Mascini *et al.*, 2001 & 2001]. The intercalating compound, such as aflatoxin B1, is influencing the oxidation signal of the guanine moieties of the DNA. Investigations were made on alternative biosensing principles; using supported bilayer lipid membranes (s-BLM), which showed an increased ion current following application of aflatoxin M1 [Siontorou *et al.*, 1998]. Those

phospholipids bilayers were also used for immobilisation of oligonucleotides or antibodies and biospecific interactions of the e.g. aflatoxin M1 could be detected by electrochemical impedance spectroscopy [Vagin *et al.*, 2003].

### 1.9.2 Surface plasmon resonance-based optical biosensors

Surface plasmon resonance (SPR) is a phenomenon that occurs upon a metal (Au) interface between an optical dense medium ( $n_1$ ) and an optical rare one ( $n_2$ ). Polarized light is totally internal reflected when the angle of reflection is larger than the critical angle of incidence. An evanescent wave is generated at the reflecting surface, which penetrates several hundred nanometers (nm) in the surrounding medium [Otto, 1968].

Biacore technology utilises the natural phenomenon of surface plasmon resonance (SPR), where detection is carried out with a diode array detector (DAD) that measures the shift in angle of incidence (change in refractive index ( $n$ ) caused by mass changes on the sensor surface. Association and dissociation of molecules to the sensor surface can be followed by converting the shift in angle of incidence into resonance units (RU) and monitoring in a sensorgram (resonance units (RU) versus time (min)). The Biacore system is using SPR to perform label-free direct immunoassays in a flow-through format. This can be utilized to screen kinetics and affinities of biomolecules [Malmquist & Karlsson, 1997; Markey, 1999].

Figure 1.8 below describes the detection principle incorporated into any Biacore device currently on the market.

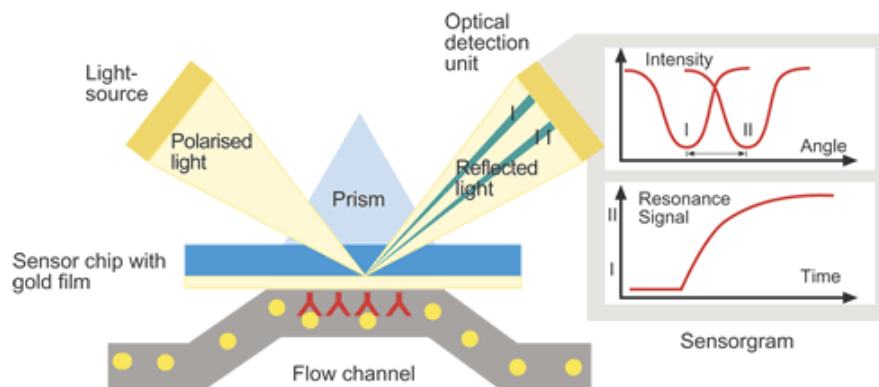


**Figure 1.8:** Biacore detection utilising surface plasmon resonance [Biacore™].

The device can be used for many applications such as concentration analysis [Karlsson *et al.*, 1993] or epitope mapping [De La Lastra *et al.*, 1999]. Biospecific interaction analysis (BIA) is consistently used to establish kinetic rates and affinities of binding interactions by assessing the kinetic rate constants for association and dissociation of an analyte to an immobilised ligand [Malmquist, 1993]. The observed binding interactions can be simple protein-protein interactions, antibody-antigen, or DNA hybridisation. More specialised interactions such as peptide-protein or lectin-carbohydrate require more sensitive modifications.

Optical biosensor development for mycotoxins is commonly based on immunoanalytical methods. Polyclonal antibodies were used in a surface plasmon resonance-based immunoassay for aflatoxin B1 [Daly *et al.*, 2000]. Deoxynivalenol sensing by SPR-based immunoassays using polyclonal antibodies has been reported by Schnerr *et al.* [2002]. An SPR-based inhibition assay was developed for deoxynivalenol, using monoclonal antibodies as recognition elements [Tudos *et al.*, 2003]. A biosensor for multiple mycotoxin analysis was also investigated by van der Gaag *et al.* [2002], where an immunochemical biosensor assay for the detection of multiple mycotoxin (i.e. aflatoxin, zearalenone, deoxynivalenol, and ochratoxin A) was described. An SPR immunosensor with real-time measurement and flow-trough format (Biacore) was also introduced by van der Gaag *et al.* [2003] for the detection of mycotoxins in food and feed. Whole cell recognition elements were used in a biosensor for the mycotoxins patulin, diacetoxyscirpenol, roquefortine, and T-2 toxin by Benitez *et al.* [1994]. Thompson and Maragos [1999] designed a fibre-optic immunosensor that has the potential for screening corn for fumonisins with a detection limit of  $10 \mu\text{g L}^{-1}$ . Scheper *et al.* [1994] presented a paper on optical sensors for biotechnology applications, where two fibre optic based immunosensor are described for mycotoxins.

### **1.10 Biomimetics**

To date, many analytical methods are based on natural recognition elements, such as antibodies, enzymes, and protein receptors. Although of fundamental importance, these methods sometimes suffer from features such as low stability and high production costs. Nevertheless, new and more specific stationary phases are needed for analytical

methods like high-performance liquid chromatography (HPLC). Thus, alternative techniques to produce materials for separation chemistry are therefore of great interest and value. One of nature's most important results of evolution is a system capable of distinguishing one molecule from another. Molecular recognition is the basis for most biological processes, such as ligand-receptor binding or substrate-enzyme reactions and is therefore of universal interest. If nature can produce enzymes, receptors and antibodies by evolution, molecular engineers should be able to develop materials with similar properties by design. Some common biomimetic recognition elements are described in the following section.

Biomimetic recognition elements such as molecular imprinted polymers (MIP) offer several applications in areas such as analysis, sensing, extraction, or pre-concentration of components [Haupt, 2002]. It is possible to design and produce tailor-made, stable recognition matrices for a wide range of analytes that can be employed in a multitude of analytical formats [Ramstrom, 2001]. The construction and operation of fibre-optic sensing devices based on molecularly imprinted polymers and the advantages of using molecularly imprinted polymers as artificial recognition systems in sensor technology were discussed by Kritz *et al.* [1995] and Haupt and Mosbach [2000]. MIPs were also used as recognition element in a surface plasmon resonance sensor [Lotierzo *et al.*, 2004]. Molecular imprinted polymers for mycotoxins were discussed by Mahony *et al.* [2005] being applied as stationary phase recognition matrix in HPLC and SPE. A MIP that recognized ochratoxin A was produced by Turner *et al.* [2004]. Other MIPs towards ochratoxin A for solid-phase extraction and sample clean-up from red wine are described by Lindner *et al.* [2002 and 2004], Jodlbauer *et al.* [2002] and Maier *et al.* [2004].

Other biomimetic recognition elements are aptamers, which are single-stranded oligonucleotide that assumes a specific, sequence-dependent shape and bind to a target molecule based on a key-lock fit. Aptamers are screened using SELEX (Systematic Evolution of Ligands by EXponential amplification), which is an *in vitro* combinatorial chemistry process used to identify aptamers to a target from large pools of diverse oligonucleotides [Wilson and Szostak, 1998]. Aptamers possess numerous advantages



that make them preferred candidates for drug development such as better stability (pH, temperature) than proteins [Mascini, 2003].

Peptides are also used as recognition elements. Molecular recognition by peptides is known for a number of biochemical processes, such as signal transduction (e.g. neuropeptides), metabolism (e.g. hormones), cell growth (e.g. Ras-protein, p53), and immune defense (e.g. MHC-receptors) [Schmuck, 2001]. Peptide receptors are relatively small enough to offer uncomplicated and fully understood structures, while being sufficiently complex to offer unique binding sites. The molecular recognition by peptides is based on several non-covalent interactions, such as (1) H-bridge-bonding, (2) salt-bridges, (3) hydrophobic and (4) van der Waals interactions (Table 1.7).

**Table 1.7:** Types of intermolecular forces [Selassie *et al.*, 2003].

Bond type	Bond strength (bond enthalpie) [kJ/mol]
Covalent	40-140
Ionic (Electrostatic)	5
Hydrogen	1-10
Dipole-Dipole	1
Van der Waals	0.5-1
Hydrophobic	1

Artificial peptides can be designed to interact specifically with a target molecule. Combinatorial libraries of up to a million synthetic peptides are screened for ligands with improved selectivity for a specific target analyte [Schmuck, 2001].

### 1.10.1 Peptide structure and synthesis

The primary structure of a peptide is the sequence of its monomer units (amino acid residues). The secondary structure is the spatial arrangement of the peptide chain under the influence of hydrogen bonding between the various amino acid residues. The secondary structure can be rationalized in terms of the rules formulated by Linus Pauling and Robert Corey. The essential feature of the Pauling and Corey rules is the stabilization of structures by hydrogen bonds involving the planar amide bond. The

amide bond can act both as a donor of the H-atom (the NH- part) and as an acceptor (the CO- part).

A peptide bond (Figure 1.9) is a covalent bond between a carboxyl- and an amino-group formed in a condensation reaction.

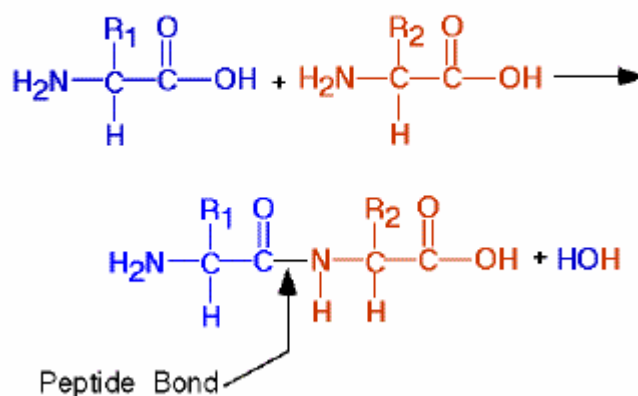


**Figure 1.9:** Peptide bond formation from amino acid monomers.

To abide by the rules, hydrogen bonding occurs between peptide links of the same chain in the  $\alpha$ -helix or links different chains as is the  $\beta$ -pleated sheet [Atkins, 1996]. The fact that peptides fold spontaneously, implies that all the information required specifying the structure is inherent in the sequence. The three methods of secondary structure prediction are those of Lim [1974], Chou and Fasman [1978], and Robson *et al.* [1978]. None gives predictions consistently more than 55 percent correct in assigning amino acids to three states: helix, sheet, and turn.

Peptide formation occurs naturally as condensation between the  $\alpha$ -COOH group of one amino acid and the  $\alpha$ -NH group of another forming an amide. In peptide synthesis, coupling of amino acids is done by the (1) azide-, (2) carbodiimide- and (3) active ester-method. To meet the solubility problems posed by the minimal nature of the protection in synthesis, polar, but chemically uncreative, substituents are employed as protecting groups. Furthermore, there are -SH, imidazole-, and guanido- protection methods. The various coupling and protection reagents can be deployed in practice in either of two

ways. In ‘stepwise synthesis’ one starts with the terminal residue and adds the others in the correct order, one by one, until the molecule is finished. Almost all coupling methods involve the activation of the  $\alpha$ -COOH group and begin with the carboxyl-terminal (opposite direction of biosynthesis). In “fragment condensation” synthesis separate portions of the sequence are assembled in a series of independent stepwise syntheses. These portions are then combined into larger fragments until all are joined in the final molecule [Offord, 1980].

## 1.11 Computational chemistry

Computational (bio)-chemistry is dealing with all of the three aspects of (bio)chemistry, namely: structure, reaction and function. Molecular modelling (computational modelling) can be defined as the application of computers to generate, manipulate, calculate and predict realistic molecular structures and associated properties. Molecular modelling can be also used as computer-aided rational drug design tool [Cramer, 1983]. In contrast to the combinatorial chemistry approach, computational modelling employs structure-based design. Molecular structures are represented numerically by simulating molecule behaviour with quantum equations and classical physics. Computational modelling programs generate and present molecular data including geometries (bond lengths, bond angles, torsion angles), energies (heat of formation, activation energy, etc.), electronic properties (moments, charges, ionization potential, electron affinity), spectroscopic properties (vibrational modes, chemical shifts) and bulk properties (volumes, surface areas, diffusion, viscosity) [Richon *et al.*, 1994]. This can be a powerful tool for conformational studies of molecules, such as drugs, proteins and other macromolecules [Tsai, 2002].

### 1.11.1 Force Fields

Force fields (molecular mechanics) are functions that associate energy with a given nuclear conformation and thus rely on the Born-Oppenheimer approximation. The calculation of the structure and energy of molecules is based on nuclear motions. Electrons are not considered explicitly, but rather it is assumed that they will find their optimum distribution once the positions of the nuclei are known. This assumption is based on the Born-Oppenheimer [1927] approximation of the Schrodinger equation [1926]:

$$H\Psi = E\Psi$$

Equation VIII

The energy of the system  $E$  is relative to a system, in which all atomic particles are separated to infinite distances.  $\Psi$  is the wave function, which defines the Cartesian and spin coordinates of the atomic particles and  $H$  is the Hamiltonian operator which

includes terms for both potential and kinetic energy. However, the Schrodinger equation can be solved only for very small molecules such as hydrogen or helium. Approximations must be introduced in order to extend the utility of the method to polyatomic systems. One approximation attempts to differentiate nuclei and electrons. The Born-Oppenheimer approximation states that nuclei are much heavier and much more slowly than electrons. Thus, nuclear motions, vibrations and rotations can be studied separately from electrons; the electrons are assumed to move fast enough to adjust to any movement of the nuclei [Richon, 1994]. Two types of force fields are known for both small and macromolecules:

**Class I** force field:

- Parameterized primarily from experimental data and mostly based on small molecule model systems
- 10 - 100 parameters
- Emphasis on thermodynamic properties in the condensed phase
- Condensed phase implicitly taken into account in parameterization  
Examples: MM1/MM2 [Allinger *et al.*, 1989], CHARMM [Brooks *et al.*, 1983], OPLS [Jorgensen and Tirado-Rivers, 1988], AMBER [Weiner *et al.*, 1984], and SYBYL [Clark *et al.*, 1989]
- Evolution: mid-1960's to present

**Class II** force field:

- Accounts for properties of more diverse systems such as isolated molecules in the gas phase, molecules in condensed phases, and macromolecular systems
- Emphasis on high precision reproduction of geometries and dipole moments
- Extensive parameterization for many different classes of organic molecules;
- >100 parameters
- MM3 and MM4 [Allinger *et al.*, 1989 & 1996]
- Evolution: mid-1980's to present

These two classes of force fields are increasingly merging as macromolecular force fields increasingly include arbitrary small molecules, e.g. for protein-ligand simulations [Jacobson, 2003].

The forces holding atoms together (bond length, bond angles, or non-bonded interactions) can be described by potential energy functions of structural characteristics and the combination is referred to as the force field. Atoms can be considered as spheres and bonds as springs. The mathematics of spring deformation can be used to describe the ability of bonds to stretch, bend, and twist as shown in Figure 1.10 [Steinbach, 2005].

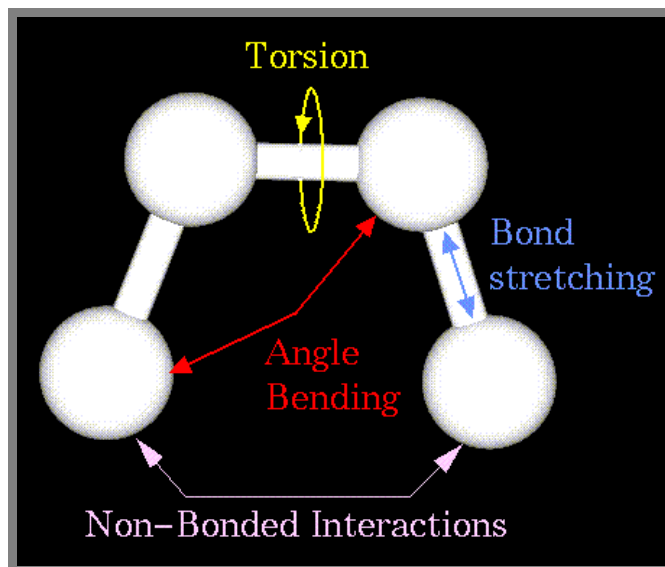


**Figure 1.10:** A molecule is viewed as a collection of points (atoms) connected by rods (bonds) with different elasticity (force constants) [Steinbach, 1996].

Non-bonded atoms (greater than two bonds apart) interact through van der Waals attraction, steric repulsion, and electrostatic attraction/repulsion. These properties are easiest to describe mathematically when atoms are considered as spheres of characteristic radii. Molecular mechanics predicts the energy associated with a given conformation of a molecule. The calculated energy can not be given absolute but relative quantities, since the energy zero is arbitrary. One can only compare energies calculated for different (two or more) configurations of chemically identical systems [Steinbach, 2005]. The molecular energy is calculated term by term, comparing bond parameter values that are taken from either experimental data or from *ab initio* (quantum mechanics) calculations.

A simple molecular mechanics energy equation including parameters that are contributing to the prediction of energies by molecular mechanics is given by Steinbach [1996]:

$$\text{Energy [E]} = E_{\text{Stretching}} + E_{\text{Bending}} + E_{\text{Torsion}} + E_{\text{Non-Bonded Intact}} \quad \text{Equation IX}$$

Engler *et al.* [1973] initially found that relative energies are determined more reliably than absolute enthalpy calculations and now supports Allinger's [1989] conclusion that the molecular mechanics method, in principle, must be considered to be competitive with experimental determination of the structures and enthalpies of molecules. In that context, Apostolakis and Caflisch [1999] discussed the estimation of (relative) binding affinities, which is from a theoretical point of view, the most challenging part of ligand design. In their paper, they reviewed three methods for the estimation of binding energies: (1) quantitative structure-activity relationships (QSAR); (2) empirical energy functions and (3) free energy calculations based on molecular dynamics simulations.

The optimal force field is context-dependent as there have been numerous reviews on comparing different force fields [Engler *et al.*, 1973; Clark *et al.*, 1989; Roterman *et al.*, 1989; and Apostolakis & Caflisch, 1999]. Furthermore, revisions within a single force field and the choice of solvent model for each application make the choice difficult.

### 1.11.2 Minimisation

As part of a force field, energy minimisation results in geometry optimisation of the molecular structure [Tsai, 2002]. The most stable conformation of a molecule can be found by minimising its free energy. Energy is a function of the atomic coordinates and force constant definitions as described in section 1.11.1. Based on the force constants and associated parameters the computational program generates a set of atomic coordinates which correspond to a minimum of energy. This is accomplished by a minimisation procedure that is an iterative method in which the atomic coordinates are modified from one iteration to the next in order to decrease energy.

A minimisation method is for instance molecular mechanics 'MM3' developed by Allinger *et al.* [1989]. MAXIMIN2 is the standard minimisation program applied in

SYBYL and uses the TRIPOS force field parameters. MAXIMIN is describing that energy can be minimised while maintaining specified geometric relationships within and/or among given sets of atoms [Labanowski *et al.*, 1986].

The goal of energy minimisation is to find a route (consisting of variation of the intramolecular degrees of freedom) from an initial conformation to the nearest minimum energy conformation using the smallest number of calculations possible. With molecular modelling of proteins, the molecule is placed in an imaginary box and periodic boundary conditions are set at a dielectric constant of 1 (vacuum) – 80 (water) [Joergensen, 1983]. The setting of the dielectric constant in minimisation procedures is crucial to the outcome of the entire model. The relationship between an initial and minimum energy conformation is shown in the following hypothetical energy surface (Figure 1.11):

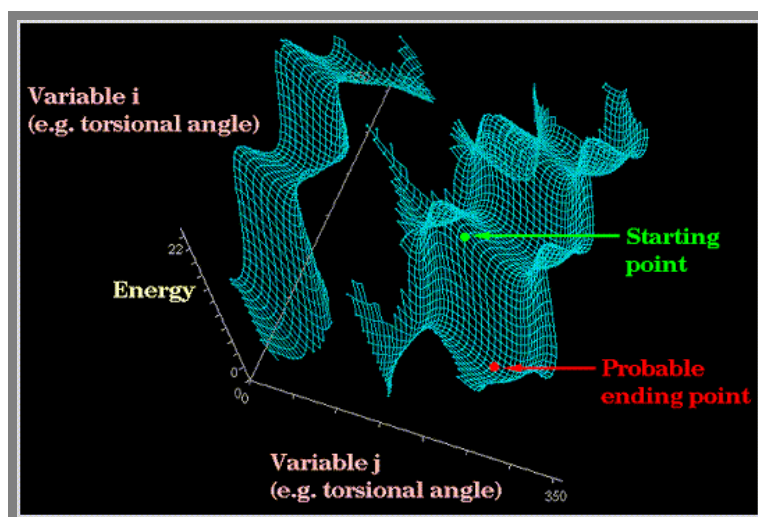


**Figure 1.11:** The energy minimisation principle [Steinbach, 1996].  $P$  (●) is the initial point on the energy surface. The energy minimum (●) can be characterized by a small change in energy and/or a zero gradient between steps towards a minimum. At a minimum of the potential energy surface, the net force on each atom vanishes, therefore the stable configuration [Tsai, 2002].

The inclusion of electrostatic interactions can play a critically important role in molecules where H-bonding and other electrostatic interactions are involved. Therefore, a number of applications used in SYBYL calculate partial charges in molecules, such as Pullman- or Gasteiger-Hueckel-charges [Tripos bookshelf, 2002]. Solvation can also have a strong effect on the energies of different conformations. It influences the H-bonding pattern, solute surface area, and hydrophilic/hydrophobic group exposures of



protein molecules. Empirical potential energy functions for proteins may be used to study protein stability and motion. However, it is difficult to evaluate these functions because most protein crystal structures are not accurate enough to act as test cases. Whitlow and Teeter [1986] empirically examined how well potential energy minimisation can model the high resolution crystal structure of the hydrophobic protein Crambin [Hendrickson & Teeter, 1981] and found that, empirically, the best overall conditions for minimisation are employing Jorgensen's van der Waals radii [1981].

### **1.11.3 Simulated annealing**

Another optimisation technique is known as simulated annealing, which was introduced by Kirkpatrick *et al.* [1983] as similar to evolutionary algorithms. Simulated annealing locates local minima (low-energy state) by annealing in a multivariate objective function [Donnelly, 1986]. To simplify, the idea comes from the industrial process of *annealing* in which a material is heated to above a critical point to soften it, then gradually cooled in order to erase defects in its crystalline structure by producing a more stable and regular lattice arrangement of atoms [Haupt & Haupt, 1998]. The annealing function is using constant temperature simulations on molecules to explore the conformational space available to a molecular system. This is done by simulating motions at a very high temperature, where nearly all conformations are energetically accessible. Thus, energetic barriers can be exceeded to find conformations with energies lower than the local minimum energy found by energy minimisation. [Steinbach & Brooks, 1994]. Then, the molecule is slowly cooled down to room temperature or below and settles into a natural conformation at that temperature.

Annealing can be repeated many times to explore all possible conformations energetically attainable at a given temperature. That way, several different low energy conformations of a single molecule or different low energy configurations of a system of molecules (e.g ligand docked to a receptor) are obtained. The conformations obtained by simulated annealing are further minimised to ensure that the system is truly in a low energy state [Tripos bookshelf, 2002]. Practically, a molecular conformation is minimised using MAXMIN, then annealed and again minimised.

#### 1.11.4 Introduction to SYBYL and the Tripos force field

Tripos' program SYBYL applies a genetic algorithm, which is a programming technique that is used for solving problems and modelling evolutionary systems [Forrest, 1993; Mitchell, 1996]. SYBYL provides the fundamental components for understanding molecular structure and properties with an emphasis on the discovery of lead candidates [Van Opdenbosch *et al.*, 1985]. Geometry optimisation (minimisation) is performed via molecular mechanics or quantum mechanical methods to produce high quality models [Blanco, 1991]. SYBYL offers a variety of force fields as well as several options for computing or importing atomic charges. Several algorithms are available for generating solvent models. The force fields in SYBYL have been extensively tested and validated against the literature. The validation of the Tripos force field 5.2 was based upon crystal structures of small molecules and peptides [Clark *et al.*, 1989]. SYBYL also includes implementations of the 'Amber united-atom and all-atom' force fields [Cornell *et al.*, 1995; Weiner *et al.*, 1984 & 1986; Singh and Kollmann, 1984] as well as MMFF947-9 and MM2 [Halgren, 1990, 1996 & 1999; Burkert and Allinger, 1982].

#### 1.11.5 Introduction to Leapfrog

Structure-based virtual screening has emerged as a reliable, cost-effective and time-saving technique for the discovery of lead compounds. LeapFrog is an example of a software design tool as part of SYBYL (Tripos Inc.) which generates a virtual library of functional monomers containing electrostatic, hydrophobic, and dipole-dipole interactions as well as van der Waals forces or reversible covalent bonds. A molecular model of the template molecule is prepared (charges of each atom are calculated and the structure is refined using molecular mechanics methods). Each of the monomers from the virtual library is probed around the template molecule to investigate possible interactions. A new, potentially active receptor molecule is designed by repeatedly making small structural changes, rapidly evaluating the binding energy of the new compound, and keeping or discarding the changes based on the results [Dixon *et al.*, 1993; Payne *et al.*, 1993]. Unlike other methods, LeapFrog does not require an experimentally known receptor site; it can generate receptor-site models directly from CoMFA (Comparative Molecular Field Analysis) or other models [Cramer *et al.*, 1988].

The generation of new compounds begins with a pool of potential monomers (e.g. amino acids) and a cavity (shown as a box) in which to place them with the target molecule (e.g. ochratoxin A). In each step of this virtual screening process called ‘electrostatic screening’ (Figure 1.12), an existing monomer and a particular atom are randomly selected. Each stage of polymer growth is evaluated according to a molecular mechanics-based energy function, which considers van der Waals interactions, internal strain energy of the lengthening polymer and desolvation of the overall structure [Moon *et al.*, 1991].

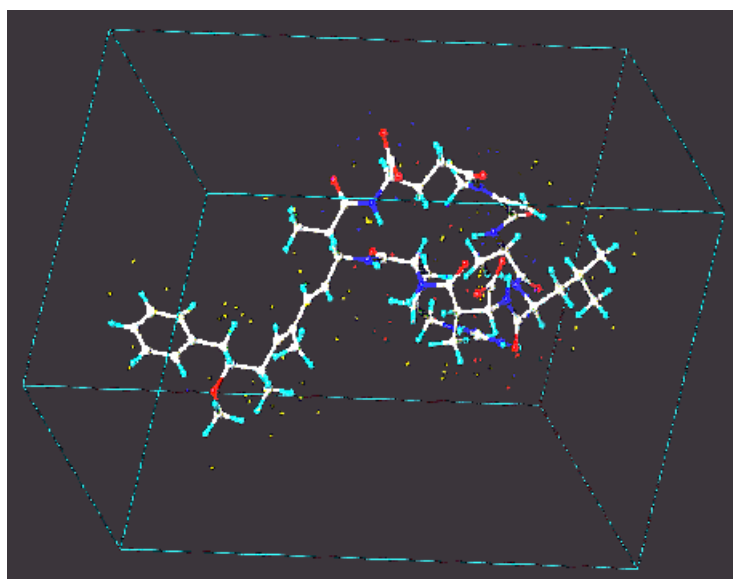


**Figure 1.12:** Leapfrog electrostatic screening displaying all possible site points for the interactions of a molecular template with suitable monomers [Chianella *et al.*, 2002].

Molecules grown by this procedure are subjected to follow-up evaluation in which an approximate binding enthalpy is determined. Therefore, LeapFrog samples the environment surrounding the polymer and determines three major components of binding energy. The direct enthalpies  $\Delta H$  of binding (electrostatic, steric and H-bonding enthalpies) are always calculated. Cavity desolvation energy and polymer desolvation energies are optionally included. An estimate of synthetic difficulty can also be calculated [Goodford, 1985]. The scoring function calculates the binding energy ( $\text{kcal mol}^{-1}$ ) of the resulting structure and if low enough, the new polymer is added to the pool of molecules available for the next move. Over a large number of such moves, the average binding energy of the pool improves [Tripos bookshelf, 2002]. An alternative scoring function that can be used in *de novo* ligand design estimates the binding energy

for a given molecular complex of known 3D structure [Boehm, 1993]. The program LUDI, designed by Boehm [1992] is similar in its application and function to LeapFrog.

### 1.11.6 Docking with FlexiDock

*In vivo*, a detailed description of for example ligand–receptor association leads to a delicate balance between van der Waals and electrostatic interactions, hydrogen bonding, solvation effects, and conformational entropy, all of which are difficult to compute accurately [Janin, 1995; Gilson *et al.*, 1997]. Tingjun and Xiaojie [2004] have discussed the basic ideas and computational tools for virtual screening and scoring functions in molecular docking. Docking procedures aim to identify the energetically most favourable docking structures to predict the affinity between the ligand and receptor. Thus, the goal of molecular docking is to search for the structure and stability of the molecular complex with the global minimum energy, as opposed to minimisation and annealing search for local minima. Molecular docking requires a target receptor structure with or without a bound ligand, the molecules of interest or a database containing existing or virtual compounds for the docking process. A computational framework allows the implementation of the desired docking and scoring procedures. The three-dimensional structure of the receptor-ligand complex has to be detailed at atomic resolution. Since molecules are dynamic, flexibility and motion are clearly important to the biological functioning of proteins and peptides. However, most docking algorithms assume the receptor to be rigid (as flexibility is difficult to compute) whereas the conformation of the ligand is mostly regarded as flexible [Krovat *et al.*, 2005]. Further discussion on recent progressions in molecular docking has been reviewed by Krovat *et al.* [2005] and the computational concepts that have been extended from rigid-body to flexible docking, as well as important strategies for flexible docking and design were reviewed by Rosenfeld *et al.* [1995]. Alberts *et al.* [2005] presented an algorithm for integrating protein binding-site flexibility into *de novo* ligand design and docking processes. The approach allows dynamic rearrangement of for example amino acid side chains during the docking and design simulations. In addition, molecular dynamics simulations, computing the motion of atoms in the molecule according to Newton's law of motion, are applied to calculate the forces acting on the atoms, and thus provide

information about possible conformations, thermodynamic properties, and dynamic behaviour of molecules according to Newton's mechanics.

Scoring of docking processes is still regarded as one of the major challenges in the field of molecular docking. The purpose of the scoring procedure is the identification of the correct binding pose by its lowest energy value, and the ranking of receptor-ligand complexes according to their binding affinities [Muegge and Rarey, 2001]. Genetic algorithm-based Flexible Docking (FlexiDock) provides a means of docking ligands into protein active sites [Tripos bookshelf, 2002].

### 1.11.7 Current research in peptide modelling

SYBYL's ligand-based design techniques use information about one or several known templates (ligands) as a basis for the design of lead compounds (e.g. peptide receptors). Research performed using SYBYL among other force fields for peptide design include peptide ligand-receptor interactions [Singh *et al.*, 1991], or peptide design with enzyme characteristics [Hahn *et al.*, 1990]. Further studies are summarized in Table 1.8.

**Table 1.8:** Research on peptide receptors and synthetic peptides [Tripos<sup>TM</sup>].

Title	Application	Reference
A novel method for the modelling of peptide ligands to their receptors.	SYBYL	Singh <i>et al.</i> [1991]
Computer model of a bovine type I collagen microfibril.	SYBYL	Erickson <i>et al.</i> [1997]
Development of a unique 3D interaction model of endogenous and synthetic peripheral benzodiazepine receptor ligands.	Structure-Based Design	Cinone <i>et al.</i> [2000]
Conformational restriction of the phenylalanine residue in a cyclic opioid peptide analogue: effects on receptor selectivity and stereospecificity.	SYBYL	Schiller <i>et al.</i> [1991.]
Role of the conformational element in peptide-receptor interactions. Studies with cyclic opioid peptide analogs.	/	Schiller <i>et al.</i> [1988]
The use of a proline ring as a conformational restraint in CCK-B receptor "dipeptoids."	Molecular Mechanics	Fincham <i>et al.</i> [1992]
CoMFA investigations on two series of artificial peptide inhibitors of the serine protease thermolysin. Synthesis of an inhibitor of predicted greater potency.	CoMFA, Peptides Proteins, QSAR	Brandt <i>et al.</i> [1995]
Computer design of bioactive molecules: a method for receptor-based de novo ligand design.	Docking, LeapFrog	Moon <i>et al.</i> [1991]
The computer program LUDI: A new method for the de novo design of enzyme inhibitors."	LUDI	Böhm <i>et al.</i> [1992]

Peptides represent a difficulty because of their great conformational flexibility. The design of peptides, amides and peptidomimetics using amino acids as building blocks is described by Boehm [1996] using the computer program LUDI as *de novo* design tool. Current research using LeapFrog as *de novo* design tool includes the structure-based design of enzyme inhibitors [Jordan *et al.*, 2001] using the LeapFrog program to develop a docking model for interaction of ligands with the active site of an enzyme. Modelling of enzyme-peptide inhibitor complexes was performed by Singh *et al.* [1991], whereas other investigations included the structure-based design of protein-binding ligands [Dong *et al.*, 2006]. The successful design of a molecular imprinted polymer for microcystin-LR using a computational approach (SYBYL, LeapFrog) has been shown by Chianella *et al.* [2002]. The *de novo* designed MIP was later on implemented into a MIP-based sensor using a solid phase extraction cartridge [Chianella *et al.*, 2003].

### **1.12 Aims and Objectives**

The aim of this thesis was to develop an affinity sensor for ochratoxin A for determination in wine samples. Comprising the required elements of specificity, sensitivity, time and cost-effectiveness, the biosensor has to be carefully assembled.

Two types of recognition elements were considered; one is a commercially available antibody specifically binding ochratoxin A and the other a synthetic peptide receptor for ochratoxin A, which is designed in this research project using computational modelling. Peptides have various advantages in terms of molecular stability and availability, compared to antibodies, which are being more commonly used in immunosensors. Also, the production of antibodies for a specific molecule can be time and cost-consuming and generally requires animal resources.

The first stage of the biosensor development involves the parallel execution of computational design of peptide receptors for ochratoxin A and the consecutive characterisation of both the antibody and peptide recognition elements using binding assays.

The second stage comprises the construction of the transducer component of the biosensor for both types of recognition elements. The transducer relates the biological signal (as a result of a binding interaction) via a detector towards an electronic data output. Electrochemical detection was chosen using an electrode as transducer. The proposed sensor format was a mediated amperometric immunosensor using screen-printed electrodes directly transducing the current response arising from an indirect competitive enzyme-linked immunoassay. The screen printed electrode sensor is compared to a microelectrode array platform in the context of miniaturisation and portability of the sensor device.

Complexity of wine plays a significant role as all the components of wine have to be considered for achieving interference-free and sensitive detection. The proposed biosensor shall be used to monitor ochratoxin A contamination (possibly on-site the



wine yard) and prevent wine samples that show ochratoxins A contamination above the permissible limit to reach the consumer. That way, the health risk imposed by ochratoxin A consumption may be decreased significantly. The required objectives of the project were carried out as follows:

I. Reagent preparation

- Immunoaffinity purification of selected antibodies for ochratoxin A
- Conjugation of ochratoxin A to horseradish peroxidase

II. Enzyme immunoassay development and affinity characterisation of antibodies

- Incorporation of immuno-reagents into a colorimetric enzyme immunoassay using solid phase microtitre plate supports
- Optimisation of assay parameters (time, temperature and reagent concentration and composition)
- Characterisation of antibody suitability for immunosensor analysis
- Immunoassay format design
- Affinity characterisation of antibodies and cross-reactivity

III. Immunosensor development incorporating the developed immunoassay format

- Fabrication of screen printed electrodes and assembly of the immunosensor
- Electrochemical characterisation of produced sensor supports and incorporated electro-active reagents
- Transfer of the selected antibody and competitive immunoassay format to the electrochemical sensor support
- Optimisation of the amperometric signal sensitivity for enzyme immunoassay transduction
- Determination and optimisation of ochratoxin A standards using the assembled immunosensor

IV. Immunosensor application to wine samples

- Characterisation of the effects from wine sample components on sensor performance
- Establishment of a calibration curve using the immunosensor in wine matrix
- Application of the sensor to determine ochratoxin A contamination in real wine samples

V. Validation against standard methods

- Compare the immunosensor performance to HPLC standard analysis and a commercially available immunoassay test kit.

VI. Computational modelling of peptide recognition elements

- *De novo* design of peptide receptors for ochratoxin A and synthetic peptide library construction
- Characterisation of peptide sequences *in silico* using ligand-receptor docking algorithms

VII. Binding assay and affinity characterisation of peptides

- Synthesis of selected lead peptide sequences for *in vitro* analysis
- Characterisation of peptide suitability for immunosensor analysis using binding assays
- Affinity characterisation of peptide recognition elements

An outline of the consecutive milestones carried out in this thesis is illustrated in the flow chart in Figure 1.13.

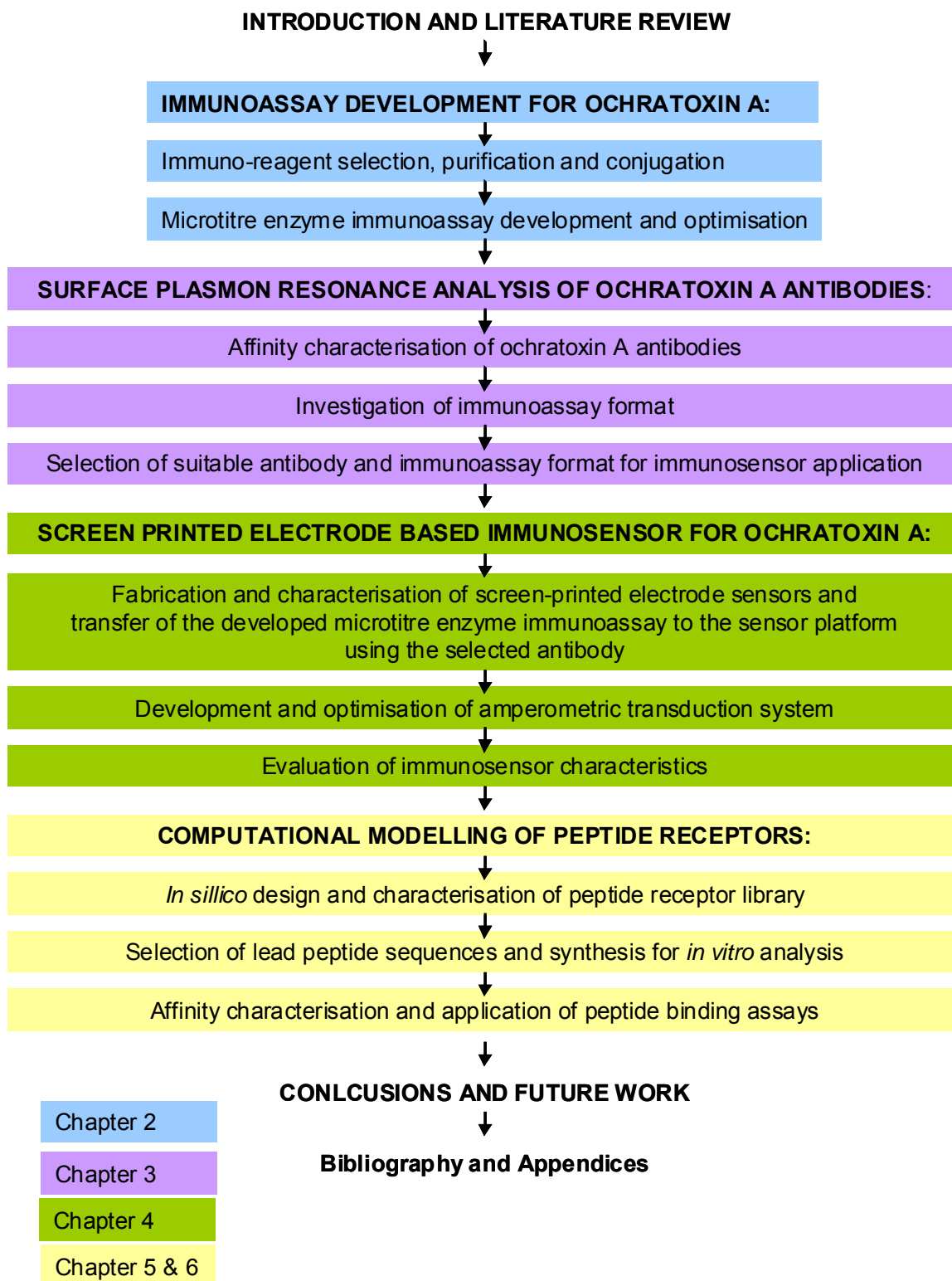


**Figure 1.13 :** Flowchart outlining the consecutive milestones carried out in this thesis.

## **CHAPTER 2 : IMMUNOASSAY DEVELOPMENT FOR OCHRATOXIN A**

### ***2.1 Introduction***

Antibodies are commonly used as recognition elements in binding assays since they can display great selectivity and sensitivity for their antigen. Binding assays involving antibodies are known as immunoassays. When the detection is based on the use of an enzyme label, the method is known as enzyme linked immunosorbent assay. This technique was used in this work to characterise a commercially available polyclonal anti-ochratoxin A antibody (Biogenesis Ltd., UK). The antibody had been raised against ochratoxin A conjugated to the carrier-protein bovine serum albumin (BSA). The manufacturer stated that the specific antibody recognition for ochratoxin A was 100% and cross-reactivity for BSA (adsorbed) was < 0.1%.

In this work, an ELISA test based on the reagents available was developed. By characterising antibody binding and optimising assay conditions, the assay can be specifically tailored to achieve lower detection limits and sensitivity, a wider dynamic range and higher signal:noise ratio. The limit of detection (LOD) regarding the direct and indirect competitive detection format is compared. Furthermore, the possibility to circumvent the need for sample clean-up and pre-concentration is part of the investigation.

## 2. 2 Materials

### 2.2.1 Chemicals and Immunoreagents

All the chemicals used were of analytical grade and these are listed in Table 2.1.

**Table 2.1:** List of chemicals and supplier.

Trivial name	Chemical name	Source
BSA	Bovine serum albumin	Sigma-Aldrich,UK
Casein	Casein from bovine milk	Sigma-Aldrich,UK
C <sub>6</sub> H <sub>8</sub> O <sub>7</sub>	Citric acid	Merck, Germany
EDAC	<i>N</i> -Ethyl- <i>N'</i> -(3dimethylaminopropyl) carbodiimide hydrochloride	Sigma-Aldrich, UK
H <sub>2</sub> O <sub>2</sub>	Hydrogenperoxide solution 30%	Sigma-Aldrich,UK
HRP	Peroxidase from horseradish, Type VI-A	Sigma-Aldrich, UK
OPD	o-Phenylenediamine dihydrochloride	Sigma-Aldrich,UK
NaH <sub>2</sub> PO <sub>4</sub>	Sodiumdihydrogenphosphate	Merck, Germany
Na <sub>2</sub> CO <sub>3</sub>	di-Sodiumcarbonate	Merck, Germany
NaHCO <sub>3</sub>	Sodiumhydrogencarbonate	Merck, Germany
Na <sub>2</sub> HPO <sub>4</sub>	di-Sodiumhydrogenphosphate	Fluka, UK
NHS	<i>N</i> -Hydroxysulfosuccinimide sodium	Sigma-Aldrich, UK
TMB	3,3',5,5'-Tetramethylbenzidine	Sigma-Aldrich, UK
Tween 20	Polyethylene glycol sorbitan monolaurate	Sigma-Aldrich, UK
Ochratoxin A	(R)-N-[(5-chloro-3,4-dihydro-8-hydroxy-3-methyl-1-oxo-1H-2-benzopyran-7-yl) carbonyl]-L-phenylalanine ( <i>Aspergillus ochraceus</i> )	Sigma-Aldrich, UK
Ochratoxin A-BSA	Ochratoxin A ( <i>Aspergillus ochraceus</i> ) conjugated 3 mol per mol bovine serum albumin	Sigma-Aldrich, UK
ochratoxin A-polyclonal antibody	Class: IgG-purified; Species: rabbit; antigen: ochratoxin A-BSA, Concentration: 1 mg ml <sup>-1</sup>	Biogenesis Ltd, Poole, UK
α rabbit IgG-HRP	Class: IgG; Species: goat; antigen: rabbit-Fc, Concentration: 1mg ml <sup>-1</sup>	Dako,Kopenhagen,DK

Due to the potentially carcinogenic properties of ochratoxin A, safety precautions were applied, such as wearing gloves, protection glasses and a mask when handling the powder. The powder was generally dissolved in ethanol or buffer upon arrival and stored in a locked fridge for toxic reagents according to safety instructions.

### 2.2.2 Equipment

The material and equipment used in this work were dialysis cassette Slide-A-Lyzer® 10K (Pierce, Rockford, IL, USA), microtitre plates MaxiSorb™ (Nunc Brand products, DK), FLUOstar Galaxy plate reader (BMG Labtechnologies Inc, US) and Micro titre plate Incubator/ Shaker HT (Labsystems iEMS, USA).

### 2.2.3 Buffer solutions

The compositions of the buffers used are listed below:

#### **Coupling buffer (CB):**

---

*0.05 M Carbonate buffer (pH 9.6)*

2.65 g NaHCO<sub>3</sub>  
3.5 g Na<sub>2</sub>CO<sub>3</sub>  
dissolved in 1 l H<sub>2</sub>O. pH adjusted to 9.6.

#### **Coating buffer (PBS):**

---

*0.1 Phosphate buffered Saline ( pH 7.4)*

2.96 g NaH<sub>2</sub>PO<sub>4</sub>  
11.5 g Na<sub>2</sub>HPO<sub>4</sub>  
8.4 g NaCl  
dissolved in 1 l H<sub>2</sub>O. pH adjusted to 7.4.

#### **Washing buffer (PBST):**

---

*0.1 M Phosphate buffered saline with Tween (pH 7.4)*

2.96 g NaH<sub>2</sub>PO<sub>4</sub>  
11.5 g Na<sub>2</sub>HPO<sub>4</sub>  
5.84 g NaCl  
0.05% (= 0.5 ml) Tween20  
dissolved in 1 l H<sub>2</sub>O. pH adjusted to 7.4.

#### **Substrate buffer:**

---

*44 mM PCB (pH 5.5)*

4.6 g Citric acid (mono- hydrate)  
7.1 g Na<sub>2</sub>HPO<sub>4</sub>  
dissolved in 1 l H<sub>2</sub>O. pH adjusted to 5.5.

**Blocking solution:**

---

1 mg ml<sup>-1</sup> BSA (dissolved in PBS, pH 7.4)  
1 mg ml<sup>-1</sup> casein (dissolved in PBS, pH 7.4)

**Substrate solution:**

---

22 mg ml<sup>-1</sup> OPD  
5 μl 30 % H<sub>2</sub>O<sub>2</sub>  
dissolved in PCB, pH 5.5.

## **2.3 Methods**

### **2.3.1 Immunoaffinity purification of antibody with BSA**

The polyclonal antibody from Biogenesis Ltd was BSA-purified to prevent cross-reacting with BSA. This is done by immobilising a saturating BSA concentration (100 mg L<sup>-1</sup>) to the polystyrene surface of a microtitre plate. The polyclonal ochratoxin A antibody (1 mg ml<sup>-1</sup>) was added (200 μl/well) and left to incubate at room temperature for 2 hours. Cross-reacting polyclonal antibody is bound to the surface-adsorbed BSA, whereas the unbound IgG is removed from the well. BSA-bound antibody is discarded.

### **2.3.2 Ochratoxin A-BSA coating procedure**

Distinct concentrations of ochratoxin A-BSA were immobilised on the polystyrene surface of a microtitre plate (MaxiSorb<sup>TM</sup>) by physical adsorption according to Nunc Bulletin No.1 (2) [Nuncbrand, DK]. The polyclonal ochratoxin A-antibody (Biogenesis Ltd., UK) had been IgG-purified by the manufacturer, so no further purification was necessary. The secondary anti-rabbit-IgG antibody labelled with horse radish peroxidase (Dako Denmark A/S) is recognizing species-specific the F<sub>c</sub> fragment of the applied antibody.

Ochratoxin A-BSA concentrations were coated by adding 100  $\mu\text{l}$ / well solution to the microtitre plate according to Table 2.2.

**Table 2.2:** Ochratoxin A-BSA coating concentrations.

MTP (row)	Ochratoxin A-BSA [ $\mu\text{g L}^{-1}$ ]		
1A	50,000	100,000	750
1B	25,000	10,000	100
1C	10,000	1,000	10
1D	7,500	100	1
1E	5,000	10	
1F	1,000	1	
1G	750	0.1	
1H	500	0	
2A	100		
2B	50		
2C	10		
2D	5		
2E	1		
2F	0.5		
2G	0.1		
2H	0		

Coating was performed (if not stated otherwise\*<sup>1</sup>) in coating buffer (100 mM Carbonate buffer, pH 9.6) for 16 hours at 4°C, followed by washing the plates three times (150  $\mu\text{l}$ / well) using phosphate buffered saline containing Tween 20 (PBST, pH 7.4). Free binding sites on the polystyrene surface were blocked using 1% (w/v) BSA in PBS (pH 7.4) using a volume of 100  $\mu\text{l}$ /well) and incubated at 4°C for 2-6 hours, followed by washing. A dilution of 1/200 from 1 mg ml<sup>-1</sup> stock solution (unless stated otherwise\*<sup>2</sup>) anti-ochratoxin A antibody solution (PBS, pH 7.4) was applied (100  $\mu\text{l}$ /well) and incubated at 4°C for about 18 hours followed by washing. Finally, a dilution of 1/2000 anti-rabbit-IgG-HRP was added (100  $\mu\text{l}$ /well) and incubated at 4°C for 1.5 hours. Before adding the substrate solution, the plate was washed again three times (150  $\mu\text{l}$ /well) with PBST. The o-phenylenediamine (OPD) was prepared in substrate buffer (pH 5.5), whereas H<sub>2</sub>O<sub>2</sub> was added just before adding the solution to the microtitre plate (100  $\mu\text{l}$ /well). Incubation was performed at room temperature (RT) for 5 minutes before measuring the absorbance at 492 nm (or alternatively 450 nm when using TMB/H<sub>2</sub>SO<sub>4</sub> system) in a plate reader.



\*<sup>1</sup> Influence of ochratoxin A-BSA coating concentrations ( Table 2.2, column 3) and time was examined at incubation times of the coating step varying from 0.5; 2; 4; 16 and 48 hours to determine the optimal coating time.

\*<sup>2</sup> Antibody dilution of 1/1000 – 1/10.000 was used when investigating the effect of antibody dilution.

### 2.3.3 Temperature, antibody concentration and blocking reagent addition to the coating buffer

Ochratoxin A-BSA (30 mg L<sup>-1</sup>) was added to the wells (100 µl/well) of a microtitre plate. Incubation was performed at 4°C for 18 hours, followed by washing three times 150µl/ well with phosphate buffered saline containing Tween 20 (PBST). Free binding sites on the polystyrene surface were blocked with either 1% (w/v) casein or 1% (w/v) BSA blocking solution (100 µl/well) and incubated at 4°C for 2 hours, followed by washing. Ochratoxin A-BSA coating (Table 2.3, column 2) was investigated at three different temperatures: 4°C; room temperature (RT), and 37°C. Two different blocking agents, bovine serum albumin (BSA) and casein were investigated and the addition of casein (0.1 % w/v) to the coating buffer.

**Table 2.3:** Antibody dilutions for indirect immunoassay.

MTP (row)	Ochratoxin A-antibody (0.95 mg ml <sup>-1</sup> )	
1A	1/100	1/100
1B	1/500	1/200
1C	1/1000	1/500
1D	1/2000	1/1000
1E	1/4000	1/2000
1F	1/5000	1/5000
1G	1/10000	1/10000
1H	0	Blank

All antibody dilutions (Table 2.3, column 1) deposited at a volume of 100 µl/well were incubated for 4 hours at 4°C, room temperature (RT) and 37°C, respectively. The incubation was followed by washing the wells three times (150 µl/ well) with PBST. A dilution of 1/2000 HRP-labelled secondary antibody was added (100 µl/well) and incubated at 4°C for 1.5 hours and then unbound material washed off. The o-

phenylenediamine (OPD) and H<sub>2</sub>O<sub>2</sub> substrate solution was added (100 µl/well) and incubated at room temperature (RT) for 5 minutes before measuring the absorbance at 492 nm in a plate reader.

The addition of casein (0.1 % w/v) to the coating buffer was investigated for two fixed ochratoxin A-BSA coating concentrations (25 and 50 mg L<sup>-1</sup>) and a dilution series of anti-ochratoxin A-antibody concentrations (Table 2.3, column 2). Secondary antibody and substrate detection was performed as described above.

### 2.3.4 Indirect non-competitive ochratoxin A immunoassay

Free ochratoxin A (Table 2.4) was coated (100 µl/well) onto the microtitre plate at 4°C for about 18 hours, followed by washing three times 150µl/ well with phosphate buffered saline containing Tween 20 (PBST). Free binding sites on the polystyrene surface were blocked with 1% (w/v) casein blocking solution (100 µl/ well) and incubated at 4°C for 2 hours, followed by washing. Each antibody concentration (100 µl/well) was incubated at 4°C, room temperature (RT) and 37°C for 4 hours (Table 2.4, column 1).

**Table 2.4:** Ochratoxin A concentrations adsorbed onto a polystyrene surface.

MTP (row)	Ochratoxin A [µg L <sup>-1</sup> ]
1A	10,000
1B	5,000
1C	1,000
1D	10
1E	1
1F	0

The incubation was followed by washing and addition of 1/2000 HRP-labelled secondary antibody (100 µl/ well) that was incubated at 4°C for 1.5 hours. The o-phenylenediamine (OPD)/ H<sub>2</sub>O<sub>2</sub> substrate solution was added (100 µl/well) and incubated at room temperature (RT) for 5 minutes before measuring the absorbance at 492 nm in a plate reader.

### 2.3.5 Indirect competitive ochratoxin A (-BSA) immunoassay

The competitive format allows ochratoxin A or ochratoxin A-BSA to compete for anti-ochratoxin A-antibody binding sites with immobilized ochratoxin A-BSA. The concentration of the immobilised ochratoxin A-BSA was 30,000  $\mu\text{g L}^{-1}$  to reach surface saturation and the antibody (2500  $\mu\text{g L}^{-1}$ ) was pre-mixed with each competitor concentration, respectively. The concentration range for competing ochratoxin A-BSA was 0.1 to 30,000  $\mu\text{g L}^{-1}$  and for competing un-conjugated ochratoxin A was 1 to 10,000  $\mu\text{g L}^{-1}$  (Table 2.5).

**Table 2.5:** Competitor concentrations pre-mixed with ochratoxin A-antibody.

Standard	Ochratoxin A [ $\mu\text{g L}^{-1}$ ]	Ochratoxin A-BSA [ $\mu\text{g L}^{-1}$ ]
1A	10,000	30,000
1B	5,000	10,000
1C	1,000	1,000
1D	100	100
1E	1	10
1F	0.1	1
1G	0	0

Ochratoxin A-BSA (30,000  $\mu\text{g L}^{-1}$ ) was coated onto each well (150  $\mu\text{l}$ /well) at 37°C on a plate shaker (400 rpm) for 1.5 hours. Washing was performed three times (150  $\mu\text{l}$ /well) with PBST. Free binding sites on the polystyrene surface was blocked with 1% w/v casein (150  $\mu\text{l}$ /well) at 4°C for 2 hours and subsequently washed. Pre-incubation of 1/400 diluted ochratoxin A-antibody with distinct competitor concentrations was performed for 0.5 hours and then added to the microtitre plate (150 $\mu\text{l}$ /well). Incubation was done at room temperature (RT) on a plate shaker (400 rpm) for about 16 hours. After washing with PBST, the secondary (1/2000) was added (150 $\mu\text{l}$ /well) and incubated at RT for 1.5 hours. The plate was washed and the o-phenylenediamine (OPD)/ H<sub>2</sub>O<sub>2</sub> substrate solution was added (100  $\mu\text{l}$ /well) and incubated at room temperature (RT) for 5 minutes before measuring the absorbance at 492 nm in a plate reader.

### 2.3.6 Production of ochratoxin A-HRP conjugate

The conjugation method was adapted from Chu *et al.* [1976]. Ochratoxin A (2 mg) was suspended in 400  $\mu\text{l}$  ethanol (98%) and mixed with 463  $\mu\text{l}$  of 32.5  $\text{mg ml}^{-1}$  EDAC and 862  $\mu\text{l}$  of 8.7  $\text{mg ml}^{-1}$  NHS (PBS, pH 7.4). The solution was stirred for 12 hours at room temperature, then horseradish peroxidase (4 mg dissolved in 1ml PBS, pH 6.5) was added to the solution and stirred for another 12 hours at room temperature adding up to a total reaction volume of 2.72 ml. The conjugate was dialysed against PBS, pH 7.4 for 48 hours at room temperature using a dialysis cassette with a MWCO of 10,000 Da. The A280 for HRP was determined 1.043, which corresponds to a concentration of 43  $\text{mmol L}^{-1}$  and Em 335 nm for ochratoxin A of 0.441, which corresponds to 66  $\text{mmol L}^{-1}$ . The approximate HRP/ochratoxin A ratio is 1.5 which corresponds to 1-2 molecules of ochratoxin A bound to each molecule HRP.

### 2.3.7 Activity characterisation of ochratoxin A-HRP conjugate

A dilution series of ochratoxin A-HRP was prepared in PBS, pH 7.4 (1/1; 1/10; 1/50; 1/100; 1/200; 1/500 and 1/1000 from stock solution of 1.9  $\text{mg mL}^{-1}$ ). Each microtitre plate well contained 100  $\mu\text{l}$ ; then the tetramethylbenzidine (TMB)/ $\text{H}_2\text{O}_2$  substrate solution was added (100  $\mu\text{l}$ / well) and incubated at room temperature (RT) for 5 minutes before stopping the reaction using 10%  $\text{H}_2\text{SO}_4$  and measuring the absorbance at 450 nm in a plate reader.

### 2.3.8 Direct non-competitive ochratoxin A-HRP immunoassay

Protein A (100  $\mu\text{g L}^{-1}$ ) was coated to a microtitre plate by adsorption for 18 hours at 4°C, the non-adsorbed part removed by washing three times with PBST (150  $\mu\text{l}$ /well). Anti-ochratoxin A-antibody concentration (2.5  $\mu\text{g L}^{-1}$ ) was incubated with adsorbed protein A for 2 hours at room temperature and the unbound material removed by washing three times with PBST (150  $\mu\text{l}$ /well). The surface was blocked with 1% w/v casein (150  $\mu\text{l}$ /well) at 4°C for 2 hours. A dilution of 1/100 ochratoxin A-HRP (1.9  $\text{mg ml}^{-1}$ ) was added to incubate with the immobilised antibody for 2 hours at room temperature. The plate was then removed by washing three times with PBST, tetramethylbenzidine (TMB)/ $\text{H}_2\text{O}_2$  substrate solution added (100  $\mu\text{l}$ /well) and incubated

at room temperature for 5 minutes before adding 10% H<sub>2</sub>SO<sub>4</sub> and measuring the absorbance at 450 nm in a plate reader.

### 2.3.9 Wine sample analysis

#### 2.3.9.1 Indirect competitive immunoassay for wine analysis

Ochratoxin A-BSA (30,000 µg L<sup>-1</sup>) was coated onto each well (150 µl/well) at 37°C using a plate shaker (400 rpm) for 1.5 hours. Washing was performed three times (150 µl/ well) with PBST. Free binding sites on the polystyrene surface were blocked with 1% casein (150 µl/well) at 4°C for 2 hours. A volume of 50 µl wine sample was diluted 1:2 with dilution buffer (5% w/v NaHCO<sub>3</sub> and 1% w/v PEG). The diluted wine sample was pre-incubated with 1/400 dilution ochratoxin A-antibody (1 mg ml<sup>-1</sup>) for 0.5 hours and then added (150µl/ well) to the microtitre plate (Table 2.6).

**Table 2.6:** Wine samples pre-mixed with ochratoxin A-antibody

MTP	Sample ID and standards			
A	red01	red09	white06	Standard 0 ng L <sup>-1</sup>
B	red02	red10	white07	Standard 25 ng L <sup>-1</sup>
C	red03	red11	white08	Standard 75 ng L <sup>-1</sup>
D	red04	white01	white09	Standard 225 ng L <sup>-1</sup>
E	red05	white02		Standard 675 ng L <sup>-1</sup>
F	red06	white03		Standard 2025 ng L <sup>-1</sup>
G	red07	white04		
H	red08	white05		

Incubation was done at room temperature (RT) on a plate shaker (400 rpm) for about 16 hours. After washing three times (150 µl/well) with PBST, the secondary IgG-HRP (1/2000) was added to each well (150µl/well) and incubated at RT at 400 rpm for 1.5 hours. The plate was the washed three times (150 µl/well) with PBST and the tetramethylbenzidine (TMB)/H<sub>2</sub>O<sub>2</sub> substrate solution (100 µl/well) incubated at room temperature (RT) for 5 minutes before stopping the reaction using 10% H<sub>2</sub>SO<sub>4</sub> and measuring the absorbance at 450 nm in a plate reader.

### **2.3.9.2 Wine analysis using an immunoassay test kit (Ridascreen)**

Wine samples were prepared following two protocols. The first method performs sample clean-up and pre-concentration according to the OchraTest™ (Vicom Ltd., UK) procedure as follows: A volume of 5 ml wine was added to 5 ml of diluting solution (5% NaHCO<sub>3</sub> +1% PEG, pH 8.3) and mixed. The Ochratest™ immunoaffinity column was connected to a pumpstand and 10 ml diluted sample solution was passed through the column at a flow rate of 1-2 drops/second using a syringe. The column was washed with 5 ml washing solution (2.5% NaCl + 0.5% NaHCO<sub>3</sub>) at a flow rate of 1-2 drops/second and then dried. Ochratoxin A was eluted by passing 2 ml methanol, at a flow rate of 1 drop/second, through the column. The methanol eluate was evaporated to dryness at 50°C under Nitrogen atmosphere and re-dissolved immediately in 250 µL PBS, pH 7.4. The second method applies dilution to reduce possible interferences as a simple alternative to extensive sample clean-up procedures. All wine samples were diluted 1:2 in dilution buffer (5% NaHCO<sub>3</sub> and 1% PEG) and processed by taking 50 µl of either immunoaffinity-treated or diluted wine sample and adding it to the microtitre plate (coated with adsorbed ochratoxin A-antibodies) of the ochratoxin A test kit (Ridascreen®). A volume of 100 µl/well of 1/500 diluted ochratoxin A-HRP conjugate (test kit) was added and incubation performed at room temperature for 2 hours. The plate was washed three times using a spray water bottle and the TMB chromogen (50µl) and substrate (50µl) solution was added immediately and incubated for up to 10 minutes before stopping the reaction using 10 % H<sub>2</sub>SO<sub>4</sub> and reading the absorbance at 450 nm in a plate reader.

### **2.3.9.3 Wine analysis using HPLC**

Wine samples were prepared according to the OchraTest™ AOAC HPLC procedure for wine and beer as follows. A wine sample (5 ml) was diluted 1:1 with dilution buffer (1% PEG + 5% NaHCO<sub>3</sub>, pH 8.3) and mixed vigorously. The Ochratest™ immunoaffinity column was connected to a column stand and 10 ml sample dilution was added to the column reservoir. The solution was manually passed through the column at a flow rate of 1-2 drops/second using a syringe (according to OchraTest™ manual instructions). The column was washed with 5 ml washing solution (2.5% NaCl

+ 0.5% NaHCO<sub>3</sub>) and then dried by passing air through the column. Ochratoxin A was eluted by passing 2 mL 99% methanol at the same flow rate. The eluate was evaporated to dryness at 50 °C under Nitrogen. The eluate was re-dissolved immediately in 250 µL HBS buffer, pH 7.4 for the immunoassay test kit application and in HPLC mobile phase, water: acetonitrile: glacial acetic acid (51:47:2), pH 3.2, for HPLC analysis. The HPLC system used consisted of a Millipore Water 600E system controller, a Millipore 712 WISP autosampler and a Millipore Waters 470 scanning fluorescence detector (Millipore Corporation, MA, USA) with excitation at 330 nm and emission at 460 nm). The samples were separated using a C18 Luna Spherisorb ODS2 column (150 x 4.6 mm, 5 mm) (Phenomenex, Macclesfield, U.K.), with a guard column of the same material. Run time for samples was 15 min with OTA being detected at about 5.75 min. The flow rate of the mobile phase was 1 ml min<sup>-1</sup> and the injection volume per sample 50 µl. Standards used were 50–1200 ng ml<sup>-1</sup>.

## **2.4 Results and Discussion**

To achieve a good signal:noise ratio and low detection limits as well as reproducibility and a relevant dynamic range, ideal concentrations of each assay reagent are established empirically. To establish the optimal dilutions checkerboard titrations are performed, by varying the concentrations of two components of the assay. That way, optimal ochratoxin A-BSA coating concentration and antibody concentration were established. Blocking reagents BSA and casein were validated. By varying incubation times and temperatures, the optimal assay parameters were characterised. For detection, the enzyme label horseradish peroxidase was chosen as it is commonly used in colorimetric assays as it is stable, has a relatively high turnover rate and can be used with many chromogenic substrates. A direct and indirect immunoassay format developed in this work is compared against each other and the literature.

### **2.4.1 Ochratoxin A-BSA coating concentration**

Preliminary ochratoxin A-BSA coating concentration and the anti-ochratoxin A-antibody concentration were determined using a titration assay. Primarily, the polyclonal antibody was BSA-purified to reduce cross-reaction with the BSA-conjugate. Ochratoxin A-BSA adsorption was chosen as the BSA-conjugate is easily adsorbed to the polystyrene surface of a micro titre plate and the passive immobilisation does not necessarily affect the ochratoxin A epitope. A broad concentration range of 0.1 – 50,000  $\mu\text{g L}^{-1}$  ochratoxin A-BSA was immobilised to establish the dynamic range of the assay. Figure 2.1 describes three saturation curves for increasing ochratoxin A-BSA coating concentrations, where each curve depicts a distinct dilution of polyclonal anti-ochratoxin A-antibody used for the binding interaction (Figure 2.1).



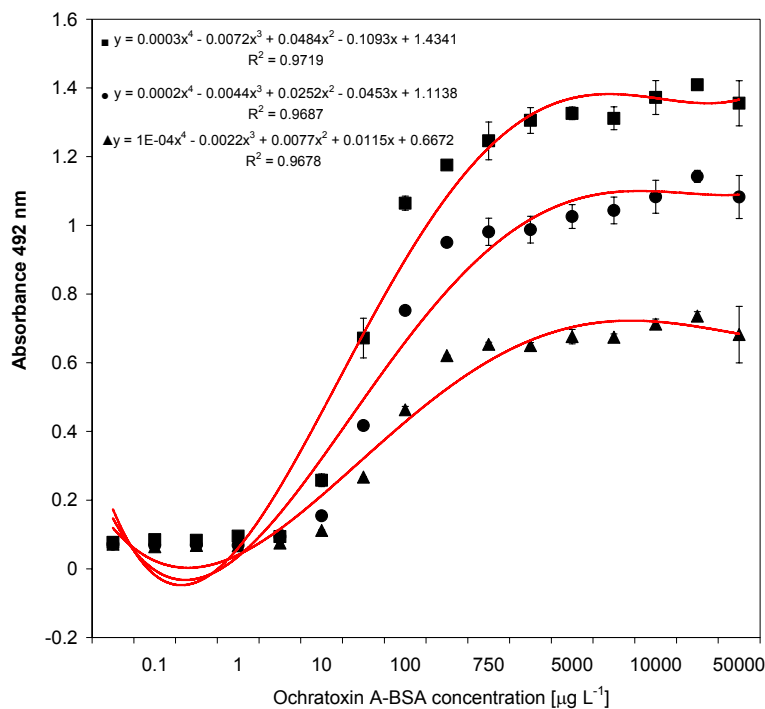


**Figure 2.1:** Serial dilution curve of adsorbed ochratoxin A-BSA. The ochratoxin A-antibody is binding at three distinct dilutions (■ 1/2000; ● 1/4000, and ▲ 1/6000) diluted from stock solution of  $1 \text{ mg ml}^{-1}$ . Absorbance was at 492 nm by monitoring the catalysis of OPD with  $\text{H}_2\text{O}_2$  by HRP. Each error bar represents standard deviation of three replicates. The curves were fitted using a 4-parameter fit.

The absorbance increased (Figure 2.1) with the antibody concentration (reduced dilution) and also with the increasing ochratoxin A-BSA concentration confirming interaction of antibody with ochratoxin A-BSA. All antibody dilutions reached saturation at an ochratoxin A-BSA coating concentration of  $750 \text{ } \mu\text{g L}^{-1}$ .

The dynamic range of the assay is the linear part of the binding curve. In the following plot (Figure 2.2), the dynamic range was fitted by linear regression.

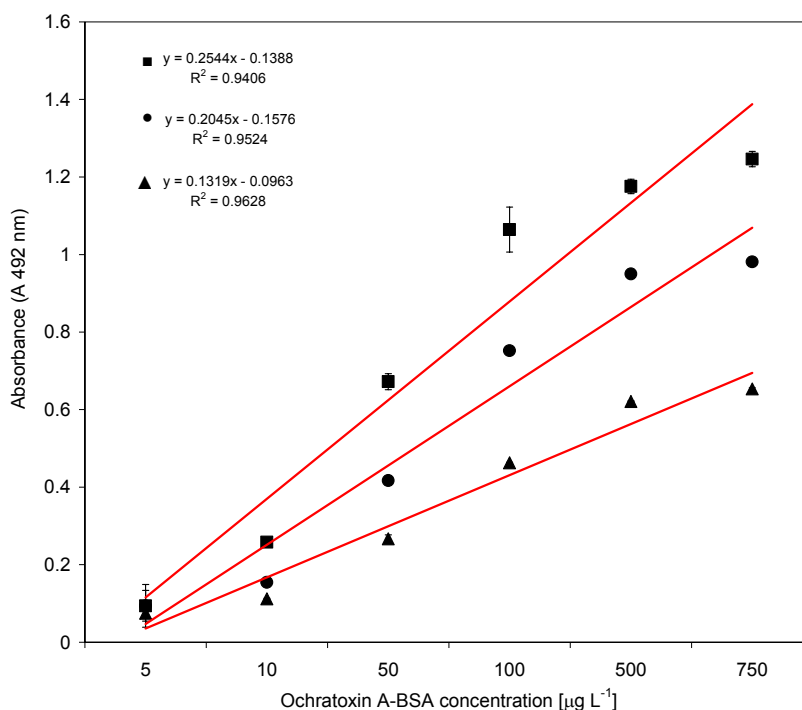


**Figure 2.2:** Logarithmic scale of the dynamic working range showing three anti-ochratoxin A-antibody dilutions (■ 1/2000; ● 1/4000, and ▲ 1/6000) made from stock solution of  $1 \text{ mg ml}^{-1}$ . Absorbance was at 492 nm by monitoring the catalysis of OPD with  $\text{H}_2\text{O}_2$  by HRP. Each error bar represents standard deviation of three replicates. Linear regression depicts corresponding equations and R-squared values.

The dynamic range depicted in Figure 2.2 covers an ochratoxin A-BSA concentration range from  $5\text{-}750 \mu\text{g L}^{-1}$ . The widest dynamic range was observed at an antibody dilution of 1/2000 ( $500 \mu\text{g L}^{-1}$ ). The best signal/noise ratio of this assay was also observed with 1/2000 antibody dilution.

The limit of detection (LOD) is the lowest quantity of a substance that can be distinguished from the blank value within a stated confidence limit [Currie, 1997]. The detection limit for this assay was determined as 10 % absorbance signal distinction from the blank absorbance (0.07) and was calculated to be about  $5\text{-}10 \mu\text{g L}^{-1}$  ochratoxin A-BSA for all antibody concentrations.

### 2.4.2 Increased dynamic range of the assay

To decrease the limit of detection, ochratoxin A-antibody dilutions were further optimised in order to establish, if higher dilutions can be used while reaching a sufficient binding interaction. To increase the sensitivity of the assay, ochratoxin A-BSA coating concentration was increased to  $100,000 \mu\text{g L}^{-1}$  to increase the binding capacity when using more diluted antibody concentrations (Figure 2.3).

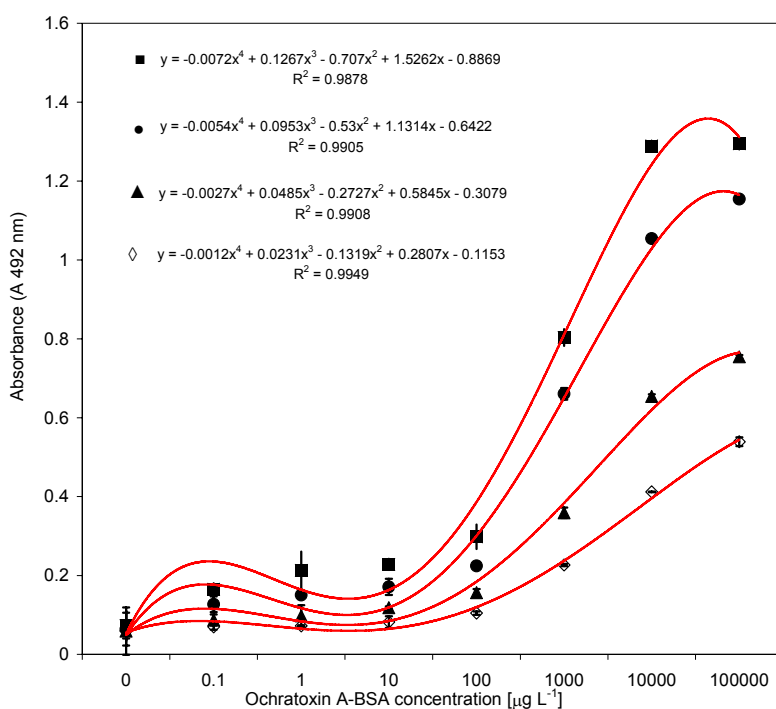


**Figure 2.3:** Serial dilution curve of ochratoxin A-BSA adsorbed to the wells of a microtitre plate. The anti-ochratoxin-antibody is shown binding at four distinct dilutions (■ 1/1000; ● 1/2000, ▲ 1/5000, and ◇ 1/10,000) from stock solution  $1 \text{ mg ml}^{-1}$ . The highest antibody concentration 1/1000 achieved saturation which indicates its molecular excess on the microtitre plate. Absorbance was determined at 492 nm by monitoring the catalysis of OPD with  $\text{H}_2\text{O}_2$ . Each error bar represents standard deviation of two replicates. The curves were fitted using a 4-parameter fit.

The blank absorbance was  $0.06 \pm 0.006$  (0.1 or lower is recommended), which confirmed the absence of unspecific binding. The signal:noise ratio was best for the antibody dilutions 1/1000 ( $1000 \mu\text{g L}^{-1}$ ) and 1/2000 ( $500 \mu\text{g L}^{-1}$ ). The dynamic range covers an ochratoxin A-BSA concentration range from  $100 - 10,000 \mu\text{g L}^{-1}$  for the antibody dilutions 1/1000 ( $1000 \mu\text{g L}^{-1}$ ) to 1/2000 ( $500 \mu\text{g L}^{-1}$ ) showing an expansion of the dynamic range towards higher ochratoxin A-BSA concentrations as compared to Figure

2.2. The detection limit for this assay is  $>10\mu\text{g L}^{-1}$ . Also, the absorbance signal for similar ochratoxin A-BSA coating concentrations was lower as compared to Figure 2.1, which becomes particularly obvious with an antibody dilution of 1/2000. At a concentration of  $100\text{ }\mu\text{g L}^{-1}$  ochratoxin A-BSA, the absorbance results in 1.06 as seen in Figure 2.1, whereas the same coating concentration in Figure 2.3 results in an absorbance signal of 0.22. This shows that the assay in Figure 2.1 shows the better sensitivity of the two assays and that higher coating concentrations are not improving the sensitivity or the dynamic range of the assay.

Higher antibody dilutions (1/5000 - 1/10,000) are also not recommended as the signal:noise ratio decreases substantially and saturation is not reached. The optimal antibody dilution of 1/2000 ( $500\text{ }\mu\text{g L}^{-1}$ ) is 5 - 20 times higher than the dilution recommended by the manufacturer Biogenesis Ltd which is 1/100-1/400 (stock concentration  $1\text{ mg ml}^{-1}$ ). The  $A_{50}$  value (signal at 50% absorbance) indicated an optimal coating concentration for ochratoxin A-BSA of about  $700\text{ }\mu\text{g L}^{-1}$  at an antibody dilution of 1/2000 ( $500\text{ }\mu\text{g L}^{-1}$ ).

### **2.4.3 Ochratoxin A-BSA coating incubation time**

A range of four ochratoxin A-BSA coating concentrations ( $1\text{-}750\text{ }\mu\text{g L}^{-1}$ ) were selected from the linear portion of the dynamic range shown in Figure 2.2 covering the optimal coating concentration  $A_{50}$  (established in Section 2.4.2, Fig. 2.3). Incubation times of the coating step varied from 0.5 to 48 hours to determine the optimal coating incubation time. A 5 fold excess of the optimal ochratoxin A antibody dilution of 1/2000 ( $500\text{ }\mu\text{g L}^{-1}$ ), that is 1/200 ( $5000\text{ }\mu\text{g L}^{-1}$ ), was used to reach saturation. Saturation was performed to ensure that the incubation time is the only parameter influencing the binding interaction.

Also, higher concentrations of specific antibodies allow for the shortening of the incubation time and thus will allow determination of the shortest possible incubation time under these conditions. An incubation temperature of  $4^{\circ}\text{C}$  was applied to diminish the effect of possible non-specific interactions that are more likely to arise with higher

temperatures. The binding capacity dependence on incubation time is shown in Figure 2.4.

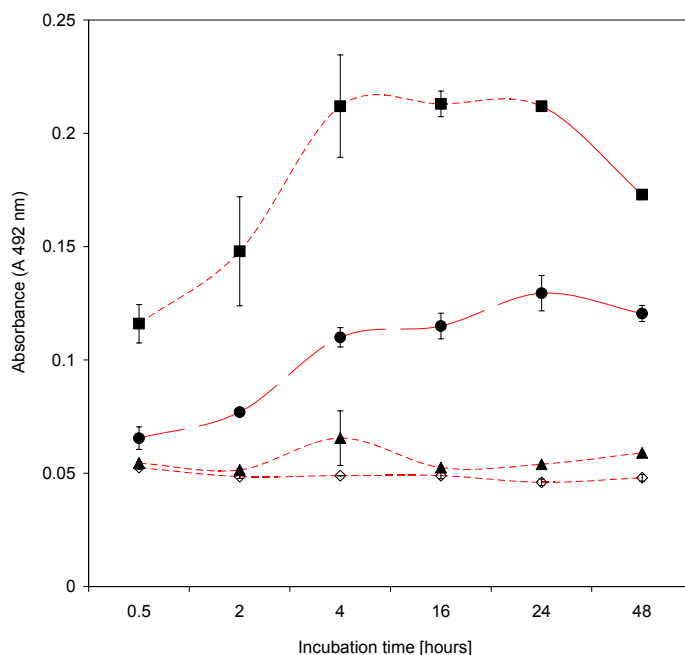


**Figure 2.4:** Different concentrations of adsorbed ochratoxin A-BSA is shown as a function of coating time. Ochratoxin A-BSA was adsorbed to the wells of a microtitre plate at coating concentrations (■ 750 µg L<sup>-1</sup>; ● 100 µg L<sup>-1</sup>; ▲ 10 µg L<sup>-1</sup> and ◇ 1 µg L<sup>-1</sup>). The anti-ochratoxin-antibody was added at 1/200 dilution made from stock solution 1 mg L<sup>-1</sup> and incubated overnight at 4°C. Absorbance was determined at 492 nm monitoring the catalysis of OPD with H<sub>2</sub>O<sub>2</sub>. Each error bar represents standard deviation of two replicates.

Figure 2.4 illustrates the distinct increase in signal with increasing ochratoxin A-BSA coating concentrations for the two highest coating concentrations 100 and 750 µg L<sup>-1</sup>. Using a coating concentration of 750 µg L<sup>-1</sup> ochratoxin A-BSA, 4 hours coating was necessary to ensure maximum adsorption. Coating times above 24 hours (24 – 48 hours incubation) showed a significant decrease in signal by about 19 % (decrease from 100 % at maximum absorbance signal at 4-24 hours) to 81 % decrease in absorbance signal at 48 hours incubation.

There is a strong possibility of denaturation when biomaterials are incubated for longer periods of time and even more when using high temperatures. It was shown that ochratoxin A-BSA physically adsorbed to the plate did not desorb during 24 hours of incubation for coating concentrations 100 and 750 µg L<sup>-1</sup>. Coating concentration below

1-10  $\mu\text{g L}^{-1}$  showed no significant signal increase which leads to the conclusion that these concentrations are too low using the given antibody concentrations.

#### **2.4.4 Antibody incubation time, temperature and blocking reagent**

Equilibrium in antigen-antibody reactions is often reached more quickly at 37°C compared to room temperature or lower temperatures. As binding interaction reaches equilibrium faster, an increase in incubation temperature allows for a greater dilution of the antibody or a shortened incubation time, which would be both advantageous. However, high incubation temperatures can result in denaturation of biomaterials. In this experiment, the influence of temperature was determined. In addition, the antibody incubation time was varied for each temperature as to investigate how temperature and time relate for the antibody binding interaction.

Coating was performed with the established range of ochratoxin A-BSA coating concentrations (1 - 750  $\mu\text{g L}^{-1}$ ). The assay was performed at three different temperatures: 4°C; room temperature (RT), and 37°C to characterise temperature influence on ochratoxin A-BSA coating and antibody-ochratoxin A binding interaction.

The incubation times for ochratoxin A-antibody were in the range of 0.5 - 48 hours. The influence of antibody incubation time at 4°C incubation temperature for BSA (A) and casein (B) blocking is shown in Figure 2.5.

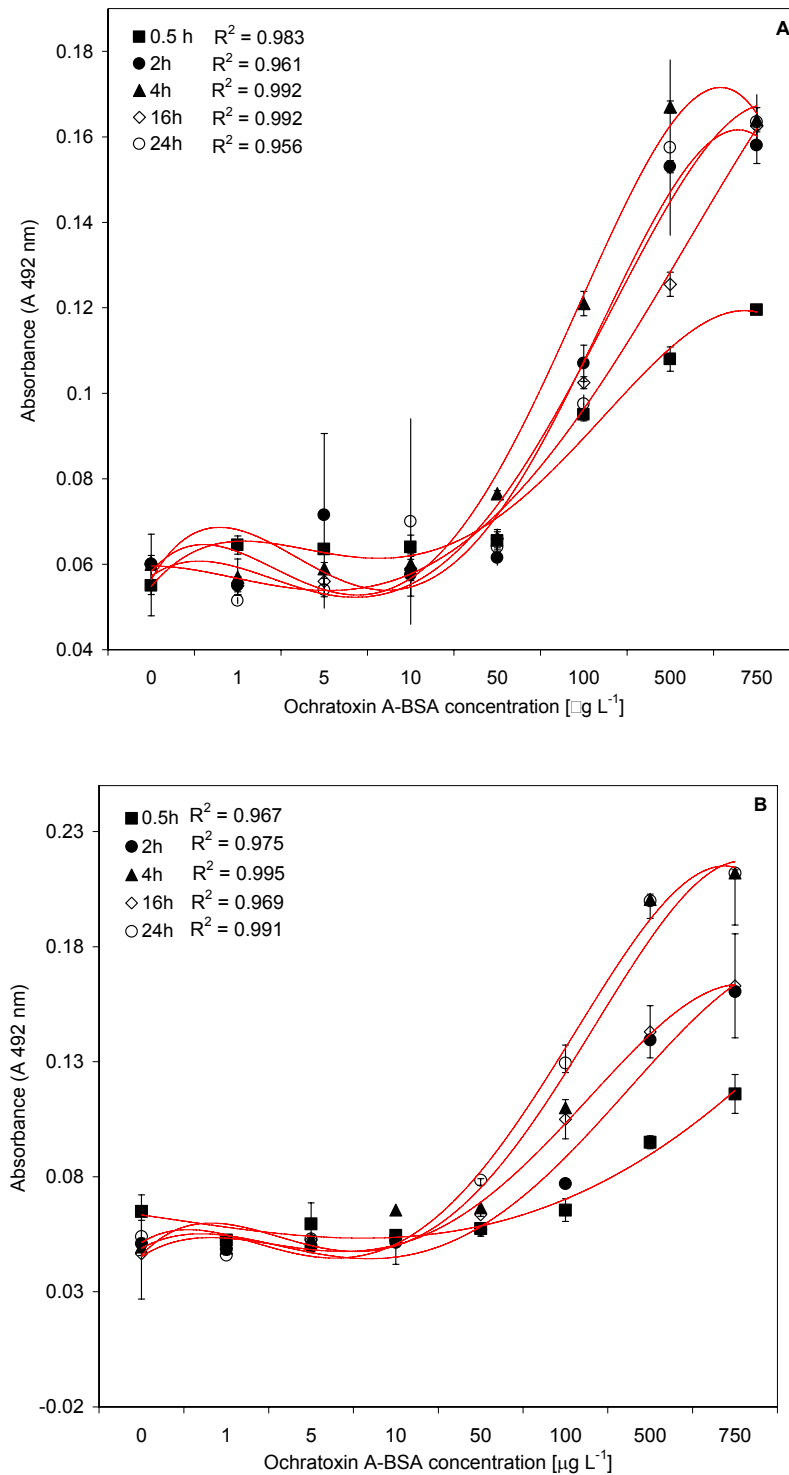


**Figure 2.5:** Serial dilution curve of ochratoxin A-BSA at 4°C incubation temperature versus incubation time (■ 0.5, ● 2; ▲ 4, ◇ 16, and ○ 24 hours) of anti-ochratoxin A-antibody. The anti-ochratoxin-antibody was added at 1/200 dilution made from stock solution 1 mg L<sup>-1</sup> and incubated overnight at 4°C. Blocking reagent was bovine serum albumin (A) and casein (B). Absorbance was determined at 492 nm monitoring the catalysis of OPD with H<sub>2</sub>O<sub>2</sub>. Double measurements were performed and the standard deviation is depicted as error bars.

At an incubation temperature of 4°C (Figure 2.5), the absorbance signal ranged between 0.05 – 0.25 absorbance units, which is compared to previous curves of the same assay design, relatively low and probably a result of experimental error in the microplate assay design. However, a signal increase for a range of increasing antibody incubation times (depicted as curves) was observed for increasing ochratoxin A-BSA concentrations. At 4°C incubation temperature, there is a significant increase antibody incubation time above 0.5 hours for both BSA and casein blocking (Figure 2.5). As the signal reaches a plateau as shown in Figure 2.5A, equilibrium (antibody binding 500 µg L<sup>-1</sup> ochratoxin A-BSA) is reached after 4 hours as the signal does not change much with higher incubation times.

Figure 2.5B depicts that equilibrium was not reached before an incubation time of four hours and required higher coating concentrations to reach a signal plateau. Generally, the signal did not seem to decrease thereby suggesting a low dissociation rate of the antigen-antibody complex. However, the signal curve at 16 hours (Figure 2.5B) showed less binding than at 2, 4, and 24 hours, which is likely due to an experimental error.

Figure 2.6 illustrates the binding at room temperature (RT) showing a signal range of 0.05 – 0.3 OD. An increase in signal with increasing antibody incubation time was also observed. A major characteristic compared to incubation at 4°C is a clearer distinction of curves for every incubation time. When blocking with BSA, the signal reached a plateau at 4 hours at a coating concentration of 500 µg l<sup>-1</sup> ochratoxin A-BSA. Lower incubation times showed a significantly lower signal. However, a signal decrease was observed at incubation times 16-24 hours (Figure 2.6 A). When blocking with casein, the signal increased from 0.5 to 4 hours and then stabilised. An incubation of 16 hours showed again a drop in signal. No plateau was reached at 24 hours (Figure 2.6 B).



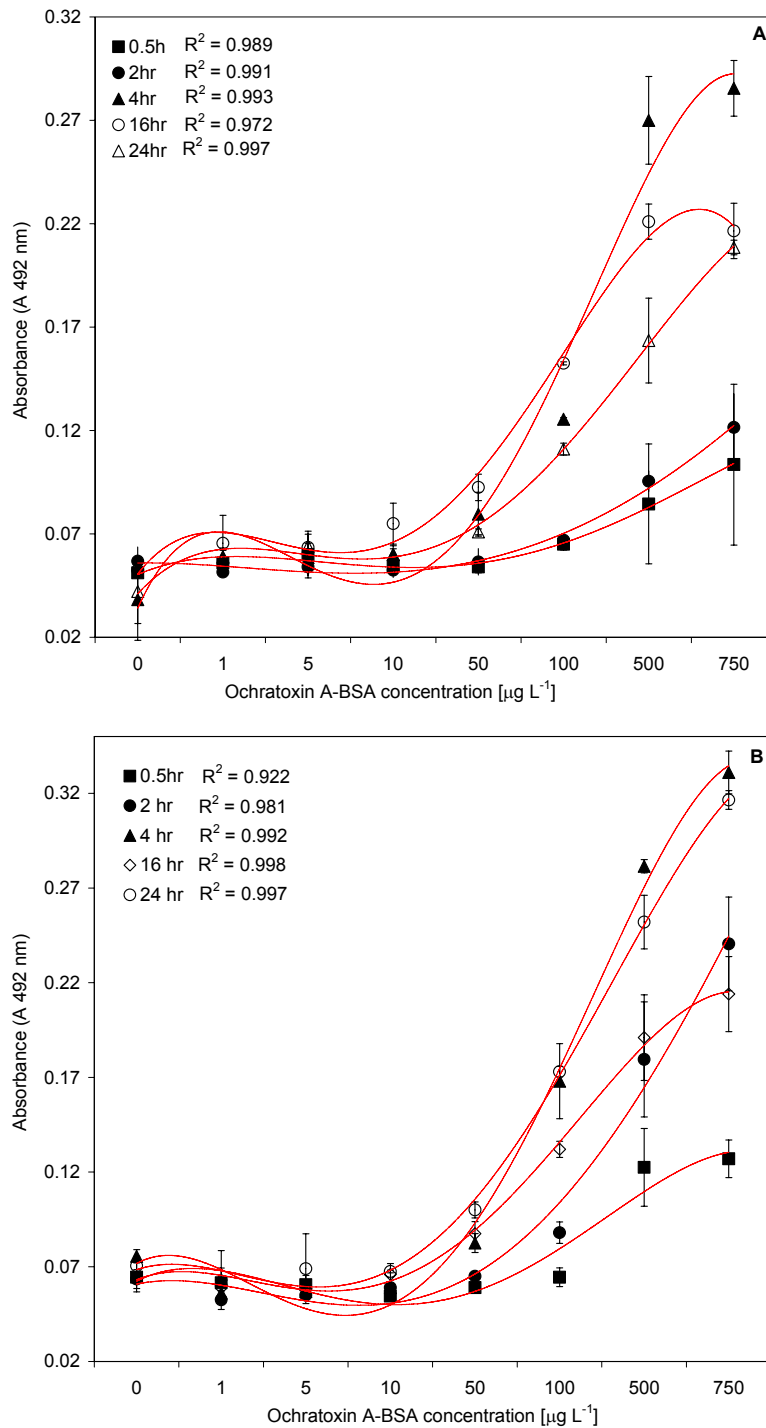


**Figure 2.6:** Serial dilution curve of ochratoxin A-BSA at room temperature versus incubation time (■ 0.5, ● 2; ▲ 4, ◇ 16, and ○ 24 hours) of anti-ochratoxin A-antibody. The anti-ochratoxin-antibody was added at 1/200 dilution made from stock solution 1 mg L<sup>-1</sup>. Blocking reagent was bovine serum albumin (A) and casein (B). Absorbance was determined at 492 nm monitoring the catalysis of OPD with H<sub>2</sub>O<sub>2</sub>. Double measurements were performed and the standard deviation is depicted as error bars.

Figure 2.6 confirms that incubation at room temperature allows for a more reliable distinction between incubation times. It is also shown that the standard deviation seems to be generally lower for casein blocking. Generally, an incubation time of 0.5 - 2 hours would be sufficient to result in significant binding, however, to reach a binding equilibrium, higher incubation times are of advantage. Although at incubation times above 24 hours, desorption of the coated ochratoxin A-BSA may occur.

The Figure below shows the binding curves at 37°C (Figure 2.7). The signal ranged between 0.05 – 0.25 absorbance units which is a further increase in binding capacity. Both graphs showed an increase in signal with increasing incubation time 0.5 to 4 hours. Thus, Figure 2.7 confirms the data obtained at room temperature (Figure 2.6A), which is an optimal incubation time of 4 hours when using the BSA block. It also becomes evident, that at 37°C, incubation times from 16-24 hours result in a decrease in overall signal.

Overall, the standard deviations increases with increasing temperature, whereas BSA blocking shows higher standard deviation values than casein at 4°C and room temperature, whereas at 37°C incubation, the standard deviation between BSA and casein seem to be similar. Incubation at room temperature and 37°C resulted in an optimal antibody incubation time of four hours. Incubation at 4°C showed lower signal values, but an optimal incubation time of 2 hours.

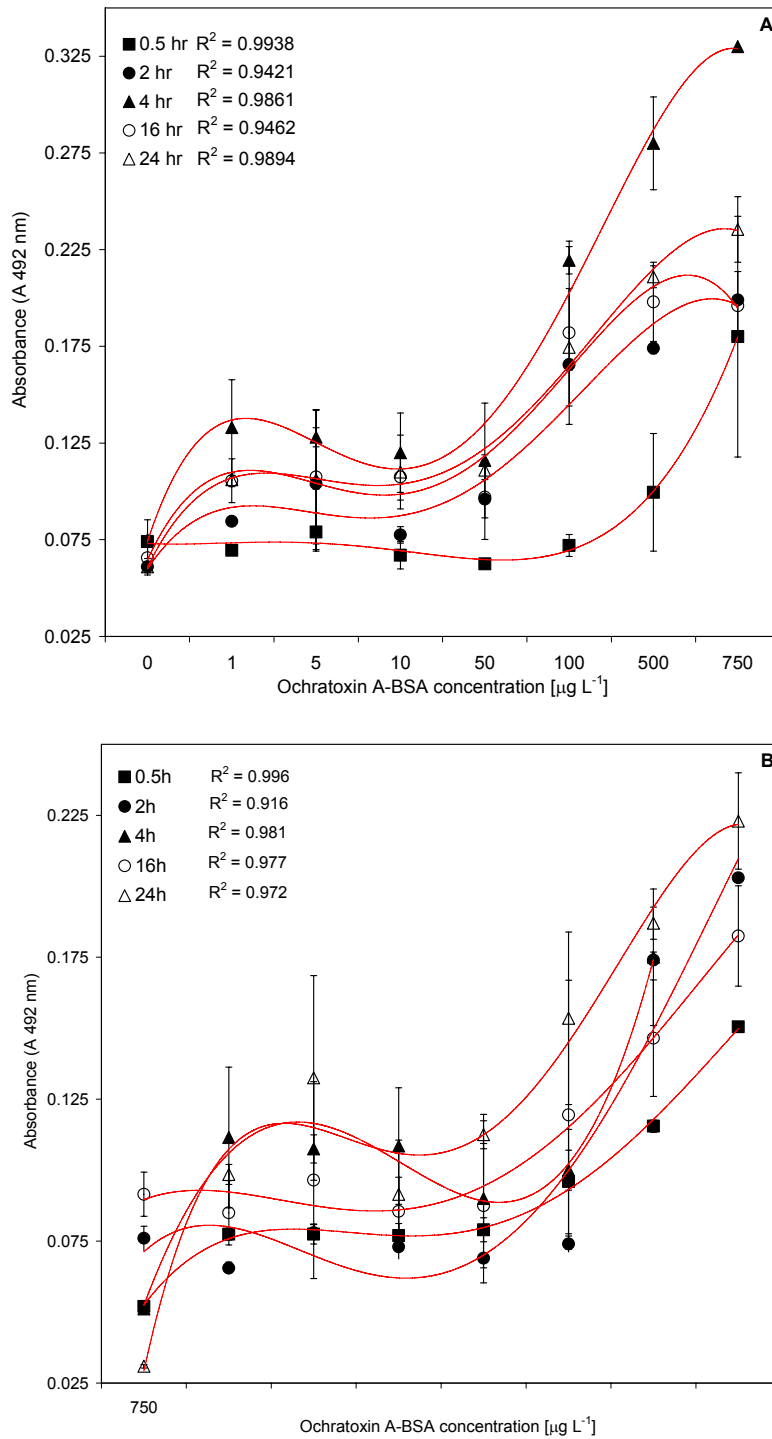


**Figure 2.7:** Serial dilution curve of ochratoxin A-BSA at 37°C incubation temperature versus incubation time (■ 0.5, ● 2; ▲ 4, ◇ 16, and ○ 24 hours) of anti-ochratoxin A-antibody. The anti-ochratoxin-antibody was added at 1/200 dilution made from stock solution 1 mg L<sup>-1</sup>. Blocking reagent was bovine serum albumin (A) and casein (B). Absorbance was determined at 492 nm monitoring the catalysis of OPD with H<sub>2</sub>O<sub>2</sub>. Double measurements were performed and the standard deviation is depicted as error bars.

Overall, binding equilibrium (signal plateau) 4°C, to a lesser extent at room temperature, but was not reached at 37°C. It is not known whether temperature promotes the antigen-antibody reaction selectively rather than the various reactions that give rise to background noise. Here, the lowest temperature seems to promote the antigen-antibody interaction better than higher temperatures. Also, regarding the blocking reagents, BSA blocking generally seems to assist the equilibrium, whereas with casein blocking a plateau is only reached at 4°C. As the standard deviation of BSA is clearly larger at 4°C and room temperature incubation, the casein block seems to be better for this application. The effect of temperature on antigen-antibody binding interaction shows that the binding capacity is increased with increasing temperature; however, binding equilibrium decreases with increasing temperature. Therefore, it was concluded that future binding assays will be performed at optimal incubation temperature of 4°C (or for maximum binding capacity at room temperature) using casein blocking and an incubation time of ochratoxin A-antibody of 4 hours.

#### **2.4.5 Calculation of the functional affinity constant**

The term ‘functional affinity’ describes the interaction of an immobilised antigen with its corresponding antibody without the influence of multi-valence. Introducing a solid phase such as a microtitre plate (for the immobilisation of one of the reactants) complicates the determination of affinity [Underwood *et al.*, 1993]. Diffusion effects play an important role in heterogeneous binding by slowing down the association and dissociation rate, thus affecting the attainment and/or the position of the equilibrium. Moreover, surface effects such as antigen-density dependent steric hindrance and bivalent antibody binding can influence the estimation of the affinity constant [Nygren and Stenberg, 1989, Underwood, 1993]. The method developed by Beatty *et al.* [1987] belongs to the class of solid phase affinity measurements which directly estimates the affinity constant from solid-phase binding of the antibody. This method uses serial dilution of both antigen (coated to the plate) and antibody for measuring affinity constants using the ‘Law of Mass Action’.

However, Beatty *et al.* [1987] assume that the reaction reaches equilibrium and therefore justifying the use of the Law of Mass Action. According to Loomans *et al.*

[1995], these assumptions are theoretical questionable and developed an improved method to determine the functional affinity constant by the coating conditions, and not by any other limiting experimental conditions such as multi-valent binding, steric hindrance or severe diffusion effects. Figure 2.8 depicts absorbance change for serial dilution of antibody binding to seven decreasing ochratoxin A-BSA coating concentrations.

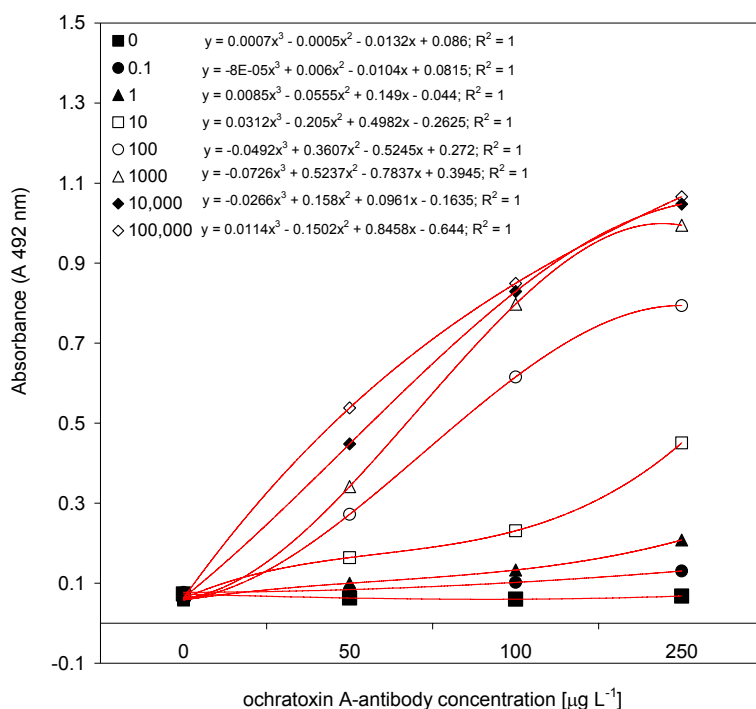


**Figure 2.8:** Experimental signal curve for anti-ochratoxin A antibody at 7 different ochratoxin A-BSA coating concentrations (■ 0, ● 0.1, ▲ 1, □ 10, ○ 100, △ 1000, ◆ 10,000, and ◇ 100,000 µg L<sup>-1</sup>). Absorbance was determined at 492 nm monitoring the catalysis of OPD with H<sub>2</sub>O<sub>2</sub>. The curves were fitted using a 4-parameter fit.

From Figure 2.8, the functional affinity constant ( $K_{aff}$ ) was calculated by selecting the antibody dilution, which was necessary to achieve 50% of the maximum absorbance value ( $A_{50}$ ). This antibody dilution was used in the following equation, derived from the Beatty formula [Beatty *et al.*, 1987]:

$$K_{aff} = (n-1) / 2(n [Ab'] - [Ab]) \quad \text{Equation X}$$

The terms [Ab] and [Ab'] equal the antibody concentration at  $A_{50\%}$  each corresponding for [Ag] and [Ag'], respectively; and  $n = [Ag] / [Ag']$ . [Ag] is the varying ochratoxin A-

BSA concentration; [Ab] is the varying antibody concentration. Here, the terms [Ag] and [Ag'] equal 1000 and 10,000  $\mu\text{g L}^{-1}$  ochratoxin A-BSA, since an approximate  $A_{100\%}$  was observed. The calculated functional affinity for this interaction, assuming a molecular weight of the antibody at 150 kD, was calculated  $1.66 \cdot 10^{11} \text{ M}^{-1}$ . It was noted that the affinity value is about 2-3 magnitudes higher than expected for a common antibody-antigen interaction. For solid-phase measurements, as compared to liquid-phase equilibrium measurements, some authors report higher affinity values [Pellequer and van Regenmortel, 1993]. These differences have been primarily explained by differences in kinetic rates as a result of diffusion limitations [Nygren and Stenberg, 1992]. It also needs to be pointed out that the Beatty equation was developed for monoclonal antibody interaction. Since polyclonal antibodies display a mixture of affinities, one can only estimate an average avidity for the polyclonal antibody mixture.

#### **2.4.6 Ochratoxin A coating to solid phase support**

The preceding experiments were all performed using the ochratoxin A-BSA conjugate since it is easy to immobilise by simple physical adsorption. Nevertheless, the attempt was made to immobilise ochratoxin A to polystyrene. In contrast to the adsorption of high molecular weight proteins, the immobilisation of small low molecular weight molecules is quite a challenge.

Physical adsorption is depended on van der Waals forces which are determined by the dipole moment of a molecule which in return is dependent on the molecules polarity, size, and length. Ochratoxin A possesses a much lower dipole moment, than for example aflatoxin B1 (low polar, non-ionisable), due to its low polar, ionisable nature [Dakovic *et al.*, 2005]. In the following experiment, the adsorption of ochratoxin A to a microtitre plate surface and its non-competitive interaction with anti-ochratoxin A-antibody was investigated (Figure 2.9).

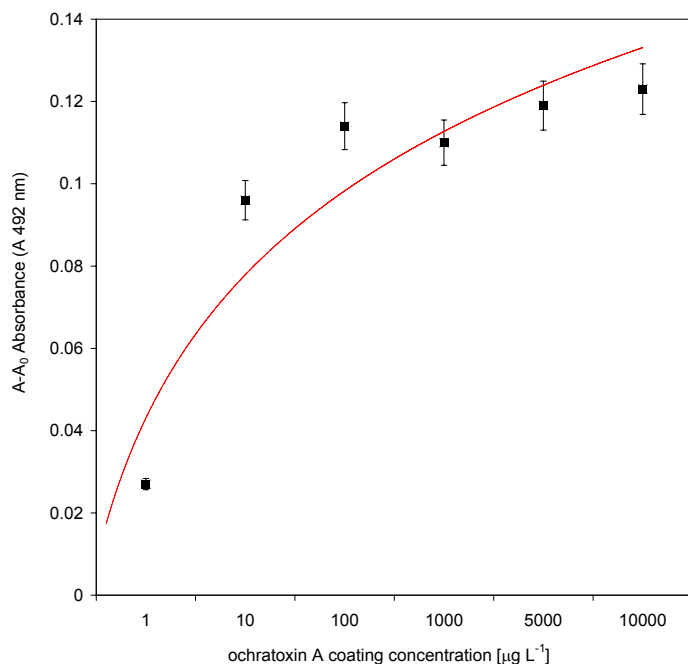


**Figure 2.9:** Signal curve of increasing ochratoxin A coating concentration (■). The signal curve depicts signal – background (blank reference). Absorbance is measured at 492 nm monitoring the catalysis of OPD with H<sub>2</sub>O<sub>2</sub>. Double measurements were performed and the standard deviation is depicted as error bars.

Figure 2.9 shows that the adsorption of ochratoxin A on polystyrene at basic pH occurred to a much lesser extent than with using its BSA conjugate. With increasing ochratoxin A coating concentration, the signal increased as well (Figure 2.10) at a fixed antibody concentration. This indicates a certain amount of physical adsorption taking place and confirms that the anti-ochratoxin A-antibody is binding to adsorbed ochratoxin A.

However, the absorbance signal ranged only between 0.03 – 0.12 absorbance signal and can be barely distinguished from the background. An explanation for the low signal range could be that the antigen-antibody binding interaction is prone to steric hindrance. However, the small signal range can also be directly related to the amount of adsorbed ochratoxin A and that the interacting part of the ochratoxin A molecule is not accessible to the antibody caused by establishment of a surface assembled monolayer which could hinder antibodies from recognizing the antigenic epitope (e.g. ochratoxin A) that may become buried during immobilisation of a tightly packed monolayer [Butler *et al*, 2000]. Summarizing, the physical adsorption of unconjugated ochratoxin A, however desirable

in terms of monovalent antigen-antibody interaction, is not recommended due to its low immobilisation yield and increased steric hindrance of the interaction.

#### 2.4.7 Indirect competitive immunoassay using ochratoxin A (- BSA)

A competitive assay approach is used in combination particularly with small haptens which only display one epitope; this format should yield more specific and sensitive results. The indirect detection approach via a secondary antibody is used to increase detection signal and sensitivity of the antigen-antibody interaction determination [O'Shannessy, and Faegerstam, 1993].

The competitive immunoassay format promotes competition of ochratoxin A (-BSA), for anti-ochratoxin A-antibody binding sites with immobilized ochratoxin A-BSA. The concentration of the immobilised ochratoxin A-BSA was  $30 \text{ mg L}^{-1}$  to reach surface saturation and the antibody concentration  $2.5 \text{ mg L}^{-1}$  ( $1/400$ ) was pre-mixed with each ochratoxin A-BSA competitor concentration, respectively. The concentration range for competing ochratoxin A-BSA was  $0.1$  to  $30,000 \text{ } \mu\text{g L}^{-1}$  (Figure 2.10) and for competing un-conjugated ochratoxin A was  $1$  to  $10,000 \text{ } \mu\text{g L}^{-1}$  as shown in Figure 2.11.

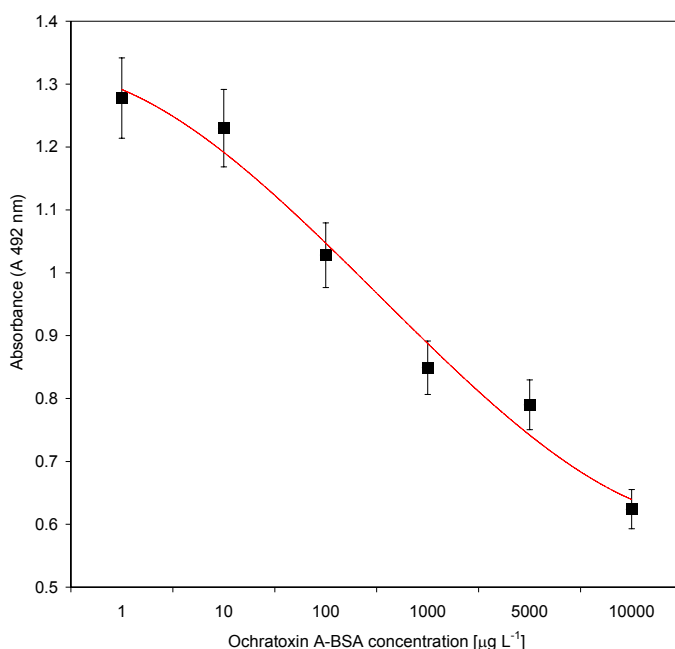


**Figure 2.10:** Signal curve (blank corrected) shows increasing concentrations of ochratoxin A-BSA competitor (■). Absorbance is measured at 492 nm monitoring the catalysis of OPD with  $\text{H}_2\text{O}_2$ . Standard deviation is depicted as error bars.



Figure 2.11 illustrates the absorbance signal increase with decreasing ochratoxin A-BSA competitor concentration and ranging between 0.6 – 1.3 absorbance units. The high background is directly related to the high amount of ochratoxin A-BSA adsorbed to the surface. BSA is prone to non-specifically interact with other biomolecules. To improve the signal background, a coating concentration of 0.1-5 mg L<sup>-1</sup> should be chosen instead. The detection limit was determined 1-10 µg L<sup>-1</sup> ochratoxin A-BSA (10% above blank signal).

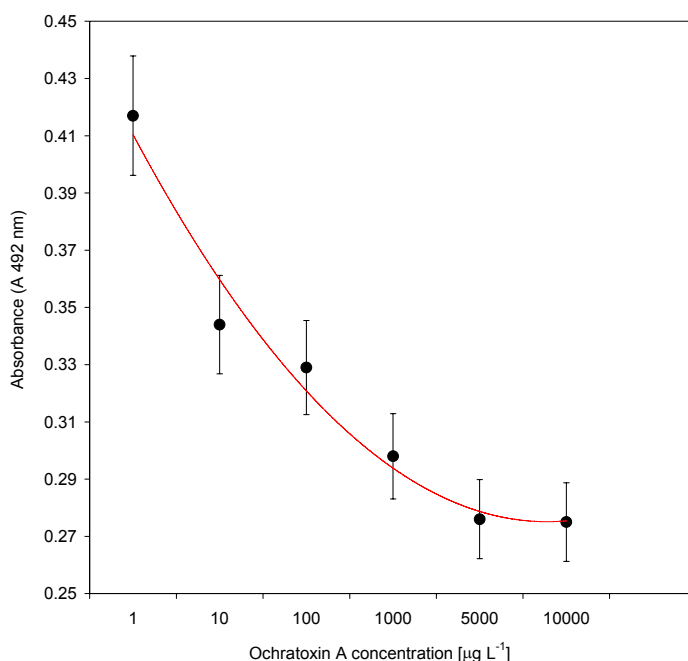


**Figure 2.11:** Signal curve (blank corrected) shows increasing concentrations of ochratoxin competitor (●). Absorbance is measured at 492 nm monitoring the catalysis of OPD with H<sub>2</sub>O<sub>2</sub>. Standard deviation is depicted as error bars.

As seen in Figure 2.11, the absorbance signal is increasing with decreasing ochratoxin A competitor concentration and ranging between 0.27 – 0.49 absorbance units, which is significantly less than observed with ochratoxin A-BSA competitor in Figure 2.11. Nevertheless, the lowest detectable signal is 1 µg L<sup>-1</sup> ochratoxin A (10% above blank signal). The slope of the signal curve showed a steeper increase with lower ochratoxin A concentrations (Figure 2.11) than with ochratoxin A-BSA (Figure 2.10), indicating that even lower ochratoxin A competitor concentrations could be measured and a LOD below 1 µg L<sup>-1</sup> can be expected for ochratoxin A. To establish the appropriate immunoreagent concentration a two-dimensional checkerboard titration needs to be performed to determine optimal coating concentration of ochratoxin A-BSA and

antibody concentration. In a competitive assay, saturating concentrations are less favourable, thus an antibody concentration that shows a signal of around 1.0 absorbance units and an antigen concentration at 70% saturation is optimal.

#### 2.4.8 Direct non-competitive ochratoxin A-HRP immunoassay

The indirect assay format resulted in detection limits for ochratoxin A at about  $1 \mu\text{g L}^{-1}$ . A direct approach can enhance the detection signal, since it is less prone to non-specific binding as there are fewer steps in the assay. Here, a direct immunoassay for ochratoxin A was performed using ochratoxin A-HRP as label. As ochratoxin A-HRP is not commercially available, the conjugate was prepared in-house as described in Section 2.3.6. The conjugate was tested for its enzyme activity using UV spectroscopy at 492 nm by adding a fixed substrate/chromogen solution to increasing HRP-conjugate concentrations (Figure 2.12).

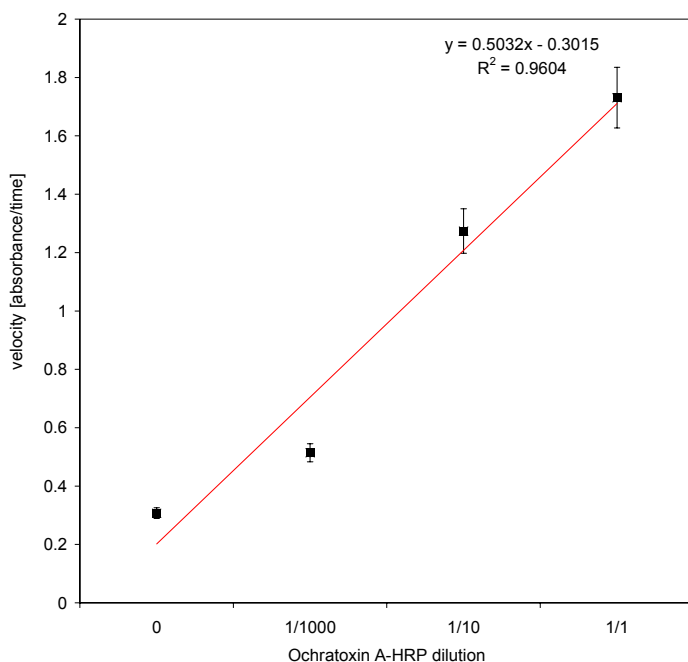


**Figure 2.12:** Spectrophotometric investigation of ochratoxin A-HRP activity upon substrate addition [■]. Absorbance was determined at 450 nm monitoring the catalysis of TMB with  $\text{H}_2\text{O}_2$  and plotted against ochratoxin A-HRP dilution factor.

Upon enzyme substrate/chromogen addition, an increase of signal was observed in Figure 2.12 corresponding to increasing HRP-conjugate concentration. The enzyme activity is defined by the reaction velocity/enzyme volume at constant total solution

volume. At excess substrate concentration, the enzyme activity should be constant showing a linear increase of enzyme reaction velocity with the enzyme concentration as seen in Figure 2.12. This indicates that the enzyme activity was retained through the conjugation process. A clear distinction of signal could be observed at a dilution larger than 1/50.

Ochratoxin A antibody immobilisation to the microtitre plate via, a) physical adsorption and b) site-directed immobilisation to adsorbed Protein A, was investigated. Site-directed immobilisation can enhance sensitivity of a direct assay by making the antigen binding sites more approachable. The comparison resulted in a stable signal increase over a wide range of ochratoxin A-HRP concentrations when using protein A. Therefore, one can assume that an antibody immobilisation approach via protein A generally results in a more sensitive signal. A series of ochratoxin A-HRP conjugate dilutions was tested in a direct approach with  $2.5 \mu\text{g L}^{-1}$  (1/500 dilution) antibody immobilised via protein A (Figure 2.13).

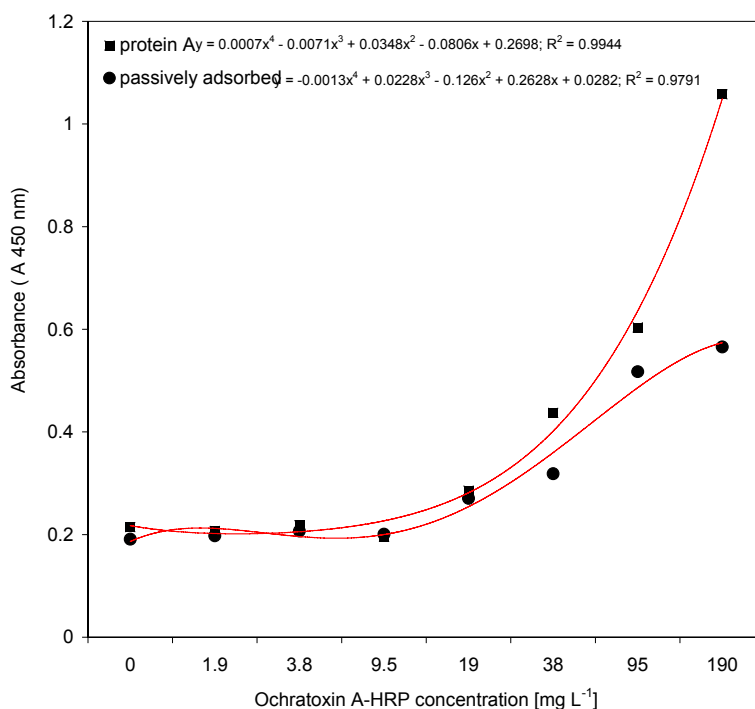
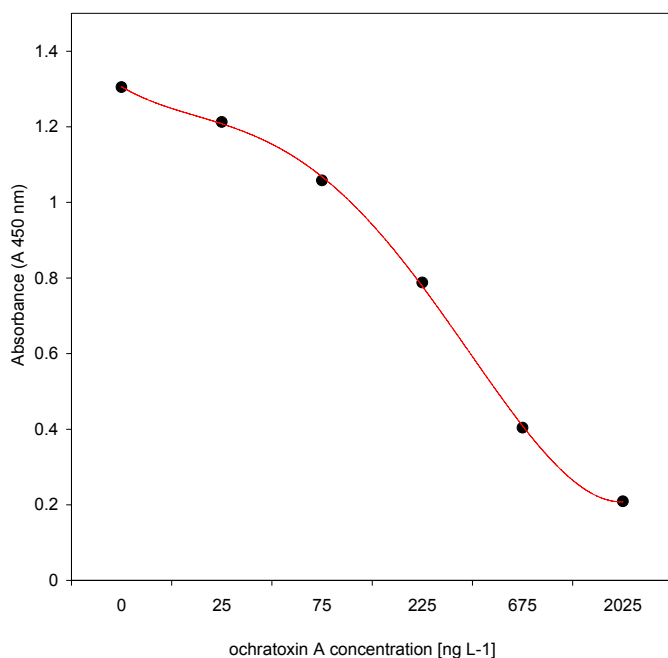


Figure 2.13: Signal curve of immobilised ochratoxin A-antibody ( $2.5 \mu\text{g L}^{-1}$ ) via protein A (■) and passive adsorption (●) interacting directly with increasing ochratoxin A-HRP concentration. Absorbance was determined at 450 nm monitoring the catalysis of TMB with  $\text{H}_2\text{O}_2$ .

The signal curve in Figure 2.13 describes a linear correlation of increasing ochratoxin A-HRP concentration (decreasing dilution factor) binding directly to ochratoxin A antibody. The signal ranged from 0.2 - 0.8 absorbance units. The ochratoxin A-HRP dilution  $1/100$  is the limit of detection (absorbance signal 10% above the blank signal). To specifically determine how strongly the ochratoxin A-HRP conjugate binds to the antibody the affinity of the interaction has to be determined using Biacore analysis.

#### 2.4.9 Analysis of wine samples using an indirect enzyme immunoassay

The indirect assay format was chosen over the direct format for preliminary wine sample analysis. A standard curve was produced using ochratoxin A standards (Figure 2.14) included in the test kit (Ridascreen<sup>TM</sup>). The same ochratoxin A standards were used for the indirect immunoassay format and in the Ridascreen test kit immunoassay. The ochratoxin A standards from the test kit are specifically made for standard analysis alongside various sample matrices. However, those sample matrices are expected to be pre-treated and in the case of wine, diluted and clean-up by IAC.



**Figure 2.14:** Standard curve of ochratoxin A using the indirect competitive assay for wine sample analysis. Ochratoxin A standard concentrations (0, 25, 75, 225, 675 and 2025 ng L<sup>-1</sup>) were obtained from the Ridascreen test kit. Absorbance was monitored at 450 nm using TMB/H<sub>2</sub>O<sub>2</sub>.

As the applied wine samples were simply diluted buffer, the standard curve lacks comparison to standards which are prepared in wine to determine the matrix effect.

The following results were obtained when comparing to the standard curve (Figure 2.14). For the indirect competitive immunoassay analysis, wine samples were diluted 1:2 in sodium carbonate buffer, pH 9.6, whereas the Ridascreen assay was performed with pre-concentrated samples subjected to immunoaffinity clean-up as suggested by the manufacturer. Concentration of ochratoxin A in the wine samples are summarised in Table 2.7.

**Table 2.7:** Wine samples analysed with indirect competitive assay and commercial immunoassay kit (Ridascreen) compared to HPLC data as verification method.

<b>Wine sample</b>	<b>HPLC</b>	<b>Ridascreen kit</b>	<b>Indirect competitive immunoassay</b>
<b>White Wine</b>	<b>Ochratoxin A [<math>\mu\text{g L}^{-1}</math>]</b>		
Canti Catarratto Chardonnay, Italy-Sicily 2005 (batch 1)	1.337	0.398	0.39
Canti-Chardonnay Pinot Grigio, Italy 2005 (batch 1)	1.629	0.411	0.42
Canti Catarratto Chardonnay, Italy-Sicily 2005 (batch 2)	1.338	0.410	0.41
Bordeaux, France 2005	0.998	0.405	0.43
Soave, Italy-Verona 2005	1.094	0.409	0.39
Pinot Grigio, Italy 2005	0.813	0.385	0.56
Canti-Chardonnay Pinot Grigio, Italy 2005 (batch 2)	0.020	0.397	0.54
Canti-Chardonnay Pinot Grigio, Italy 2005 (batch 3)	0.536	0.392	0.45
Soave Classico, Italy 2005	1.260	0.392	0.43
<b>Red wine</b>			
France, 2001	0.572	0.389	
Canti, Italy, 2006	0.379	0.4	0.56
Cabernet Sauvignon, Chile, 2005	0.439	0.328	0.56
Italy, 2006	0.556	*	*
Bordeaux, France, 2005	0.321	0.375	0.47
Cru,S	0.138	0.403	0.46
Mon,France, 2005	0.213	0.379	0.76
South Africa, 2006	0.354	0.314	0.64
unknown origin	0.722	0.396	0.59

\*- depicts a signal below the detection limit

This suggests that the two immunoassay methods show data within the methods standard error. This supports the hypothesis that the indirect competitive assay developed throughout this thesis is as sensitive as the direct assay format used in the test kit. Also, the sample dilution could be increased 5 fold and still achieve sensitive detection. Thus, the indirect competitive format is being implemented into immunosensor development. However, the variation compared to the HPLC data is, especially with white wine samples, is very high. Higher values suggest that ochratoxin A is determined more sensitively using HPLC with fluorescence detection than colorimetric solid state immunoassays. Regarding the pre-concentration and clean-up procedure, one can assume that clean-up by dilution and immunoaffinity chromatography perform both similarly good (regarding the data correlation) and bad (regarding the comparison to HPLC data).

## **2.5 Concluding remarks**

The coating concentration for ochratoxin A-BSA was established in Figure 2.1 and 2.2 and resulted in a preliminary LOD of 5-10  $\mu\text{g L}^{-1}$  ochratoxin A-BSA coating over a dynamic range of 5-750  $\mu\text{g L}^{-1}$ . The antibody dilution range was further decreased over a wider dynamic range of coating concentration (100-10,000  $\mu\text{g L}^{-1}$  ochratoxin A-BSA), however, resulted in lower sensitivity (LOD > 10  $\mu\text{g L}^{-1}$ ). Optimal coating time was established as 4 hours for a coating concentration of 750 (50+/-)  $\mu\text{g L}^{-1}$  whereas >24 hours incubation will lead to signal decrease and sensitivity loss (Figure 2.3). The indirect competitive assay, using a coating concentration of 30  $\text{mg L}^{-1}$  ochratoxin A-BSA when testing with an antibody solution of 2.5  $\text{mg L}^{-1}$  showed improved sensitivity when of 1-10  $\mu\text{g L}^{-1}$  ochratoxin A-BSA and indicating <1  $\mu\text{g L}^{-1}$  ochratoxin A competitor. However, the signal noise in the competitive assays was comparatively high (Figure 2.10), possibly as a result of non-specific interactions involving the BSA conjugate, whereas the signal noise was less when applying ochratoxin A only (Figure 2.11). The choice of blocking agent is also of vital importance for the signal/noise ratio, thus casein block generally resulted in better signal/noise ratio than BSA. Therefore, it was concluded that future binding assays will be performed at optimal incubation temperature of 4°C (or for maximum binding capacity at room temperature) using casein blocking and an incubation time of ochratoxin A-antibody of 4 hours.

Furthermore, the affinity of the interaction of immobilised ochratoxin A-BSA with a range of antibody concentrations could be established using a solid-phase immunoassay without steady-state equilibrium. The affinity constant was  $1.66 \times 10^{11} \text{ M}^{-1}$ .

This work can be directly compared to the work published by Alarcon *et al.* [2004], who also using the polyclonal antibody from Biogenesis for ochratoxin A detection. The paper discusses interference resulting from the antibody cross-reacting with BSA as a standard curve for a competitive assay was not achievable. The indirect immunoassay was repeated with BSA-purified antibody but it was not possible to achieve the required sensitivity. They also encountered low reproducibility and non-specific binding (high blank values). The indirect assay presented in this work, however, using the same BSA-purified ochratoxin A antibody (while also applying the same method of BSA-purification) shows comparably good reproducibility and sensitivity (Figure 2.11, 2.12). Alarcon *et al.* [2004] proposed a direct immunoassay instead with a limit of detection of  $0.18 \mu\text{g L}^{-1}$  ochratoxin A applying the parameters  $20 \text{ mg L}^{-1}$  anti-IgG capture antibody,  $26 \text{ mg L}^{-1}$  ochratoxin A antibody (Biogenesis) using an ochratoxin A-AP conjugate. The detection limit of the direct immunoassay is lower than the detection limit for the indirect assay presented in this work for an indirect assay ( $<1 \mu\text{g L}^{-1}$  ochratoxin A).

Detection limits of immunoassay based test kits range from  $0.1 - 3 \mu\text{g L}^{-1}$ , where the direct binding format falls in the detection range of  $0.1-2 \mu\text{g L}^{-1}$  (Immunoscreen®Ochra, Tecna Lab, It; MycoMonitor®, Helica USA) and the indirect immunoassay format of  $0.3 - 3 \mu\text{g L}^{-1}$  ochratoxin A (Transia®Plate, DiffChamb AB; Biokits®Ochratoxin A Assay kit, Telpel Biosystems Ltd.). The test kit from Ridascreen that was used in this work for comparison states a detection limit of  $0.025 - 0.625 \mu\text{g L}^{-1}$ . This shows that the indirect immunoassay based methods generally show a smaller detection range and less sensitivity for ochratoxin A. The indirect assay developed in this work showed that a LOD of  $\mu\text{g L}^{-1}$  can be achieved and therefore places the hereby developed assay alongside the commercial test kits.

Also, detection of ochratoxin A in chillies was performed using a polyclonal detection antibody and an indirect competitive ELISA format, thereby achieving a detection limit

of  $0.1 \mu\text{g L}^{-1}$  [Thirumala-Devi *et al.*, 2000]. The polyclonal antibody used was raised against ochratoxin A-BSA, which, according to the authors did not increase non-specific binding. Another indirect competitive ELISA used of monoclonal antibodies and resulted in a less sensitive detection limit of  $3.75 \mu\text{g kg}^{-1}$  ochratoxin A in green coffee [Fujii *et al.*, 2006]. This is compared to an ELISA also using monoclonal antibodies, but in a direct competitive format, resulting in a detection limit of  $0.01\text{-}0.1 \mu\text{g L}^{-1}$  in coffee extract [Ueno *et al.*, 1999]. Recently, Yu *et al.* [2005] developed a direct competitive ELISA with a detection limit of  $0.90 \mu\text{g L}^{-1}$  for ochratoxin A in various agricultural commodities, which shows the potential of polyclonal antibodies being used in a sensitive direct assay format. This shows that the use of polyclonal or monoclonal antibodies does not necessarily have an affect on assay sensitivity, as both the indirect and direct ELISA, when using either antibody, show similar sensitivity. Also, generally, the indirect ELISA does show the same sensitivity as the direct format and one can summarise that the lowest detection limits for immunoassays for ochratoxin A detection using either polyclonal or monoclonal antibodies is about  $0.1 \mu\text{g L}^{-1}$ . Another test kit designed to detect ochratoxin A by a membrane-based flow-through enzyme immunoassay using monoclonal antibodies were studied by screening cereals (wheat, rye, maize and barley) and resulted in a limit of detection for ochratoxin A of  $4 \mu\text{g kg}^{-1}$  [De Saeger *et al.*, 2002], which is in the range of commercial immunoassay based kits and was marketed as a flow-through ELISA kit for ochratoxin A by Toxi-Test (Belgium). In comparison, a direct competitive enzyme immunoassay for ochratoxin A in chillies developed by Saha *et al* [2007] showed a detection limit for ochratoxin A of only  $10 \mu\text{g kg}^{-1}$ , which is comparatively high for a direct immunoassay format. They have also determined ochratoxin A in wine and coffee with a detection limit in wine of  $1 \mu\text{g L}^{-1}$  and coffee of  $2.5 \mu\text{g kg}^{-1}$  [Saha *et al.*, 2006]. The method itself, based on focused absorption of a sample and reagents through an aqueous network of capillary channels formed between a nitrocellulose membrane and a wetted absorbent body, could cause the relatively high detection limit or the method of detection which is based on densitometric analysis. The latter has been extensively used for TLC analysis of ochratoxin A and has been show limits in terms of sensitivity and selectively, thus it could also result in a high background noise. Saha *et al.* [2006] also points out that the quality of the immobilized antigen or antibody spots on the



membranes is highly operator-dependent and spotting by conventional methods often leads to heterogeneous spot morphologies and deposition inconsistencies. It can be summarised that membrane-based immunoassays generally show higher detection limits than conventional ones.

Current research in ochratoxin A using immunoassays is often based around antibody production and characterisation [Chu *et al.*, 1976; Candlish *et al.*, 1986; Gyongyosi-Horvath *et al.*, 1996], or in immunoaffinity column applications [Goryacheva *et al.*, 2006] and multi-analyte analysis [Saha *et al.*, 2007] and some specialised application include the application of colloidal gold direct competitive immunoassay with a detection limit of  $1.0 \mu\text{g L}^{-1}$  [Wang *et al.*, 2007] and a gel-based direct competitive ELISA for ochratoxin A in beer resulting in a detection limit of  $0.2 \mu\text{g L}^{-1}$ .

This research shows that the immunoassay developed in this work has the potential of improving its detection limit below  $1 \mu\text{g L}^{-1}$  and that both direct and indirect format using both polyclonal and monoclonal antibodies are capable of achieving a very sensitive detection limit in various sample commodities.

Furthermore, throughout the immunoassay development in this work, it became apparent that there was a need for comparison with another ochratoxin A antibody, particularly one that has no likelihood of cross-reacting with BSA. Even though, a cross-reaction with BSA could not be positively confirmed, especially results from Section 2.4.4 indicated the involvement of BSA in high standard deviation of the signal. Therefore, a more accurate method to characterise antibody binding to ochratoxin A was needed. Biospecific interaction analysis such as surface plasmon based Biacore technology can be used for monitoring binding interaction, kinetic rates and cross-reactivity towards BSA. Affinity data for one or more antibodies can be quickly obtained and compared to the solid phase immunoassay data. As the solid phase immunoassay was developed to optimise the ochratoxin A binding assay for eventual sensor development, the Biacore analysis can be used to compare antibody affinities and cross-reactivity to screen the optimal antibody to be used as recognition element in sensor construction.

## **CHAPTER 3 : SURFACE PLASMON RESONANCE ANALYSIS OF OCHRATOXIN A ANTIBODIES**

### **3.1 Introduction**

Different ochratoxin A antibodies available commercially allow for optimal sensor development by selecting the best antibody to be implemented as recognition element in the immunosensor. Therefore, antibodies need to be characterised for their binding ability for ochratoxin A. To investigate the effect of ligand immobilisation in a direct and indirect binding format, a number of antibody receptors can be screened for common characteristics such as binding recognition of ochratoxin A and the strength of the interaction. Different antibodies can bind an analyte with the same affinity even though the kinetic rates are different. Binding interaction analysis was performed using surface plasmon resonance to investigate the affinity and kinetics of several antibodies interacting with ochratoxin A. The surface plasmon resonance phenomenon and its use in binding interaction analysis have been described by Johnsson *et al.*, [1991]. Sensors based on surface plasmon resonance (SPR) have been reviewed by Homola *et al.* [1999] and the use of a SPR biosensor for mycotoxin analysis binding to specific antibodies was described by van der Gaag *et al.* [2003] and will be discussed in this chapter.

The objective of this work was the development of a binding assay for ochratoxin A detection using a commercial biosensor based on surface plasmon resonance (Biacore). In the process, the affinity of anti-ochratoxin A antibodies B (Biogenesis Ltd) and antibody A (Acris GmbH) for immobilised ochratoxin A-BSA conjugate is monitored. Upon antibody immobilisation while using ochratoxin A-BSA as analyte, the difference in affinity is compared. A competitive binding assay was developed on the SPR sensor and investigated whether the SPR biosensor can be used for wine analysis.

As both antibodies are polyclonal (subject to availability), the affinity measured will be a combination of affinities and thus the results will display avidity. The immobilisation of ochratoxin A-BSA conjugate compared to antibody immobilisation should show a variation in affinity as the immobilisation will especially affect the antibody binding capacity. By testing different antibodies and different formats of binding, the resulting

data will allow estimation about which binding assay format will be optimal for the proposed sensor and also which antibody should be used as recognition element.

The affinity of the antibodies is also expected to be high for the ochratoxin A-BSA conjugate since it has 3-6 mol ochratoxin A per molecule of BSA (Sigma-Aldrich Ltd., UK) that can lead to enhanced avidity as a result of the increased number of binding sites. Multiple binding sites are also likely to cause a problem when analysing the kinetics and affinity using standard binding models.

## **3.2 Experimental**

The ochratoxin A-BSA conjugate, ochratoxin A and BSA, acetate buffer and glycine was purchased from Sigma Aldrich Ltd., UK. The CM5 sensor chips, HEPES buffered saline (HBS-EP), 1 M ethanolamine, pH 8.5, 0.4 M EDC (N-(3-dimethylaminopropyl)-N'-ethylcarbodiimide) and 0.1 M NHS (N-hydroxysuccinimide) as well as the BIAcore 3000™ used for the analysis were from BIAcore (Uppsala, Sweden). The ochratoxin A-antibodies were from Biogenesis Ltd. (UK) and Acris GmbH (Germany) and are hereafter referred to as ochratoxin A antibody B (Biogenesis) and A (Acris).

## **3.3 Methods**

### **3.3.1 Amine coupling of ochratoxin A-BSA to the CM5 sensor chip**

The binding interaction analysis of ochratoxin-BSA with the anti-ochratoxin antibodies (Biogenesis Ltd. (now known as MorphoSys UK Ltd.) & Acris GmbH) were carried out on a CM5 (carboxymethylated dextran on gold) sensor chip. HBS (0.01 M HEPES pH 7.4, 0.15 M NaCl, 3 mM EDTA, 0.005% Surfactant P20) was used as running and dilution buffer. The CM5 surface was activated using 0.4 M N-(3-dimethylaminopropyl)-N'-ethylcarbodiimide (EDC) and 0.1 M N-hydroxysuccinimide (NHS), according to BIAcore instruction manual, applying amine coupling. Amine coupling involves the activation of carboxy-groups present on the sensor surface by a mixture of NHS and EDC to give reactive succinimide esters. Ligands passed over the surface react with their primary amines with the succinimide esters and link the ligand covalently to the carboxymethylated dextran surface. In brief, a 1:1 mixture of

EDC/NHS was passed over the surface for 6 minutes at a flow rate of 5  $\mu\text{l min}^{-1}$ . The ligand ochratoxin A-BSA was diluted in 10 mM acetate buffer, pH 4.5 to a concentration of 100  $\mu\text{g ml}^{-1}$ . The injection volume was 75  $\mu\text{l}$  at a flow rate of 5  $\mu\text{l per minute}$  for 15 minutes. Every flow cell of a sensor chip was immobilised separately. Non-bound binding sites were subsequently deactivated by injecting 35  $\mu\text{l}$  1M ethanolamine-HCl, pH 8.5 for 7 minutes. Calibration was executed at a flow rate of 5  $\mu\text{l min}^{-1}$  and regeneration was performed of the surface using 15  $\mu\text{l}$  20 mM Glycine-HCl, pH 2.0 for 3 minutes. Antibody A and B analytes were injected at a volume of 50  $\mu\text{l}$  at a flow of 5  $\mu\text{l per minute}$ . This was followed by a dissociation phase of about 7 minutes, regeneration by 15  $\mu\text{l}$  20 mM Glycine-HCl plus 2 minutes to stabilise the baseline before another injection.

The immunogen used for the production of the polyclonal antibody from Acris GmbH is a synthetic peptide corresponding to part of the native molecule conjugated to bovine serum albumin, whereas the immunogen used for the antibody manufactured by Biogenesis Ltd. is a BSA conjugate of ochratoxin A. The specificity of the antibody was determined by the manufacturer as for ochratoxin A 100%, ochratoxin B 1%, BSA (absorbed) <0.1% for both antibodies. Both antibodies were Ig purified. There has been a report of the Biogenesis antibody to be showing cross-reaction with BSA [Alarcon *et al.*, 2004]. Therefore, BSA was co-immobilised on a reference flow cell as negative control for both antibodies, thus allowing subtraction of any cross-interaction of BSA from the specific binding event.

### **3.3.2 Amine coupling of ochratoxin A antibody to the CM5 sensor chip**

Ochratoxin A antibody B was immobilised using amine coupling using the procedure described for ochratoxin A-BSA. The analyte (ochratoxin A-BSA and ochratoxin A-HRP) were injected at a volume of 25  $\mu\text{l}$  at a flow rate of 5  $\mu\text{l per minutes}$ . Competitive reactions were performed by pre-incubation of a fixed ochratoxin A- antibody concentration (5  $\text{mg L}^{-1}$ ) with varying ochratoxin A concentrations (0.1; 1; 10; 50 and 100  $\mu\text{g ml}^{-1}$ ) for 15 minutes and then injected a volume of 50  $\mu\text{l}$  at a flow rate of 5  $\mu\text{l per minutes}$ . The kinetic parameters of the binding reactions were determined using

BIAevaluation 3.2 software (Karlsson *et al.*, 1994) and statistically validated using the chi-square distribution (also chi-squared or  $\chi^2$  distribution), which is one of the most widely used theoretical probability distributions in inferential statistics, i.e. in statistical significance tests. The resonance signal is displayed in resonance units (RU) that can be directly related to a specific biomolecule mass on the sensor chip surface.

A binding interaction is comprised of the analyte transfer from the bulk solution onto the surface and the subsequential binding of the analyte to the surface bound ligand. The analyte transfer from the bulk solution onto the surface is termed mass transfer and is dependent on diffusion and convection (in a flow system). The mass transfer depends on the flow cell dimensions, the diffusion coefficient of the analyte and the flow rate, whereas the rate of the binding interaction depends on the association and dissociation constants of the analyte, the concentration of the analyte on the surface and the surface binding capacity [Glaser, 1993]. Checking for mass transfer limitations is done by injecting the analyte at different flow rates. The association and dissociation rate constants should be the same between different flow rates when mass transfer limitations are not present.

### **3.3.2.1 Production of Ochratoxin A-HRP conjugate**

The ochratoxin A-HRP conjugation method was adapted from the method according Chu *et al.* [1976]. Ochratoxin A (2 mg) was suspended in 400  $\mu$ l ethanol (98%) with 15 mg EDAC and 7.5 mg NHS (in PBS, pH 7.4) and stirred for 12 hours at room temperature. Horseradish peroxidase (4 mg, dissolved in PBS, pH 6.5) was added to the solution and stirred for another 12 hours at room temperature. The conjugate was dialysed against PBS, pH 7.4 for 48 hours at room temperature using a dialysis cassette with a MWCO of 10.000.

### **3.3.2.2 Wine sample preparation**

All wine samples were purchased from major UK supermarkets within a price range of £3-5. The wine samples for Biacore analysis were pre-treated using immunoaffinity clean-up according to the “OchraTest™ AOAC HPLC procedure for wine and beer” in

accordance with the work published by Visconti *et al.* [1999]. Wine (5 ml) was added to 5 ml of diluting solution (1% polyethylene glycol (PEG) + 5% NaHCO<sub>3</sub>, pH 8.3) and mixed vigorously. The Ochratest™ immunoaffinity column was connected to a pumpstand and 10 ml diluted sample solution was added to the column reservoir, whereas the solution was passed through the column at a flow rate of 1-2 drops/second using a syringe. The column was washed using 5 ml washing solution (2.5% NaCl + 0.5% NaHCO<sub>3</sub>) and then dried. Ochratoxin A was eluted by passing 2 mL methanol, at a flow rate of 1 drop/second, through the column and the eluate was evaporated to dryness at 50°C under Nitrogen. The eluate was re-dissolved immediately in 250 µl HEPES buffer, pH 7.4 for Biacore analysis.

### 3.3.2.3 Control experiments

To establish what type of binding model would fit the interaction; a linked reaction experiment is carried out. A fixed concentration of ochratoxin A-BSA analyte (10 mg L<sup>-1</sup>) is passed over a sensor surface with immobilised ochratoxin A antibody. The binding interaction is observed at different flow rates (1 and 5 µl min<sup>-1</sup>) resulting in different length of association and dissociation phase. The Biaevaluation software 3.2 aligns both curves at the injection stop marker (end of association). The dissociation phase is analysed by observing if the dissociation phases overlay. A 1:1 binding or heterogenous ligand binding model will result in overlaying dissociation curves, whereas overlapping dissociation curves indicate a more complex binding model.

The mass transfer control experiment involves both ochratoxin A antibodies being passed over a sensor surface with immobilised ochratoxin A-BSA. The binding interaction is observed at increasing flow rates (5, 15 and 75 µl min<sup>-1</sup>) and the association ( $k_a$ ) and dissociation constant ( $k_d$ ) of the resulting sensorgrams are obtained and plotted versus the flow rate. Mass transfer is flow rate-dependent and an increase in flow rate will result in increased  $k_a$  and  $k_d$  if mass transfer is involved in the interaction.

BSA cross-reactivity was assessed by passing varying antibody concentrations over a sensor surface immobilised with BSA. The sensorgrams of the association and

dissociation were monitored and the binding interaction evaluated using Biaevaluation software 3.2.

The immobilised biomolecule will be referred to as ligand, whereas the interacting partner free in solution will be referred to as analyte according to the definition used with Biacore. In the following section, the anti-ochratoxin A polyclonal antibody purchased from Acris Antibodies GmbH will be abbreviated as ‘antibody A’ and the one from Biogenesis Ltd. as ‘antibody B’.

### 3.4 Results and Discussion

#### 3.4.1 Immobilisation of Ligands

The amount of biomolecule to be immobilised to the sensor chip surface depends on the molecular weight of the immobilised ligand and also of the analyte. According to the Biacore description, when using large molecular weight ligands and analytes (such as ochratoxin A-BSA and specific antibody), as much as possible of the ligand should be immobilised. High surface density allows rapid binding at low analyte concentrations, thereby improving sensitivity. When measuring kinetics, a lower amount of immobilised ligand is generally preferred to reduce adverse effects such as mass transport limitations of the analyte. The ligands used in this work and their respective immobilisation level (RU) on the CM5 chip surfaces is shown in Table 3.1.

**Table 3.1:** Immobilisation levels of ligands immobilised on carboxymethylated gold surface via amine coupling.

Ligand	Immobilisation level [RU]	Analyte
Ochratoxin A-BSA	6460 RU	Ochratoxin A antibody
Ochratoxin A antibody B	5400 RU	Ochratoxin A-BSA
Ochratoxin A antibody A	2380 RU	Ochratoxin A-BSA

The immobilisation level can be calculated according to the estimation that 1 RU is about equal to  $1 \text{ pg mm}^{-2}$  of ligand immobilised [Biacore Evaluation Handbook, 1998]. The net surface plasmon resonance signal for immobilized ochratoxin A-BSA, with a MW  $\approx 67211\text{-}68422 \text{ g mol}^{-1}$  (3-6 mol ochratoxin A at MW  $403.81 \text{ g mol}^{-1}$  per mol BSA at MW  $66000 \text{ g mol}^{-1}$ ), was 6460 resonance units after completion of the chip regeneration cycle, which corresponds to  $6.5 \text{ ng/mm}^2$  ( $95\text{-}96 \text{ fmol/mm}^2$ ). The net surface plasmon resonance signal for immobilized ochratoxin A-antibody B, with a MW  $\approx 150000\text{-}180000 \text{ g mol}^{-1}$  was 5400 resonance units after completion of the chip regeneration cycle, which corresponds to  $5.4 \text{ ng/mm}^2$  ( $30\text{-}36 \text{ fmol/mm}^2$ ). The net surface plasmon resonance signal for immobilized ochratoxin A-antibody A, with a MW  $\approx 150000\text{-}180000 \text{ g mol}^{-1}$  was 2380 resonance units after completion of the chip regeneration cycle, which corresponds to  $2.38 \text{ ng/mm}^2$  ( $13\text{-}15 \text{ fmol/mm}^2$ ).



### 3.4.2 Binding interaction analysis of ochratoxin A antibodies

Sensorgrams show binding interactions in real-time as a plot of time (seconds) versus response signal (RU). Kinetics and affinities are defined by the association rate constant  $k_a$  [ $M s^{-1}$ ], dissociation rate constant  $k_d$  [ $s^{-1}$ ], the affinity constant  $K_A$  [ $M^{-1}$ ] and the equilibrium dissociation constant  $K_D$  [ $M$ ].

### 3.4.3 Immobilised ochratoxin A-BSA-conjugate

The Figure below (Figure 3.1) illustrates the covalent immobilisation of the ochratoxin A-BSA ligand to the carboxymethylated dextran on the CM5 sensor chip surface.

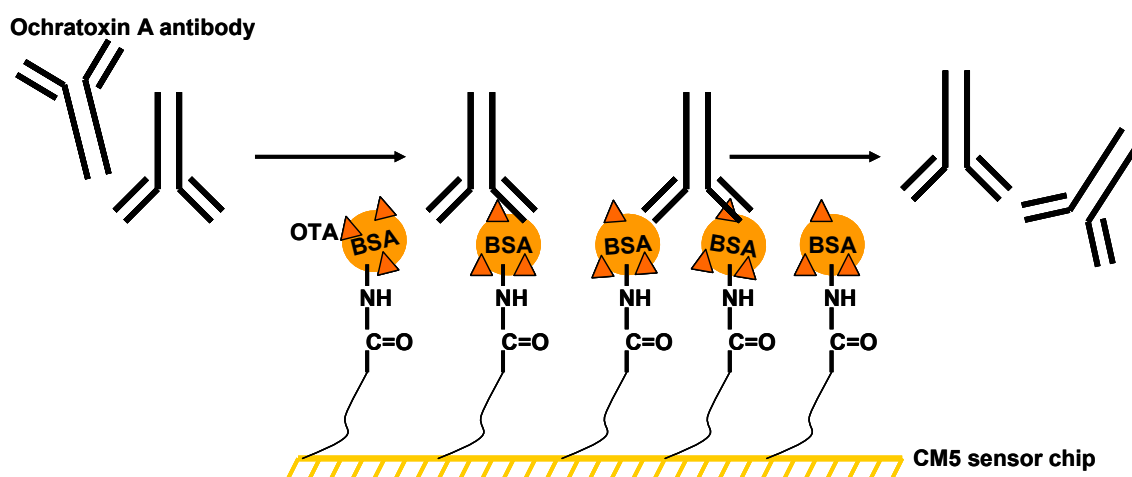


**Figure 3.1:** Covalently immobilised ochratoxin A-BSA is linked to the sensor chip surface through a carbodiimide linker. The illustration represents amine coupling. The ochratoxin A antibody is passed over the surface at a set flow rate displaying association and dissociation from the immobilised ochratoxin A-BSA ligand.

#### 3.4.3.1 Ochratoxin A-BSA ligand with antibody B analyte

To assess the binding interaction of antibody B to immobilized ochratoxin A-BSA, a range of antibody analyte concentrations was injected over the ochratoxin A-BSA ligand surface. Here, the reference is a blank surface that was blocked with ethanolamine. Any cross-reactivity of antibody B to BSA will be included in the response units of the curves shown in Figure 3.2.

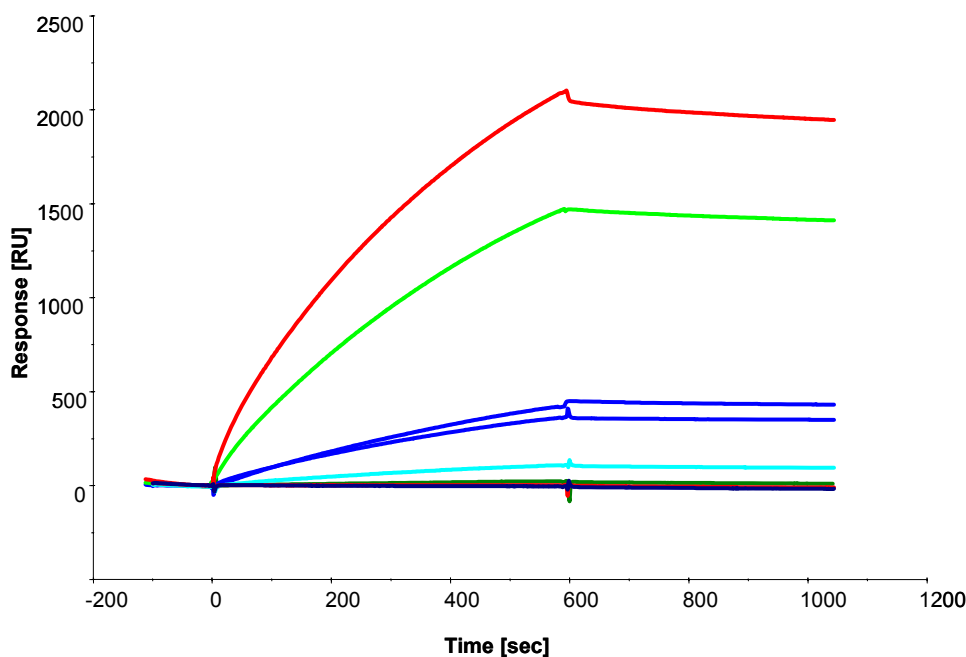
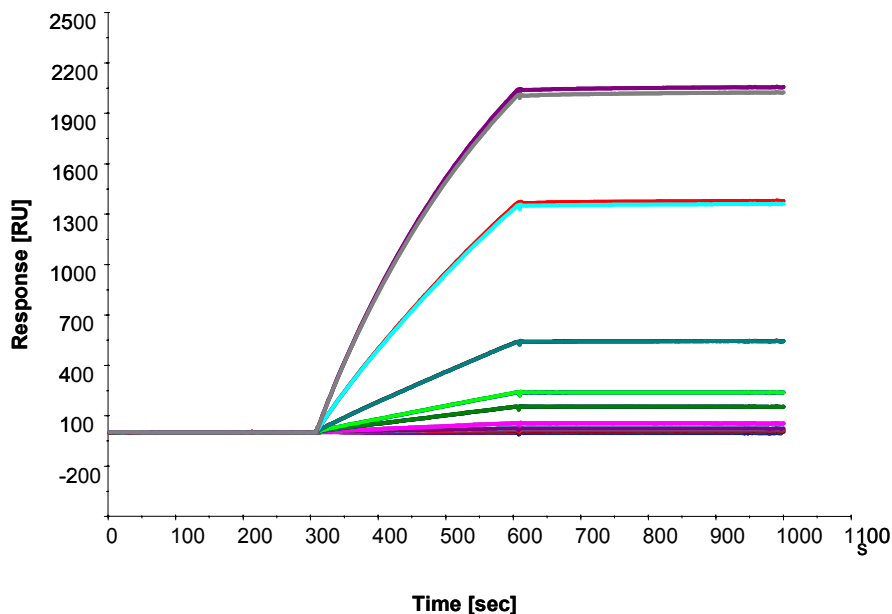


**Figure 3.2:** Sensorgram of response unit versus time illustrating the binding of ochratoxin A-antibody (Biogenesis) to immobilized ochratoxin A-BSA. A medium concentration ( $10 \mu\text{g ml}^{-1}$ ) antibody was measured in duplicate to assess the reproducibility of the method. The ochratoxin A-antibody concentrations as displayed from top to bottom ranged from 100, 50, 10, 5, 2, 1 and  $0 \text{ mg L}^{-1}$ . The zero concentration is equivalent to the same volume of buffer injected over the surface. All curves were subtracted by a blank reference surface (ethanolamine blocked).

Figure 3.2 shows that the response signal decreases according to the decreasing antibody concentration binding to the surface-bound ligand. Measurements are reproducible as indicated by the concentration duplicate ( $10 \text{ mg L}^{-1}$  antibody B). High association and low dissociation rates were observed suggesting high affinity of the interaction. The sensitivity of the binding interaction was estimated at  $2 \text{ mg L}^{-1}$  antibody B with a response of 20 RU. The higher antibody concentrations had shown reproducible and distinct binding curves and were therefore selected in duplicate for the kinetic assessment (sensorgram not shown). For the kinetic evaluation, the reality of the binding cannot be truly assessed using the available fitting models. The kinetic model is complex since the immobilised ochratoxin A-BSA offers three or more binding sites whereas the antibody analyte suggests bivalent binding and the cross-reactivity towards BSA has to be included as well. The 1:1 Langmuir model was chosen as it shows the best  $\chi^2$  value for the fit. The model is not displaying the true binding rates but suggests that the interaction is strong with an association rate constant of  $k_a = 4.36 \times 10^3 \text{ Ms}^{-1}$  and

a dissociation rate constant of  $k_d = 7.82 \times 10^{-5} \text{ s}^{-1}$  resulting in affinity of  $K_A = 5.58 \times 10^7 \text{ M}^{-1}$  and  $K_D = 1.79 \times 10^{-8} \text{ M}$ .

In the following experiment, immobilised BSA is used as reference and the response signal subtracted automatically by BIAevaluation from the specific binding event. Here, only the antibody binding to ochratoxin A will be included in the response units of the curves shown in Figure 3.3.



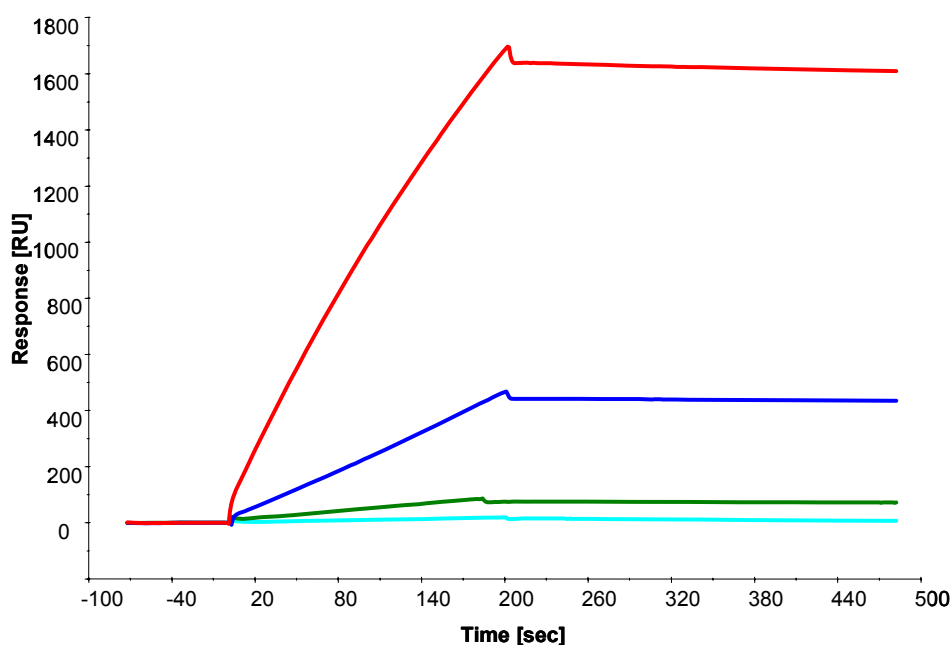
**Figure 3.3:** Sensorgram of response unit versus time illustrating the binding of ochratoxin A-antibody (Biogenesis) to immobilized ochratoxin A-BSA. A medium concentration ( $10 \mu\text{g ml}^{-1}$ ) antibody was measured in duplicate to assess the reproducibility of the method. The ochratoxin A-antibody concentrations as displayed from top to bottom ranged from 100, 50, 20, 10, 5, 2, 1, 0.5, 0.2, 0.1, 0.05 and 0  $\text{mg L}^{-1}$ . The zero concentration is equivalent to the same volume of buffer injected over the surface. All curves were subtracted by a blank reference surface (BSA blocked).

Figure 3.3 illustrates the sensorgrams showing a steeper, faster association rate and much slower dissociation, which indicates that the specific interaction has high affinity. The 1:1 Langmuir model suggests that the interaction is quite strong with  $k_a = 5.13 \times 10^3 \text{ Ms}^{-1}$  and  $k_d = 5.22 \times 10^{-9} \text{ s}^{-1}$  resulting in affinity of  $K_A = 9.84 \times 10^{11} \text{ M}^{-1}$  and  $K_D = 1.02 \times 10^{-12} \text{ M}$ . The evaluation confirms that the antibody binds very strongly and only dissociates very slowly from ochratoxin A. The affinity shows a 4 orders of magnitude increase compared to the binding event where a mixture of specific binding and cross-reaction with BSA is monitored (Figure 3.2). The LOD at a maximum response of 5 RU is

corresponding to an antibody concentration of  $0.2 \text{ mg L}^{-1}$ , increasing the sensitivity ten fold.

### 3.4.3.2 Ochratoxin A-BSA ligand with antibody A

The same experiment was also performed with antibody A. Selected antibody concentrations were investigated on the same ochratoxin A-BSA surface and the reference is a blank surface that was blocked with ethanolamine. Any binding of the antibody to BSA will be included in the response units of the curves shown in Figure 3.4.



**Figure 3.4:** Sensorgram of response unit versus time illustrating the binding of ochratoxin A-antibody (Acris) to immobilized ochratoxin A-BSA. All curves are reference subtracted. The ochratoxin A-antibody concentrations as displayed from top to bottom ranged from 10, 5, 2, 1, 0.5  $\text{mg L}^{-1}$  and zero injection (PBS). The zero concentration is equivalent to the same volume of buffer injected over the surface. All curves were subtracted by a blank reference surface (ethanolamine blocked).

The sensorgram in Figure 3.4 illustrates the binding interaction of the antibody A with immobilized ochratoxin A-BSA at distinct concentrations. The lowest concentration of  $0.5 \text{ mg L}^{-1}$  showed a maximum response of 17 RU, whereas the corresponding analysis of antibody B had shown a similar response (of 20 RU) at  $2 \text{ mg L}^{-1}$  suggesting that antibody A is more sensitive than B. The sensorgram also indicates a bulk refractive

index change (The refractive index change RI is seen as signal spike at injection start and end). The highest antibody concentration ( $10 \text{ mg L}^{-1}$ ) displays a RI value of 60 RU, the lower concentrations range between 10-20 RU, thus confirming that the RI is concentration dependent. The kinetic evaluation, using the 1:1 Langmuir model as described earlier, suggests that the interaction is quite strong with  $k_a = 2.07 \times 10^4 \text{ Ms}^{-1}$  and  $k_d = 8.59 \times 10^{-5} \text{ s}^{-1}$  resulting in affinity of  $K_A = 2.41 \times 10^8 \text{ M}^{-1}$  and  $K_D = 4.16 \times 10^{-9} \text{ M}$ .

Having immobilised BSA as reference and the response signal subtracted automatically from the specific binding event the resulting sensorgram is shown in Figure 3.5.

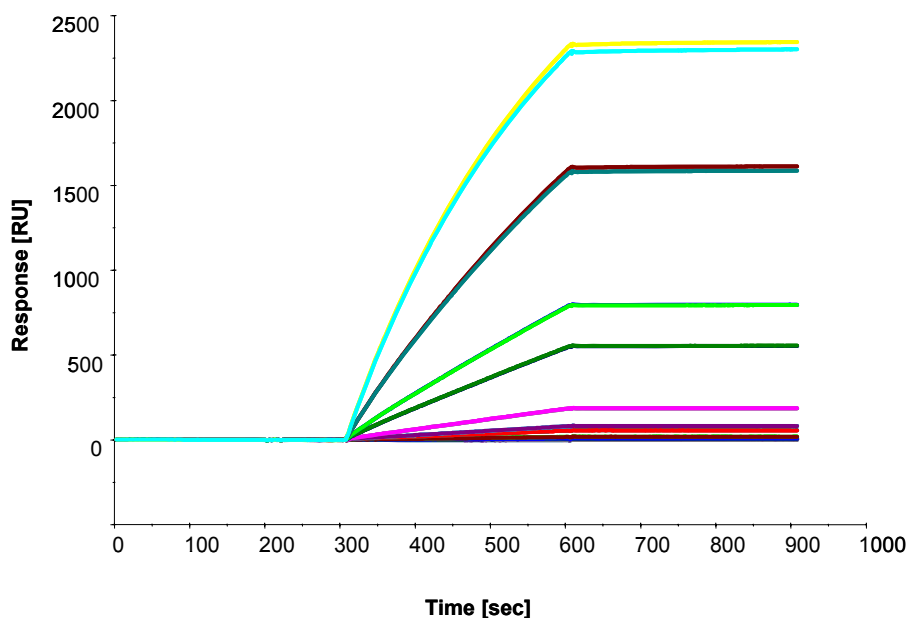


**Figure 3.5:** Sensorgram of response unit versus time illustrating the binding of ochratoxin A-antibody (Acris) to immobilized ochratoxin A-BSA. All curves are BSA reference subtracted. The ochratoxin A-antibody concentrations as displayed from top to bottom ranged from 100, 50, 20, 10, 5, 2, 1, 0.5, 0.2, 0.1, 0.05 and 0  $\text{mg L}^{-1}$ . The zero concentration is equivalent to the same volume of buffer injected over the surface. All curves were subtracted by a blank reference surface (BSA blocked).

Figure 3.5 shows sensorgrams displaying fast association and low dissociation rates, which are also observed in Figure 3.4 when using a blank surface as reference. The 1:1 Langmuir model suggests that the interaction is strong with  $k_a = 8.4 \times 10^3 \text{ Ms}^{-1}$  and  $k_d = 3.29 \times 10^{-8} \text{ s}^{-1}$  resulting in affinity of  $K_A = 2.55 \times 10^{11} \text{ M}^{-1}$  and  $K_D = 3.92 \times 10^{-12} \text{ M}$  confirming that the antibody has very high affinity and only dissociates very slowly from the ochratoxin A. The affinity shows a three orders of magnitude increase

compared to the binding event where a mixture of specific binding and cross-reaction with BSA is monitored (Figure 3.4). The LOD at a maximum response of 6 RU is corresponding to an antibody concentration of  $0.1 \text{ mg L}^{-1}$ , which is a five fold increase in sensitivity in respect to the binding interaction, monitored using ethanolamine blocking as reference.

Comparing Figure 3.2 to 3.4, antibody A shows a magnitude higher affinity and 4 orders of magnitude better sensitivity than antibody B. Taking into account the cross-reactivity of the antibodies towards BSA (Figure 3.3 and 3.5), antibody B shows slower dissociation rates resulting in three times higher affinity of antibody B for the immobilized ochratoxin A-conjugate than antibody A. However, antibody A shows better sensitivity in comparison (two fold more sensitive). This shows that the cross-reactivity towards BSA has sufficient impact on the overall binding interaction to affect the overall affinity. For accurate kinetics and affinity, a BSA reference should be used at all time using this binding format.

### 3.4.4 Immobilised antibody

As a comparison the antibody was immobilised and the ochratoxin A-BSA conjugate used as analyte as illustrated in Figure 3.6. Here, the influence of cross-reaction with BSA cannot be reference subtracted, as the conjugate is injected as analyte. Only immobilised ligands can be used as reference using the BIAevaluation software 3.2. This has to be taken into consideration when analysing affinity of the binding interactions.

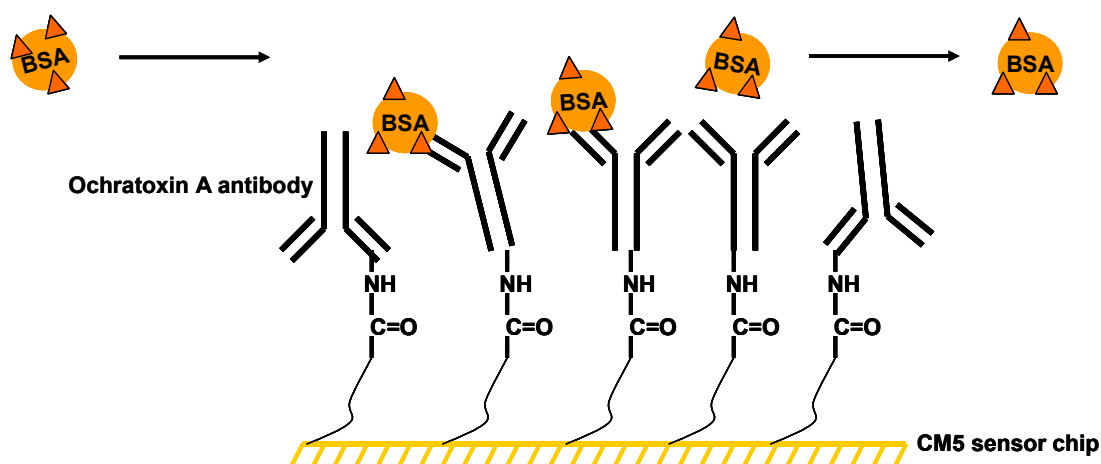


**Figure 3.6:** Covalently immobilised ochratoxin A antibody is linked to the sensor chip surface through a carbodiimide linker. The illustration represents amine coupling. The ochratoxin A-BSA analyte is passed over the surface at a set flow rate displaying association and dissociation from the immobilised ochratoxin A antibody ligand.

#### 3.4.4.1 Antibody B ligand with ochratoxin A-BSA analyte

Anti-ochratoxin A antibody B itself was successfully immobilized onto a CM5 chip surface to investigate a direct assay format. The activity of an antibody could be decreased due to non-site-specific immobilisation which might hinder the access to its antigen-binding site; nevertheless the ochratoxin A-BSA analyte showed sensitive binding as seen in Figure 3.7.

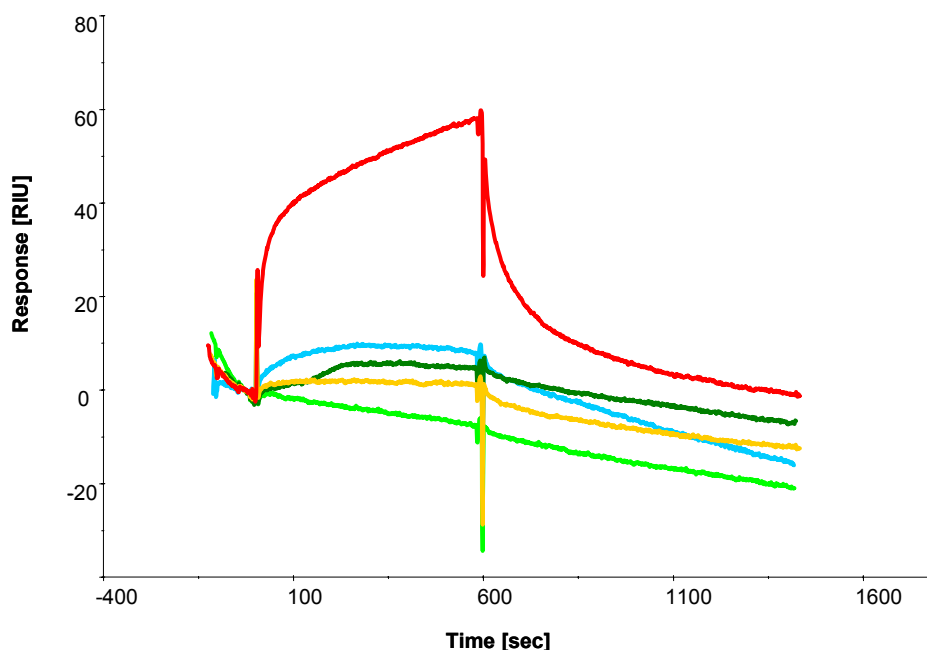


**Figure 3.7:** Sensorgram of response unit versus time illustrating varying ochratoxin A-BSA concentrations (top to bottom: 100, 10, 1, 0.1 and 0.01 mg L<sup>-1</sup>) binding immobilized anti-ochratoxin A antibody (Biogenesis). All curves are reference subtracted with non-specific IgG used as blank.

The overall signal response shown in Figure 3.7 was clearly lower and the drifting baseline implies that the immobilised antibody is leaking off the surface due to insufficient covalent attachment. This assumption was made as the drift had been observed over several hours of flowing buffer over the surface, but did not stabilise. The low response unit can be a result of activity of the immobilised antibody and the decreasing surface coverage of the antibody as it is leaking off the surface over time. The curve displaying the highest ochratoxin A-BSA analyte concentration (red) might indicate a biphasic binding event as the association and dissociation curves seem to progress at two stages. This can be seen as the initial association progresses very quickly however does not proceed into a signal plateau as expected for a steady state reaction but progresses by further increase in signal, which indicates a second binding phase. This can be a result of multiple binding events as ochratoxin A-BSA has on average 3-6 epitopes, as a result of binding cooperativity and also as a result of the antibody cross-reacting with BSA at a different affinity. Analysing the data with 1:1 binding kinetics, the average kinetics and affinity for antibody B binding immobilized ochratoxin A-BSA are:  $k_a = 2 \times 10^4 \text{ Ms}^{-1}$ ,  $k_d = 3 \times 10^{-3} \text{ s}^{-1}$  and  $K_A = 6 \times 10^4 \text{ M}^{-1}$ ,  $K_D = 3 \times 10^{-6}$

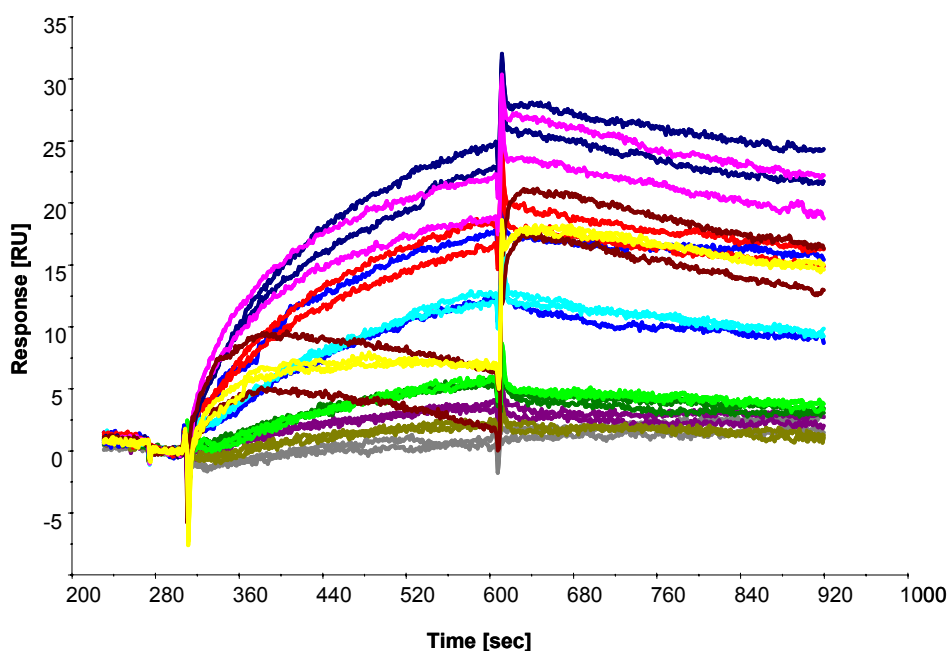


M. The affinity of the binding interaction was about two to three magnitudes lower having the antibody immobilized instead of ochratoxin A-BSA, as compared to the binding interaction (blank reference) shown in Figure 3.2 as it also includes BSA cross-reaction. The lower affinity is mainly due to the increase in dissociation rate, which indicates a slight activity loss of the immobilised antibody and thus a decrease in binding strength. The sensitivity of the binding interaction though was sufficiently low at a concentration of  $1 \text{ mg L}^{-1}$ .

#### 3.4.4.2 Antibody A ligand with ochratoxin A-BSA analyte

Antibody A was also immobilized onto a CM5 chip surface to investigate a direct assay format using ochratoxin A-conjugates.

Figure 3.8 below shows a steady baseline and no signal drift indicating a stable immobilisation of antibody. This is also corresponding well with the overall signal response, which was lower than shown with antibody B (Figure 3.7).



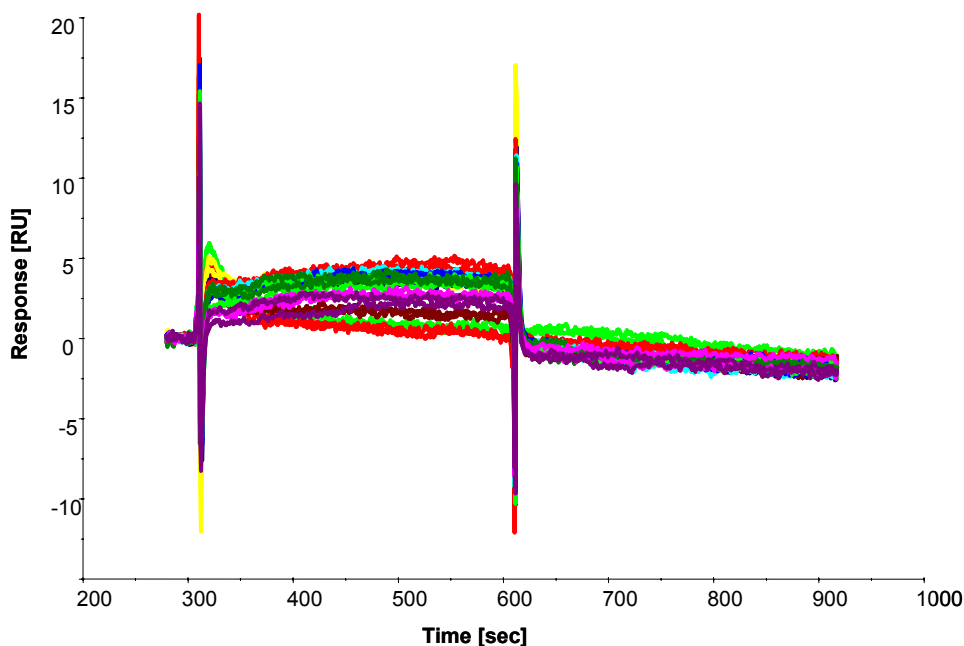
**Figure 3.8:** Sensorgram of response unit versus time illustrating the binding of ochratoxin A-BSA to immobilized ochratoxin A-antibody (Acris). All curves are reference subtracted with non-specific IgG used as blank. All conjugate concentrations were measured in duplicate to assess the reproducibility of the method. The ochratoxin A-BSA concentrations as displayed from top to bottom ranged from 100, 50, 20, 10, 5, 2, 1, 0.5, 0.2, 0.1 and  $0 \text{ mg L}^{-1}$ .

Figure 3.8 shows a reduced binding response at similar ochratoxin A-BSA analyte concentrations. This is probably a result of the activity loss upon non-site-directed immobilisation. Also, the immobilisation level of antibody A was only 2380 RU compared to 5400 RU for antibody B, indicating lower binding capacity. Fitting basic kinetic model 1:1 Langmuir binding to the curves results, the kinetics and affinity of the binding interaction are summarized as follows:  $k_a = 1.41 \times 10^5 \text{ M}^{-1} \text{ s}^{-1}$ ,  $k_d = 4.75 \times 10^{-4} \text{ s}^{-1}$  and  $K_A = 2.96 \times 10^8 \text{ M}^{-1}$ ,  $K_D = 3.38 \times 10^{-9} \text{ M}$ .

#### **3.4.4.3 Antibody A ligand with ochratoxin A-HRP analyte**

A commercially available ochratoxin A-HRP conjugate is not available except for those being included in binding assay kits, which are generally expensive. As a cost-effective alternative, an in-house prepared ochratoxin A-HRP conjugate (as described in section 3.3.2.1) has shown good enzyme activity containing a crude mixture of HRP and HRP-conjugate. The ratio of ochratoxin A per mol horseradish peroxidase was not analysed and therefore is not known.

To assess the composition of the conjugate, one has to employ for instance Matrix-Assisted Laser Desorption/Ionisation (MALDI) Time-of-Flight (TOF) mass spectrometry. At this point, this method is not available. Therefore, the success of the conjugation with ochratoxin A was verified using binding analysis. Antibody A was chosen for this experiment (Figure 3.9) as it had previously shown higher sensitivity for the ochratoxin A-BSA conjugate.



**Figure 3.9:** Sensorgram of response unit versus time illustrating the binding of ochratoxin A-HRP (Horseradish peroxidase) to immobilized ochratoxin A-antibody (Acris; amine coupling). All curves are reference subtracted with non-specific IgG used as blank. All conjugate concentrations were measured in duplicate to assess the reproducibility of the method. The ochratoxin A-BSA concentrations as displayed from top to bottom ranged from 100, 50, 20, 10, 5, 2, 1, 0.5, 0.2, 0.1 and 0 mg L<sup>-1</sup>.

The sensorgram (Figure 3.9) shows very little response with the highest ochratoxin A-HRP concentrations resulting in about 5 RU (five fold less response than with ochratoxin A-BSA). The residuals analysis shows a variation in signal of  $\pm 0.8$  RU. It was assumed that ochratoxin A-HRP interacts with the immobilised antibody as a clear association phase that can be observed in contrast to the zero concentration (blank injection).

Therefore, the sensorgrams were fitted to the kinetic model 1:1 Langmuir binding, which gives a  $\chi^2$  value of 1.01 as indicator of good statistical value. The kinetics of the binding interaction is  $k_a = 0.0173 \text{ Ms}^{-1}$  and  $k_d = 1.01 \times 10^{-5} \text{ s}^{-1}$ ,  $K_A = 1.71 \times 10^3 \text{ M}^{-1}$  and  $5.84 \times 10^{-4} \text{ M}$ . The affinity evaluation confirms very little affinity, as a result of very fast association and dissociation, of the conjugate for the immobilised antibody A. This indicates that the conjugation ratio of mol ochratoxin A to mol HRP is probably low suggesting that the conjugate should not be used in sensitive binding assays.

Due to the lack of a suitable reference cell, in retrospective, a simple injection of BSA alone could have been used as a reference to the injection of ochratoxin A-BSA and ochratoxin A-HRP by subtracting the sensorgram of the BSA injection from the signal curve.

### 3.4.5 Immobilised ochratoxin A-BSA with ochratoxin A competitor

Competitive assays differ from direct binding analysis as the binding interaction is not entirely happening on the ligand surface (surface affinity) but also in the analyte solution (solution affinity) as illustrated in Figure 3.10.

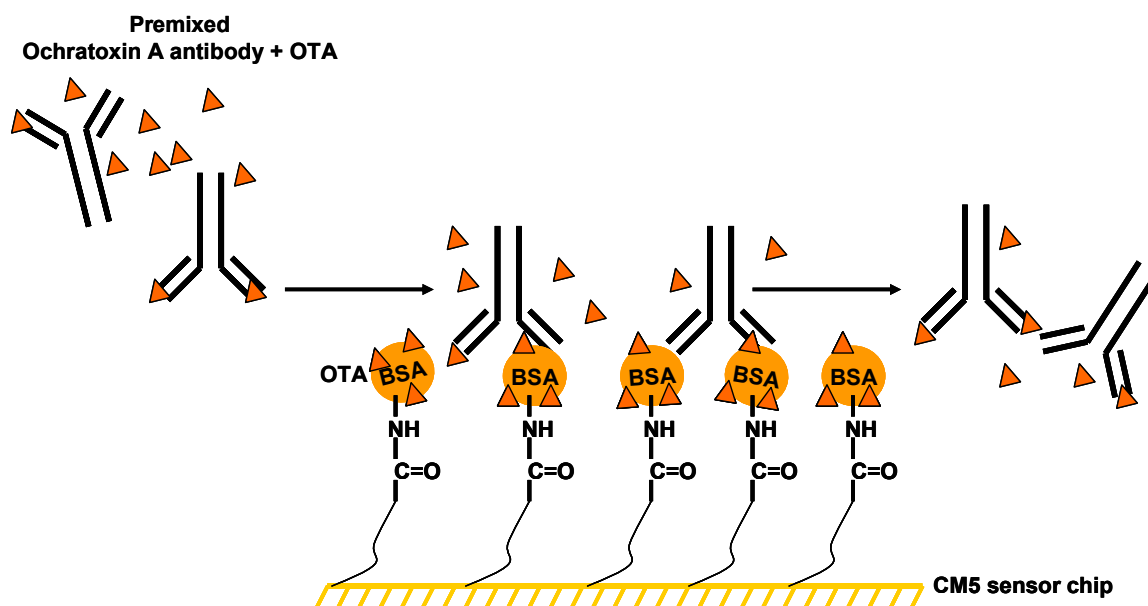


**Figure 3.10:** Covalently immobilised ochratoxin A-BSA is linked to the sensor chip surface via amine coupling. The ochratoxin A antibody is premixed with varying ochratoxin A concentrations and the solution is then passed over the sensor surface at a set flow rate illustrating the competitive reaction of premixed ochratoxin A and immobilised ochratoxin A-BSA ligand for antibody binding sites.

#### 3.4.5.1 Ochratoxin A-BSA ligand with antibody B and ochratoxin A competitor

A competitive assay using ochratoxin A antibody B analyte and ochratoxin A as competitor is shown in Figure 3.11.

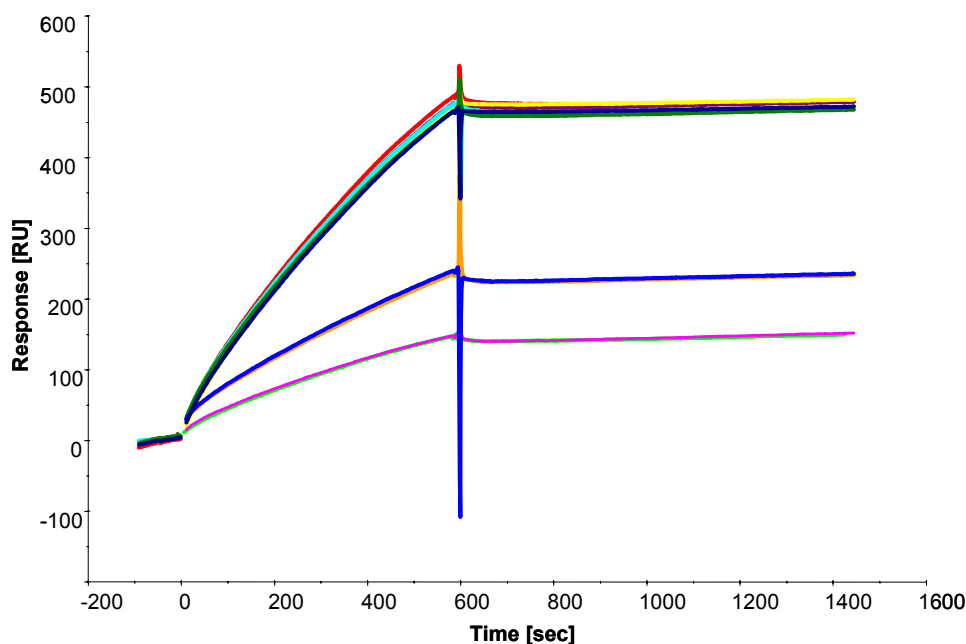


**Figure 3.11:** Sensorgram of response unit versus time illustrating the binding of ochratoxin A-antibody (Biogenesis) to ochratoxin A in solution competing with immobilized ochratoxin A-BSA. The measurement was performed in duplicate and the ochratoxin A concentrations in solution with the antibody are displayed in duplicate from top to bottom: 0, 0.0001; 0.001; 0.01; 0.1; 1; 10 and 100 mg L<sup>-1</sup> ochratoxin A standard.

The sensorgrams in Figure 3.11 illustrate that with the increase in ochratoxin A concentration, antibody B will predominantly bind the free analyte than to immobilized ochratoxin A-BSA surface resulting in a decrease in signal. The response signal drops with increase in ochratoxin A competitor in solution. However, no competition could be observed with ochratoxin A standard concentrations below 0.1 mg L<sup>-1</sup>. This could be due to the cross-reaction with immobilised BSA-conjugate as competitive standard curve with ochratoxin A-BSA could not be obtained.

### 3.4.5.2 Ochratoxin A-BSA ligand with antibody A and ochratoxin A competitor

A competitive assay using the second ochratoxin A antibody (A) with ochratoxin A in solution as competitor is shown in Figure (Figure 3.12).

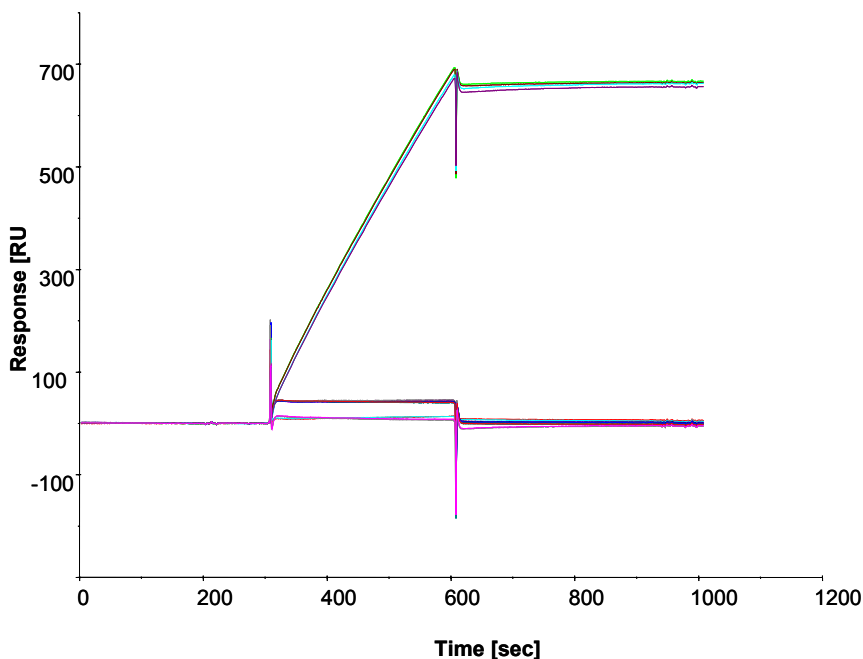


**Figure 3.12:** Sensorgram of response unit versus time illustrating the binding of ochratoxin A-antibody (Acris) to ochratoxin A in solution competing with immobilized ochratoxin A-BSA. The measurement was performed in duplicate and the ochratoxin A concentrations in solution with the antibody are displayed in duplicate from top to bottom: 0, 0.0001; 0.001; 0.01; 0.1; 1; 10 and 100 mg L<sup>-1</sup> ochratoxin A standard.

Figure 3.12 shows the response signal drop with increase in ochratoxin A competitor in solution indicating the competition of ochratoxin A with immobilised ochratoxin A-BSA for antibody A binding sites. No competition was observed with lower ochratoxin A standard concentrations below 0.001 mg L<sup>-1</sup>. This indirect competitive assay shows that both antibodies show some sensitivity for the ochratoxin A standard, particularly antibody A which shows a 100 times better sensitivity than antibody B. However, the influence of BSA cross-reactivity leads to a non-linear relationship of response signal versus ochratoxin A standard concentration when attempting a standard curve. Therefore, the competitive assay has to be improved by either affinity purifying the antibodies using a BSA-immunoaffinity column or by adding BSA to the buffer solutions used for binding interaction to reduce non-specific binding.

### 3.4.6 Wine sample analysis

As antibody A had shown better sensitivity in the competitive assay (Figure 3.12) it was used when monitoring a number of standard ochratoxin A concentrations in a competitive format to establish a standard curve that can be used alongside wine analysis. The indirect competitive assay has been optimised regarding the cross-reactivity with BSA by adding  $10 \text{ mg L}^{-1}$  BSA to antibody A solution before it was premixed with an ochratoxin A standards and injected over the immobilised ochratoxin A-BSA conjugate. The competitive binding interaction is shown in Figure 3.13.

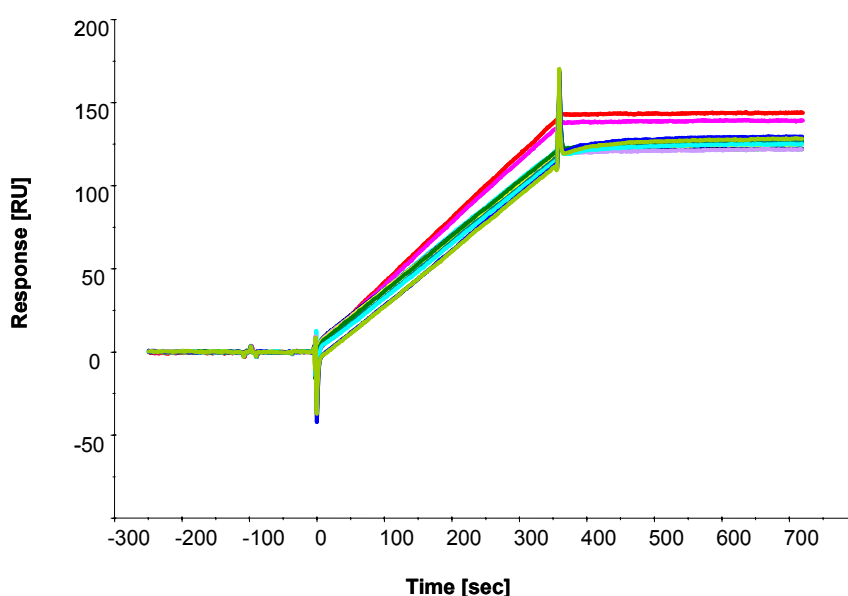


**Figure 3.13:** Sensorgram of response unit versus time illustrating the binding of ochratoxin A-antibody (Acris) to ochratoxin A in solution competing with immobilized ochratoxin A-BSA. The reference surface is blocked with BSA and used as blank. The measurement was performed in duplicate and the ochratoxin A concentrations in solution with the antibody are displayed in duplicate from top to bottom: 0, 0.0001; 0.001; 0.01; 0.1; 1; and  $10 \text{ mg L}^{-1}$  ochratoxin A standard (in HEPES buffer pH 7.4).

The overall response signal is much lower shown in Figure 3.13 compared to the untreated (no BSA additive) assay shown in Figure 3.12. The optimised assay shows a much more refined decrease of response signal with increasing ochratoxin A standard concentration. The response signal at the end of the dissociation phase indicates the amount of analyte (antibody A) bound to the ligand surface (ochratoxin A-BSA). At the end of dissociation all loosely bound biomaterial is washed off and the response unit should directly correspond to the antibody concentration bound to the surface and thus



inversely to the ochratoxin A standard concentration. By plotting the RU values at the end of dissociation of each sensorgram against the respective ochratoxin A concentration, a standard curve is presented (Figure 3.14).

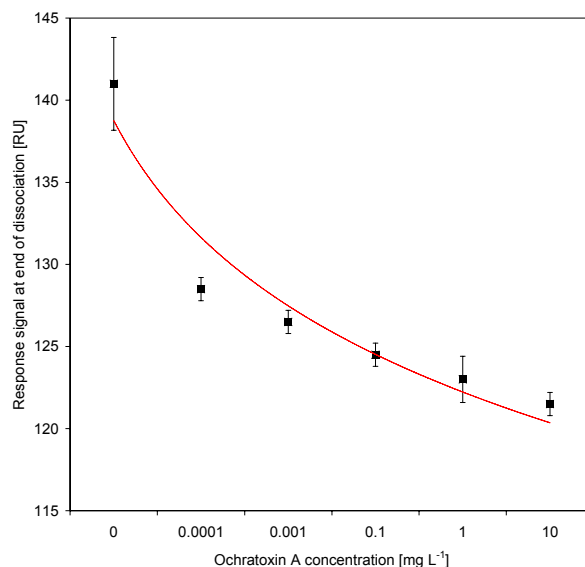


**Figure 3.14:** Standard curve displaying response signal [RU] versus ochratoxin A standard concentration: 0; 0.0001; 0.001; 0.1 and 10 mg L<sup>-1</sup> in HBS, pH 7.4.

The plot in Figure 3.14 shows the decrease of signal with increasing ochratoxin A competitor concentration. It appears that the sensitivity could be high for this method as there is a clear signal distinction between the 0.1  $\mu\text{g L}^{-1}$  and zero concentration. To emphasize the linear decrease of the signal with concentration the data have been normalised by the response signal by the blank response and multiplied by 100 (Figure 3.15).

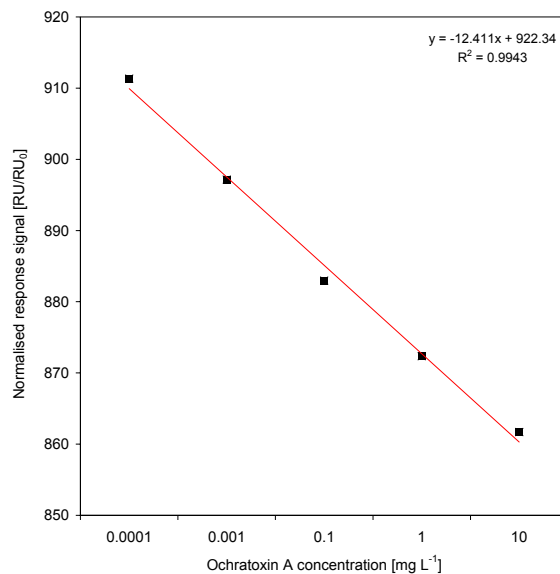


**Figure 3.15:** Normalised response signal [RU] times 100 versus ochratoxin A standard concentration: 0; 0.0001; 0.001; 0.1 and 10 mg L<sup>-1</sup>.

The blank response is the zero concentration for ochratoxin A, which should show maximum, non-competed binding of the antibody to ochratoxin A-BSA. Figure 3.15 confirms the linear dependency of ochratoxin A concentration and response signal and illustrates the dynamic range of the binding assay of 0.1  $\mu\text{g L}^{-1}$  to 10 mg L<sup>-1</sup> with a sensitivity of below 0.1  $\mu\text{g L}^{-1}$ . The sensitivity of this assay is compared to a multi analyte biosensor for mycotoxins by van der Gaag *et al.* [2003], who describe a similar competitive binding assay for ochratoxin A, except for using a non-commercial monoclonal antibody and having an ochratoxin A-derivative immobilised on the sensor surface. The assay results in a sensitivity value of 0.1  $\mu\text{g L}^{-1}$ , which is in about the same range of magnitude as presented here.

These standards were recorded along side a number of selected red wine samples that have been pre-treated using immunoaffinity chromatography and were re-dissolved in HEPES buffered saline, pH, 7.4. Wine samples were premixed with a fixed concentration of antibody A (2.5  $\mu\text{g L}^{-1}$ ) and passed over the sensor surface. Any ochratoxin A present in a wine sample binds the antibody and is competing with immobilized ochratoxin A-BSA. The following sensorgram shows the competitive analysis of a number of wine samples (Figure 3.16).

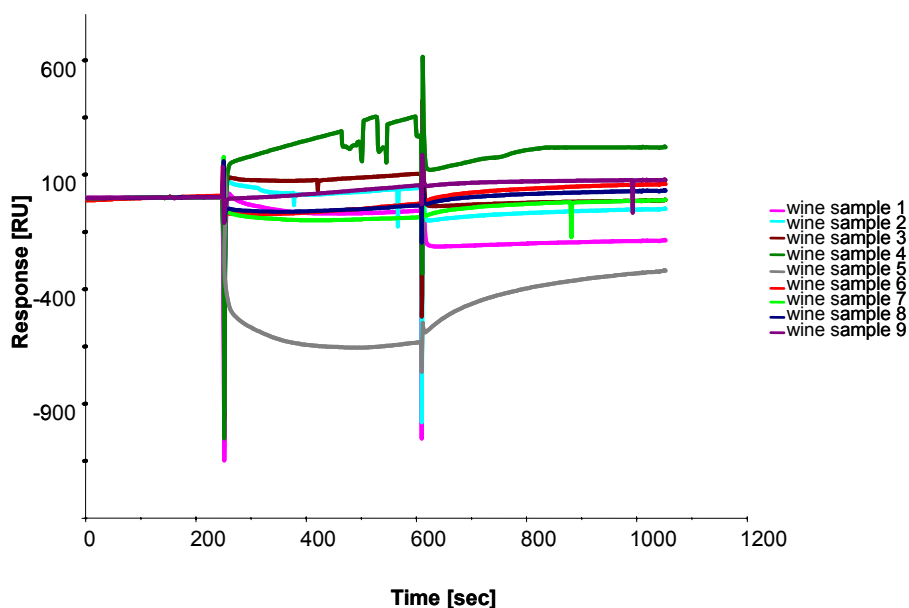


**Figure 3.16:** Sensorgram of response unit versus time illustrating wine samples premixed with ochratoxin A antibody A passed over the sensor surface. Any ochratoxin A present in a wine sample binds the antibody and is competing with immobilized ochratoxin A-BSA. Signal spikes result from interfering substances present in wine.

This (Figure 3.16) shows the sensorgrams depicting the signal response resulting from the ochratoxin A present in wine samples. Signal spikes result from interfering substances present in wine that affect the refractive index change on the sensor surface. A clear increase in signal during the association phase can only be seen with wine sample 4 (121 RU), 6 (15 RU) and 9 (50 RU).

All other curves show a negative response or interferences in signal. This is probably related to the clean-up procedure of wine samples and the remainder of interfering particles in the concentrate, which might indicate that the immunoaffinity (IAC) clean-up procedure is not removing isolated ochratoxin A from the wine sample but also other, possibly interfering, substances. Another possibility is that the solvent (methanol) used for ochratoxin A extraction was not completely evaporated when redissolving ochratoxin A in HEPES buffer and that the methanol could have an effect on the refractive index of the injected sample solution and thus causes the signal spikes. To be able to measure ochratoxin A concentration in processed wine samples, the indirect competitive assay needs further improvement.

### 3.4.7 Control experiments

Some control experiments were carried out to determine the binding model of multivalent ochratoxin A-BSA and the bivalent antibody. Other control experiments involved the investigation of the common mass transfer effect and also the binding interaction of both antibodies to the BSA reference surface is investigated.

#### 3.4.7.1 Multi-valance of the binding interaction

To establish what type of binding model would fit the interaction; a linked reaction experiment is carried out. A fixed concentration of ochratoxin A-BSA analyte is binding to immobilized ligand (antibody A) at different flow rates. By aligning the curves at the injection stop marker (end of association), the dissociation phase is analysed (Figure 3.17).

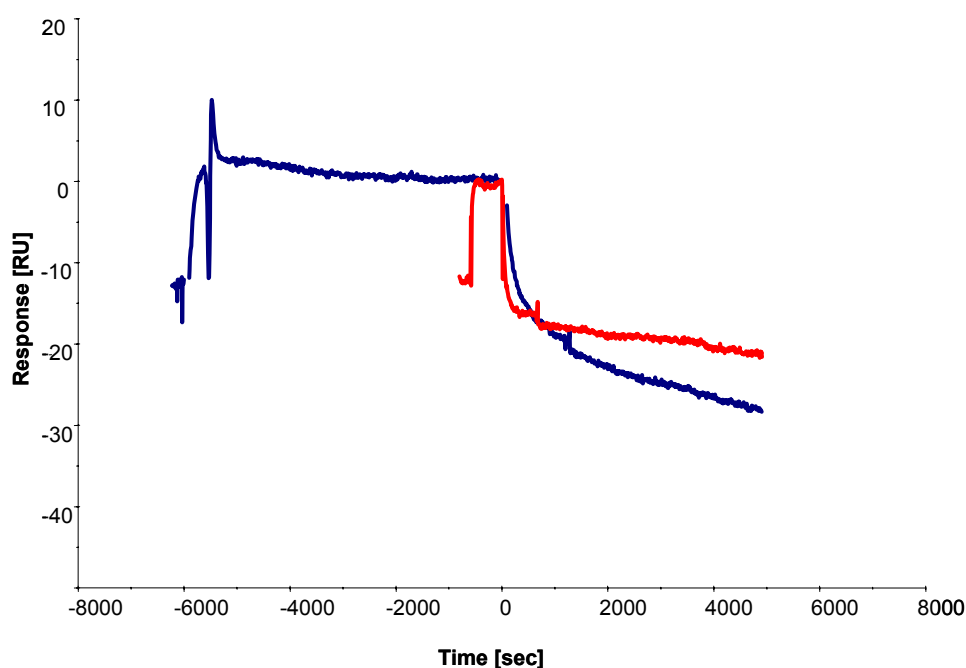


**Figure 3.17:** Sensorgrams of response unit versus time showing a fixed concentration of ochratoxin A-BSA ( $10 \text{ mg L}^{-1}$ ) analyte binding to immobilized ochratoxin A-antibody at two distinct flow rates:  $1 \text{ } \mu\text{l min}^{-1}$  (blue) and  $5 \text{ } \mu\text{l min}^{-1}$  (red).

For a 1:1 binding or heterogenous ligand, the dissociation curves should match. As seen in Figure 3.17, the dissociation phase at the different flow rates do not match, as the faster flow rate yields a dissociation curve above the slower one. This indicates that the

binding event is clearly more complex than a 1:1 binding or heterogeneous ligand model. The suggested models are bivalent analyte for analytes with two ligand binding sites or heterogeneous analyte, when a competing reaction occurs. Here, with ochratoxin A-BSA as analyte, a multivalent interaction is assumed, when the antibody is the analyte, it is clearly a bivalent interaction as long as the immobilized ligand is monovalent. With ochratoxin A-BSA immobilized, the model would fit the heterogeneous ligand model, as long as the analyte is monovalent. Multivalent ligands behave as separate binding sites, whereas multivalent analytes lead to avidity effects which are difficult to analyse. Since both reagents are multivalent, a perfect fit cannot be established easily.

### 3.4.7.2 Mass transfer control experiment

When the association rate constant ( $k_a$ ) is greater than  $1 \times 10^6 \text{ M}^{-1} \text{ s}^{-1}$  then the measured rate of binding interaction may reflect the transfer of analyte to the surface rather than the reaction rate itself (Chaiken, 1993). The mass transfer control experiment for antibody A and B analytes to immobilised ochratoxin A-BSA is depicted in Figure 3.18 and 3.19.

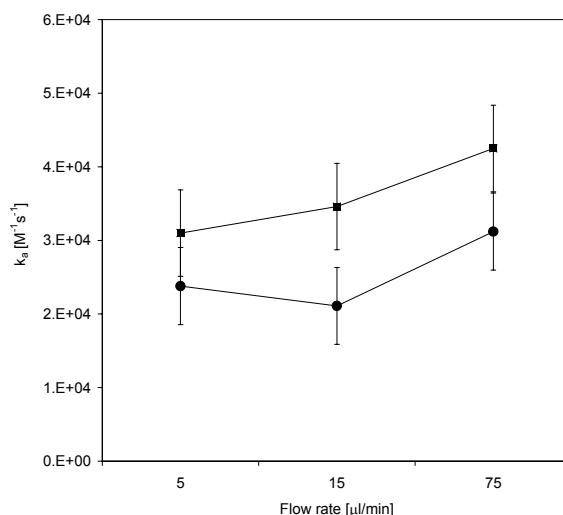


**Figure 3.18:** Association rate constant  $k_a$  versus increasing flow rate. Ochratoxin A antibodies (antibody A (■) and antibody B (●)) are passed over a sensor surface with immobilised ochratoxin A-BSA. The binding interaction is observed at increasing flow rates (5, 15 and  $75 \mu\text{l min}^{-1}$ ) and the increasing association constant ( $k_a$ ) is related to mass transfer.

A  $k_a$  value as high as  $1 \times 10^6 \text{ M}^{-1} \text{ s}^{-1}$  has not been observed in the presented experiments, however, mass transfer limitation are likely. This was identified by varying the flow rate, since mass transfer is influenced by flow whereas the reaction rate is flow independent. As seen in Figure 3.18 above, the  $k_a$  value increases slightly with increasing flow rate ( $75 \mu\text{l min}^{-1}$ ). If mass transport limitation is involved, a higher flow rate will also decrease the dissociation rate constants (Figure 3.19) until the mass transport limitation is slower than the binding kinetics.

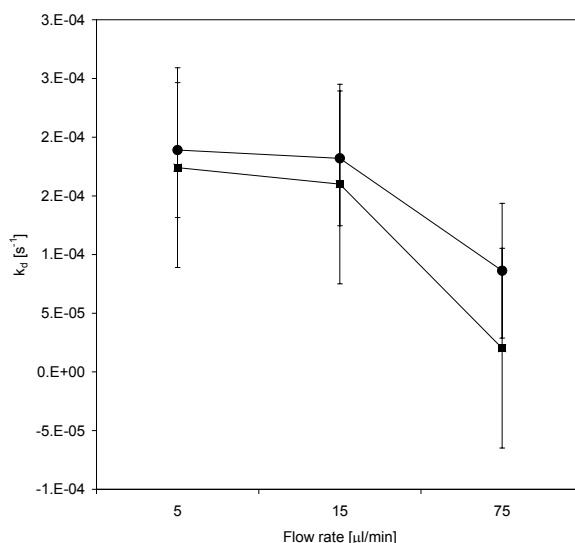


**Figure 3.19:** Dissociation rate constant  $k_d$  versus increasing flow rate. Ochratoxin A antibodies (antibody A (■) and antibody B (●)) are passed over a sensor surface with immobilised ochratoxin A-BSA. The binding interaction is observed at increasing flow rates ( $5, 15$  and  $75 \mu\text{l min}^{-1}$ ) and the increasing dissociation constant ( $k_d$ ) is related to mass transfer.

The dissociation rate constant  $k_d$  decreased significantly at  $75 \mu\text{l min}^{-1}$  (Figure 3.19). It can be assumed that there is minor mass transfer, indicated by the variation in association and dissociation rate constant, for both antibodies. However, the variation is within the standard deviation in both plots. Therefore, the mass transfer should not limit the interaction of the antibody analytes with immobilised ochratoxin A-BSA and the observed binding rate as depicted in Figure 3.3 and 3.5 is confirmed as the true, unlimited binding rate of the binding interaction.

### 3.4.7.3 BSA cross-reactivity

BSA cross-reactivity can be easily assessed by monitoring varying antibody concentrations on a single flow cell immobilised with BSA. In the following experiment, the flow cell response signal that has been reference subtracted from sensorgrams in Figure 3.3 is shown in Figure 3.20 for antibody B binding BSA.

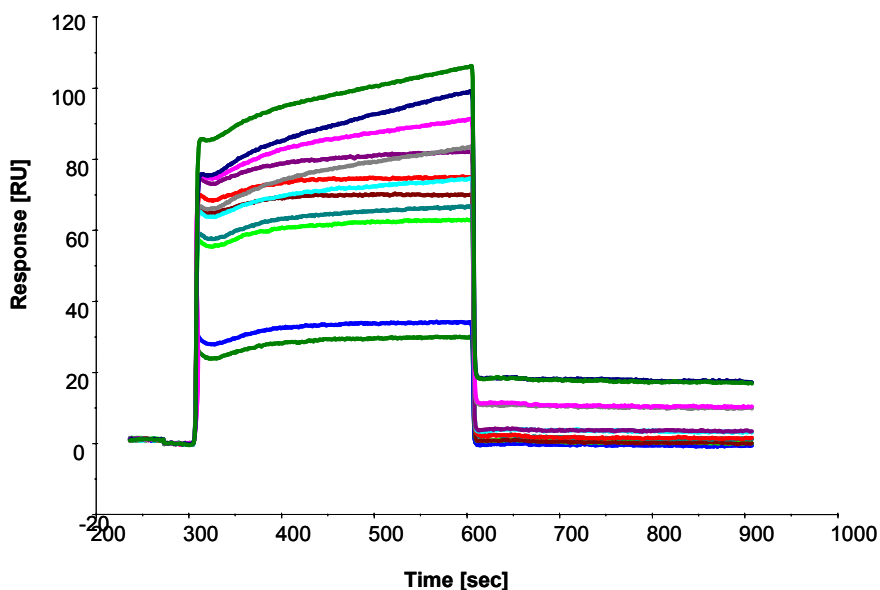


**Figure 3.20:** Sensorgram of response unit versus time illustrating the binding of antibody B to immobilized BSA (bovine serum albumin). All antibody concentrations are displayed from top to bottom ranged from 100, 50, 20, 10, 5, 2, 1, 0.5, 0.2, 0.1, 0.05 and 0 mg L<sup>-1</sup>.

The flow cell response signal that has been reference subtracted from sensorgrams in Figure 3.5 is shown in Figure 3.21 for antibody A binding BSA. It seems that there is a population of antibodies that show fast kinetics with BSA and dissociation is fast and completed right at the beginning of the dissociation phase.

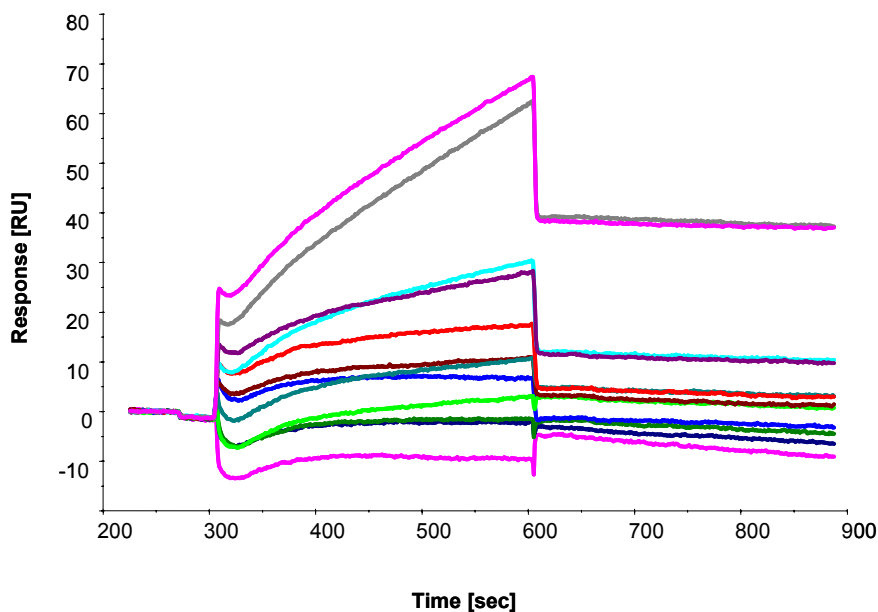


**Figure 3.21:** Sensorgram of response unit versus time illustrating the binding of antibody A to immobilized BSA (bovine serum albumin). All antibody concentrations are displayed from top to bottom ranged from 100, 50, 20, 10, 5, 2, 1, 0.5, 0.2, 0.1, 0.05 and 0 mg L<sup>-1</sup>.

As seen in Figure 3.20, it seems that antibody B binds with a greater capacity to immobilised BSA as the signal response is greater for similar antibody concentrations. In Figure 3.21, the beginning of the association appears to be slower than the end of association displaying two phase association kinetics which indicates two distinct populations of polyclonal antibodies binding BSA. Also, the dissociation of antibody B (Figure 3.20) from BSA is fast indicated by an instant drop in signal after end of association, whereas antibody A displays slower dissociation kinetics, which are not completed right at the start of the dissociation phase. This would indicate that antibody A is cross-reacting with BSA to a greater extent than antibody B.

Antibody B results in the following kinetic and affinity with a  $\chi^2$  value of 0.9:

$$k_a = 3.03 \times 10^5 \text{ M}^{-1} \text{ s}^{-1}, k_d = 7.49 \times 10^{-4} \text{ s}^{-1} \text{ and } K_A = 4.04 \times 10^8 \text{ M}^{-1}, K_D 2.47 \times 10^{-9} \text{ M}.$$

Antibody A results in the following kinetic and affinity with a  $\chi^2$  value of 9.05

$$k_a = 2.41 \times 10^3 \text{ M}^{-1} \text{ s}^{-1}, k_d = 6.36 \times 10^{-4} \text{ s}^{-1} \text{ and } K_A = 3.79 \times 10^6 \text{ M}^{-1}, K_D 2.64 \times 10^{-7} \text{ M}.$$



The overall affinity of the antibody A for BSA is actually two magnitudes lower than with antibody B as a result of a fast association rate displayed in Figure 3.21. The affinity indicates that the antibody A is cross-reacting with BSA with less strength.

### **3.5 Concluding remarks**

The binding interaction analysis using Biacore shows several advantages compared with standard immunoassay techniques, such as the real-time, high throughput monitoring of association and dissociation rates and also the sensitivity of the detection. However, the standard immunoassay could be optimised further.

In this work, antibody A had shown better sensitivity in the competitive assay (Figure 3.12) it was used when monitoring a number of standard ochratoxin A concentrations in a competitive format to establish a standard curve that can be used alongside wine analysis. Figure 3.14 and 3.15 confirms the linear dependency of ochratoxin A concentration and response signal and illustrates the dynamic range of the binding assay of  $0.1 \mu\text{g L}^{-1}$  to  $10 \text{ mg L}^{-1}$  with a sensitivity of below  $0.1 \mu\text{g L}^{-1}$ . The sensitivity of this assay was directly compared to a multi analyte biosensor for mycotoxins by van der Gaag *et al.* [2003], who produced calibration curves for the mycotoxins, zearalenone, aflatoxin B1, and Ochratoxin A. The detection limit for all mycotoxins was between  $0.1$  to  $0.4 \mu\text{g L}^{-1}$ . The indirect competitive binding assay for ochratoxin A was similar to this work, except for using a non-commercial monoclonal antibody and having an ochratoxin A-derivative immobilised on the sensor surface. The assay results in a detection limit of  $0.1 \mu\text{g L}^{-1}$  ochratoxin A, which is in about the same range presented here.

Deoxynivalenol (DON) sensing from wheat extracts by SPR-based immunoassays has been reported by Schnerr *et al.* [2002], who used a similar indirect competitive assay using polyclonal antibodies as described in this work, resulting in a working range between  $0.13$  and  $10.0 \text{ mg L}^{-1}$  of DON and a detection limit of  $2.5 \mu\text{g L}^{-1}$ . Another SPR-based inhibition assay was developed for deoxynivalenol, using monoclonal antibodies as recognition elements. The assay was based on the competition for antibody binding between the immobilized deoxynivalenol conjugate on the sensor and the free deoxynivalenol molecules in the test solution. The working range of the assay was

between 2.5 and 30  $\mu\text{g L}^{-1}$  [Tudos *et al.*, 2003]. Polyclonal antibodies were used in a surface plasmon resonance-based immunoassay for aflatoxin B1, resulting in a linear range of 3- 98  $\mu\text{g L}^{-1}$  [Daly *et al.*, 2000]. Alternatively, Thompson and Maragos [Maragos & Thompson, 1999] designed a fibre-optic immunosensor that has the potential for screening corn for fumonisins with a detection limit of 10  $\mu\text{g L}^{-1}$ . Optical waveguide lightmode spectroscopy (OWLS) has been applied for aflatoxin B1 and ochratoxin A determination using monoclonal antibodies in both direct and indirect competitive binding format. The sensitivity of the competitive assay ranged between 0.5 – 10  $\mu\text{g L}^{-1}$  for both aflatoxin B1 and ochratoxin A.

This shows that few SPR-based immunosensors have been tried for ochratoxin A analysis, but a view were developed for deoxynivalenol showing good sensitivity of about 2.5  $\mu\text{g L}^{-1}$ . Other sensors were based on fibre-optic or OWLS technology, showing less sensitivity as compared to SPR immunosensors. The work presented here shows that SPR could be a sensitive technique as an alternative method for ochratoxin A analysis in wine, which shows the required sensitivity and applicability for multiple sample analysis. However, the equipment and maintenance is costly and requires trained personell, thus a cheap, disposable sensor platform has an advantage.

The antibodies analysed with SPR technology were examined to be chosen for the electrochemical immunosensor and should show sufficiently high affinity and sensitivity in an indirect detection format. Taking the influence of BSA cross-reactivity into account, antibody B showed higher affinity for ochratoxin A, whereas antibody A displayed better sensitivity of the assay. After careful consideration, antibody A was chosen as recognition element for the electrochemical immunosensor development. One reason is that sensitivity of the assay has priority over affinity, especially since the difference in affinity is minor and antibody A shows high affinity by itself. Secondly, an indirect binding assay should not involve the immunogen to avoid further cross-reactivity and as the immunogen for antibody B was ochratoxin A-BSA conjugate and for antibody A the immunogen was a peptide mimicking the conjugate, the latter antibody A was suited better for the application even though Figure 3.20 and 3.21 indicate that polyclonal antibody A involves a population of antibodies recognizing BSA non-specifically.

## CHAPTER 4 : SCREEN PRINTED ELECTRODE BASED IMMUNOSENSOR FOR OCHRATOXIN A

### 4.1 Introduction

Bioanalytical assays such as immunoassays, which use specific antigen-antibody interaction, are commonly applied in many fields including biological and medical research, e.g. testing for environmental pollutants such as pesticides, in clinical drug tests, tumour markers, or food toxins. Immunoassays combined with electrochemical methods have been proven to be sensitive analytical tools obtaining detection limits down to  $10^{-15}$  M and offer reduced instrumentation costs compared to their optical counterparts.

Warsinke *et al.* [2000] already showed electrochemical immunoassays as promising alternatives to existing immunochemical tests for their use in opaque or optically dense matrices and the application of potentiometric, capacitive and amperometric transducers for direct and indirect electrochemical immunoassays. Amperometric transducers are preferred due to their fast detection, broad linear range and low detection limit. Competitive and non-competitive amperometric immunoassays have been developed with redox compounds or enzymes as labels. Amperometric screen-printed electrode sensors based on a sensitive immunoassay format represent a promising tool for the specific and sensitive analysis of ochratoxin A. The performance and reproducibility of an electrochemical immunosensor depend mainly on the communication of detection system and transducer and also on the immobilisation procedure involved.

In this work the development of a disposable immunosensor on screen-printed gold electrodes for the analysis of ochratoxin A (OTA) contamination in wine samples is presented.

To date, there is no known immunosensor applying screen-printed gold electrodes and using the indirect competitive immunoassay format for the detection of ochratoxin A in wine. Previous work using a screen-printed electrode sensor for ochratoxin A analysis has been conducted using a carbon working electrode [Alarcon *et al.*, 2006] as well as a

sample clean-up. In this paper, however, we report the first use of screen-printed gold electrodes (SPGE) as an attractive alternative to the common carbon electrode. Major difficulties in the immunosensor development are primarily related to immobilising biomolecules that remain biologically active and secondly to generate a sensitive signal free of interferences arising due to complex sample matrices [Corgier *et al.*, 2005]. Interferences arising from wine are generally due to its polyphenols, which are easily oxidised on the working electrode [Avramescu *et al.*, 2001].

To tackle the problem arising from a complex sample matrix such as wine, the electrode surface was modified with a polyanionic reagent to diminish possible non-specific interaction and interference from wine components. This technique also allows for simple dilution of the sample prior to measurement instead of elaborative sample clean-up and pre-concentration procedures. The assay format is an indirect system, using immobilised ochratoxin A-BSA conjugate, a specific ochratoxin A antibody and a HRP-labelled anti-IgG antibody. The electrochemical detection involves chronoamperometry and uses a TMB/H<sub>2</sub>O<sub>2</sub> substrate catalysed by horseradish peroxidase that has been widely used for screen printed immunosensors [Butler *et al.*, 2006; Connely *et al.*, 2006 and Crew *et al.*, 2007].

The sensor was characterised using cyclic voltammetry and optimised resulting in a sensitive biosensor for ochratoxin A utilizing screen-printing technology with amperometric detection. The performance of the immunosensor for ochratoxin A standard solutions and real wine samples was cross-examined in relation to a standard enzyme immunoassay test kit (Ridascreen®) and HPLC analysis [European Standard, 2006].

The procedure for ochratoxin A determination in wine using the proposed screen-printed immunosensor is considered to be economical and has a high potential for automation and miniaturisation. The suggested immunosensor design is illustrated in Figure 4.1.

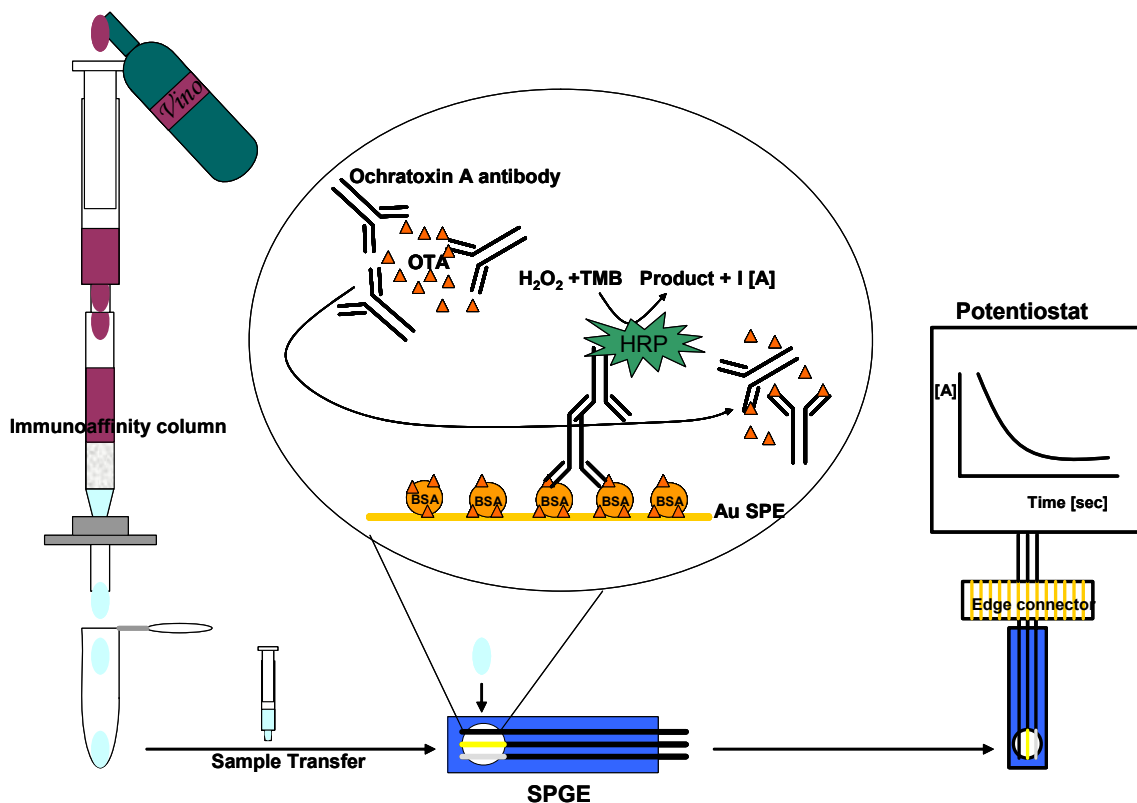


**Figure 4.1:** The immunosensor procedure proposed for ochratoxin A analysis using immunoaffinity purification of wine samples, transfer of the sample extract to the immunoassay-modified screen-printed gold electrode and measurement using chronoamperometry.

This (Figure 4.1) displays the immunosensor design for ochratoxin A in wine samples. The first step shows the immunoaffinity chromatography of wine samples using affinity extraction columns such as OchraTest<sup>TM</sup> and collection of concentrated ochratoxin A extract in buffer. The concentrated samples were transferred to the immunoassay modified electrode surface of the screen-printed gold electrode and upon addition of reactant, an amperometric signal change (current, I) can be observed over time.

## 4.2 Experimental

Anti-ochratoxin A antibodies were purchased from Acris GmbH (Germany). Secondary antibody (rabbit IgG-HRP) was from Dako (DakoCytomation, Denmark). The 3,3',5,5'-tetramethylbenzidine (TMB) solution containing hydrogen peroxide (H<sub>2</sub>O<sub>2</sub>) was purchased from Europa Bioproducts Ltd. (UK). Hydroquinone, polyvinylalcohol (PVA), polyvinylpyrrolidone (PVPP), polyethylene glycol (PEG), dextran (MW 10,000), 30 % hydrogen peroxide solution, 5% Nafion solution, and di-sodium phosphate and sodiumhydrogen phosphate as well as ochratoxin A-BSA conjugate and ochratoxin A was purchased from Sigma Aldrich Ltd. (UK). Sodium chloride, chloroacetic acid, sodium hydroxide and hydrochloric acid and potassium chloride were obtained from Fluka (UK). *N*-ethyl-*N*'-(3-dimethylaminopropyl)-carbodiimide (EDC), *N*-hydroxysuccinimide (NHS) and 0.1 M ethanolamine was from Biacore AB (Uppsala, Sweden).

Phosphate buffered saline, pH 7.4, containing KCl, was prepared according to the following recipe: NaH<sub>2</sub>PO<sub>4</sub> (2.96 g), Na<sub>2</sub>HPO<sub>4</sub> (11.5 g) and NaCl (8.4 g) are dissolved in 1L H<sub>2</sub>O. The pH was adjusted to 7.4, followed by 1:2 dilution with 0.2 M KCl in H<sub>2</sub>O, yielding a final concentration of 50 mM PBS, pH 7.4, containing 0.1 M KCl.

Screen printing gold ink R-464 (DPM-78) was purchased from Ercon Inc. (USA). Electrodag graphite ink (Electrodag 423 SS) and silver/silver chloride ink (Electrodag 6037 SS) is from Acheson Industries Inc. (USA). The insulating ink (242-SB) is an epoxy-based protective coating ink obtained from Agment ESL (Reading, UK). Melinex sheets were obtained from Cadillacprinting Ltd. (Swindon, UK). The edge connector with ribbon data cable (DG41U) was purchased from Maplin Electronics Ltd. (Milton Keynes, UK). Wine samples were chosen from distinct origins and grape species and all purchased from local stores in the lower to middle price range. Synthetic wine was kindly provided by Mariluz Rodriguez, prepared at the University of Valladolid, Spain, according to "Estacion Enologica of Rioja" (see also Appendix 1).

### 4.3 Methods

A DEK 248 screen-printing system (produced by DEK, UK) was used to fabricate the electrodes. Cyclic voltammetry experiments and chronoamperometry studies were performed using a Galvanostat/Potentiostat from Autolab (EcoChemie, Utrecht, Netherlands). A PC equipped with data acquisition and treatment software (GPES3) was used to record the signal generated in the electrochemical cell and received via the potentiostat.

#### 4.3.1 Fabrication of screen printed electrodes

Stainless steel screens with a screen mesh size of 200 counts per inch were used to print the electrodes. The DEK 248 parameters were adapted according to the standard operating procedure summarised in Table 4.1.

**Table 4.1:** Screen printer DEK 248 parameters for screen printing electrodes onto a polyester substrate using imaged screens.

Parameter	Action
Menu	Default
Menu name	Default
Print Mode	Double Squeegee
Print gap	2.6 cm
Deposits	1 (Carbon ink), 2 (Ag/AgCl and
Forward speed	66 mm s <sup>-1</sup>
Reverse speed	66 mm s <sup>-1</sup>
Inspection rate	0
Alignment rate	0
Front limit	54 mm
Rear limit	420 cm
Hop-over	26 mm
Separation speed	10%
Table-In delay	0 sec
Squeegee delay	0 sec
Hop-over delay	0 sec
Squeegee pressure	4 psi

The protocol in Table 4.1 was used to prepare the screen-printed electrodes (Figure 4.2) consisting of a gold working electrode ( $1.3 \text{ mm}^2$  planar area), carbon counter electrode and Ag/AgCl reference electrode. The screen-printed electrodes were mass fabricated in-house by a multi-stage screen-printing process using a DEK model 248 machine (DEK, Weymouth, UK). The electrodes were printed onto  $250 \text{ }\mu\text{m}$  thick Melinex ST725 polyester sheet obtained from Cadillac Plastic (Swindon, UK).

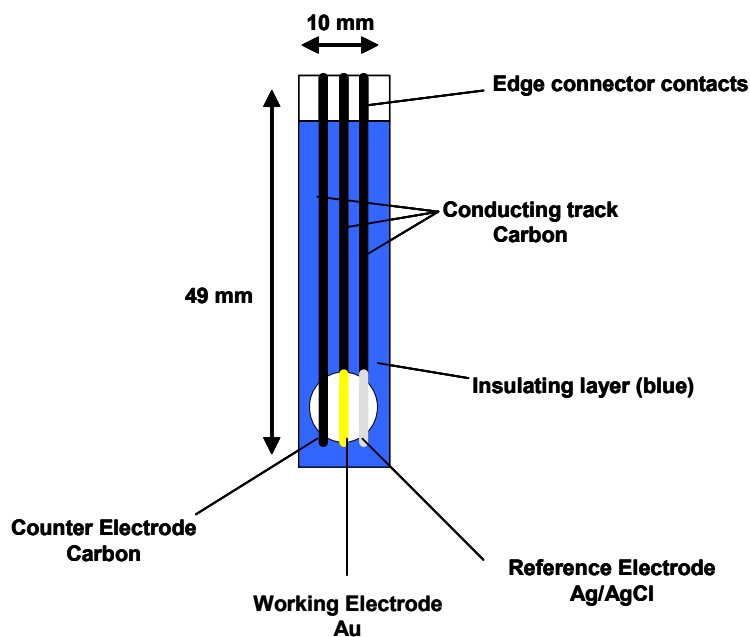


**Figure 4.2:** Three-electrode design of screen printed gold electrodes fabricated in-house at Cranfield University, 2006.

At first, the conducting basal tracks were printed using graphite based ink in one single deposit and dried in an oven at  $100^\circ\text{C}$  for 15 minutes. In the second step, a double deposit of silver/silver chloride in silver paste was printed onto one of the terminal basal tracks and dried in an oven at  $100^\circ\text{C}$  for 15 minutes. For screen-printed gold electrode construction, the centre terminal basal track was re-printed with one deposit of gold ink at an increased carriage speed of  $66 \text{ mm s}^{-1}$  and then dried at  $100^\circ\text{C}$  for 15 minutes. In the last step, the basal tracks were insulated with a protective coating ink leaving a defined circular shaped area ( $3.2 \text{ mm}^2$ ) for the electrical contact in measurements. The insulation layer was cured at  $100^\circ\text{C}$  for 1 hour in order to stabilise the epoxy resin. The sheets were left thereafter to dry in a drying cabinet at room temperature overnight. About 100 electrodes are printed per sheet at a time; and can be cut into individual



electrodes. Prior to use, the screen printed electrodes are treated at 120°C for 30 minutes and then cooled to room temperature under nitrogen atmosphere. In the following, the screen printed gold electrodes are generally abbreviated as SPGE, screen printed carbon electrodes as SPCE.

### 4.3.2 Electrochemical noise of screen printed electrodes

Electrochemical noise refers to naturally occurring fluctuations in potential and current flow. Electrochemical noise (EN) monitoring can be further subdivided into electrochemical potential noise (EPN) measurements and electrochemical current noise (ECN) measurements. Electrochemical noise measurements to date have been performed entirely on the subject of corrosion [Hickling *et al.*, 1998; Eden, 2000]. The noise impact of the electrode material can be determined using a zero resistance ammeter (ZRA). A ZRA is a current to voltage converter that produces a voltage output proportional to the current flowing between its two input electrodes at zero internal resistance. The ZRA system used in this work has been manufactured by Capsis Ltd. [Oxford, UK] and generally used to detect localized corrosion mechanisms in real time.

From the three-electrode design of the screen printed electrodes, the counter and working electrode were connected to a ZRA and assumed as two ‘identical’ working electrodes during this measurement. In this context the gold microelectrodes introduced in Chapter 1 (Section 1.8.6) are implemented into the study as comparison to screen printed electrodes. The gold (Au) microelectrode comprised also a three-electrode design, which consists entirely of gold electrodes; one can be modified with Ag/AgCl as reference electrode. The SPCE has been produced in-house in the same design as the SPGEs and compared to an industrially manufactured SPCE (Dupont Ltd., UK) of similar design. In the case of SPCE and gold microelectrodes, the assumption of connecting ‘identical’ working electrodes is valid; however, the SPGE was connected assuming Au and Carbon electrode to be ‘identical’ working electrodes and was thus expected to show different noise patterns due to their dissimilar materials.

### 4.3.3 Voltammetric studies

The screen-printed electrodes were inserted applying a 'push-fit' action via their carbon basal track into a 34-way edge connector connected via a ribbon data cable. Each basal track is connected via a single pin and the copper outlets of the ribbon cable were manually soldered to crocodile clamps that were connected to a '3-copper core (non-plated) individually screened cable' leading towards the PC-controlled Autolab potentiostat/galvanostat that is run by the software package type GPES 3 (Eco Chemie B.V., NL). Up to four electrodes can be fitted and monitored simultaneously; here, three electrodes were attached simultaneously for triplicate measurement.

#### 4.3.3.1 Cyclic voltammetry

From the Autolab software, the option cyclic voltammetry (CV) was selected from the menu and parameters set as describe below. The cyclic voltammogram was monitored applying a start potential of -0.8 V, first vertex potential of 1.0 V and second vertex potential of -0.2 V. The step potential was 0.0027 V and CV was performed at a scan rate of 50 mV s<sup>-1</sup> for three cycles.

#### 4.3.3.2 Cyclic voltammetric studies of TMB

Hydroquinone and 3,3',5,5'-tetramethylbenzidine (TMB) were examined with cyclic voltammetry to characterise their redox reaction on SPGEs. A solution of 20 µl TMB at a concentration of 0.1 µg L<sup>-1</sup> in H<sub>2</sub>O and 0.1 µg L<sup>-1</sup> Hydroquinone in H<sub>2</sub>O deposited (liquid/spot) onto a bare SPGE. TMB has been extensively used as colorimetric substrate for the assay of horseradish peroxidase (HRP). According to the manufacturer, the TMB solution (Europa Bioproducts Ltd.) is optimized with respect to TMB and hydrogen peroxide concentrations and yields a linear response with the concentrations of HRP usually employed in immunologic assays. It also contains stabilisers.

The possibility of using SPGEs as sensors with the ready-made TMB solution was investigated by cyclic voltammetry. All voltammograms were recorded in electrolyte buffer, since a constant concentration of chloride ions is needed in order to stabilise the Ag/AgCl reference electrode. Cyclic voltammetry parameters were set to a start potential of -0.8 V, first vertex potential of 1.0 V and second vertex potential of -0.2 V

and step potential was 0.0027 V. Varying scan rates were monitored for 25; 50; 75; 100; 150; 200; and 400  $\text{mV s}^{-1}$  over three cycles. When comparing TMB to 50 mM PBS, pH 7.4 containing 0.1M KCl, the scan rate was set to 50  $\text{mV s}^{-1}$ .

#### **4.3.3.3 Redox peak characterisation**

Horanyi *et al.* [1983] observed that chloride ions actively participate in the electro-oxidation of gold by voltammetric characterisation of a gold working electrode with chloride containing electrolyte. To conduct the voltammetric characterisation of the SPGE, a voltage sweep (start potential of -0.8 V, first vertex potential of 1.0 V and second vertex potential of -0.2 V, scan rate of 50  $\text{mV s}^{-1}$ , three cycles) was applied to the working electrode (Au) and the current response monitored using 20  $\mu\text{l}$  0.1 M KCl deposited on the SPGE and SPCE.

#### **4.3.3.4 Redox peak (interference) investigation**

Interference studies were performed, by depositing 10  $\mu\text{l}$  of Nafion solution (Nafion perfluorinated ion-exchange resin 5 wt%, Aldrich, UK) onto the electrode area of a SPGE and depositing 5  $\mu\text{l}$  to the reference electrode area only, respectively. The Nafion solution was incubated on SPGE at room temperature for one hour. The SPGE was washed in water and 10  $\mu\text{l}$  0.1 M PBS, pH 7.4 containing 0.1 M KCl was added to the whole electrode surface for a blank reading. To determine the characteristics of Nafion in combination with TMB, 10  $\mu\text{l}$  TMB solution was added subsequently. The Nafion-modified SPGE were characterised using cyclic voltammetry at a potential range between -0.2 and 0.8 V at a scan rate of 50  $\text{mV s}^{-1}$  over three cycles.

#### **4.3.3.5 Voltammetric studies of ochratoxin A-BSA adsorption**

A volume of 20  $\mu\text{l}$  ochratoxin A-BSA ( $100 \text{ mg L}^{-1}$ ) has been left to adsorb for 8 hours on the gold working electrode (room temperature, humidity chamber). As comparison, 20  $\mu\text{l}$  ochratoxin A-BSA ( $100 \text{ mg L}^{-1}$ ) has been deposited onto the gold working electrode of another SPGE just prior to measurement. Voltammetric characterisation of adsorbed and non-adsorbed ochratoxin A-BSA was performed immediately by cyclic voltammetry at a scan rate of 100  $\text{mV s}^{-1}$  over three cycles. Both electrodes were

measured simultaneously. The peak shift upon protein adsorption compared to the cyclic voltammogram obtained from freshly applied ochratoxin A-BSA solution was compared.

#### **4.3.3.6 Voltammetric studies of wine samples**

Cyclic voltammetry was used to observe the electrochemical behaviour of wines and assess possible interferences regarding the sensor sensitivity. For this purpose, voltammograms were recorded for different wine solutions using the same three-electrode configuration as described. These solutions were 10-fold dilutions in 0.1M phosphate buffer pH 7.4 of either kind of wine solution and synthetic wine as control. Synthetic wine is prepared solving 32 organic compounds usually found in the headspace (volume left at the top of a filled container (e.g. bottle) before sealing) of wines in 12 % ethanol as summarised in Appendix 1. The potential was scanned between  $-0.2$  and  $0.8$  V at a scan rate of  $50 \text{ mV s}^{-1}$  for three cycles. A random red wine sample was analysed using cyclic voltammetry to assess the interferences arising from polyphenols during the amperometric measurement. The red wine (sparkling Lambrusco) was treated prior to measurement by bubbling with  $\text{N}_2$  to remove any bubbles. A volume of  $20 \mu\text{l}$  was deposited onto a bare SPGE and a cyclic voltammogram recorded at a potential range between  $-0.2$  and  $0.8$  V at a scan rate of  $50 \text{ mV s}^{-1}$  over three cycles. In comparison, a 1:10 sample dilution (0.1M phosphate buffer pH 7.4, 0.1 M KCl) was monitored and also a 1:10 diluted sample pre-treated with a saturating concentration of PVPP (Polyvinylpolypyrrolidone).

#### **4.3.4 Amperometry**

Prior to use, the SPGEs were baked at  $100^\circ\text{C}$  for 30 minutes to remove any particles from the surface, then each SPGE was cleaned with distilled water using a spray flask and dried under  $\text{N}_2$ .

##### **4.3.4.1 Amperometric studies of TMB/ $\text{H}_2\text{O}_2$ (HRP)**

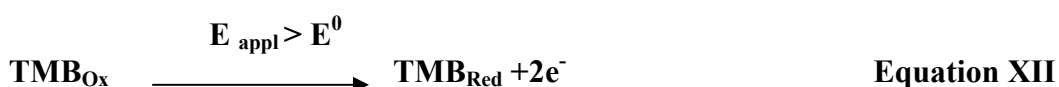
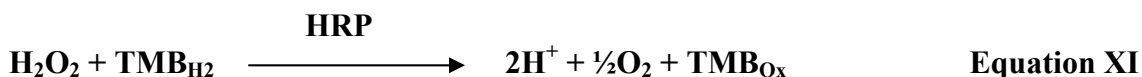
The amperometric investigation was performed by a) stepamperometry to determine the optimal potential of TMB solution and b) chronoamperometric investigation of

subsequent addition of hydrogen peroxide and TMB followed by HRP enzyme. First, stepamperometry was performed to assess the optimal working potential for TMB on SPGE. For this, 20  $\mu\text{l}$  TMB solution was deposited on the SPGE area and a step-wise potential (-600; -400; -200; -100; 0; +100; +200; +400; +600 mV) was applied for 100 seconds per step. The current response was monitored in comparison to a SPGE with electrolyte buffer. The stable current at 50 seconds of each step potential was plotted versus the applied electrochemical potential.

Secondly, chronoamperometry was used to evaluate the potential of screen-printed electrodes as sensors using TMB. The potential was set constant to -150 mV. Pre-anodization was performed by applying a potential at +1 V versus Ag/AgCl for 10 s in 10  $\mu\text{l}$  electrolyte solution (pH 7.4 PBS containing 0.1M KCl). The preanodization procedure can not only make the screen-printed electrodes more electroactive towards TMB oxidation but also provide low susceptibility to electrode fouling [Prasad *et al.*, 2006]. Dissolution of gold is observed at potentials above +0.9 V. The pre-anodization is followed by an equilibration period ( $E = -150$  mV) of 10 seconds. The measurement starts at time zero where the electrolyte solution is monitored as baseline. At time 100 seconds, 10  $\mu\text{l}$  of 3 %  $\text{H}_2\text{O}_2$  was deposited on the electrodes in such a manner that the liquid area was covering all electrodes, then another 10  $\mu\text{l}$  of TMB solution at time 300 seconds was added and the change in current monitored for another 300 seconds.

In another experiment the baseline current is monitored for 100 seconds, then 20  $\mu\text{l}$  of a TMB/ $\text{H}_2\text{O}_2$  mix (15  $\mu\text{l}$  TMB, 5  $\mu\text{l}$   $\text{H}_2\text{O}_2$ ) was added and compared to the addition of TMB/  $\text{H}_2\text{O}_2$ / HRP mix (15  $\mu\text{l}$  TMB, 5  $\mu\text{l}$  3%  $\text{H}_2\text{O}_2$  and 1  $\mu\text{l}$  1:10 dilution HRP in PBS, pH 6.5). The current change was monitored for another 100 seconds.

The electrochemical reaction follows the equation:



Care has been taken that the measurement is performed at an acid pH wherein the enzymatic product, yellow diimine, is stable and yields 2 electrons by TMB oxidation. The TMB solution, according to the manufacturer, is dissolved in citric acid buffer, pH 3.3 (Europa Bioproducts Ltd., UK)

#### 4.3.4.2 Chronoamperometric characterisation of ochratoxin A-BSA

The SPGE was treated by liquid/spot deposition with a volume of 20  $\mu\text{l}$  per SPGE at a range of ochratoxin A-BSA concentrations ( $0.5 - 100 \text{ mg L}^{-1}$  in 0.1 M PBS, pH 7.4), which were adsorbed for 2 hours. All incubations were performed at  $37^\circ\text{C}$  in a humidity chamber. After washing off unbound excess by PBST followed by  $\text{H}_2\text{O}$ , the surface was blocked with 1 % PVA for one hour. A saturating anti-ochratoxin A antibody concentration of 20  $\mu\text{l}$   $20 \text{ mg L}^{-1}$  was incubated for one hour. Secondary antibody (rabbit-IgG-HRP) was added at a dilution of 1:2000 ( $0.5 \text{ mg L}^{-1}$ ) for another hour. The reaction layer of the described immunosensor is illustrated in Figure 4.3.

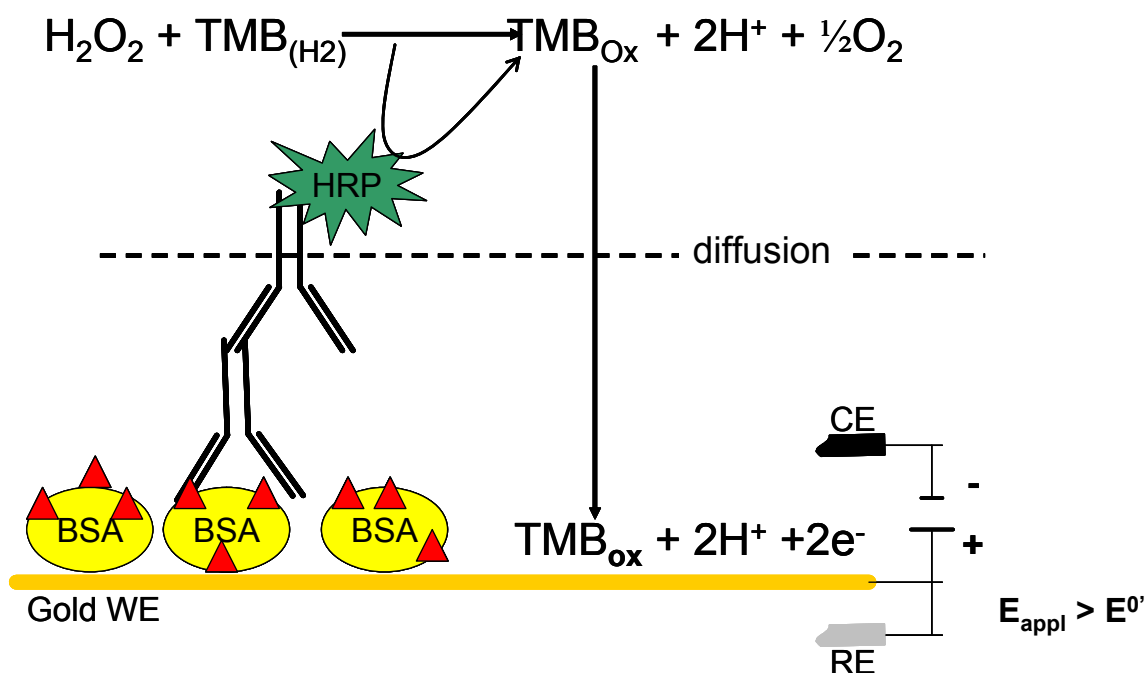


**Figure 4.3:** Immunoassay layer on SPGE showing HRP catalysed reaction of  $\text{H}_2\text{O}_2$  and TMB at a gold working electrode with a set potential.

The measurement was performed at a constant potential of -150 mV in 50 mM PBS, pH 7.4, containing 0.1 M KCl for a time frame of 100 seconds (baseline current). Upon the addition of TMB/H<sub>2</sub>O<sub>2</sub> solution a decrease in current is proportional to the HRP catalysis rate, which, in return, is directly proportional to the varying amount of ochratoxin A-BSA adsorbed on the surface.

#### **4.3.4.3 Chronoamperometric characterisation of anti-ochratoxin A antibody**

A SPGE was modified with a saturating concentration of 10 mg L<sup>-1</sup> ochratoxin A-BSA (20 µl per sensor SPGE) by adsorption for 2 hours. All incubations were performed at 37°C in a humidity chamber. After washing off unbound excess by PBST followed by H<sub>2</sub>O, the surface was blocked with 1 % PVA for one hour. The optimal anti-ochratoxin A antibody concentration was investigated using a dynamic range of 1-100 mg L<sup>-1</sup> antibody applied by liquid/spot deposition of 20 µl per SPGE for one hour. Secondary antibody (rabbit-IgG-HRP) was added at a dilution of 1/2000 (0.5 mg L<sup>-1</sup>) for another hour. The measurement was performed at a constant potential of -150 mV in 50 mM PBS, pH 7.4, containing 0.1 M KCl over 100 seconds (baseline current). TMB/H<sub>2</sub>O<sub>2</sub> solution (heated to 37°C, 80 µl/ SPGE) was then added and the current monitored for another 100 seconds. The baseline current was subtracted from the signal current and plotted against the ochratoxin A-BSA concentration. Upon the addition of TMB/H<sub>2</sub>O<sub>2</sub> solution a decrease in current is proportional to the HRP catalysis rate, which, in return, is directly proportional to the varying anti-ochratoxin A antibody concentrations bound to the fixed amount adsorbed ochratoxin A-BSA.

#### **4.3.4.4 Ochratoxin A biosensor development**

An indirect immunoassay format had been investigated prior to the biosensor development on solid phase supports and showed a limit of detection (LOD) of 1 µg L<sup>-1</sup> ochratoxin A in phosphate buffer, pH 7.4 (Chapter 2). Thus, an indirect detection format was chosen for the electrochemical immunosensor.

The immunosensor has been initially optimised with respect to coating and operating pH, ochratoxin A-BSA and ochratoxin A antibody concentration as well as range of

ochratoxin A standard concentrations and HRP/TMB/H<sub>2</sub>O<sub>2</sub> loading. The final protocol resumes with the drop deposition of 20 µl 10 mg L<sup>-1</sup> ochratoxin A-BSA conjugate in 50 mM PBS, pH 7.4 onto the gold surface of the working electrode. The droplet was adsorbed for two hours. Non-covalent immobilisation was chosen as the gold surface allows for easy adsorption of biomolecules as a result of hydrophobic and thiol–gold interactions [Horisberger & Vauth, 1984]. After washing off unbound excess by PBST followed by PBS, the entire SPGE electrode area was blocked by dipping the electrode into 1% PVA solution for one hour. Specific ochratoxin A antibody (20 µl of 10 mg L<sup>-1</sup> in 0.1 M PBS, pH 7.4) was added to 10 µl ochratoxin A competitor of different concentrations, mixed briefly and deposited to the gold surface. Binding interaction was allowed for two hours and unbound material washed off. Then, the horseradish peroxidase (HRP)–labeled secondary antibody (0.5 mg L<sup>-1</sup> in 0.1 M PBS, pH 7.4) was added for one hour. All incubations were performed at 37°C in a humidity chamber. The amount of bound ochratoxin A antibody is determined in an indirect detection format, thus the signal is inversely proportional to the ochratoxin A sample concentration. Chronoamperometry was monitored at a set potential of -150 mV. The electrodes were equilibrated to stabilise the background current for 10 seconds at -150 mV. The measurement starts at time zero where the electrolyte buffer is monitored as baseline for 50 seconds. The TMB reaction solution is added to the electrode area in excess (50 µl). The current-time response is monitored for another 250 seconds (total measurement time per electrode is 300 seconds).

#### **4.3.4.5 Surface modification of SPGE**

Carboxymethylated dextran (CMD) was prepared according to the literature [Hermanson, 1996; Surugiu *et al.*, 2001]. The procedure adds 1 ml of 40 mg ml<sup>-1</sup> dextran to a solution consisting of 1 M chloroacetic acid in 3 M NaOH. The mixture was allowed to react while stirring for 2 hours at room temperature. The reaction was stopped by adding 4 mg NaH<sub>2</sub>PO<sub>4</sub> per ml of dextran solution and the pH was adjusted to neutral with HCl. The excess of reactants was removed by dialysis towards 0.1 M PBS, pH 7.4 at room temperature for 24 hours.



The gold working electrode of each SPGE was modified by adsorbing a volume of 3  $\mu\text{l}$  of carboxymethylated dextran (CMD) solution to the bare gold surface. The SPGE was then air-dried at room temperature. To protect the carbon counter electrode and Ag/AgCl reference electrode, a 2  $\mu\text{l}$  droplet of 6 % D-(+) Trehalose-dihydrate in 10 % Gelantine was deposited onto each electrode track.

The CMD-modified gold working electrode was activated by liquid/spot deposition using 5  $\mu\text{l}$  of a 1:2 mixture of 0.05 M NHS and 0.2 M EDC. Then, a solution of 20  $\mu\text{l}$  10 mg  $\text{L}^{-1}$  ochratoxin A-BSA conjugate in 0.1 M PBS, pH 7.4 was added and left to incubate for two hours at 37°C in a humidity chamber. The SPGE were washed using PBST followed by PBS. The activated carboxymethylated dextran was blocked by depositing of 2.5  $\mu\text{l}$  0.1 M ethanolamine, pH 8.5, onto the gold working electrode and incubating at 37°C for 30 minutes. Another blocking step of 1 % PVA was introduced covering the entire electrode area for 30 minutes. After washing off excess biomaterial, 20  $\mu\text{l}$  ochratoxin A antibody was premixed with distinct ochratoxin A concentrations and added to the electrode surface. Subsequent steps using the secondary antibody and detection with HRP/TMB/ $\text{H}_2\text{O}_2$  was performed as described above in Section 4.3.4.4.

#### **4.3.4.6 Sample preparation and analysis**

The three-electrode screen printed electrode assembly, was subjected to electrolyte buffer (10  $\mu\text{l}$ ) containing 0.1 M KCl for baseline establishment. The amperometric measurement procedure was initiated at +1 V pre-anodization and the electrochemical response was allowed to equilibrate for 10 s, after which the TMB/ $\text{H}_2\text{O}_2$  solution was deposited on the working electrode which was set at a potential of -150 mV versus the Ag/AgCl reference. The change in response was monitored after TMB/ $\text{H}_2\text{O}_2$  addition for 200 seconds.

The wine samples used for the sensor analysis were diluted 1:2 in carbonate buffer containing PEG (5%  $\text{NaHCO}_3$  + 1% PEG, pH 8.3) to stabilise the pH at 7-8. A volume of 10  $\mu\text{l}$  of each dilution was pre-mixed (1:2 dilution) with 10  $\mu\text{l}$  of a fixed concentration of 5  $\mu\text{g L}^{-1}$  (1:200 dilution) antibody A and deposited onto the immunosensor surface. Standard curves were prepared with every assay.

Sensor performance was compared against a standard ochratoxin A immunoassay test method based on a commercially available colorimetric test kit (Ridascreen, UK) and the initially in-house developed indirect competitive immunoassays. Samples were tested in accordance with the supplied protocol and the absorbance was measured at 450 nm.

The official method recommended for ochratoxin A determination in beer and wines is based on HPLC. This method is the European Standard (prEN 14133) with the reference number EN 14133:2003/AC and the document title “Foodstuffs - Determination of ochratoxin A in wine and beer - HPLC method with immunoaffinity column clean-up”, published in 2006. This protocol comprises quantification using HPLC with fluorescence detection and immunoaffinity chromatography for sample clean-up and pre-concentration in accordance with the work published by Visconti *et al.* [1999].

Wine (5 ml) was added to 5 ml of diluting solution (1% polyethylene glycol (PEG) + 5% NaHCO<sub>3</sub>, pH 8.3) and mixed vigorously. The Ochratest™ immunoaffinity column was connected to a pumpstand and 10 ml diluted sample solution was added to the column reservoir, whereas the solution was passed through the column at a flow rate of 1-2 drops/second using a syringe. The column was washed using 5 ml washing solution (2.5% NaCl + 0.5% NaHCO<sub>3</sub>) and then dried. Ochratoxin A was eluted by passing 2 mL methanol, at a flow rate of 1 drop/second, through the column and the eluate was evaporated to dryness at 50°C under Nitrogen. The eluate was re-dissolved immediately in HPLC mobile phase, Water/acetonitrile/glacial acetic acid (51:47:2), pH 3.2, for HPLC analysis.

HPLC was performed according to a modified method published by Visconti *et al.* [1999]. Fifty microlitre re-dissolved eluate (equivalent to 0.5 ml wine) was injected via an autoinjector loop injection system over a RP-C<sub>18</sub> column. The mobile phase consisted of a mixture of acetonitrile/water/acetic acid (51:47:2) eluted at a flow-rate of 1 ml min<sup>-1</sup> and a fluorescence signal was monitored over an acquisition time of 15 minutes (Excitation 333 nm, Emission 460 nm). Quantification of ochratoxin A was performed by measuring peak areas at ochratoxin A retention time and comparing them

with the standard curve. A standard curve was produced from ochratoxin A concentrations 0; 0.001; 0.01; 0.1; 1; and 10 mg L<sup>-1</sup> dissolved in HPLC mobile phase.

#### **4.3.4.7 Microelectrode arrays –preliminary characterisation-**

Microelectrodes composed of a 5x5 microelectrode array with a size of 20 µm and a separation distance of 200 µm were prepared at the Tyndall Institute for sensor research (Cork, Ir). Preliminary characterisation of the microelectrodes was conducted using TMB solution containing hydrogen peroxide as a representative electroactive species. TMB and hydrogen peroxide were tested on the AuME using cyclic voltammetry by adding 10 µl of the mixed solution to the electrode array area. Cyclic voltammetry parameters were set to a start potential of -0.8 V, first vertex potential of 1.0 V and second vertex potential of -0.2 V. The step potential was 0.0027 V. Varying scan rates were monitored for 25; 50; 75; 100; 150; 200; and 400 and mV s<sup>-1</sup>. When comparing TMB to 0.1 M PBS, containing 0.1M KCl, the scan rate was set to 50 mV s<sup>-1</sup>.

The amperometric investigation was performed by a) step amperometry to determine the optimal potential of TMB solution b) chronoamperometric investigation of subsequent addition of hydrogen peroxide and TMB followed by HRP (horse radish peroxidase). A volume of 10 µl TMB solution was deposited on the gold microelectrode area and a step-potential (-600; -400; -200; -100; 0; +100; +200; +400; +600 mV) was applied for 100 seconds per steps. The current response was monitored in comparison to a SPGE with electrolyte buffer. The stable current at 50 seconds of each step potential was plotted versus the electrochemical potential.

Chronoamperometric measurement was performed at a potential of +150 mV. The measurement starts at time zero where 10 µl electrolyte solution (pH 7.4 PBS containing 0.1M KCl) was deposited onto the gold microelectrode and the current monitored as baseline. At about 50 seconds, 10 µl of TMB solution was added and the change in current observed over time for 200 seconds.

#### 4.3.4.8 Preliminary direct immunosensor

Protein A (20  $\mu\text{l}$ ; 5  $\text{mg L}^{-1}$ ) 0.1 M PBS, pH 7.4 was applied to the SPGE by drop deposition onto the gold working electrode and adsorbed for one hour. The ochratoxin A antibody was incubated at a dilution of 1:200 (5  $\text{mg L}^{-1}$ ) with protein A modified for 1 hour. After washing off unbound excess by PBST followed by PBS, the entire SPGE electrode area was blocked by dipping the electrode into 1% PVA solution for one hour. Ochratoxin A antibody (5  $\mu\text{l}$ ; 1:10 dilution in 0.1 M PBS, pH 7.4) was added to 5  $\mu\text{l}$  ochratoxin A competitor of varying concentrations, mixed briefly and deposited to the gold surface. Binding interaction was allowed for two hours and unbound material washed off. All incubations were performed at 37°C in a humidity chamber. The amount of bound ochratoxin A-HRP is determined in direct detection format, thus the signal is directly proportional to the ochratoxin A sample concentration. Chronoamperometry was monitored at a set potential of -150 mV. The electrodes were equilibrated to stabilise the background current for 10 seconds at -150 mV. The measurement starts at time zero where the electrolyte buffer is monitored as baseline for 50 seconds. The TMB reaction solution is added to the electrode area in excess (50  $\mu\text{l}$ ). The current response is monitored over time.

## 4.4 Results and discussion

### 4.4.1 Electrode fabrication and configuration

The picture (Plate 4.1) documents the produced electrode designs connected via an edge connector and ribbon data cable to a static potentiostat (Autolab, Eco Chemie BV, NL).

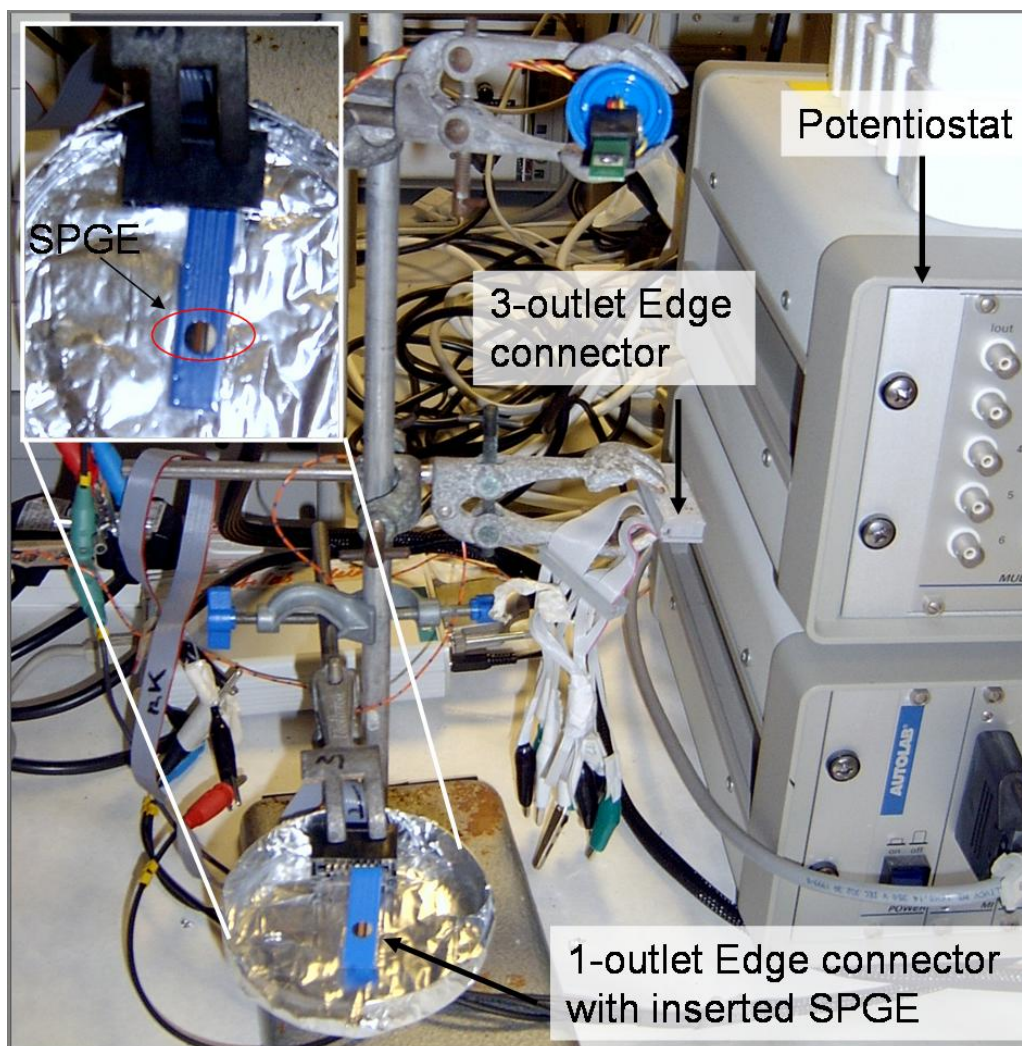


**Plate 4.1:** Illustration of the screen printed gold electrode (SPGE) with working electrode (WE), counter electrode (CE) and reference electrode (RE) connected via a 1-outlet edge connector (insert) with ribbon data cable to a potentiostat (Autolab). Three electrodes can be fitted into the 3-outlet edge connector for simultaneous multiple measurements.

This instrumental setup was applied throughout this work unless stated otherwise.

#### 4.4.2 Economical aspects of screen printed electrode-based sensor

The described ochratoxin A biosensor has several advantages over the reference immunoassay method such as the simplicity of the procedure and the equipment, as well as the short time required for one assay and its production costs. The cost of gold ink is compared to carbon ink more expensive, e.g. 50 g E4464 gold ink costs an equivalent of £746.640 (\$1,473.65\*). However, the overall cost of each sensor is comparably cost-effective and cheaper compared to commercially available sensors. In Table 4.2, a number of commercial available screen printed gold electrodes are summarised and their cost compared to the in-house manufactured SPGEs.

**Table 4.2:** End-user prices of screen printed gold electrodes per piece (valid 2007).

Source	Screen printed electrode type	Price per SPGE [£ ]*
Cranfield University –produced in-house–	WE Au , CE Carbon, RE Ag/AgCl Carbon basal track	0.4
Florence Sensors	Three electrode design Au working electrode	1,2 (≥ 400) 1.4 (80 to 380) 2.0 (20 to 60)
DropSens Sensors	Three electrode design Au working electrode 220AT&220BT	1,2 (Ink AT) 1,2 (Ink BT)
BVT Technologies	WE Au, CE Au, RE Ag/AgCl Silver basal track	1.35 (250) 0.67 (>250)

\* Prices in Euro converted to GBP according to 1 EUR = 0.678997 £, and 1\$ = 0.506 £

The cost for one electrode of the in-house produced SPGE design (assuming 100 SPE per sheet and 20 sheets per 50 g ink), is about 40 pence, which is still 1.5 - 3 times less than the commercially available screen printed gold electrodes from e.g. BVT technologies [Brno, CR]. However, the production costs for the in-house produced electrodes do not include the cost for personell, which should be taken into account.

### 4.4.3 Electrochemical noise of screen printed electrodes

Upon establishment of an electrochemical cell potential between two working electrode, a galvanic currents arises due to the surface condition and local chemistry differences between the two. The cell potential depends on the potentials of the electrodes involved, thus the SPGE displays a cell potential established from carbon (counter electrode) and gold (working electrode). SPCE displays a cell potential from carbon (counter electrode) and carbon (working electrode) and ME from gold (counter electrode) and gold (working electrode). Connection of the electrodes to the zero resistance ammeter (ZRA), the potential noise is observed over time. The cell potential establishment with time after connection of the electrodes is dependent on the electrode material and its influence on the cell potential. Figure 4.4 depicts the characteristic cell potential patterns for all screen printed electrodes and a gold microelectrode.

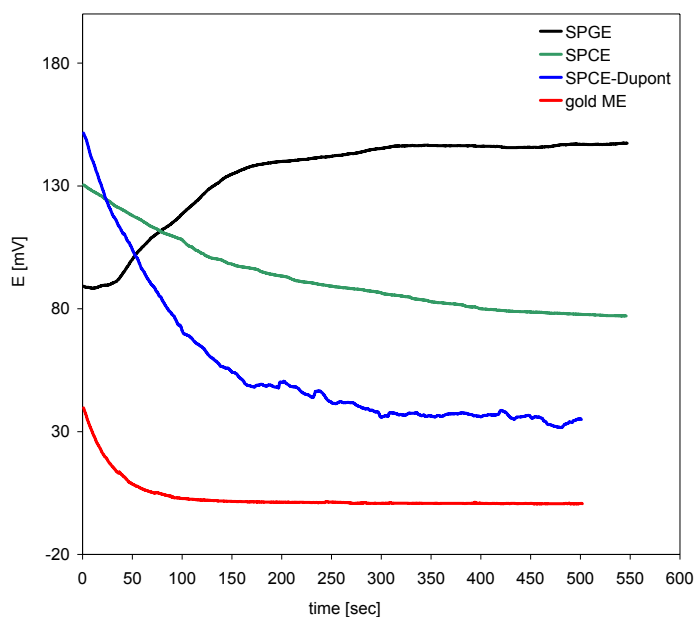


**Figure 4.4:** Electrochemical potential [mV] illustrated versus time [seconds]. Curves display the potential noise of the cell potential [mV] for SPGE (black), SPCE (green), SPCE-Dupont (blue) and gold microelectrode AuME (red).

As Figure 4.4 shows, the noise of the electrochemical potential is different for the combination of working and counter electrode (WE-CE) that are Au-C (SPGE) and C-C (SPCE) and Au-Au (ME) electrodes. The ‘dimeric’ electrode (WE-CE) design, in the case of AuME and SPCE results in a decrease of potential within the first 150-200

seconds, whereas with SPGE a potential increase is observed. It can also be seen that the AuME reaches its cell potential plateau already after 50-100 seconds, thus indicating less potential noise, which agrees with the micro-manufacturing process and thus thinner and more even layer of gold. It was also observed, that the in-house produced carbon electrode (SPCE) takes the longest to reach its cell potential plateau (up to 300 seconds). Summarising, the AuME showed the lowest potential noise (13.6 mV), whereas the SPCE showed the highest. SPGE (in-house, 146.2 mV) and SPCE (Ind., 36.2 mV) showed mirrored curve patterns which is due to the fact that the SPGE is a non-identical electrode setup, causing a shift in cell potential dependant on the Au electrode potential. The potential differences between SPCE (79.2 mV) and SPCE (Ind), was about 40 mV due to the slight differences of the local chemistry and surface conditions. Practically, the screen printed electrodes used in this work need to be connected in electrolyte 150 +/-50 seconds prior to the measurement to let the cell reach its potential plateau, otherwise, the measurement will be compromised by the increase or decrease in potential during the first 150 seconds. The noise of the electrochemical current was also monitored for the screen printed electrodes and the microelectrode and depended on the cell potential. The current noise is depicted in Figure 4.5.

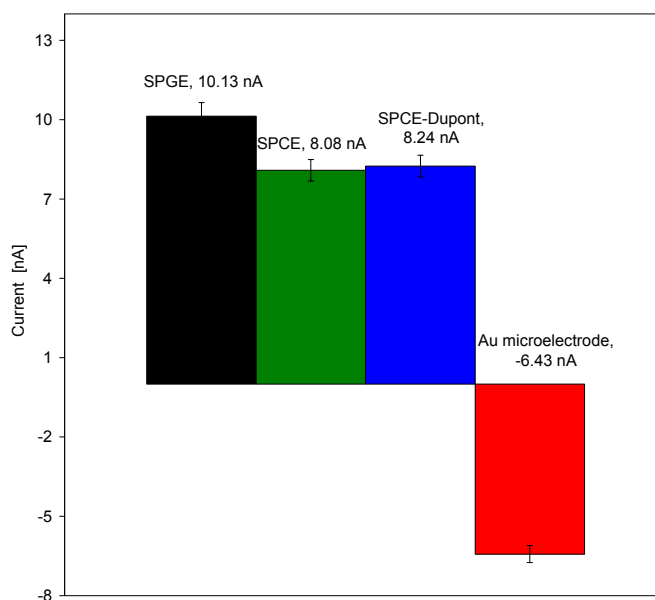


**Figure 4.5:** Electrochemical current [ $\mu\text{A}$ ] depicted as columns comparing the current noise for screen-printed gold (SPGE), carbon (SPCE), carbon (SPCE-Dupont) and gold (Au) microelectrodes. The current noise was determined as an average value of an alternating current signal over 600 seconds.



The presence of current noise indicates that there existed a potential difference between two working electrodes, as seen in Figure 4.5. A range of 3 – 10 nA as current noise value is acceptable for this application. Whereas the SPGE displayed a higher average current noise over time, it showed the least standard deviation. This indicates that due to the dissimilarity of gold-carbon electrode (SPGE) and its resulting electrochemical cell potential a higher noise current is observed over time than for carbon-carbon electrodes (SPCE).

However, observing the standard deviation of average current, the SPGE design shows the lowest alternation in current compared to SPCEs and is similar to the standard deviation displayed by the gold microelectrode. The microelectrode displayed negative current noise values in contrast to the screen printed electrodes, which arises due to the gold-gold connection and direction of current flow. An increase in background current indicates the formation of redox active groups, thus, the SPGE seem to be more redox active than the SPCEs.

#### **4.4.4 Choice of electroactive species 3,3',5,5'-tetramethylbenzidine**

There are a number of possible substances that can be used as electrochemical mediator for horseradish peroxidase catalysed reactions [Volpe *et al.*, 1998]. Here, we investigate two possible substances, 3,3',5,5'-tetramethylbenzidine (TMB) and hydroquinone to establish their electrochemical behavior at a screen printed gold working electrode polarized at -150 mV versus Ag/AgCl (Figure 4.6).

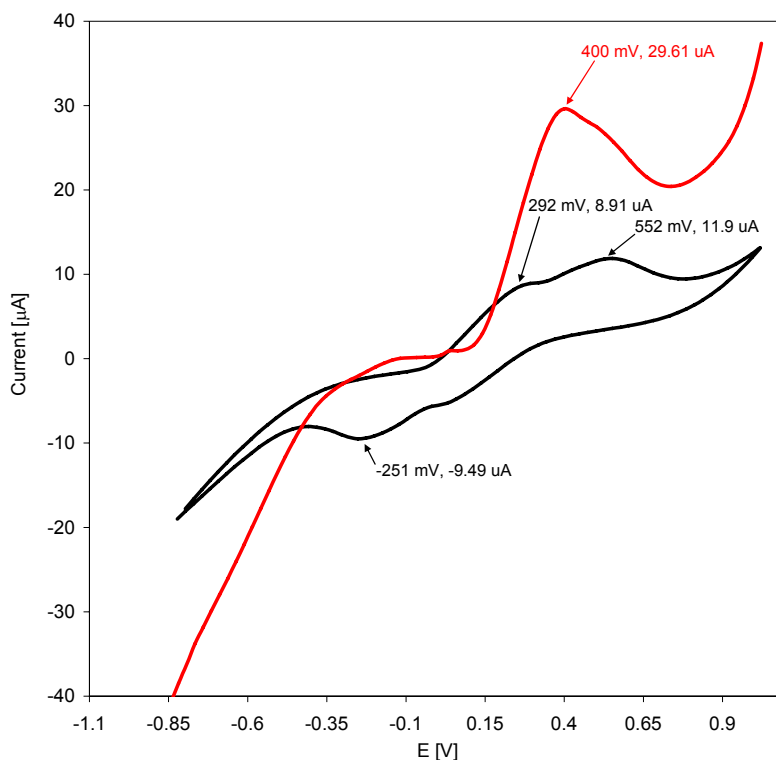


**Figure 4.6:** Current versus electrochemical potential shows the cyclic voltammograms of TMB (black) and hydroquinone (red) on bare screen-printed gold electrodes (SPGE). The cyclic voltammograms were monitored separately upon addition of 20  $\mu\text{l}$  TMB and hydroquinone at a scan rate of  $50 \text{ mV s}^{-1}$ .

Figure 4.6 shows that hydroquinone is displaying one oxidation peak at +0.4 V, TMB a peak shoulder consisting of two oxidation peaks at +0.29 V and +0.55 V, in addition to that, TMB also shows a reduction peak at -0.25 V, whereas hydroquinone does not show any change in current on the negative scan, indicating the oxidation of Hydroquinone is not reversible.

TMB is the reagent of choice for the detection with  $\text{H}_2\text{O}_2$  catalysed by HRP as the first oxidation peak and reduction peak occur at a potential which is suitable, since interferences are common above potentials of +0.4 V. Peak currents for the TMB oxidation peaks are comparable less than the hydroquinone peak current. Hydroquinone oxidation occurs at a potential that is too high and thus might be subject to interferences such as polyphenols.

#### 4.4.5 Cyclic voltammetric studies of TMB

The dependence of peak current ( $i_p$ ) on scan rate ( $\nu$ ) for the oxidation of TMB was investigated for the SPGE. There was a gradual increase in the  $i_p$  with respect to the increase in  $\nu$ . Figure 4.7 displays the increase in peak current and peak shift with increasing scan rate.

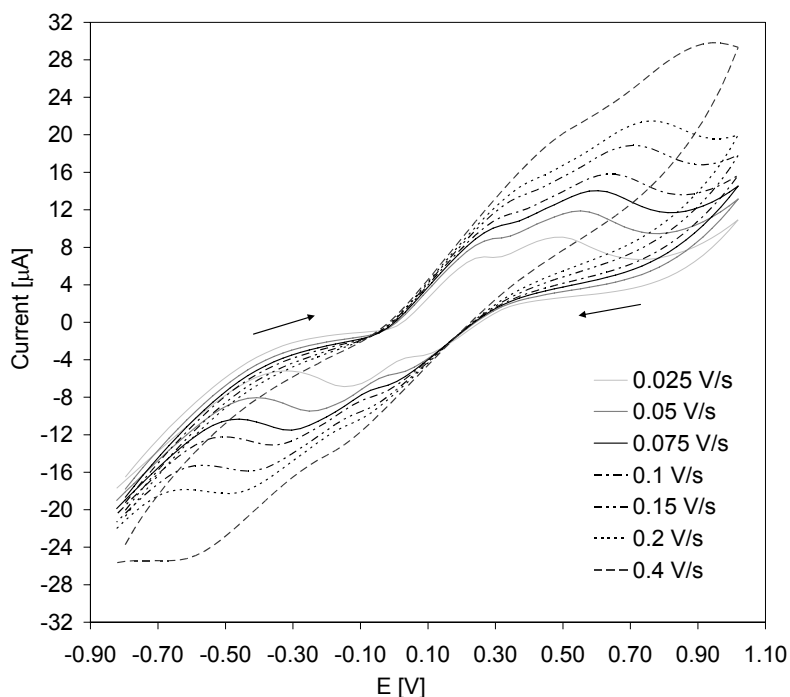
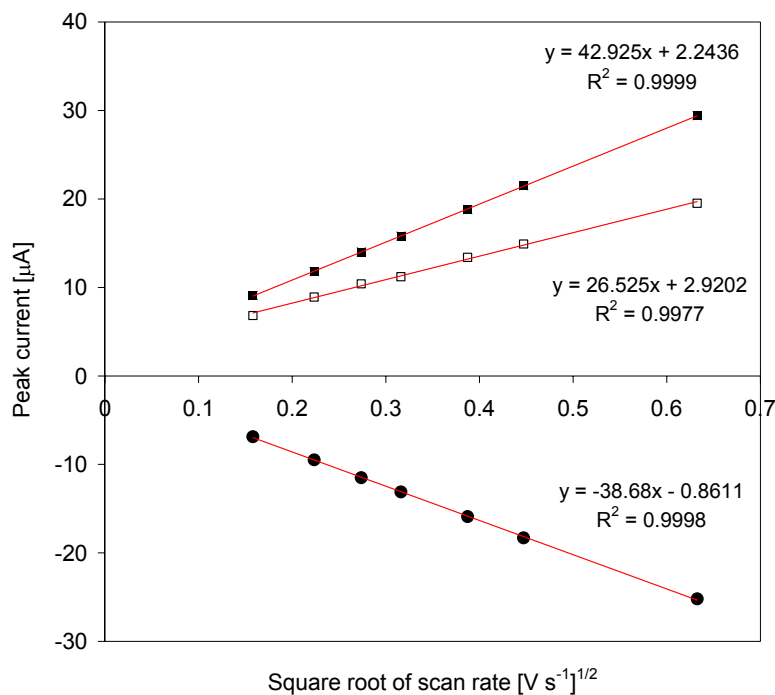


Figure 4.7: Current versus electrochemical potential shows the cyclic voltammograms (CV) of 20  $\mu\text{l}$  TMB solution on SPGE at different scan rates [ $\nu$ ]. From inner to outer cyclic voltammogram the scan rate is 25; 50; 75; 100; 150; 200; and 400  $\text{mV s}^{-1}$ .

Figure 4.7 shows all cyclic voltammograms for all scan rates that display the characteristic TMB double shoulder on the positive scan, which are considered to result from the TMB itself illustrating two 1-electron oxidation steps. One reduction peak on the negative scan is illustrating a 2-electron reduction step. The TMB peaks are most profound at scan rates in the range of 25 -75  $\text{mV s}^{-1}$ .

The anodic peak currents for both TMB peaks on the positive scan and the cathodic peak current were further evaluated by plotting the peak current versus the square root of the scan rate as shown in Figure 4.8.



**Figure 4.8:** Anodic peak currents [ $\mu A$ ] versus square root of scan rate  $\sqrt{\nu}$  [ $\sqrt{(V s^{-1})}$ ] obtained from cyclic voltammograms on bare SPGE with increasing scan rate. Linear relationship of anodic peak current  $pa_{,1}$  (□) and  $pa_{,2}$  (■) as well as the cathodic peak current  $pc$  (●) of TMB with the scan rate  $\nu$ .

Seen in Figure 4.8, shows that the anodic and cathodic peak currents ( $i_{pa}$  and  $i_{pc}$ ) display a linear dependence proportional to the square root of scan rate ( $\sqrt{Vs^{-1}}$ ). This confirms that the redox reaction is a typical surface-controlled (quasi-reversible) process and thus that the electrochemical oxidation of TMB is a diffusion-controlled electron transfer process. In contrast, a non-linear relationship would indicate an adsorption depended redox reaction.

The peak-to-peak separation was also evaluated by plotting the separation potential (E) versus the scan rate. Figure 4.9 shows that with increasing scan rate the peak-to-peak separation increases accordingly.

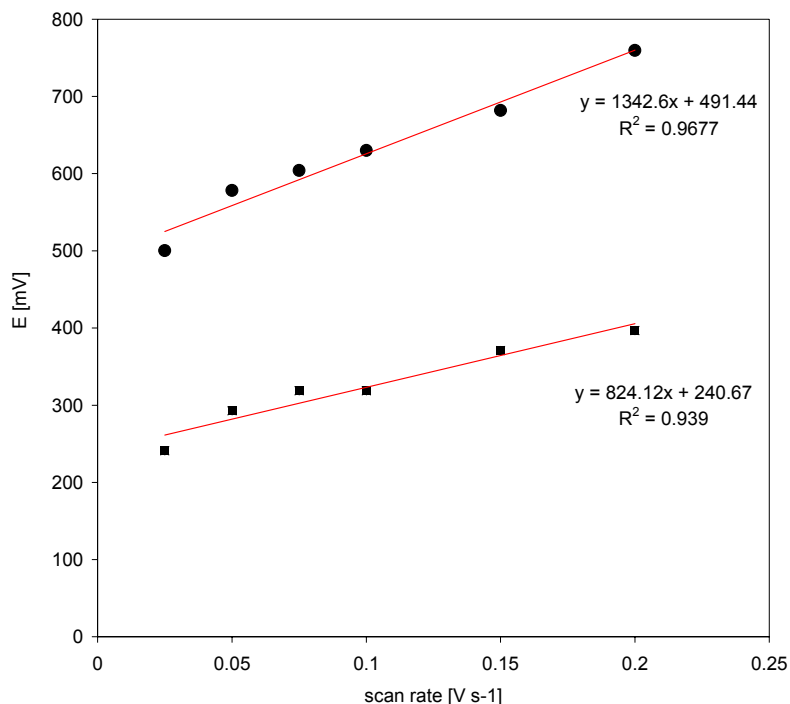


**Figure 4.9:** Linear relationship of peak separation [mV] versus scan rate  $v$  obtained from cyclic voltammograms for anodic peaks pa,1 [■] and pa, 2 [●] of TMB on a bare SPGE.

The peak-to-peak separation is seen in Figure 4.9. The lower the peak-to-peak separation, the lower the mass transfer influence on the diffusion controlled redox reaction of TMB. Thus, the smallest peak-to-peak separation of 25 mV was found for both TMB pa,<sub>1</sub> and pa,<sub>2</sub> at a scan rate in the range of 50 to 100 mV s<sup>-1</sup> which indicates a fast electron transfer rate. Therefore, the median scan rate of 50 mV s<sup>-1</sup> was assigned as standard scan rate for future measurements.

Cyclic voltammetry was also used to investigate the electrochemical behaviour of TMB with SPGE, compared to PBS buffer, pH 7.4 containing 0.1M KCl, and plain DI water using a scan rate of 50 mV s<sup>-1</sup>, as displayed in Figure 4.10.

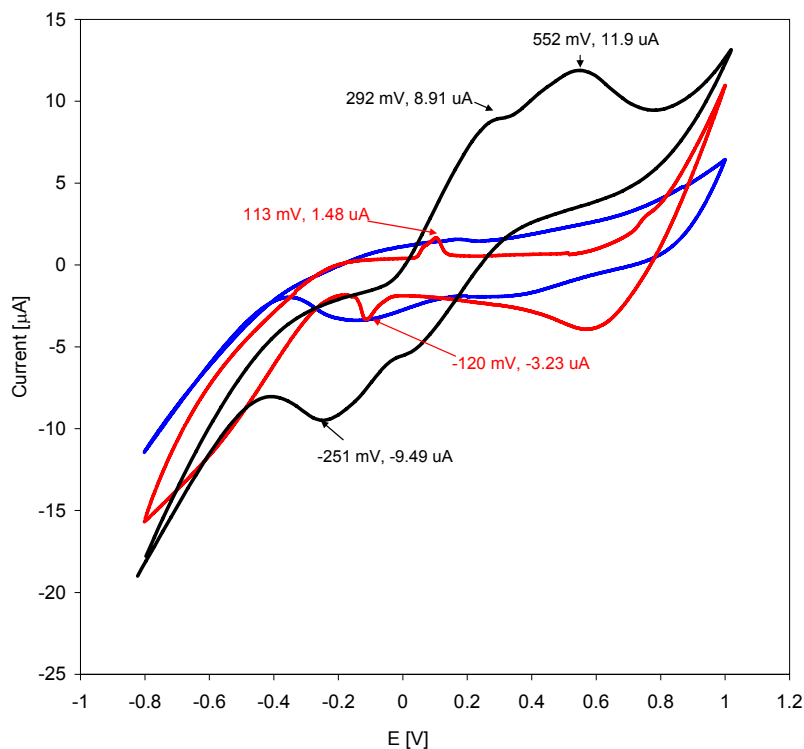


**Figure 4.10:** Cyclic voltammograms of H<sub>2</sub>O (blue); 0.1 M PBS, pH7.4, containing 0.1M KCl (red); and TMB solution (black) on bare SPGE recorded at a scan rate of 50 mV s<sup>-1</sup>.

The cyclic voltammograms in Figure 4.10 show that the peak for the oxidation of TMB on the bare screen-printed gold electrodes corresponds to +0.29 V and +0.55 V. The reduction peak is observed at -0.25 V. The peak observed scanning 0.1 M PBS containing 0.1 M KCl at +0.11 V and -0.12 V may be caused by the high salt concentration (Cl<sup>-</sup> ion) on the SPGE surface; hence, exceedingly high Cl<sup>-</sup> ions can cause interferences in potential with certain electrochemical cells [Skoog & Leary, 1992].

#### 4.4.6 Identification and characterisation of KCl peak

The first assumption from the occurrence of the redox peak at +0.11 V and -0.12 V was that characteristic element of cyclic voltammetry on gold electrodes is a set of peaks associated with the formation and dissolution of a surface oxide layer at about 1.6 V and 0.2 V, respectively [Norouzi *et al.*, 2006]. Chloride adsorption on noble metal electrodes has been mentioned in the literature, but the first direct observation of chloride adsorption on gold was made by Horanyi *et al.* [1983].

The effect of adsorbed  $\text{Cl}^-$  ion on the current of the cyclic voltammogram can be seen directly. However, current changes should mainly take place at the potential regions of the oxidation and reduction of gold. This can be seen as anodic wave on positive scan 0.8-1.1 V and on negative scan 0.8-0.6 V. In this work, however, no peak currents were observed at these potentials.

To confirm that the peaks at +0.11 V and -0.12 V are caused by  $\text{Cl}^-$  ions, a cyclic voltammogram was monitored of bare SPGE in 0.1 M KCl (Figure 4.12, A). This experiment was also performed on a carbon screen printed electrode (SPCE) to investigate whether this peak is only displayed on gold screen printed electrodes (SPGE) shown in Figure 4.11.

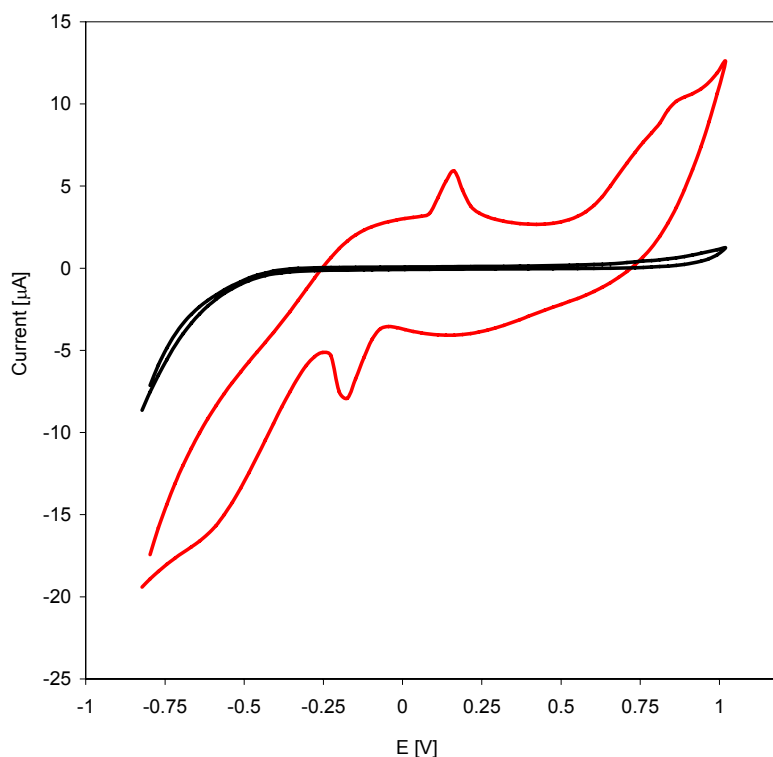


**Figure 4.11:** Cyclic voltammograms of 0.1 M KCl on bare SPGE (red) compared to bare SPCE (black) and of 0.1 M KCl on SPCE (red). Scan rate is  $50 \text{ mV s}^{-1}$ .

The cyclic voltammograms (Figure 4.11) established that the occurring redox peaks must be arising as a result of the KCl electrolyte. It furthermore has to be mentioned that, when compared to a similarly designed carbon screen printed electrode (SPCE), these redox peaks did not occur. Moreover, the SPCE did not show any change in current upon change of applied potential when subjected to 0.1 M KCl electrolyte,

except for a slight anodic peak at 0.78 V. The Ag/AgCl reference electrode provides a stable potential through the reaction:



However, for AgCl in aqueous solution there is also the solution/deposition equilibrium reaction:



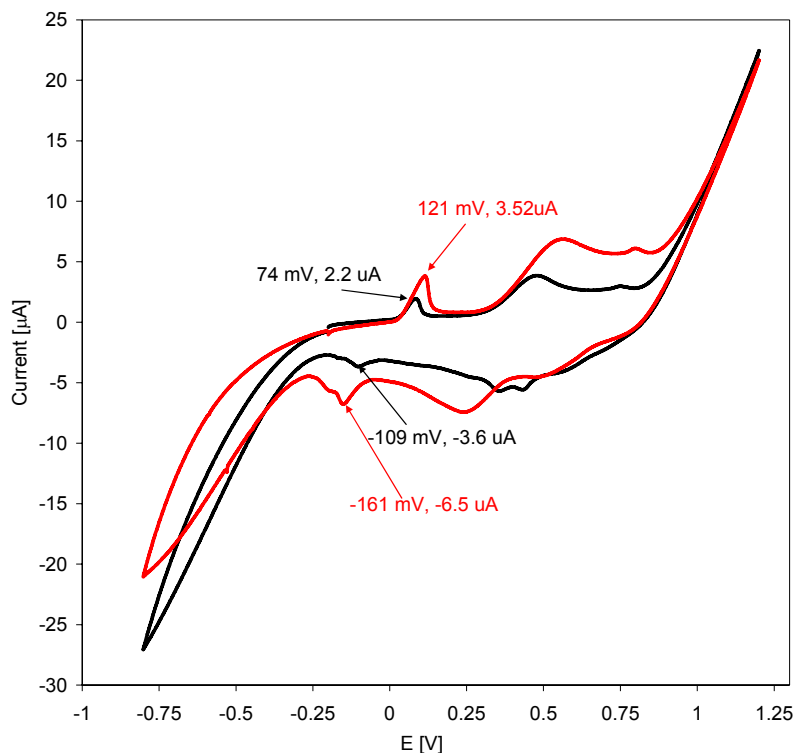
During cyclic voltammetry with a KCl solution,  $\text{Cl}^-$  is consumed during the oxidation (positive scan), which disturbs the equilibrium and causes the dissolution of AgCl. During the reduction half cycle,  $\text{Ag}^+$  is deposited on the working electrode (gold), which also causes the dissolution of AgCl. So during the entire cycle, AgCl is being dissolved. Eventually all of the AgCl is dissolved, and the reference electrode is no longer able to provide a stable potential [Cao *et al.*, 2005]. Concluding, that the ion transfer from the Ag/AgCl electrode to the electrolyte is the main cause of the interferences observed and can result in the eventual failure of the electrode [Nolan *et al.*, 1997].

#### 4.4.7 Interference control

To avoid the KCl peak for clearer measurements, since it partially overlaps with the measurement potential at -150 mV, the reference electrode needs to be stabilised. This is done by coating the reference electrode with a conductive layer that is non-permeable for silver or chloride ions and thus, will prevent electrode fouling of the reference electrodes. Such material could be Nafion (anion-exchange polymer) or modified polyurethane (redoxpolymer) and the procedure is described by Nolan *et al.* [1997].

In the following experiment the effect of Nafion on bare screen printed electrodes was characterised using cyclic voltammetry. Nafion deposition on the reference electrode alone was compared with whole SPGE deposition as shown in Figure 4.12.

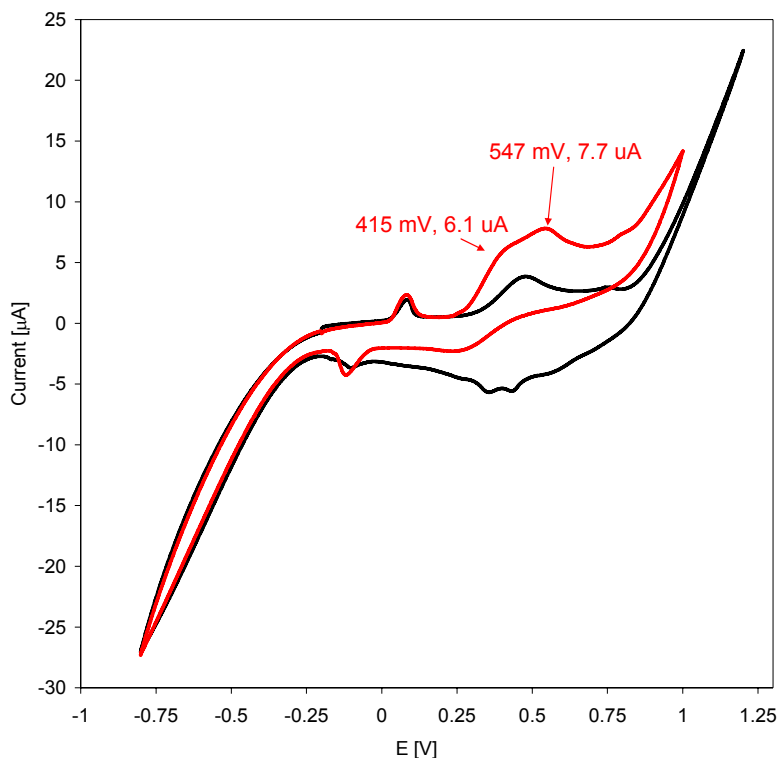




**Figure 4.12:** Cyclic voltammograms of Nafion-modified bare SPGE. Nafion-modified reference electrode is shown in black; whole (3-electrode) modified SPGE is shown in red. The cyclic voltammogram was recorded in 0.1 M PBS, pH7.4, containing 0.1 M KCl at a scan rate of  $50 \text{ mV s}^{-1}$ .

It is shown in Figure 4.12 that the re-occurring peaks characterised earlier to arise due to  $\text{Cl}^-$  ions in the electrolyte buffer, are still prominent with the Nafion coating of the electrode surface. In this experiment it could be furthermore established that the Nafion solution used causes some background noise at about  $+0.48 - 0.57 \text{ V}$  on the positive scan and  $+0.23 - 0.4 \text{ V}$  on the negative scan. The noise was more prominent when the whole 3-electrode design of the SPGE was treated with Nafion compared to the reference electrode only.

To establish if this interference would overlap with the monitoring of TMB, the SPGE with Nafion-modified reference electrode was subjected to TMB. The monitored cyclic voltammograms are shown in Figure 4.13.



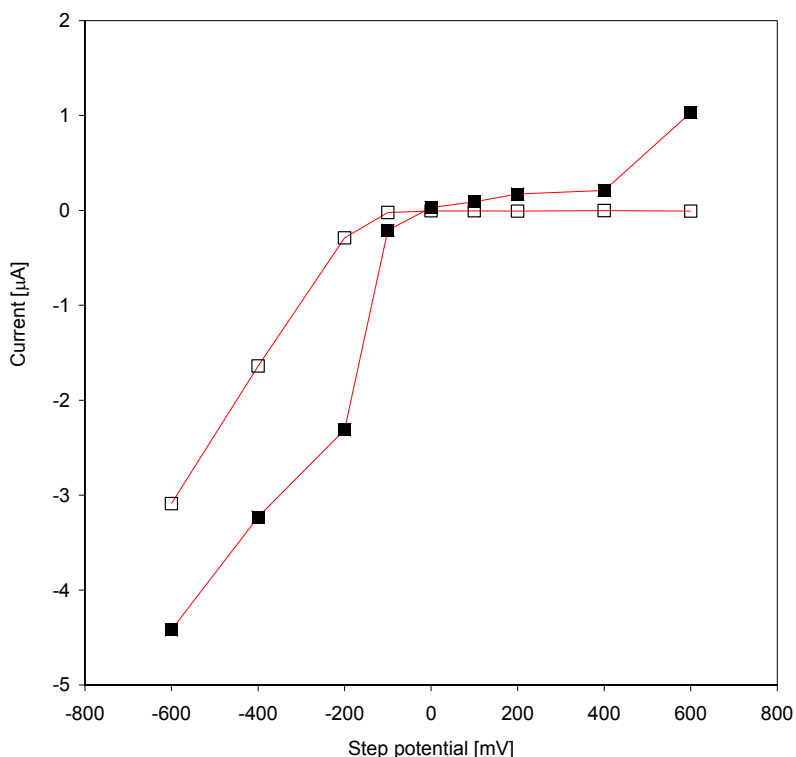
**Figure 4.13:** Cyclic voltammograms of Nafion-modified reference electrode on bare SPGE with 20  $\mu\text{l}$  added TMB solution compared to 0.1 M PBS, pH7.4, containing 0.1M KCl. Nafion-modified reference electrode in 0.1 M PBS is shown in black and with TMB is shown in red.

Figure 4.13 shows that the TMB oxidation and its occurring double shoulder on the positive scan is unaffected by the background current that arises through the Nafion modification. The increase in background charging current, when using chemically modified electrodes, has been observed by Wang and Golden [1989], who also observed a significant improvement in the magnitude and sharpness of redox peaks. They furthermore stated that the increased background current does not affect analytical measurements commonly done by a) differential-pulse voltammetry or b) fixed-potential amperometry and that c) the cyclic voltammetric peak potentials are not affected. The latter statement is verified by the occurrence of Cl-ion peaks in the same spot on both the positive and the negative scan. The fixed potential of -150 mV is also unaffected by the Nafion modification which shows no increased noise at that potential. Conclusively, one can say that Nafion-modification can be safely used on SPGE with TMB as mediator without any added interferences at a potential of -150 mV. However, the advantages of Nafion-modification are questionable since the initial effort to

stabilise the reference electrode by a conducting polymer such as Nafion, which is non-permeable for silver or chloride ions was (Figure 4.12 and 4.13) unsuccessful. Furthermore, even though the Nafion polymer is a conductive ion-exchange resin and commonly used as preconcentration agent, it appears that the resulting peak currents for the TMB oxidation dropped on average 30 % compared to the ones determined in Figure 4.10. This can be explained by the nature of the Nafion ion exchange medium is to attract specifically ions of positive charge, whereas TMB, before it gets oxidised at the electrode, is not attracted by the ion exchange medium and therefore fails to accumulate on the electrode surface. Thus, the decrease in peak current can be explained by the creation of a diffusion barrier caused by the thickness of the nafion film, which affects the flux of TMB from the bulk solution to the electrode surface. Since the Nafion modification could not be related to any significant improvement of interference reduction or measurement sensitivity, the use of Nafion-modified screen printed gold electrodes using TMB as mediator was excluded from further experiments.

#### 4.4.8 Potential selection for amperometric studies with TMB

The optimum working electrode potential for TMB was selected using step amperometry. A 20  $\mu\text{l}$  solution of 100  $\text{mg L}^{-1}$  TMB in electrolyte buffer was deposited on a bare SPGE and the potential increased step-wise (100 seconds/step). Each signal point was recorded at time 50 seconds of each step potential (Figure 4.14).



**Figure 4.14:** Current [ $\mu\text{A}$ ] versus step potential [ $\text{mV}$ ] illustrates step-amperometry of 20  $\mu\text{l}$  TMB solution on bare SPGE. The current was recorded over a hundred seconds for each step potential (-600 to +600 mV).

This (Figure 4.14) displays the current response to each potential step. The current increases more significantly within the negative potential range, where it is displayed in negative values. Within the positive potential range  $>0$  V to + 400 mV the current change in proportion to potential increase is less than at negative potentials. The highest signal: noise ratio was observed at -200 to + 200 mV as the current background (0.05 M PBS, 0.1 M KCl, pH 7.4) was near zero. The low background current is optimal for enzymatic activity determination when a small amount of catalysis product ( $\text{TMB}_{\text{ox}}$ ) needs to be measured in the presence of high concentrations of  $\text{H}_2\text{O}_2$  substrate [Volpe *et al.*, 1998; Badea *et al.*, 2004].

The effect of applied potential on the current response is summarised in Table 4.3.

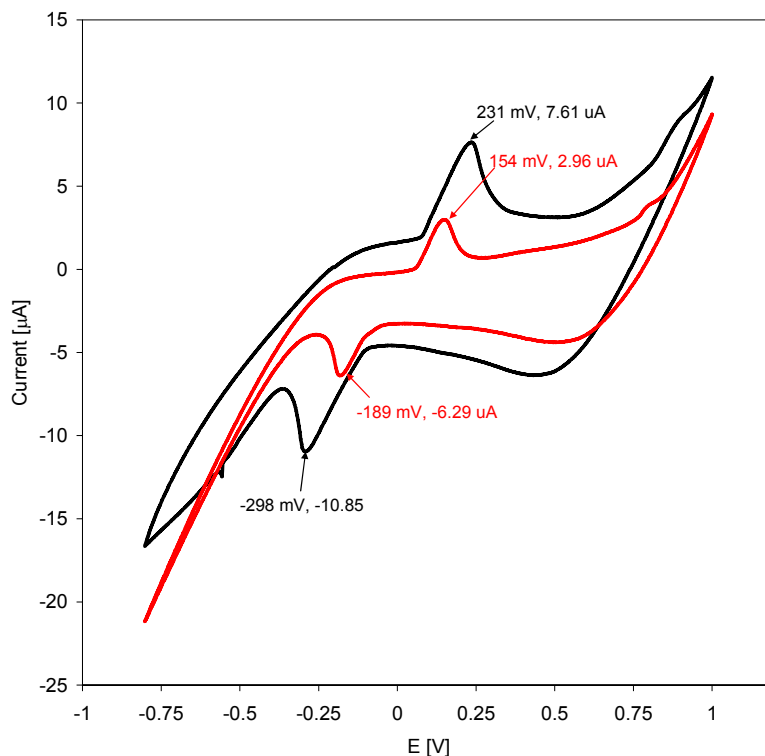
**Table 4.3:** Effect of applied potential on the current response on SPGE with TMB.

Step potential [mV]	Signal current [ $\mu$ A]	Background current [ $\mu$ A]
-600	-4.42	-3.090
-400	-3.23	-1.640
-200	-2.31	-0.290
-100	-0.21	-0.022
0	0.03	-0.005
100	0.09	-0.004
200	0.17	-0.009
400	0.21	-0.002
600	1.03	-0.008

Based upon these findings and taking into account the interferences from phenolic compounds specifically at positive potentials and less in the range of 0-100 mV, a potential of -150 mV was selected as a working potential for the chronoamperometric detection of TMB. Thus, the proposed immunosensor monitors the change in reduction current over time.

#### 4.4.9 Cyclic voltammetry of ochratoxin A –BSA adsorption

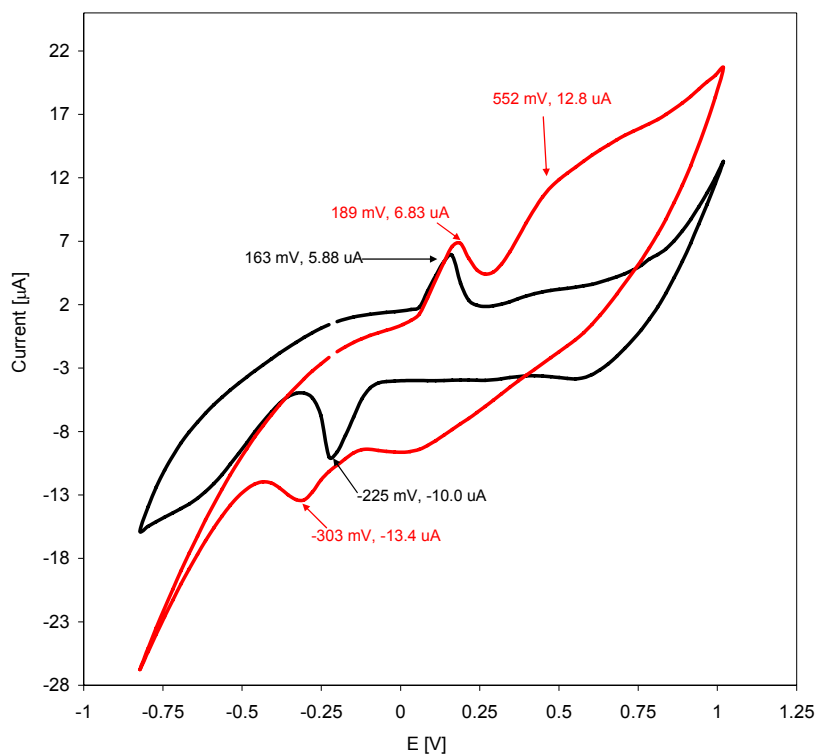
Ochratoxin A-BSA diluted in PBS, pH 7.4 containing 0.1 M KCl, was deposited onto a SPGE and compared to a SPGE modified with adsorbed ochratoxin A-BSA (Figure 4.15).



**Figure 4.15:** Cyclic voltammogram of ochratoxin A-BSA ( $0.1 \text{ mg L}^{-1}$ ) on SPGE at a scan rate of  $50 \text{ mV s}^{-1}$ . Addition of  $20 \text{ }\mu\text{l}$  ochratoxin A-BSA solution (red) added prior to measurement and after overnight adsorption of ochratoxin A-BSA (black).

As shown in Figure 4.15, a redox peak is observed at potentials  $+154 \text{ mV}$  and  $-189 \text{ mV}$  due to the  $\text{Cl}^-$  presence in the electrolyte buffer. The anodic peak potential is shifted upon ochratoxin-BSA adsorption to  $231 \text{ mV}$  and the cathodic peak potential to  $-298 \text{ mV}$ , which displays a shift of  $77$  and  $109 \text{ mV}$  respectively and is clearly related to the gold surface modification. Due to the presence of protein, the peaks on the positive and negative scans shift towards higher potentials, which is more prominently increased upon protein adsorption. The adsorbed protein layer also influences the current, particularly, the anodic current, which is increased on average about  $2 \text{ }\mu\text{A}$ , a sign of increased background interference, also a result of the adsorbed protein layer. The observed redox peaks have been identified as adsorbed ions on the gold surface that have an effect on the current. Is the gold surface exposed to protein (which can adsorb on the electrode) such as ochratoxin A-BSA, any surface redox process should become strongly inhibited. In fact, the inhibition of the surface process causes significant change in the currents at the potential region, and as a consequence the profound changes in the shape of CVs take place [Norouzi *et al.*, 2006].

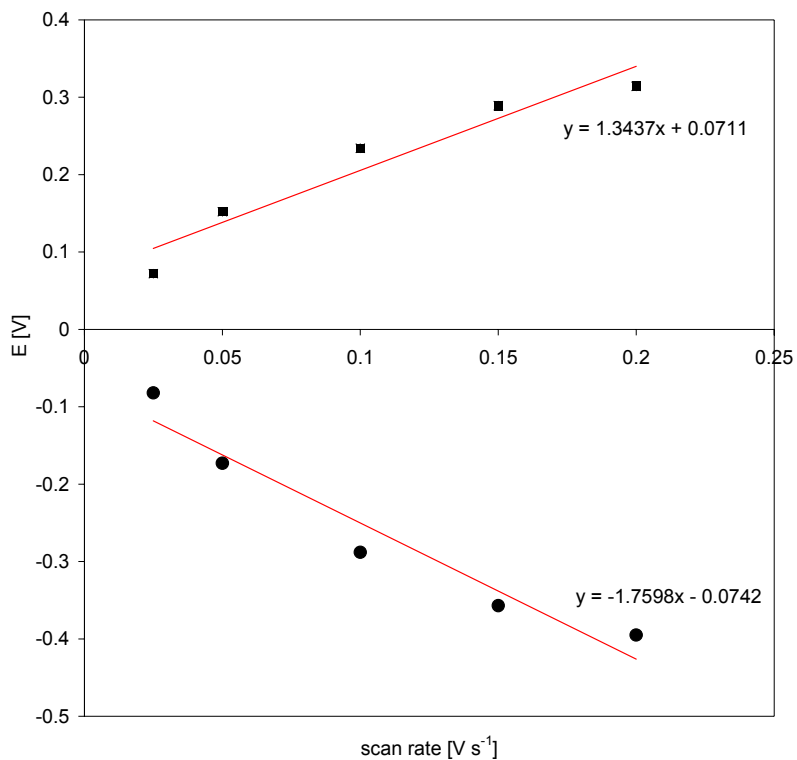
Cyclic voltammograms obtained for the oxidation of TMB on ‘indirect immunoassay’-modified SPGE to one without addition of TMB (Figure 4.16).



**Figure 4.16:** Cyclic voltammograms of 20  $\mu\text{l}$  TMB solution (red) and the control 50 mM PBS, pH 7.4, 0.1 M KCl (black) on SPGE at a scan rate of  $50 \text{ mV s}^{-1}$ .

The  $\text{Cl}^-$  peaks are observed in Figure 4.16 in both instances, which can be explained by the equilibration of the SPGE prior to measurement in 50 mM PBS, pH 7.4, containing 0.1 M KCl. Compared to the CV behaviour observed on a bare SPGE (+ 0.11 V; -0.12 V), the ‘indirect immunoassay’-modified SPGE exhibited a significant shift in  $\text{Cl}^-$  peak potential to +0.16 and -0.22 which corresponds to a shift of about 50 and 100 mV respectively. This potential shift was already observed when investigating the adsorption of ochratoxin A-BSA and can be readily explained by the increased protein layer attached to the gold surface. The positive shift in the oxidation potential also reflects the slower electron transfer reaction [Liu *et al.*, 2002].

The peak-to-peak separation was further investigated with adsorbed ochratoxin A-BSA on SPGE with increasing scan rates (Figure 4.17).



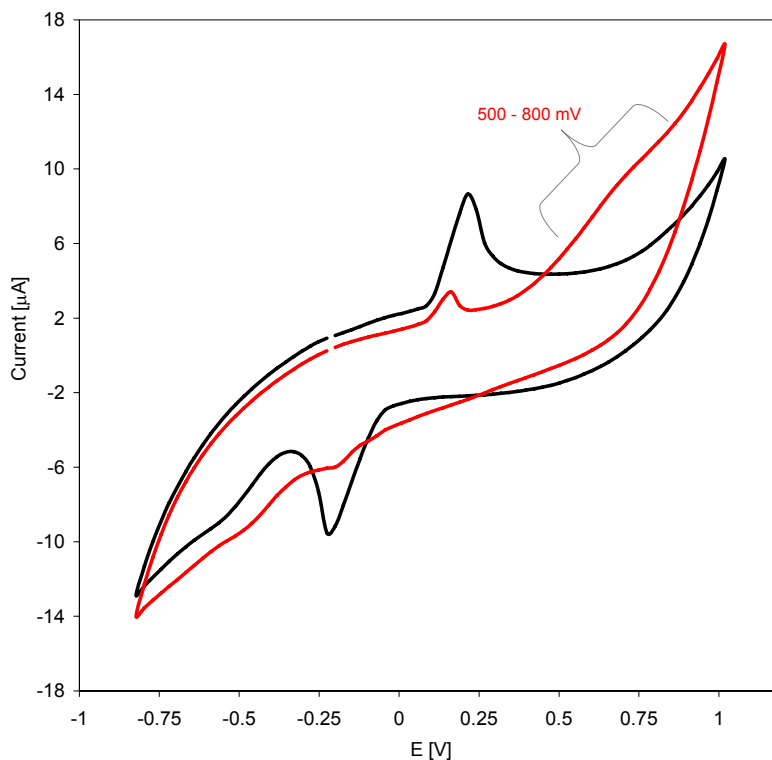
**Figure 4.17:** Plot of scan rate versus peak separation for anodic peak [■] and cathodic peak [●] of ochratoxin A-BSA (50 mM PBS, pH 7.4 in 0.1 M KCl adsorbed on SPGE at a scan rate of  $50 \text{ mV s}^{-1}$ ).

Figure 4.17 displays peak-to-peak separations of 80, 82, 55, and 25 mV at 25, 50, 100, 150, and  $200 \text{ mV s}^{-1}$  respectively, thus substantially higher than those observed on bare SPGEs; this again indicates a slower electron transfer rate.



#### 4.4.10 Electrochemical characterisation of wine

For this study cyclic voltammograms were monitored on bare SPGE with a red wine sample and compared to synthetic wine control as illustrated in Figure 4.18.



**Figure 4.18:** Cyclic voltammograms of 20  $\mu\text{l}$  red wine sample diluted in 0.1 M PBS, pH 7.4 containing 0.1 M KCl (red) compared to synthetic wine (black) and monitored on a bare SPGE at a scan rate of  $50 \text{ mV s}^{-1}$ .

This (Figure 4.18) shows the CV of red wine which exhibits an oxidation process between the potentials +0.5 and +0.8 V, indicated by the broadened peak shoulder. This observation was also made by Parra *et al.* [2004] who observed peaks at 0.45 V and 0.87 V using an unmodified carbon paste electrode (CPE) versus Ag/AgCl. According to previously published works by Kilmartin *et al.* [2001 and 2002] these peaks are related to the polyphenolic content of red wine. In particular, the peak at 0.45 V has been assigned to polyphenols containing an *ortho*-diphenol (catechol) group. In addition to that, no major peak was observed for red wine in the area of the potential selected for TMB determination (-150 mV). In this work, we also observe a distinct peak for the red wine sample at +0.16 V and -0.2 V, previously marked as a response to the Cl<sup>-</sup> ion in KCl electrolyte (+0.11 and -0.11 V) interacting with the SPGE surface.

Since the red wine was 10 fold diluted in electrolyte buffer; this peak was much more developed and the increase in oxidation current was about 5  $\mu\text{A}$  and reduction current about 3.5  $\mu\text{A}$ . Synthetic wine does not display a polyphenol peak (+0.5 and +0.8 V) as it contains much less polyphenols (Appendix A).

#### 4.4.11 Wine interference study on SPGE

Red wine should generate the most electrochemical interferences as it contains more polyphenols than white wine. The effect of dilution and the treatment with PVPP is examined in comparison. PVPP is commonly used in wine fining and known to complex with phenolic and polyphenolic components in wine and also attracts low molecular weight catechins [Morris & Main, 1995]. Using cyclic voltammetry, the electrochemical behaviour of a red wine sample was investigated in the presence of PVPP (Figure 4.19).

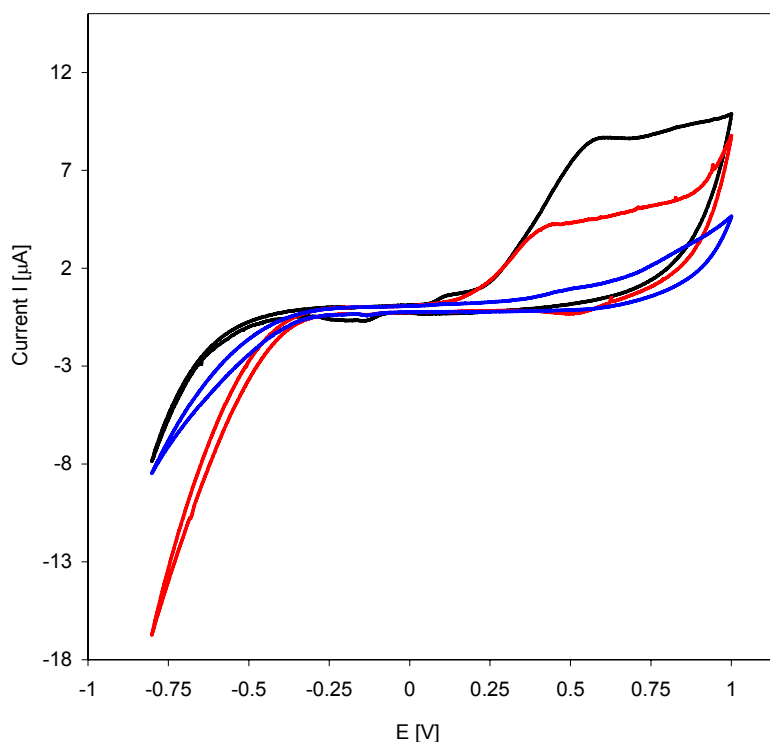


**Figure 4.19:** Cyclic voltammograms of a red wine sample (black), 1:10 diluted red wine sample (red) and 1:10 diluted red wine sample treated with PVPP (blue) on SPGE at a scan rate of  $50 \text{ mV s}^{-1}$ . Dilution buffer was 5%  $\text{Na}_2\text{CO}_3$ , 1% PEG, pH 8.3.

The cyclic voltammogram of red wine exhibits an oxidation peak between the potentials + 0.4 and + 0.8 V, indicated by the broadened peak shoulder. According to previously published works by Kilmartin *et al.* [2001 and 2002] these peaks are related to the polyphenolic content of red wine. In particular, the peak at around 0.45 V has been assigned to polyphenols containing an *ortho*-diphenol (catechol) group. The cyclic voltammograms confirm that wine does not cause much interference at a working potential of -150 mV with a peak current of 0.69  $\mu$ A. The diluted wine sample shows a 50% reduced background current, which is also observed with the PVPP treated sample. As expected, PVPP removed phenolic compounds from the sample solution, which is depicted in the cyclic voltammogram as a sharp reduction in the peak area +400 to +800 mV. However, the background current observed at -150 mV is the same range for the wine sample with and without PVPP addition. Therefore, it was found it unnecessary to treat the diluted wine samples with PVPP prior to detection. It had also been observed that the clean-up and pre-concentration procedure did not make a significant difference regarding interferences at a working potential of -150 mV and presumed a simple dilution of the sample as sufficient.

#### 4.4.12 Chronoamperometric studies of TMB/ H<sub>2</sub>O<sub>2</sub>/HRP system

The mediator TMB and HRP substrate H<sub>2</sub>O<sub>2</sub> were studied using chronoamperometry to characterise the resulting current as an effect of subsequent addition of H<sub>2</sub>O<sub>2</sub> and TMB as illustrated in Figure 4.20.

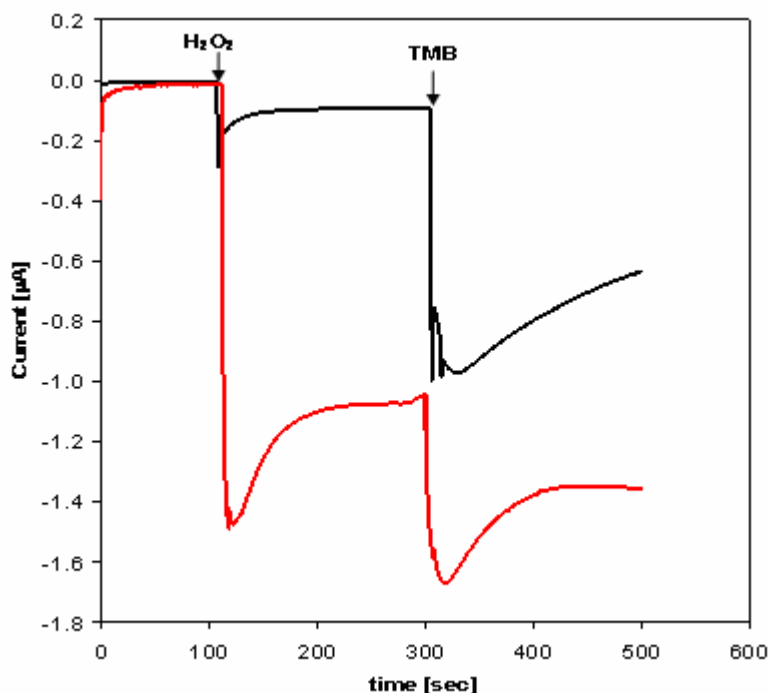


**Figure 4.20:** Chronoamperometry of current [ $\mu\text{A}$ ] versus time [sec] illustrates the current response upon the addition of H<sub>2</sub>O<sub>2</sub> and then TMB when applying zero potential (black) compared to applying a potential at -150 mV (red).

Figure 4.20 shows that the current decreases sharply upon addition of H<sub>2</sub>O<sub>2</sub> and stabilises within 50-100 seconds. At potential zero, there is barely an electrochemical net conversion of reactant visible, but the spontaneous reduction of H<sub>2</sub>O<sub>2</sub> that probably resulted from remaining charges of the previously applied conditioning potential of the electrode. However, at an applied potential of -150 mV, where the negative potential causes the reduction of H<sub>2</sub>O<sub>2</sub>, the sharp decrease ('spike') in current, confirms the initial reduction of H<sub>2</sub>O<sub>2</sub> at the electrode surface. Upon addition of TMB, there is another sharp decrease of current that stabilises within 50 seconds indicating the initial oxidation of TMB (by reducing further H<sub>2</sub>O<sub>2</sub>) at the electrode surface. At potential -150 mV, the current spike is followed by a constant increase in current, illustrating the

diffusion of TMB molecules from the bulk solution to the electrode surface. At zero potential, the current-time curve is showing different characteristics such as the steady increase indicates an ongoing diffusion of TMB to the electrode surface. This can be explained by the non-electrochemically induced reduction of  $\text{H}_2\text{O}_2$  at zero potential; thus, the net concentration of  $\text{H}_2\text{O}_2$  is higher at the point of TMB addition than the decreased concentration (reduced  $\text{H}_2\text{O}_2$ ) caused by the application of -150 mV potential. Therefore, the reaction shows a steady current increase caused by the reaction of TMB with  $\text{H}_2\text{O}_2$ . The addition of TMB results in its oxidation by  $\text{H}_2\text{O}_2$  and subsequent reduction at the gold electrode releasing further electrons.

Overall, one can conclude, that at a set potential of -150mV, the reaction rate  $\text{H}_2\text{O}_2$  alone on the gold working electrode is highest within 100 seconds from the point of deposition, after that the reaction rate is growing steadily slower, which can be also observed past the deposition of TMB.

To maximise signal sensitivity, TMB and  $\text{H}_2\text{O}_2$  should be deposited together in a freshly mixed solution, to maximise the concentration of initial  $\text{H}_2\text{O}_2$  and TMB at the start of the reaction (redox reaction taking place in the bulk solution), whereas the resulting current is entirely depended on the diffusion rate of oxidised TMB to the electrode surface. One also needs to take into account, that upon addition of the  $\text{H}_2\text{O}_2$ /TMB solution, the reaction rate will be at its steepest slope within the first 100 seconds.

This reaction can be catalysed by the presence of a redox enzyme such as horseradish peroxidase. After the establishment of a baseline at an applied potential of -150 mV, a mix of TMB and  $\text{H}_2\text{O}_2$  with and without enzyme is deposited onto the SPGE and the decrease in current observed (Figure 4.21).

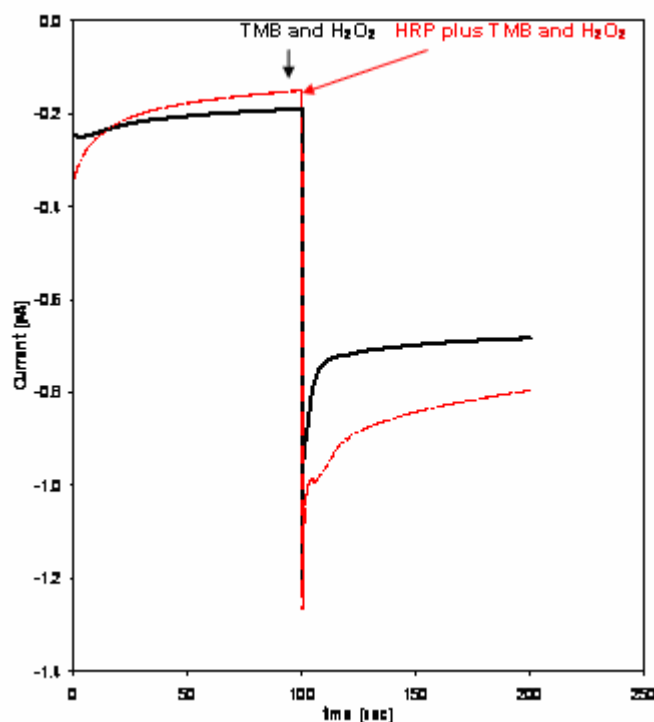


**Figure 4.21:** Chronoamperometry of current [ $\mu\text{A}$ ] versus time [sec] illustrates the current response upon the addition of TMB and  $\text{H}_2\text{O}_2$  (black) in comparison to the addition of TMB/ $\text{H}_2\text{O}_2$ /HRP (red) at an applied potential of  $-150\text{ mV}$ .

From Figure 4.21 it becomes clear that even with the addition of a low concentration of enzyme, there is a visible change in current, which decreases even further as a result of the catalysed reduction of  $\text{H}_2\text{O}_2$ . The resulting electrons were shuttled to the electrode via TMB. The higher the concentration of enzyme, the more the decrease in current is to be expected. Therefore, using a redox enzyme such as HRP as label in the immunoassay setup will result in a direct signal response with enzyme concentration, which, in turn, is depended on antibody concentration bound to immobilised ochratoxin A-BSA. This format allows for non-competitive and competitive detection of analyte. In Figures 4.20 and 4.21, one can clearly observe the electrolytic process as the current spikes as a result of electroactive species being transformed at the electrode surface. Over time, the current shows a diffusion profile according to the Cottrell equation as electroactive species diffuse from the bulk solution to the electrode surface in order to react.

#### 4.4.13 Optimal ochratoxin A-BSA concentration

In immunosensor development, the direct immunoassay format with transducer-immobilised antibodies has been traditionally used. However, the stability of the sensor relies on the quality of the immobilisation technique. Thus, an indirect competitive assay with a stable conjugate of the antigen bound to the sensor surface has been proven to produce more stable and reproducible sensors [Bier *et al.*, 1994].

An indirect assay was developed on the sensor by establishing the optimal ochratoxin A-BSA concentration to be adsorbed onto the gold surface. This was determined by immobilising varying concentrations of ochratoxin A-BSA onto the SPGE. The amount of adsorbed ochratoxin A-BSA is determined via anti-ochratoxin A antibody and secondary HRP-labelled antibody. Change in current was observed over time at a potential of -150 mV as seen in Figure 4.22.

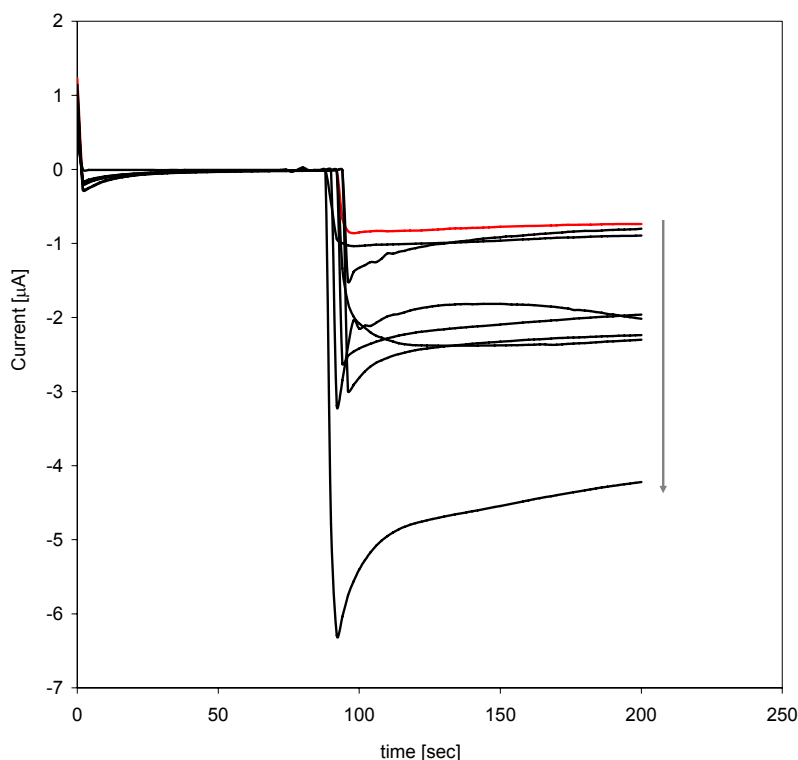


**Figure 4.22:** Chronoamperometry of current [ $\mu\text{A}$ ] versus time [sec] illustrates the current response upon the addition of TMB and  $\text{H}_2\text{O}_2$  to the immunosensor surface (non-competitive immunoassay-modified SPGE). The change in current at an applied potential of -150 mV was monitored over time. The grey arrow depicts increasing adsorbed ochratoxin A-BSA concentration (black) [0.1; 0.5; 1; 2; 5; 10; and 100  $\text{mg L}^{-1}$ ]

ochratoxin A-BSA] with decreasing current compared to the negative control BSA (red).

The amount of adsorbed ochratoxin A-BSA is directly proportional to the decrease in current observed with increasing HRP catalysis. Upon addition of TMB/H<sub>2</sub>O<sub>2</sub> (Figure 4.22), an instant decrease in current can be observed, which stabilise within 50 seconds.

The degree of current decrease changes with increasing ochratoxin A-BSA concentration towards negative current values as expected. The current [ $\mu$ A] was then plotted versus immobilised ochratoxin A-BSA concentration (Figure 4.23).

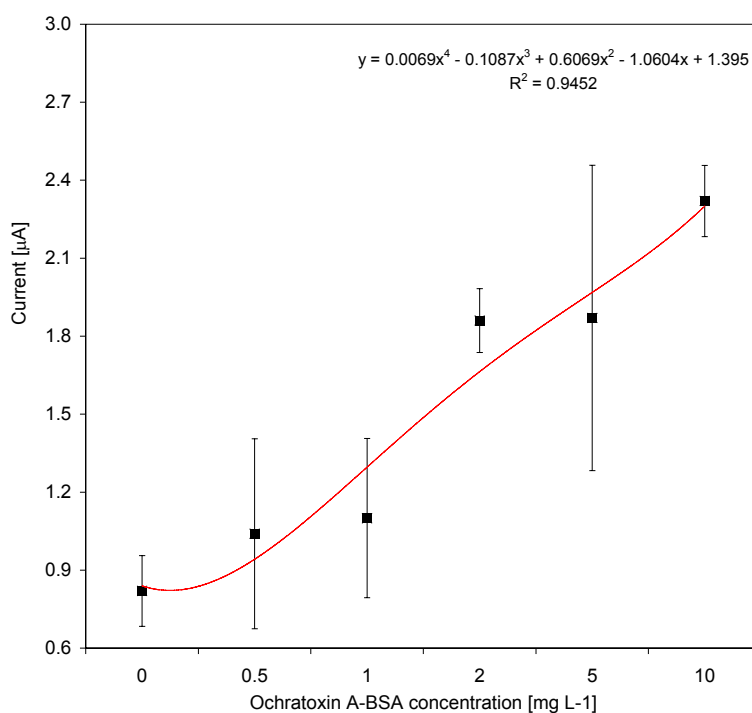


**Figure 4.23:** Current -[ $\mu$ A] versus immobilised ochratoxin A-BSA (■) concentration illustrates the current response with increasing ochratoxin A-BSA adsorbed to the SPGE.

From Figure 4.23, it was established that the current did decrease with increasing ochratoxin A-BSA concentration in the current range of -0.8 to -3.7  $\mu$ A, depicting the dynamic concentration range of adsorbed ochratoxin A-BSA. Saturation was not reached at the maximum applied concentration of 100 mg L<sup>-1</sup> ochratoxin A-BSA. Therefore, a saturation concentration and current could not be established. The lowest adsorbed concentration showing a distinguishable signal (10 % above the blank value



$I_0 = -0.84 \mu\text{A}$ ) is approximately  $0.5\text{-}1 \text{ mg L}^{-1}$  ochratoxin A-BSA with an optimal coating concentration at  $I_{50}$  of about  $2\text{-}10 \text{ mg L}^{-1}$ .

#### 4.4.14 Optimal antibody concentration

The optimal antibody concentration was determined by immobilising a fixed amount of ochratoxin A-BSA ( $10 \text{ mg L}^{-1}$ ) and incubating with distinct concentrations of antibody in the range of  $1\text{-}50 \text{ mg L}^{-1}$  (equivalent of dilutions from stock of  $1/1000$  to  $1/20$ ). Again, the amount of bound antibody was determined via a secondary HRP-labelled antibody and directly proportional to the decrease in current observed with increasing HRP catalysis. Figure 4.24 depicts a plot of current versus antibody concentration.

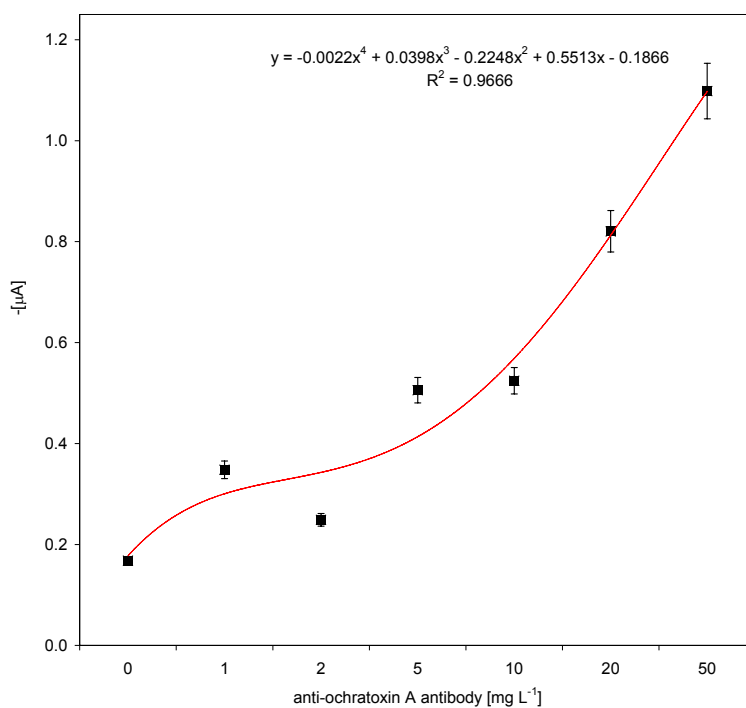


**Figure 4.24:** Current  $-I$  [ $\mu\text{A}$ ] versus immobilised anti-ochratoxin A antibody ( $\blacksquare$ ) concentration illustrates the current response with increasing antibody concentration bound to a fixed concentration of adsorbed ochratoxin A-BSA.

It can be seen from Figure 4.24, that at  $50 \text{ mg L}^{-1}$  antibody concentration, saturation of adsorbed ochratoxin A-BSA binding sites was not yet reached. This was expected since a similar range of concentrations was used as when establishing the optimal ochratoxin A-BSA concentration. It was established that the lowest antibody concentration considered to show a distinguishable signal (considered 10 % above the blank value  $I_0 =$

-0.17  $\mu\text{A}$ ) is approximately 1-2  $\text{mg L}^{-1}$  antibody (equivalent to a dilution of 1/1000 to 1/500). It was also observed that the range of current decreasing with increasing antibody concentration was low, between -0.1 to -1.1  $\mu\text{A}$ , requiring a much higher antibody concentration to reach saturation of adsorbed ochratoxin A-BSA. The optimal antibody concentration determined at  $I_{50}$  for this assay was about 15  $\text{mg L}^{-1}$ .

#### 4.4.15 Indirect competitive ochratoxin A immunosensor

The developed indirect competitive immunoassay was transferred onto the screen printed gold electrode. A range of ochratoxin A standard concentrations was applied to establish a calibration curve. A mixture of TMB and  $\text{H}_2\text{O}_2$  was added to the immunoassay on the sensor surface and the change in current was observed over time for different ochratoxin A competitor concentrations at a potential of -150 mV (Figure 4.25).

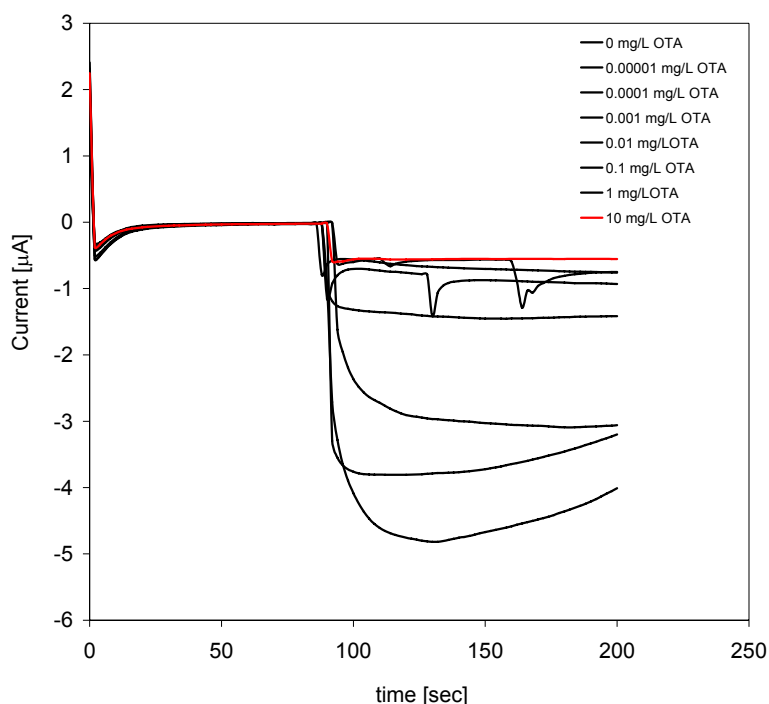


**Figure 4.25:** Chronoamperometry of current [ $\mu\text{A}$ ] versus time [sec] illustrates the current response upon the addition of TMB and  $\text{H}_2\text{O}_2$  to the immunosensor surface (indirect competitive immunoassay-modified SPGE). The change in current at an applied potential of -150 mV was monitored over time. The grey arrow depicts the increasing ochratoxin A competitor concentration (black) [0.00001; 0.0001; 0.001; 0.01; 0.1; 1; and 10  $\text{mg L}^{-1}$  ochratoxin A] inversely proportional to the current response. The negative control is 0.1 M PBS, pH 7.4 (red).

With increasing ochratoxin A competitor concentration, the less antibody is bound to the surface, thus, the less resulting decrease in current (Figure 4.25). Therefore, the decrease in current is inversely proportional to the ochratoxin A competitor concentrations. The degree of current increase changes with increasing ochratoxin A competitor concentration is inversely proportional to the non-competitive approach. The more ochratoxin A competitor, the less antibody binds to the ochratoxin A-BSA modified SPGE. The less antibody binds, the less secondary antibody binds and thus less HRP is bound to the SPGE, which results in a less negative (therefore increasing) current. The current [ $\mu\text{A}$ ] is then plotted versus ochratoxin A competitor concentration (Figure 4.26).

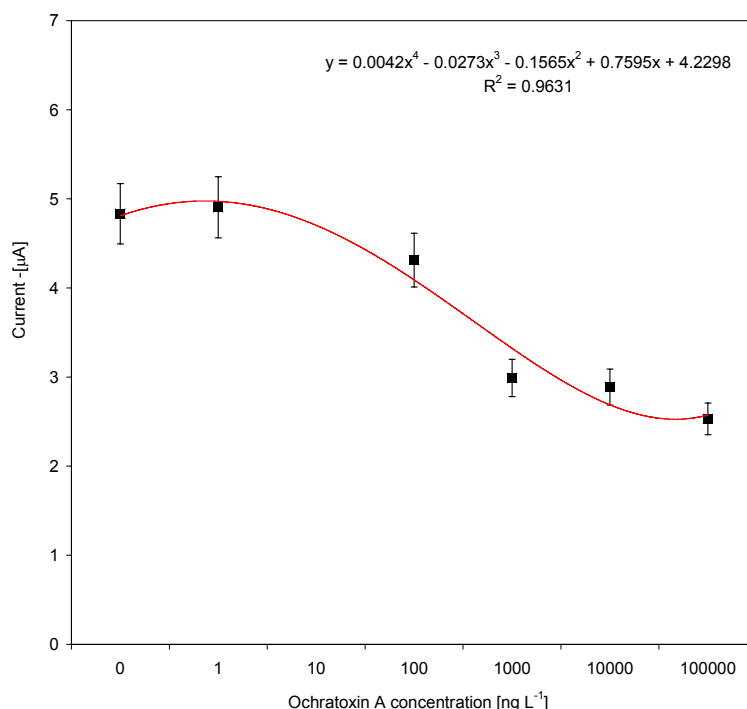


**Figure 4.26:** Competitive response curve of current -[ $\mu\text{A}$ ] versus ochratoxin A (■) competitor concentration illustrating the current response with increasing ochratoxin A [ $\mu\text{g L}^{-1}$ ] applied with fixed antibody and immobilised ochratoxin A-BSA concentration on SPGE monitored using the Autolab potentiostat. Standards are prepared in PBS, pH 7.4.

As Figure 4.26 shows, the range of ochratoxin A concentration reached from  $1 \text{ ng L}^{-1}$  to  $10 \mu\text{g L}^{-1}$  displaying a dynamic range that covers the permissible concentration of about  $2 \mu\text{g L}^{-1}$ . The plot shows linearity in the range from  $10\text{-}1000 \text{ ng L}^{-1}$  ochratoxin A with a detection limit of  $< 100 \text{ ng L}^{-1}$  ochratoxin A and a standard deviation of 6 %.

#### 4.4.16 Biosensor optimisation through surface modification

It has been discussed that significant improvement to sensor performance can be achieved by incorporation of new printed materials or support surfaces. Surface-modification (e.g. new ligands, polymers and nanostructure materials) can enhance the reproducibility and sensitivity of screen-printed based sensors [Renedo *et al.*, 2007]. In this work, a polymer was implemented into the sensor. The gold electrode was modified with carboxymethylated dextran (CMD), a carboxy-group functionalised dextran polymer mainly known in SPR measurements [Lofas & Johnsson, 1990]. This calibration graph for ochratoxin A determination (Figure 4.26) is being further improved by modifying the SPGE surface with CMD to enable the covalent attachment of ochratoxin A-BSA. The electrochemical characteristics of carboxymethylated dextran were initially characterised using cyclic voltammetry on a bare SPGE (Figure 4.27).

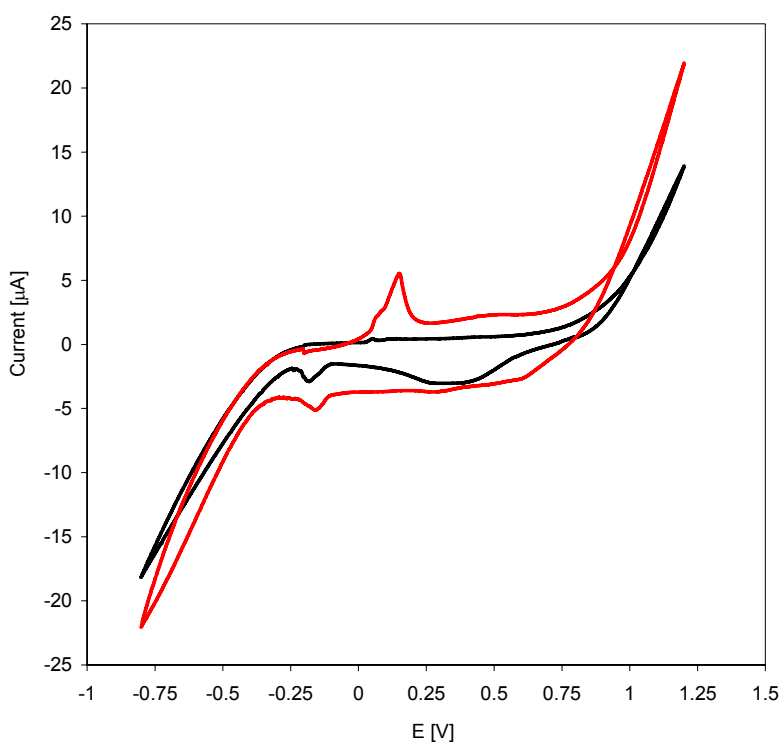


**Figure 4.27:** Cyclic voltammograms of current [ $\mu\text{A}$ ] versus potential [V] of CMD-modified SPGE illustrating adsorbed carboxymethylated dextran (CMD) (red) compared to bare SPGE in 0.1 M PBS, pH 7.4 containing 0.1 M KCl at a scan rate of  $50 \text{ mV s}^{-1}$ .

As shown in Figure 4.27, no significant oxidation or reduction peak was monitored for CMD on SPGE versus Ag/AgCl. The catalytic current did not decrease as opposed to a study by Pallarola *et al.* [2006] who observed a decrease in catalytic current with CMD modified gold electrodes suggesting that the CMD may hinder the access of the redox couple to the electrode surface. The high molecular weight dextran used in this work has a much looser and flexible structure and should not hinder the access to the electrode surface. The observed increased background current (0.5-1.5  $\mu\text{A}$  compared to electrolyte buffer background) arose probably due to surface charges through carboxy groups present in the carboxymethylated dextran as suggested for other poly-anionic surfaces (e.g. Nafion). CMD surface modification is presumed to increase stability of the active surface and decrease non-specific binding of protein and interfering wine components. Subsequently, ochratoxin A-BSA was immobilised covalently to the carboxymethylated surface via carbodiimide coupling (Figure 4.28).

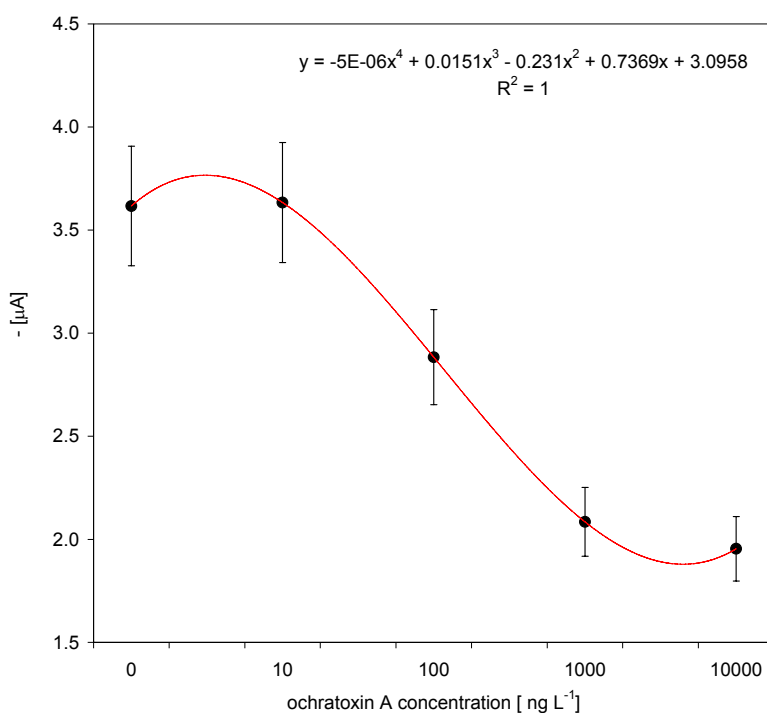


**Figure 4.28:** Competitive response curve of current  $-\mu\text{A}$  versus ochratoxin A (■) concentration illustrating the current response with increasing ochratoxin A competitor [ $\mu\text{g L}^{-1}$ ] concentration on CMD-modified SPGE monitored using the Autolab potentiostat. Standards are prepared in PBS, pH 7.4. The curve was fitted using a four parameter fit.

As Figure 4.28 shows, the range of concentration reached from  $10 \text{ ng L}^{-1}$  to  $100 \text{ } \mu\text{g L}^{-1}$  displaying a dynamic range, covering lower concentrations of interest and also covering the aim of detection of about  $2 \text{ } \mu\text{g L}^{-1}$ .

The plot shows linearity in the range from  $0.1\text{-}10 \text{ } \mu\text{g L}^{-1}$  with a detection limit of  $10 \text{ ng L}^{-1}$  and a standard deviation in the range of 8 %. This covalent immunosensor construction is about 10 times more sensitive than the immunosensor using adsorbed ochratoxin A-BSA, which can be partially explained by the increase in surface charges (surface activity) and also through the decrease in non-specific binding through covalent coupling of biomolecules.

Despite its relatively narrow linear range ( $0.1\text{-}10 \text{ } \mu\text{g L}^{-1}$ ), the biosensor described in this work appears suitable for on-site applications of wine sample contamination displaying a detection limit of  $10 \text{ ng L}^{-1}$ .

#### **4.4.17 Analysis of ochratoxin A in wine samples**

The signal current monitored for the wine samples was baseline subtracted and a 1:2 dilution of sample and a sample volume of  $10 \text{ } \mu\text{l}$  taken into account.

The calculated values for ochratoxin A contamination are listed in Table 4.4, as seen below. The results of the wine analysis are compared with two further immunoassay-based methods, the previously developed indirect competitive immunoassay and a commercial directly competitive immunoassay kit.

**Table 4.4:** Comparison of sensor and standard immunoassay test kit results for measurement of ochratoxin A in wine samples.

Wine sample	Immuno- sensor	HPLC	Immuno- assay kit
	1:2 dilution	IAC	IAC
White wine	Ochratoxin A [ $\mu\text{g L}^{-1}$ ]		
Canti Catarratto Chardonnay, Italy-Sicily 2005	1.763	1.337	0.398
Canti-Chardonnay Pinot Grigio, Italy 2005 (1)	0.748	1.629	0.411
Canti Catarratto Chardonnay, Italy-Sicily 2005	1.752	1.338	0.410
Bordeaux, France 2005	1.253	0.998	0.405
Soave, Italy-Verona 2005	1.232	1.094	0.409
Pinot Grigio, Italy 2005	0.720	0.813	0.385
Canti-Chardonnay Pinot Grigio, Italy 2005 (2)	0.563	0.020	0.397
Canti-Chardonnay Pinot Grigio, Italy 2005 (3)	0.763	0.536	0.392
Soave Classico, Italy 2005	0.854	1.260	0.392
Red wine	Ochratoxin A [ $\mu\text{g L}^{-1}$ ]		
France, 2001	0.152	0.572	0.389
Canti, Italy, 2006	*	0.379	0.4
Cabernet Sauvignon, Chile, 2005	0.285	0.439	0.328
Italy, 2006	0.182	0.556	*
Bordeaux, France, 2005	0.155	0.321	0.375
Cru,S	0.176	0.138	0.403
Mon,France, 2005	*	0.213	0.379
South Africa, 2006	*	0.354	0.314
unknown origin	*	0.722	0.396
Lambrusco,Italy,2005 sat PVPP	0.512	/	/
Lambrusco,Italy,2005 0.2% PVPP	0.523	/	/

-\*- depicts a signal below the detection limit and -/-depicts a sample not included in that method

The wine sample analysis suggested that more interference were observed with red wine than with white wine samples, possibly due to increased polyphenols in red wines. Also, the data monitored with the immunosensor and HPLC suggest that there is more ochratoxin A contamination in white wines than in red, which is generally not published in the literature as it is well established that red wines contain more ochratoxin A than white ones. On an overall note, the sensor data correlated best with the HPLC data, even though the sample pre-treatment differs substantially. Also, it can be observed that the standard deviation of the immunoassay kit compared to the sensor and HPLC data is, especially with white wine samples, very high. The wine analysis showed good results corresponding with HPLC data, however, not with the immunoassay data.

#### **4.4.18 Microelectrode immunosensor**

The trend in biosensor design moves towards miniaturisation since it saves materials and can improve performance. Microfabrication technology is a great tool for miniaturisation applying novel techniques such as photolithography or electron-beam-lithography as well as chemical and electrochemical etching to produce reactive surfaces. High density immobilisation and the use of polymer materials enables integration of core components like sampling, reaction, sensing, transduction and data processing into one entity (lab-on-a-chip).

In this work, the use of gold microelectrode arrays was described as a means of improving immunosensor performance by increasing the current density on the sensor area and thus producing an accumulative signal response. This is achieved by using microelectrode arrays. Also, the microelectrode design allows for a different diffusion profile and thus electrochemical kinetics and also for much lower samples volumes to be used. The indirect immunosensor format that has been proven to work on SPGE is transferred to the gold microelectrodes. The microelectrode array prepared at Tyndall is composed of a gold reference and counter electrode that can be modified further and a working electrode made of an array of 5x5 microelectrodes with a size of 20  $\mu\text{m}$  and a separation distance of 200  $\mu\text{m}$  (as seen Figure 1.7).



The microelectrodes were characterised using cyclic voltammetry by monitoring the dependence of peak current ( $i_p$ ) with scan rate ( $\nu$ ) for the oxidation of TMB (Figure 4.29).

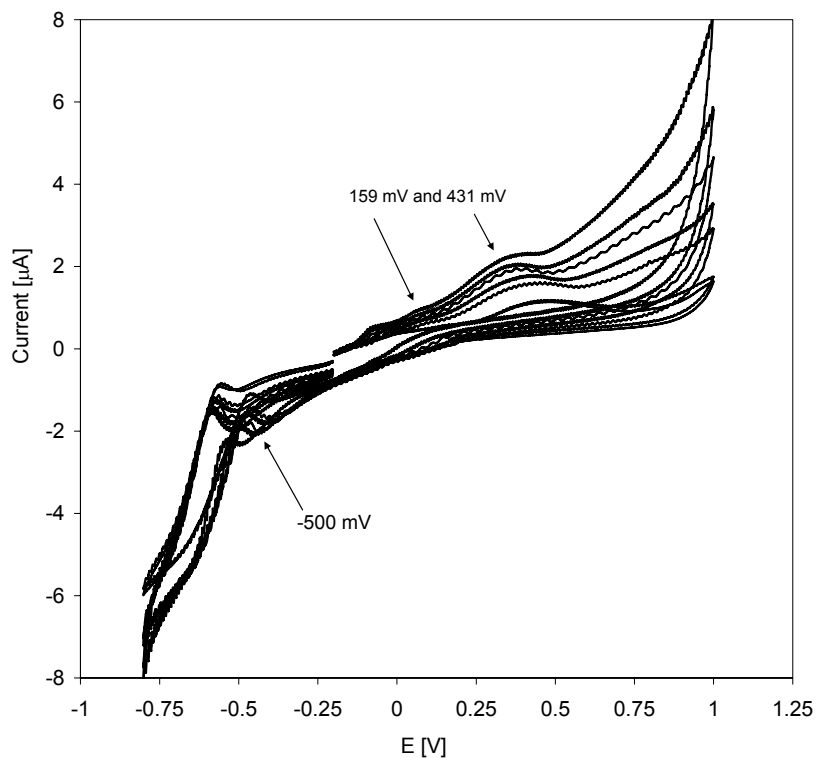


**Figure 4.29:** Current versus electrochemical potential shows the cyclic voltammograms (CV) of 10  $\mu\text{l}$  TMB solution on SPGE at different scan rates [ $\nu$ ]. From inner to outer cyclic voltammogram the scan rate is 25; 50; 75; 100; 150; 200; and 400  $\text{mV s}^{-1}$ .

Figure 4.29 shows cyclic voltammograms for all scan rates that display the characteristic TMB double shoulder on the positive scan, which are considered to result from the TMB itself illustrating two 1-electron oxidation steps. One reduction peak on the negative scan is illustrating a single 2-electron reduction step. There was a gradual increase in peak current  $i_p$  with respect to the increase in  $\nu$ . It was also observed that the cyclic voltammogram shows interferences as the current seems to be oscillating while scanning the potential.

The anodic peak currents for both TMB peaks on the positive scan and the cathodic peak current were further evaluated by plotting the anodic peak current versus the square root of the scan rate as shown in Figure 4.30.

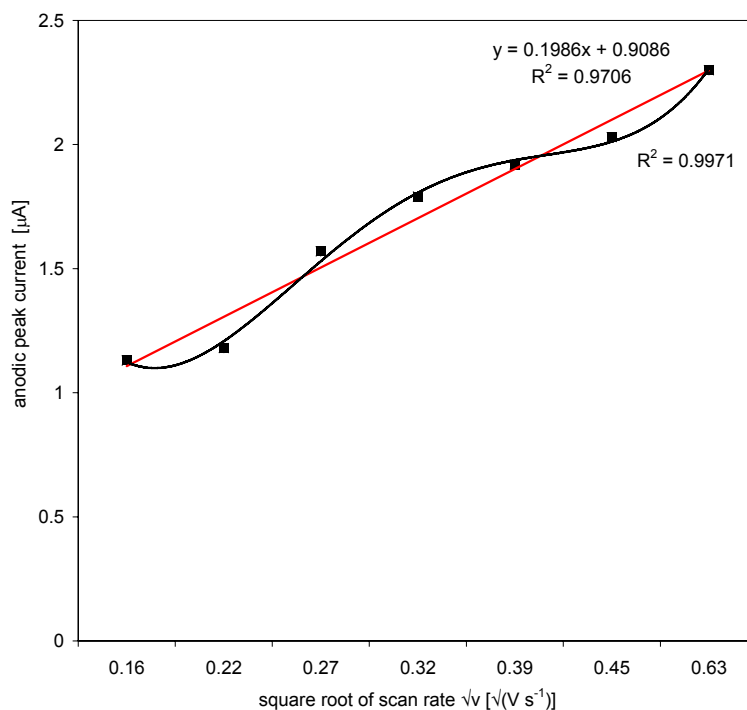


**Figure 4.30:** Anodic peak currents [ $\mu A$ ] versus square root of scan rate  $\sqrt{v}$  [ $\sqrt{V s^{-1}}$ ] obtained from cyclic voltammograms on bare gold microelectrodes with increasing scan rate.

Figure 4.30 shows that the anodic peak current ( $i_{pa}$ ) display a more non-linear relationship to the square root of scan rate ( $\sqrt{V s^{-1}}$ ). This indicates that the redox reaction of TMB on gold microelectrodes is more adsorption depended redox reaction and less diffusion-controlled electron transfer process as shown for SPGE (Figure 4.8). This could mean that the different diffusion patterns (radial versus linear diffusion) on microelectrodes influence the redox reaction of TMB or that due to lower sample volumes on microelectrodes, capillary forces prevent mixing and distribution of analyte (TMB) over the electrode surface and thus limit diffusion.

Cyclic voltammetry was also used to investigate the electrochemical behaviour of the gold microelectrodes with PBS buffer, pH 7.4 containing 0.1M KCl, and H<sub>2</sub>O using a scan rate of 50 mV s<sup>-1</sup> (Figure 4.31).

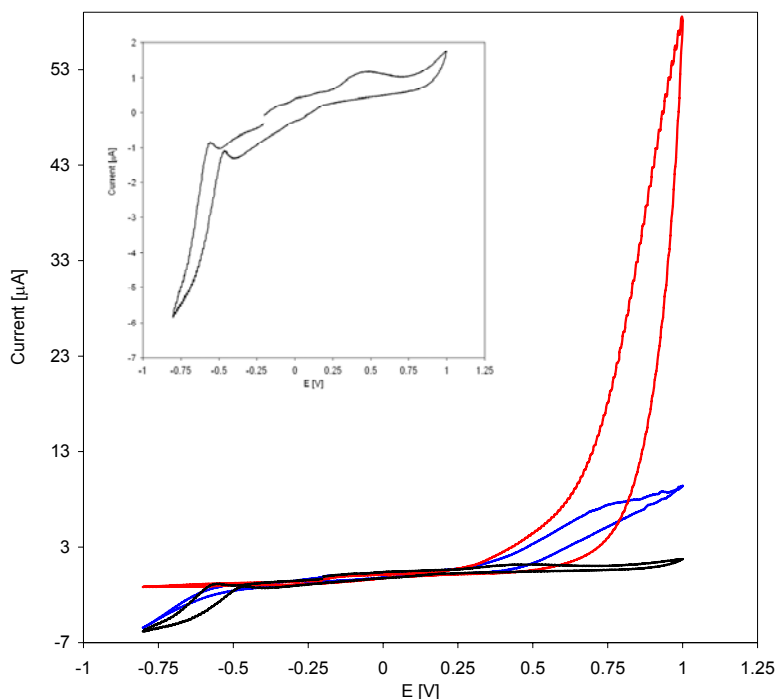


**Figure 4.31:** Cyclic voltammograms of H<sub>2</sub>O (blue); 0.1 M PBS, pH7.4, containing 0.1M KCl (red); and TMB solution (black and seen as insert) on bare gold microelectrodes recorded at a scan rate of 50 mV s<sup>-1</sup>.

The cyclic voltammograms in Figure 4.31 also show a peak for the oxidation of TMB and there are no distinctive peaks for H<sub>2</sub>O or 0.1 M PBS containing 0.1 M KCl, although the latter shows a high increase in current at potentials larger than 750 mV, which indicates possible interferences. The lack of a peak caused by the high salt concentration (Cl<sup>-</sup> ion) that had been observed on the SPGE surface (Figure 4.11) is not observed with the gold microelectrodes. Nevertheless, this could be a result of the different reference electrode used with the microelectrodes. Whereas SPGE used gold working electrode versus Ag/AgCl reference electrode, the microelectrodes have a gold working and also gold reference electrode. This might cause instability in the current response, possibly the increased current response for PBS at > 750 mV and also the slight oscillation in current signal observed in Figure 4.29.

The optimum working electrode potential for TMB on the gold microelectrodes was determined using step amperometry depositing 10  $\mu\text{l}$  TMB solution on a bare gold microelectrode and increasing the electrode potential step-wise (100 seconds/step). Each signal point was recorded at time 50 seconds of each step potential (Figure 4.32).

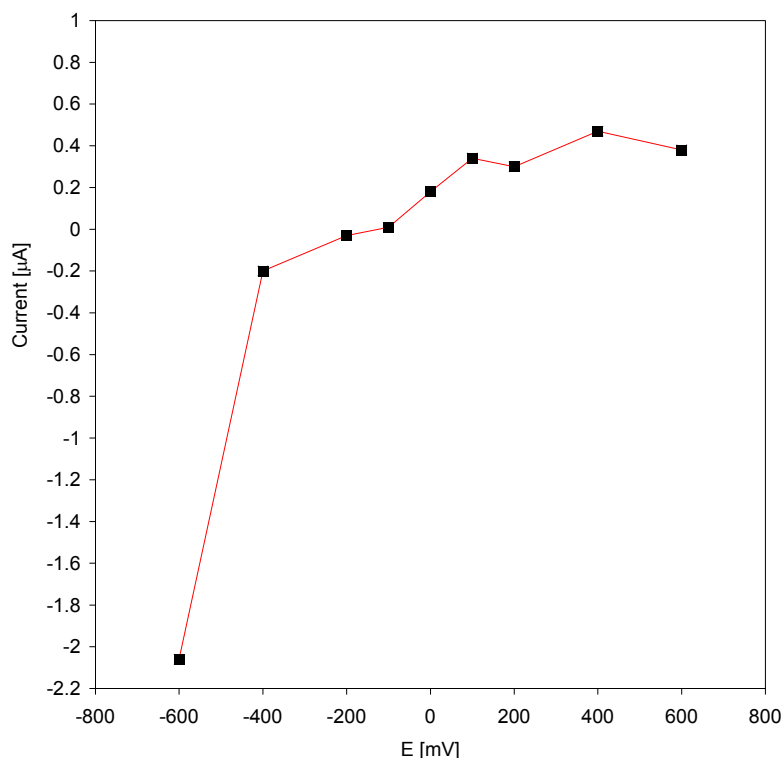
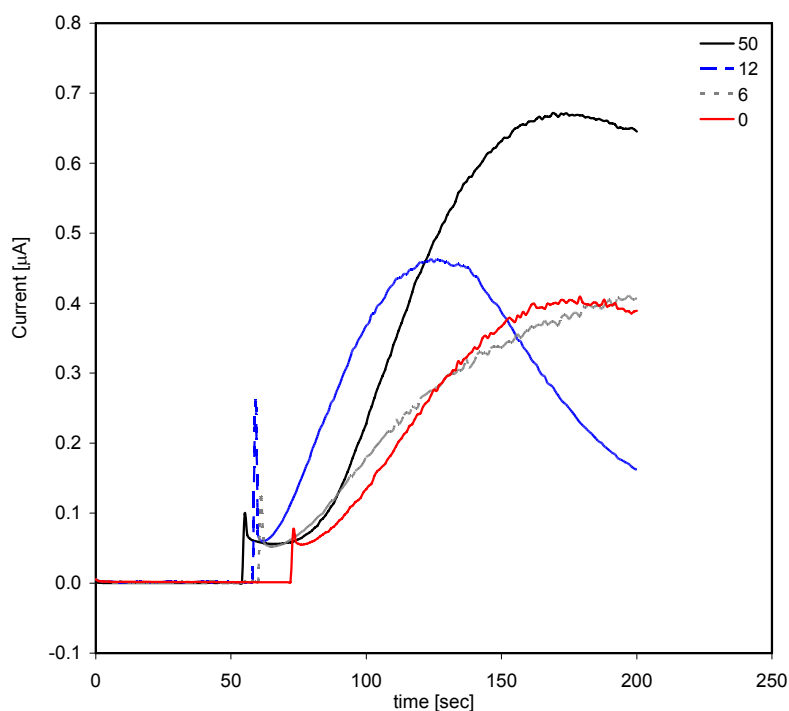


**Figure 4.32:** Current [ $\mu\text{A}$ ] versus step potential [mV] illustrates step-amperometry of 20  $\mu\text{l}$  TMB solution on bare gold microelectrodes. The current was recorded for each step potential (-600 to +600 mV) over a hundred seconds.

Figure 4.32 displays the current response to each potential step. Here, the current increases more significantly within the positive potential range between  $>100$  mV to +400 mV, whereas the current change at negative potentials is small and close to zero ampere. Therefore, a potential working potential of +150mV was chosen, since more positive potentials might result in interferences.

When performing chronoamperometry, the change in current (I) is monitored as a function of time (t). At applied positive potentials, in contrast to negative working electrode potentials, the current ‘spikes’ towards more positive current values with a ‘reverse’ decay towards more negative values as the diffusion-controlled current ‘decays’ towards zero ampere upon addition of an electroactive. The indirect

immunoassay format that has been used for the SPGE immunosensor development in Section 4.4.15 was transferred to the gold microelectrode and a small range of ochratoxin A competitor concentrations ( $1\text{-}50\text{ mg L}^{-1}$ ) was determined to obtain a preliminary standard curve. Chronoamperometry on gold microelectrodes is shown in Figure 4.33.



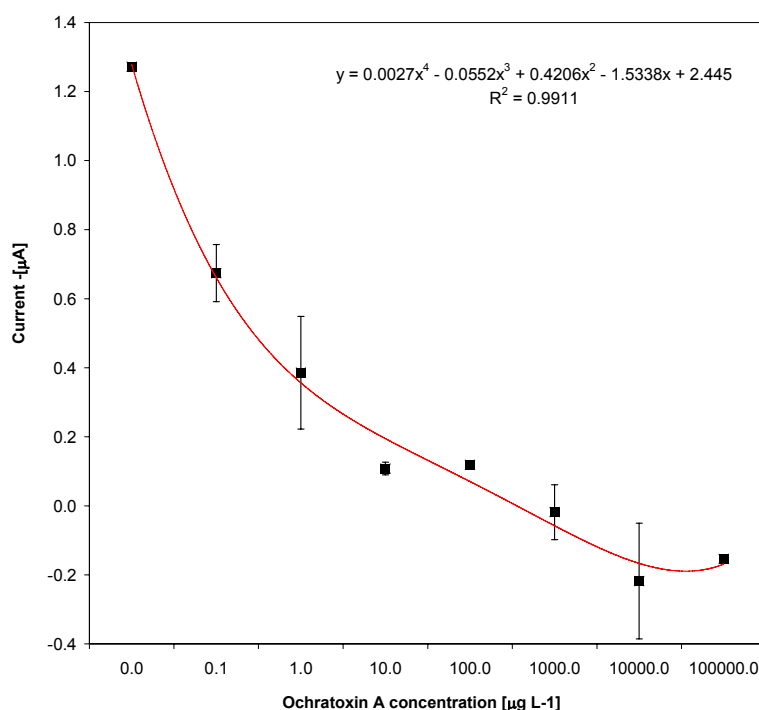
**Figure 4.33:** Chronoamperometry of current [ $\mu\text{A}$ ] versus time [sec] illustrates the current response upon the addition of TMB and  $\text{H}_2\text{O}_2$  to the immunosensor surface (indirect competitive immunoassay-modified gold microelectrode). The change in current at an applied potential of  $+150\text{ mV}$  was monitored over time. Increasing ochratoxin A competitor concentrations [ $6$ ;  $12$ ; and  $50\text{ mg L}^{-1}$  ochratoxin A] are shown in black and negative control is  $0.1\text{ M PBS}$ ,  $\text{pH } 7.4$  (red).

Figure 4.33 shows a current change over time that does not decay towards zero and is not corresponding to the Cottrell equation (Equation V) but shows a peak-shaped current increase followed by a decrease over time. It is also peculiar that the current seem to be increasing in proportion to the ochratoxin A competitor concentration instead of being inversely proportional. This indicates that the indirect competitive binding assay for ochratoxin A on the gold microelectrodes does need further characterisation of the microelectrodes and adaptation of the assay. It has also been observed that 50% of the received microelectrodes had faulty connections (as tested

with a voltameter) and as a result did not show a current signal at all. The peculiar shape of the current response upon addition of TMB/H<sub>2</sub>O<sub>2</sub> could be a result of misconnection of the microelectrodes working, counter and reference electrode.

#### 4.4.19 Preliminary direct competitive ochratoxin A immunosensor

To establish, if the direct immunoassay would work on the SPGE, a preliminary experiment was executed, where ochratoxin A antibody was immobilised on the SPGE surface via protein A. The ochratoxin A-HRP conjugate that had shown a low binding ability for the antibody in biospecific interaction analysis (Biacore) was employed for the competitive assay with ochratoxin A standards. Figure 4.34 shows the current response for a direct competitive assay on SPGE using the ochratoxin A-HRP conjugate with ochratoxin A standards.



**Figure 4.34:** Competitive response curve of current  $-\mu\text{A}$  versus ochratoxin A ( $\blacksquare$ ) concentration illustrating the current response with increasing ochratoxin A competitor [ $\mu\text{g L}^{-1}$ ] concentration on SPGE modified with protein A bound antibody. Standards are prepared in PBS, pH 7.4. The curve was fitted using a four parameter fit.

Figure 4.34 shows the range of concentration reached from  $100 \text{ ng L}^{-1}$  to  $10 \text{ mg L}^{-1}$  aim of detection of about  $2 \mu\text{g L}^{-1}$  ochratoxin A. The plot shows linearity in the range from

0.1-100  $\mu\text{g L}^{-1}$  with a lowest detectable concentration of 100  $\text{ng L}^{-1}$  ochratoxin A standard. The graph indicates that concentrations below 100  $\text{ng L}^{-1}$  could be measured sensitively and that the limit of detection is much lower. These data show that the direct format can be used on the SPGE and that the ochratoxin A-HRP conjugate does respond in an electrochemical assay when competing with ochratoxin A standards. These results can be a promising alternative to the indirect immunosensor assay.

## **4.5 Conclusions**

Cost-effective, disposable and sensitive sensors for ochratoxin A were produced by screen-printing. The initial immunosensor with ochratoxin A-BSA-adsorbed SPGEs reached a detection limit of less than 100  $\text{ng L}^{-1}$ . Further improvement was achieved when covalently immobilising ochratoxin A-BSA, and decreasing the detection limit to 10  $\text{ng L}^{-1}$ . Furthermore, the direct immunoassay format showed promising results indicating a detection limit below 100  $\text{ng L}^{-1}$ . This level of detection corresponds with the lowest level of wine contamination with ochratoxin A in Europe (0.01 – 7  $\mu\text{g L}^{-1}$ ) and outreaches the permissible limit of ochratoxin A in wine and grape containing drinks set by the European Commission ( 2  $\mu\text{g L}^{-1}$ ) as well as the desired limit of detection suggested by the GoodFood requirements.

Furthermore, each measurement takes about 200 seconds, where up to three electrodes as multiple measurement, can be monitored at the same time. The construction of each immunoassay modified electrode takes a minimum of 5 hours, including the covalent surface modification with carboxymethylated dextran, since the CMD-modified SPGEs can be produced in advance.

The screen-printed immunosensor was optimised for wine analysis, the electrochemical interferences due to phenol compounds being tackled. The solution to this problem offered in this work in order to perform accurate determinations with biosensors consisted in polarising the working electrode at -150 mV versus reference Ag/AgCl.

The developed immunosensor in the indirect format using non-modified SPGE resulted in a detection limit of 100  $\text{ng L}^{-1}$ , whereas using CMD modification of the SPGE a detection limit of 10  $\text{ng L}^{-1}$ . The non-modified SPGE method performed comparable to

a previously reported electrochemical immunosensor run with standard OTA solutions by Alarcon et al. [2006], who used monoclonal antibodies in both a direct and indirect format to determine ochratoxin A in wheat. The standard curve data of the electrochemical immunoassay resulted in a detection limit of 60 and 100 ng L<sup>-1</sup> for the direct and indirect assay format, respectively. Alarcon et al. [2004] initially had used commercially available polyclonal antibodies (Biogenesis Ltd.) in a similar assay, which had a detection limit of 180 ng L<sup>-1</sup>. The authors stated that the use of a monoclonal antibody had improved the assay performance. However, in this assay, the detection limit of 100 ng L<sup>-1</sup> was reached using polyclonal antibodies in an indirect detection format and was improved by modifying the sensor surface with carboxymethylated dextran (CMD), thereby exhibiting superior sensitivity.

Another ochratoxin A immunosensor was presented by Prieto-Simón et al. [2008], who compared polyclonal to monoclonal antibodies and also the effect of the enzyme label by studying HRP and AP-labelled secondary antibodies in an indirect assay format. They also reported better sensitivity using monoclonal antibodies confirming the statement by Alarcon et al. [2006] and the superior use of HRP-labels in electrochemical assays as electroactive interferences present in spiked wine samples did not affect HRP-labelled immunosensors, but they were likely oxidised at the working potential for AP-labelled immunosensors (0.225 V vs Ag/AgCl). The limit of detection for the HRP-labelled immunosensor was 700 ng L<sup>-1</sup> ochratoxin A (700 ng L<sup>-1</sup> using an AP-label). The results confirm that using an HRP-label will reduce interferences from electrochemical detection in wine. The group also reduced the effect of the wine pH by neutralization with buffer and removed polyphenols with PVP, which confirms the procedure used in this work, where the wine sample was diluted in carbonate buffered containing PEG to neutralize the pH and the wine was pretreated with PVPP to remove polyphenols. However, the detection limit of the work presented in this thesis is still superior to the achieved detection limit achieved by Prieto-Simón et al. [2008], which is, assumingly, entirely due to the CMD-modified SPGE. The modification with CMD will enable covalent attachment of the immunoreagents, but also enhance stability as it is known that polymers such as dextran or polyions such as PEG are used in protein stabilisation [Drago & Gibson, 2001].



The immunosensor in the indirect format using CMD modification of the SPGE exhibited superior sensitivity according to the detection limit of  $10 \text{ ng L}^{-1}$  and was then selected for the experimental work on real samples.

It has been established in Chapter 3 by surface plasmon resonance analysis that the ochratoxin A antibody was cross-reacting to a certain extent with BSA. By choosing an antibody for the immunosensor development where BSA was not used as immunogen in addition to affinity-purifying the antibody with BSA, any non-specific binding of the antibody to BSA was diminished. An in-depth literature search resulted in a novel aspect that might cause the low reproducibility of the immunoassay. Galtier *et al.* [1981] show that ochratoxin A also binds BSA non-specifically and thus affects the performance of the indirect immunosensor assay, since free ochratoxin A in solution can be adsorbed onto immobilised BSA-conjugate. This might be the reason for the low reproducibility of the SPGE immunosensor standard curve and also for the increase in current with ochratoxin A concentration determined with the microelectrodes. As ochratoxin A interacts with BSA, the toxin would also bind to the immobilised ochratoxin A-BSA conjugate instead of the antibody when using the indirect competitive format. Also, the interaction of ochratoxin A with BSA is dependent on the ionic strength of the buffer. This explains, why the results obtained with the screen-printed gold electrode immunosensor were more reproducible than with the microelectrodes, as the ochratoxin A standards used for the microelectrode standard curve were dissolved in a low ionic strength buffer. To avoid the interaction of ochratoxin A with BSA, a high ionic strength buffer can be used throughout the assay. However, the better alternative would be to remove BSA from the assay by for instance using the direct immunoassay format.

However, further optimisation of the proposed ochratoxin A immunosensor on SPGE should be carried out in order to achieve better reproducibility on SPGE. Furthermore, the preliminary result of a direct competitive immunosensor for ochratoxin A showed a detection limit of  $10 \text{ ng L}^{-1}$  and seems a promising alternative in the development of a BSA-free affinity sensor for ochratoxin A.

Microelectrode arrays as biosensor platform can monitor multiple analytes simultaneously or increase the sensitivity of single analyte analysis as the electrode array increases current density (signal). As some mycotoxins can be found alongside in the same sample matrix, a single sample deposition can be used to determine several mycotoxins quantitatively. Most mycotoxin sensor arrays are based on an immunoassay format, while using different transduction methods, whereof most are based on fluorescence determination [Prieto-Simón *et al.*, 2007]

Piermarini *et al.* [2007] describe the only electrochemical immunosensor array so far for the detection of AF B1, by using an indirect competitive immunoassay format on a 96-screen-printed electrode array format with attached 96-well microplate. The detection was carried out using an AP-labelled secondary antibody and 4-nitrophenylphosphate by intermittent pulse amperometry an applied potential of +400mV (with a pulse width of 1ms and a selected frequency of 50 Hz). AF B1 was detected in spiked corn samples at concentrations as low as 30 ng L<sup>-1</sup> allowing the measurement of multiple samples, replicates and all the corresponding controls at the same time.

Work on fluorescence sensor arrays for mycotoxins using a competitive immunoassay format with fluorescent labelled antibody were carried out comprehensive work on fluorescent biosensor arrays for mycotoxins for ochratoxin A [Ngundi *et al.*, 2005], DON [Ngundi *et al.*, 2006] and AF B1 [Sapsford *et al.*, 2006] with detection limits of ochratoxin A in several cereals ranged from 3.8 to 100 µg kg<sup>-1</sup>, while in coffee and wine, detection limits were 7 and 38 µg kg<sup>-1</sup>, respectively [Ngundi *et al.*, 2005], detection limits of deoxynivalenol ranged from 0.2 µg L<sup>-1</sup> in buffer to 50 µg kg<sup>-1</sup> in oats, and for aflatoxin B1 the detection limit in buffer was 0.3 µg L<sup>-1</sup> and increased in real samples to 1.5 and 5.1 µg kg<sup>-1</sup> (corn) and 0.6 and 1.4 µg kg<sup>-1</sup> (nuts). An SPR-based biosensor array was developed by van der Gaag *et al.* [2003] for simultaneous detection of DON, AF B<sub>1</sub>, and zearalenone, but lacked the analysis of real samples and interference analysis.

This shows that the use of microarrays for mycotoxin analysis is still in progress and the idea of an electrochemical microelectrode array is novel. The electrochemical sensor array [Piermarini *et al.*, 2007] also indicated that it is possible to achieve lower

detection limits than with fluorescence based methods. The microelectrode array in this work is preliminary used to enhance sensitivity by increased current density of the array and will evolve further into multi-mycotoxin analysis. Interference analysis and matrix effects of real samples are prioritised. The construction of a standard curve was inconclusive as the standard curve resulted in an increasing current in proportion to the ochratoxin A competitor concentration instead of being inversely proportional. This indicates that the indirect competitive binding assay for ochratoxin A on the gold microelectrodes does need further characterisation of the microelectrodes and adaptation of the assay.

## **CHAPTER 5 : COMPUTATIONAL MODELLING OF PEPTIDE RECEPTORS**

### ***5.1 Introduction***

One of nature's most important talents is evolutionary development of systems capable of distinguishing one molecule from another. Molecular recognition is the basis for most biological processes, such as ligand-receptor binding, antibody-antigen interaction or substrate-enzyme reactions, and is therefore of general interest.

To date, many analytical methods are based on biomolecular recognition elements, such as antibodies, enzymes, and protein or peptide receptors. These methods include enzyme assays and immunoassays, biosensors and various (immuno)-affinity separation techniques. Although of fundamental importance, these methods sometimes suffer from features such as low stability and reproducibility, often as a result of the implemented biomolecule.

Commercially available antibodies for ochratoxin A exist but are an expensive commodity. The production of an antibody against a small molecule is particularly difficult as small molecular weight molecules do not cause a sufficient immune response since they are not recognized as pathogens by the immune system. Antibody production can be labour-intensive, time- and cost-consuming, but is especially difficult for small molecular weight toxins such as ochratoxin A. The mycotoxin would more likely cause an acute toxic response in the boosted animal than the production of antibodies.

Therefore, one often uses carrier proteins linked with small molecular weight haptens to boost the immune response. When using toxin-protein conjugates (e.g. ochratoxin A-BSA) the concentration has to be sufficiently low, so no acute toxic effect is interfering. When using carrier proteins, the result is often a polyclonal antibody partly recognising the conjugate-structure it was raised against.

Also, common methods used in analysis such as high-performance liquid chromatography (HPLC), gas chromatography (GC), etc. require constantly new and more specific stationary phases for chromatography columns.

Thus, alternative techniques to produce new (bio)-materials for separation chemistry are therefore of great interest and value.

Peptides show advantages over other receptors, as they are known to be more stable under a wider range of physicochemical conditions (ionic strength, pH, temperature) and generally easy to synthesize.

Usually, a combinatorial approach is applied where millions of possible molecules from a library are screened to identify *in vitro* the best candidates for synthesis. The screening procedure is based on an existing library that might not contain the optimal ligand, since the produced molecular library is only containing a finite number of possibilities. The best fit (hit) can only be chosen from that confined set of molecules, which depends on the make of the library. Hence, the size of a combinatorial library is not decisive, but rather the need for more diversity within the library for a given task or problem. Therefore, a method that can screen for an infinite number of variants of peptide receptors, specific for ochratoxin A, is required.

Computational modelling can be applied for the design of peptide receptors derived from 20 standard amino acid monomers that can be combined in any possible way to built peptides displaying various lengths (dimer, trimer, oligomer, etc.) and variations into a library. From that virtual library, peptide combinations are screened for hits according to the binding energy of the interaction calculated by computational modelling algorithms. Computational modelling is a powerful tool to simulate highly specific molecular interactions cost- and time-efficiently without the need for animal recourses or bench space. Virtual peptide sequence screening showed promising results with previous designed biomimetics for small molecular weight ligands [Subrahmanyam *et al.*, 2001; Chianella *et al.*, 2002]. This work presents the design of a peptide receptor for a specific template molecule (i.e. ochratoxin A) using computer simulation technology.

## 5.2 Experimental

Molecular modelling was carried out on a Silicon Graphics (SGI) workstation running IRIX 6.6 operating system. The workstation was configured with two 195 MHz reduced instruction set processors, 712 MB memory and 12 GB fixed drive. This system was used to execute the software SYBYL 6.9.1 (Tripos Associates Inc., US).

## 5.3 Methods

Computational modelling was performed to obtain a suitable peptide receptor for the template ochratoxin A. Molecular modelling procedure was performed as follows:

- (1) Ochratoxin A structure was drawn manually using SYBYL drawing tools.
- (2) Energy minimisation generates a set of atomic coordinates which correspond to a minimum of energy to enhance the molecule geometry of ochratoxin A.
- (3) Simulated annealing searches for conformations with energies lower than the minimum of energy found by energy minimization.
- (4) LeapFrog tool designs peptide ligands for ochratoxin A by repeatedly making small structural changes and evaluating the binding energy  $E$  (kcal mol<sup>-1</sup>).
- (5) FlexiDock simulates receptor-ligand docking of LeapFrog derived sequences and their analogues.

### 5.3.1 Drawing tools

The ochratoxin molecule was drawn according to the SYBYL tutorial ‘small molecule sketching’ [Sybyl Tutorial Pages, 1999] and imported into the SYBYL program. Hydrogen atoms were added subsequently to the entire ochratoxin A structure.

### 5.3.2 Energy minimisation

The minimization tool was used to refine the molecular model of ochratoxin A. All minimisation simulations were performed using MAXIMIN2 applying the Powell method. This was conducted following the SYBYL protocol shown in Figure 5.1.

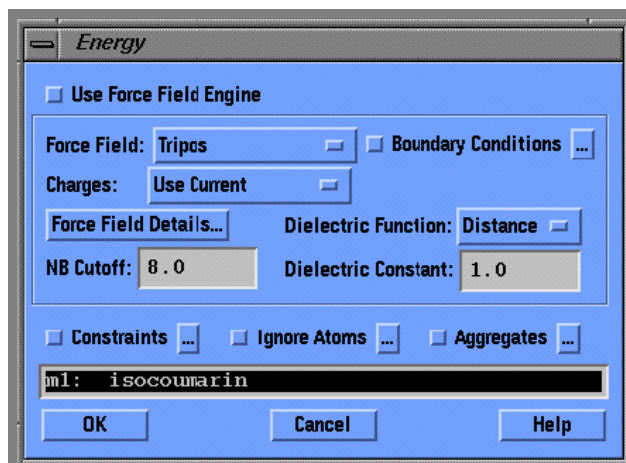


**Figure 5.1:** Setup of minimization via the SYBYL menu bar.

The Energy tool was approached via:

**Compute** >>> Minimise >>> *Modify* >>> *Energy Dialog box*

Free energy determinations should be performed with an all-atom force field that treats the aqueous environment via an explicit solvent model. The TRIPOS force field was applied for energy calculations, the utilised charges were Gasteiger-Hückel charges. The dielectric constant, which defines the screening effect on electrostatic interactions and can vary from 1 (*in vacuo*) to 80 (in water), is set to corresponded water conditions. A ‘Gradient’ with a cut-off value of  $0.001 \text{ kcal mol}^{-1}$  at a maximum of 1,000 iterations was used as summarised in Table 5.1.

**Table 5.1:** Parameters used for energy minimization.

Parameter	Value
Force field	TRIPOS
Charges	Gasteiger-Hückel
Dielectric constant	80
Termination: Gradient cut-off	$0.001 \text{ kcal mol}^{-1}$
Iterations	1000

The minimisation output consists of a report of energy, gradient, etc. for each step. The changes in molecular structure can be visualized during interactive minimisation, which is completed when the gradient reduces to the cut-off point.

### 5.3.3 Simulated annealing

In simulated annealing, as in genetic algorithms, there is a fitness function that defines a fitness landscape. Simulated annealing also adds the concept of ‘temperature’, which gradually decreases over time. At each step of the algorithm, the solution mutates (which is equivalent to moving to an adjacent point of the fitness landscape). The fitness of the new solution is then compared to the fitness of the previous solution; if it is higher, the new solution is kept. Otherwise, the algorithm makes a decision whether to keep or discard it based on temperature. If the temperature is high, as it is initially, even changes that cause significant decreases in fitness may be kept and used as the basis for the next round of the algorithm, but as temperature decreases, the algorithm becomes more and more inclined to only accept fitness-increasing changes. Finally, the temperature reaches zero and the system ‘freezes’; whatever configuration it is in at that point becomes the solution. Simulated annealing is often used for engineering design applications such as determining the physical layout of components on a computer chip [Kirkpatrick *et al.*, 1983].

The simulated annealing tool surmounts energetic barriers in a search for conformations with energies lower than the local minimum energy by simulating motions at a very high temperature, where nearly all conformations are energetically accessible. This is followed by slowly cooling down to room temperature or below. The molecule settles into a natural conformation at that temperature. This was executed following the SYBYL protocol as shown in Figure 5.2.



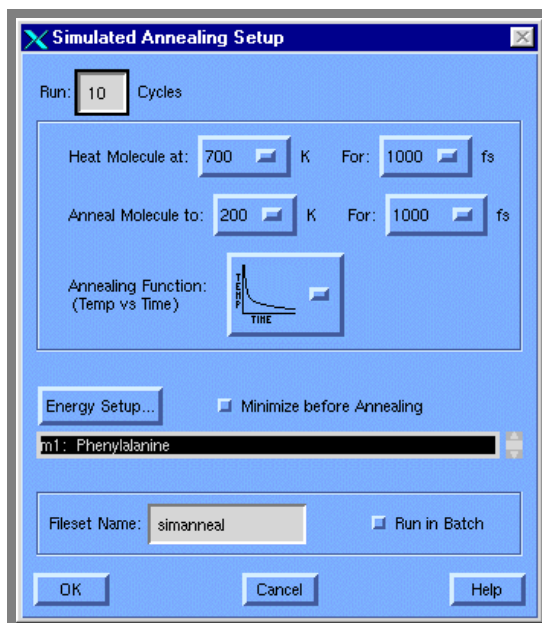


**Figure 5.2:** Setup of annealing via the SYBYL menu bar.

Parameters used to anneal the ochratoxin A structure were set according to Table 5.2. The simulated annealing setup tool was approached via:

Compute>>>Dynamics>>>Simulated Annealing dialog box

**Table 5.2:** Parameters used for simulated annealing.

Parameter	Value
RUN	10 cycles
Heat molecule at	700 K for 1000 fs
Anneal Molecule to	200K for 1000 fs

The annealing function followed a second minimization step for further structure optimization as described in Section 5.3.2.

### 5.3.4 Ligand design using LeapFrog

LeapFrog was used to screen a database of amino acid monomers for their interaction with the ochratoxin A template. Interactions predominantly take place through hydrogen-bonding and van der Waals electrostatic interactions. LeapFrog performs an evaluation of ligands (here: single and combined amino acid monomers) based on their binding score. Calculations are based on an electrostatic screening process, where LeapFrog is repetitively trying novel ligands in different positions (starting points) of

the ochratoxin A template. Depending on the calculated ochratoxin A energy, the program is adding suitable ligands to a binding score list. This procedure followed the SYBYL protocol. The LeapFrog Start-up tool was approached via:

Options >>> Tailor >>> Subject >>> **LeapFrog**

Parameters used in LeapFrog were set according to Table 5.3.

**Table 5.3:** Parameters used for LeapFrog.

Parameter	Value	
Mode	DREAM	
Move frequencies	Begin with 1000	
Input Data	Peptide	
Start with cavity molecule in M1	ON	
Calculate site points for:	ALL	Atoms
Box described by:	Corners	
Starting ligands	None	from database

The program was applied in DREAM mode for 100,000 to 1,000,000 iterations, respectively. When using a starting ligand from database, LeapFrog was started with 1,000 iterations to begin with, and then modified by adding ‘active hydrogens to the ligand’s structure for binding interaction localization.

To obtain peptide ligands, designed from only amino acid monomers, the input data was set on ‘peptide’. The program performed its calculations within a prescribed box, where the template molecule and the novel ligands are inserted to. Box dimensions (X; Y; Z) entered for a Leapfrog run is given in Table 5.4.

**Table 5.4:** LeapFrog electrostatic screening box dimensions.

<b>X</b>	-6	8
<b>Y</b>	-8	12
<b>Z</b>	-11	6

Selecting ‘Tailor’ in the LeapFrog start-up, the appearing window was set as default except for the category ‘Relative move frequencies’. The ‘Join’ parameter allows for construction of novel molecules by combining several fragments into one molecule [Boehm, 1995].

The 'Bridge' move was set to zero, since a software problem was isolated to that part by Richard Day [1999], who observed that as the amino acids were refined and joined from previous iterations, old results were not being removed and eventually all the memory of both system and virtual were being consumed. The 'Bridge' move was therefore turned off and the number of iterations doubled to allow larger fragments to grow. To enhance that feature, the 'Join' move, which joins different fragments together, was also increased. Further parameters of this category are shown in Table 5.5.

**Table 5.5:** Summary of relative move frequencies.

<b>Parameter</b>	<b>Description</b>	<b>Default</b>	<b>Modified value</b>
<b>Join</b>	Joining of different fragments	2	<b>6</b>
<b>Fuse</b>	Fuses fragments	0	0
<b>New</b>	New ligand is started by aligning fragments	5	5
<b>Fly</b>	Alternative minimum energy ligand orientations	2	2
<b>Twist</b>	Conventional minimizing	2	2
<b>Refine</b>	Improves newly found ligand	2	2
<b>Bridge</b>	Considers all fragments as bridges	2	<b>0</b>
<b>Complement</b>	Chooses moiety complementary to a cavity group as a ligand	2	2
<b>Save</b>	Saves ligands that match requirements	2	2
<b>Weed</b>	Discards the worst ligands except the top 10	0	0
<b>Crossover</b>	Generates best hybridizations among similar molecules	0	0
<b>Prune</b>	Can delete moieties of a known ligand on the basis of their energy with the receptor	0	0

The LeapFrog results for the binding scores from each run are listed. The ligands given the highest binding score (lowest binding energy) were assumed to represent the best fitting peptide ligands for ochratoxin A. The virtual peptide library database is generally stored as SLN-file. SYBYL Line Notion (SLN) is an ASCII language used to represent chemical structures, including common organic molecules, macromolecules, polymers, and combinatorial libraries. SLN is also used to express substructural (2D) queries [Ash *et al.*, 1997].

### 5.3.5 Receptor-ligand docking using FlexiDock

FlexiDock is a genetic algorithm for receptor-ligand docking. It is designed to dock a number of ligands into a receptor molecule cavity such as an enzyme macromolecule. In this application, FlexiDock is used to dock a number of LeapFrog designed peptide receptors around the ligand molecule ochratoxin A.

Effectively, the terms ligand and receptor are reversed in that context. The following docking protocol is adapted from the Tripos Bookshelf 7.2 FlexiDock™ Manual.

FlexiDock allows to "recycle" a molecular (ochratoxin A ligand) definition so that a variety of peptide receptor molecules can be investigated at once. A selection of lead sequences of the virtual database of peptide receptors designed from LeapFrog is assembled in one database file. Then, the ochratoxin A ligand file is loaded and prepared as follows:

- Empty the binding pocket: remove any existing ligand.
- Check all atom types (energy calculations are based on atom types, therefore it is important to verify that these have been assigned correctly by SYBYL)
- Removal off all water molecules (deletion of crystal water), keeping only those that may contribute to the interactions between the ligand and receptor.
- Adding hydrogens and charges (AMBER charges for ochratoxin A and Gasteiger-Hückel charges for the peptide receptors)
- Definition of ochratoxin A table bonds
- Mark the hydrogen bonding sites
- Pre-position the ligand in a virtual cavity

For each peptide receptor:

- Load the molecule into a second molecule area and prepare it.
- Add all hydrogens.
- Compute atomic charges.
- Define the ochratoxin A table bonds ( to simply define all ligand bonds as ochratoxin A table)
- Mark the hydrogen bonding sites.
- Manually position the peptide receptor in the ochratoxin A cavity.

Run FlexiDock on the entire set:

**Compute >>> FlexiDock >>> Run Existing Input Files...**

The results of the FlexiDock run are stored in the SYBYL database (e.g.: file.mdb). The resulting spreadsheet includes a column; titled 'Energy' and containing the FlexiDock score for the saved solution.

## 5.4 Results and Discussion

### 5.4.1 Minimisation and annealing

The ochratoxin A structure (Figure 5.3) was drawn from the scratch using SYBYL ‘DRAW’. In this context the ochratoxin A structure is referred to as template or as ligand, whereas the derived peptide structures are referred to as receptors.

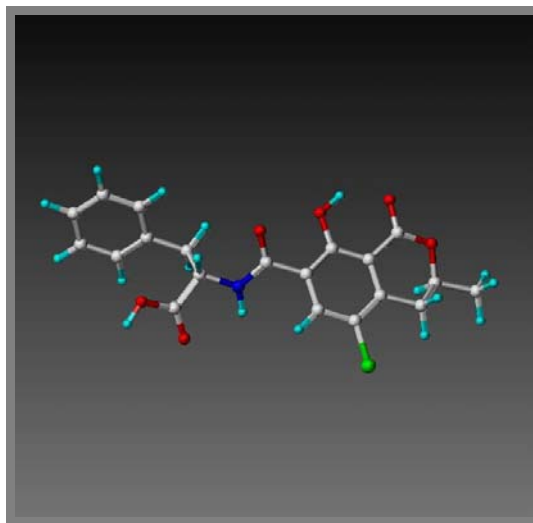


**Figure 5.3:** Minimised and annealed structure of the ochratoxin A template (shown in stick and ball).

The ochratoxin A structure was minimised, annealed and then minimised again before running the *de novo* design tool LeapFrog. Table 5.6 summarises the results of a minimization procedure for ochratoxin A, before as well as after annealing.

**Table 5.6:** Minimisation of ochratoxin A structure.

<b>Energy contribution</b>	<b>Energy [kcal mol<sup>-1</sup>]</b>
Bond stretching energy	0.526
Angle bending energy	2.233
Torsional energy	5.551
Out of plane bending energy	0.053
1-4 van der Waals energy	4.167
Van der Waals energy	-4.004
1-4 electrostatic energy	-7.855
Electrostatic energy	-5.239
<b>Ochratoxin A energy [kcal mol<sup>-1</sup>]</b>	<b>-4.569</b>

The various energy contributions that make up the overall molecular energy of ochratoxin A are listed in Table 5.6. The energies were obtained by minimising the structure (Figure 5.3) of ochratoxin A. The total energy outcome of the minimised ochratoxin A structure was  $-4.569 \text{ kcal mol}^{-1}$ . Minimisation was followed by annealing and another step of minimisation to for further optimisation of the ochratoxin A structure. The values for the energy minimisation before and after annealing vary considerably; the energy of the molecule is increased after annealing.

#### 5.4.2 Leapfrog assisted design using ochratoxin A

The *de novo* design of ligands was performed using LeapFrog, where the ochratoxin A template is initially subjected to a procedure called electrostatic screening (Figure 5.4). LeapFrog proposed novel peptide structures after about 1,000,000 iterations of trial.

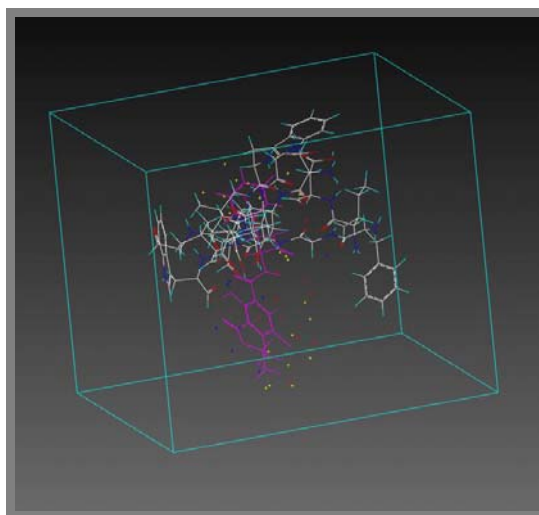


**Figure 5.4:** Electrostatic screening of the ochratoxin A template (seen in purple). Coloured dots are depicting the sites of interaction tried by the LeapFrog tool.

LeapFrog stored its best scoring results in a spreadsheet for further evaluation. The binding score, assumed to be directly related to the ochratoxin A binding energy of the binding interaction, was shown in  $\text{kcal mol}^{-1}$ .

A LeapFrog run was setup according to the protocol in Section 5.3.4. The binding energy of every single amino acid with ochratoxin A was assessed and should indicate the characteristics of each amino acid monomer in relation to ochratoxin A interaction.

The binding energies and corresponding polarity of each applied amino acid is shown in Table 5.7. The lowest binding energy is ascending which describes the binding energy for the most likely binding interaction with ochratoxin A.

**Table 5.7:** Binding energies for all 21 amino acids with ochratoxin A.

No.	Amino acid	Polarity	Binding energy [kcal mol <sup>-1</sup> ]
1	Phenylalanine (Phe)	Apolar	-33.52
2	Proline (Pro)	Apolar	-32.10
3	Valine (Val)	Apolar	-30.93
4	Isoleucine (Ile)	Apolar	-30.37
5	Leucine (Leu)	Apolar	-28.94
6	Cysteine (Cys)	Polar (non-charged)	-28.67
7	Tyrosine (Tyr)	Polar (non-charged)	-27.29
8	Methionine (Met)	Apolar	-26.33
9	Threonine (Thr)	Polar (non-charged)	-25.55
10	Tryptophan (Trp)	Apolar	-22.71
11	Alanine (Ala)	Apolar	-21.87
12	Glutamate (Glu)	Polar (negatively charged)	-20.63
13	Aspartate (Asp)	Polar (negatively charged)	-19.86
14	Asparagine (Asn)	Polar (non-charged)	-13.27
15	Lysine (Lys)	Polar (positively charged)	-11.72
16	Histidine (His)	Polar (positively charged)	-10.06
17	Glutamine (Gln)	Polar (non-charged)	-6.43
18	Arginine (Arg)	Polar (positively charged)	-5.65
19	Serine (Ser)	Polar (non-charged)	-5.23
20	Glycine (Gly)	Polar (non-charged)	-1.89

As listed in Table 5.7, the five best scoring amino acids interacting with ochratoxin A have an apolar side chain and exhibit a hydrophobic character (Phe; Pro; Val; Ile; Leu). The highest binding score was seen with Phenylalanine that contains a water-insoluble aromatic ring, which is insofar interesting, since the ochratoxin A structure contains an L- $\beta$ -phenylalanine moiety as well.

The second best binding score showed Proline (cyclic amino acid) and followed by Valine, Leucine and Isoleucine that have all aliphatic acyclic residual groups (Figure 5.5).



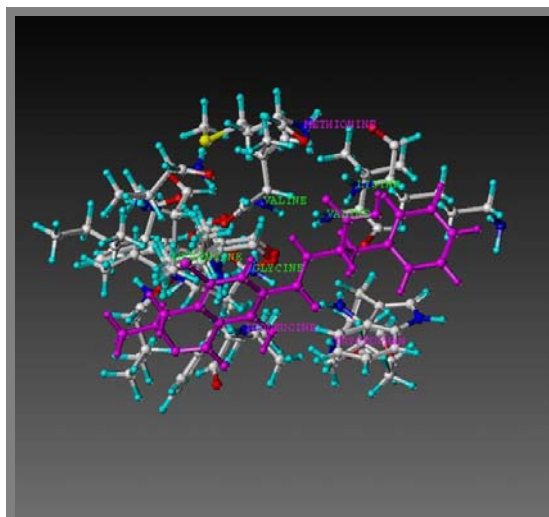


**Figure 5.5:** Ochratoxin A template (seen in purple) interacting with distinct amino acids (from left to right: isoleucine, valine, glycine, methionine, lysine and tryptophan).

The lowest binding scores were obtained by polar (charged and non-charged) amino acids (Figure 5.5) that are relatively hydrophilic due to the polar functional groups in their side chains. The lowest binding score showed Glycine, which has as side chain a hydrogen atom that has no effect on the hydrophilic character of the amino acid. These findings confirm the hydrophobicity of ochratoxin A and the likelihood of establishing hydrophobic interactions.

### 5.4.3 *De novo* designed peptides

The *de novo* design of peptide receptors was facilitated using LeapFrog in DREAM-mode, by directly proposing new lead compounds by trying all 20 amino acids listed in Table 5.7. The best interacting peptide sequences regarding binding energy and H-bonding are shown in Table 5.8.

**Table 5.8:** Binding energy and corresponding H-bonds highest scoring peptide sequences interacting with ochratoxin A generated from LeapFrog.

No.	Peptide	Sequence	H-bonds	Binding energy [kcal mol <sup>-1</sup> ]
1	Tripeptide	Ile-Gly-Ala	4	-44.55
2	Tetrapeptide	Ile-Gly-Ala-Pro	3	-44.54
3	Tetrapeptide	Ile-Gly-Ala-Gly	5	-40.05
4	Tetrapeptide	Ile-Gly-Ala-Cys	5	-38.56
5	Pentapeptide	Ile-Gly-Ala-Pro-Ala	5	-37.47

As shown in Table 5.8, the highest scoring peptide sequence was a tripeptide, which formed three H-bonds with ochratoxin A. This peptide contains two apolar (Ile and Ala) and one non-charged polar amino acid, which can act as spacer. The second best sequence was a tetrapeptide which differed in just one amino acid from the lead compound, which is Proline, another apolar amino acid.

The main assumption made from the results is that mainly apolar or non-charged amino acids are combined to a peptide sequence that is able to interact with ochratoxin A. This confirms the data obtained with single amino acid monomers shown in Table 5.7, which indicated high binding affinities for apolar amino acid monomers. Therefore, the interactions of the peptide sequence with ochratoxin A is most likely based on hydrophobic interactions. Interestingly, the number of hydrogen bonds does not seem to be directly proportional to the binding score.

The two highest scoring peptides interacting with ochratoxin A are shown in Figure 5.6.

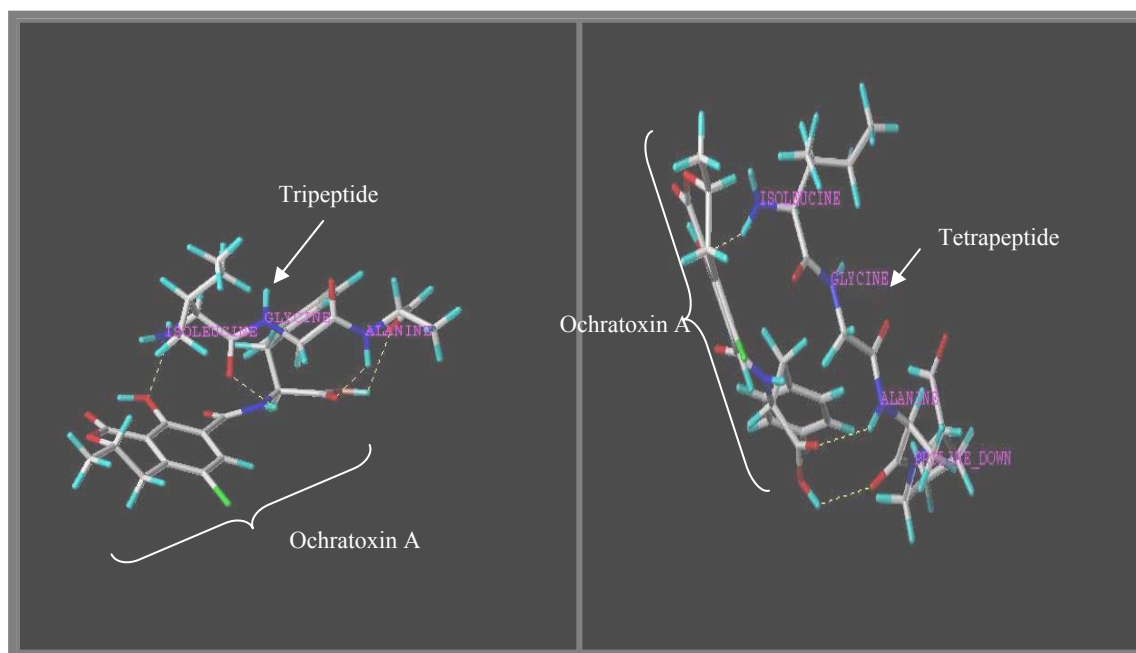


**Figure 5.6:** Left: Ochratoxin A with tripeptide (from left to right: Ile-Gly-Ala) linked via 4 H-bonds. Binding energy:  $-44.55 \text{ kcal mol}^{-1}$ . Right: ochratoxin A with tetrapeptide (from top to bottom: Ile-Gly-Ala-Pro) linked via 3 H-bonds Binding energy:  $-44.54 \text{ kcal mol}^{-1}$ .

Figure 5.6 shows that the tripeptide (left) is mainly building H-bonds with the L- $\beta$ -phenylalanine moiety of ochratoxin A. Alanine is building 2 H-bonds and Isoleucine one H-bond with the L- $\beta$ -phenylalanine moiety, whereas Isoleucine establishes another H-bond with the OH-residue of the 3,4-dihydro-3-methyl-isocoumarin part of ochratoxin A. Glycine doesn't seem to interact at all and is probably used as a spacer monomer for stabilisation. This is confirmed in the tetrapeptide structure in Figure 5.6 (right), where both Alanine and Proline establishing one H-bond each with the L- $\beta$ -phenylalanine moiety and Isoleucine one with the OH-residue of the isocoumarin moiety.

Therefore, the main interaction of the peptides seems to be localised on the L- $\beta$ -phenylalanine part of ochratoxin A based on hydrophobic interaction of mainly apolar amino acids. The sequence Ile-Gly-Ala was repeated throughout the first five lead compounds and was involved in the majority of H-bond interactions with ochratoxin A (Table 5.8). The termini of the tetramer and pentamer sequences differed in one or two amino acids such as Glycine, Cystein or Proline with Alanine, which established a fifth H-bond with ochratoxin A (Table 5.8).

#### **5.4.4 *De novo* peptide design using a starting molecule**

To optimize specificity of the binding interaction, lead sequences were implemented in the electrostatic screening process to give LeapFrog a starting point of existing H-bond-based interactions, from where it could expand the given peptide receptors with further amino acid monomers to obtain a longer, more specific sequence (lower binding energy).

LeapFrog was setup with the tripeptide and tetrapeptide chosen from Table 5.8 as starting molecules around the ochratoxin A template. Table 5.9 below shows the results of LeapFrog run applying starting molecules.

**Table 5.9:** Binding energy and corresponding H-bonds of lead peptide sequences interacting with ochratoxin A generated from LeapFrog using starting ligands.

No.	Starting ligand	Resulting Peptide	H-bonds	Binding energy [kcal mol <sup>-1</sup> ]
1	Ile-Gly-Ala	Ile-Ser-Pro	4	-38.34
2	Ile-Gly-Ala-Pro	Ile-Ser-Gly	4	-35.56

Only the two highest scoring peptide sequences are shown in Table 5.9. The resulting lead sequences were both tripeptides, which each formed 4 hydrogen-bonds with ochratoxin A. One tripeptide contained two apolar (Ile and Pro) and one non-charged polar (Serine) amino acid. The other sequence differed from the first one in just one amino acid that is a Glycine instead of the Proline. Again, mainly apolar or non-charged amino acids were combined to a peptide sequence.

The two lead peptides, interacting with ochratoxin A, are shown in Figure 5.7.

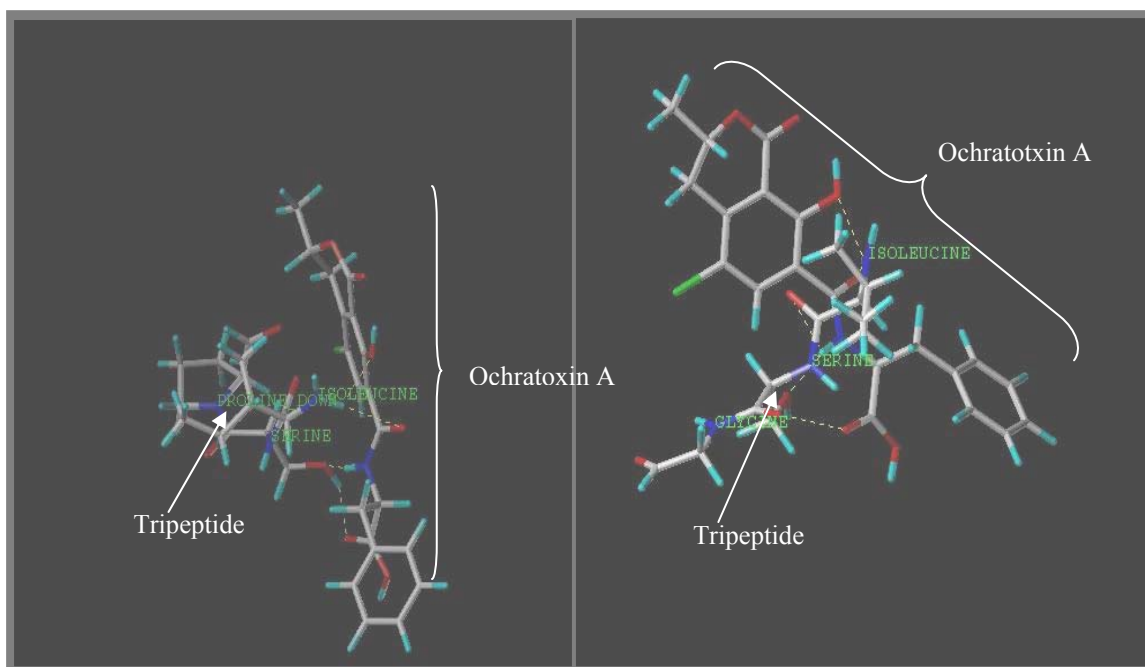


**Figure 5.7:** Peptide interaction with ochratoxin A, applying a starting ligand. Left: Ochratoxin A with tripeptide (from left to right: Pro-Ser-Ile) linked via 4 H-bonds. Binding energy:  $-38.34 \text{ kcal mol}^{-1}$ . Right: Ochratoxin A with tripeptide (from left to right: Gly-Ser-Ile) linked via 4 H-bonds. Binding energy:  $-35.56 \text{ kcal mol}^{-1}$ .

Figure 5.7 shows that one tripeptide (left) is building hydrogen bonds with ochratoxin A mainly via the amino acids Serine and Isoleucine. The residual OH-group and the NH-group of ochratoxin A's phenylalanine moiety are part of the hydrogen-bonding. The same functional groups of ochratoxin A are interacting with the amino acids of the second tripeptide, which are Isoleucine, Serine, and Glycine. The hydrogen-bonding of this modelling experiment, using starting molecules, seemed to distribute the interactions between the *de novo* designed receptor and ochratoxin A over the entire structure.

However, the resulting lead sequences shown in Table 5.9 are both very short sequences (tripeptides) with a higher binding energy than the initially obtained sequences (Table 5.8) when no starting molecule was used. Therefore, the approach of using a starting ligand to enhance specificity of the peptides was discarded.

### 5.4.5 Screening the peptide receptor library

To obtain longer peptide sequences and thus higher specificity (lower binding energy), the ‘Tailor’ option in the LeapFrog start-up was modified in the category ‘Relative move frequencies’ in its ‘join’ and ‘bridge’ parameters (see Section 5.3.4, Table 5.5). The ‘Tailor’ option allows LeapFrog to combine amino acids into short peptide sequences of 3-6 amino acids in length. By increasing the parameter ‘join’ and setting the ‘bridge’ function to zero, LeapFrog should increase the length of peptide fragments to be joined. High scoring peptide sequences interacting with the ochratoxin A template are shown in Table 5.10.

**Table 5.10:** Binding energies for the highest scoring peptide sequences.

No.	Amino acid sequence	Binding energy [kcal mol <sup>-1</sup> ]
1	Pro-Ser-Ile-Val-Glu	-46.45
2	Ile-Gly-Ala	-44.55
3	Ile-Gly-Ala-Pro	-44.54
4	Cys-Ser-Ile-Val-Glu	-42.13
5	Ile-Gly-Ala-Pro-Ala	-37.47
6	Cys-Gly-Pro-Ala-Gly-Ile	-31.85
7	Ser-Pro-Ala-Gly-Ile	-31.56

The highest scoring peptide sequences contained repetitively the amino acids Isoleucine, Glycine, Alanine and Proline as well as Valine and Glutamate. The introduction of Proline, Valine and Leucine in the peptide sequences was expected since those amino acid monomers resulted in high binding scores when modelling the amino acid monomer interactions with ochratoxin A. Alanine and Glutamate had shown medium binding interaction and Glycine has the highest binding energy and therefore the lowest binding score (Table 5.7) and is possibly not involved in any hydrogen bonding. The majority of these amino acids are apolar, which means they are difficult to dissolve in aqueous solution.

### 5.4.6 Docking simulation for lead sequence selection

By modelling the dynamics of the peptide-ochratoxin A interaction, the flexibility of the modelled sequences binding to ochratoxin A is characterised. High scoring peptides designed with LeapFrog were screened using FlexiDock, which assumes high flexibility

of the peptide around ochratoxin A. The simulation was performed using selected peptides and manually modified sequence analogues containing negatively charged amino acids such as Aspartate and Glutamate, as well as positively charged Lysine and polar (non-charged) Serine that were introduced at random positions into the sequences to improve hydrophilicity.

The final peptide design from FlexiDock contained a LeapFrog-derived peptide sequence and was terminally functionalized with a Cysteine residue to facilitate immobilisation procedures in binding assays. The final peptide sequences screened by Flexidock and corresponding binding energies are shown in Table 5.11.

**Table 5.11:** List of 11 highest ranking peptides screened with FlexiDock shown in descending order

No.	Peptide sequence	Binding energy [kcal mol <sup>-1</sup> ]	Acidic (-1) /basic(+1) rating
1	Gly-Pro-Ser-Ile-Val-Glu-Cys	-17.24	-1
2	Pro-Ser-Ile-Val-Glu-Pro-Ser-Ile-Val-Glu-Cys	-16.72	-1 -1
3	Ser-Pro-Ala-Gly-Ile	-16.07	/
4	<b>Cys-Ser-Ile-Val-Glu-Asp-Gly-Lys</b>	<b>-14.90</b>	<b>-1+1</b>
5	Cys-Gln-Ile-Val-Glu-Pro-Gln-Ile-Val-Glu	-14.63	-1 -1
6	Cys-Phe-Asp-Pro-Ala-Gly-Ile-Lys	-14.25	-1 +1
7	Cys-Phe-Asp-Ala-Pro-Ala-Gly-Ile-Lys	-13.08	-1 +1
8	Pro-Ser-Ile-Val-Glu	-12.48	-1
9	<b>Gly-Pro-Ala-Gly-Ile-Asp-Gly-Pro-Ala-Gly-Ile-Arg-Cys</b>	<b>-11.81</b>	<b>-1</b>
10	Gly-Ser-Pro-Ala-Gly-Ile-Gly	-11.78	/
11	Cys-Gly-Pro-Ala-Gly-Ile	-8.72	/

The binding energy values in Table 5.11 are similar to LeapFrog generated energy values in that large, negative binding energy is indicating a high score. However, these values are not identical to what would be obtained using the Tripos force field because different force field terms are used and a site-point matching score was included in the FlexiDock calculation. Table 5.11 lists the sequences that showed the lowest binding energy resulting from docking simulations with FlexiDock. Reoccurring sequences can be found in the highest scoring peptides such as the sequences Cys-Gly-Pro-Ala-Gly-Ile (6), Ser-Pro-Ala-Gly-Ile (7), and Pro-Ser-Ile-Val-Glu (1) derived from Table 5.10.

Other short sequences such as Pro-Ala-Gly-Ile (Table 5.8) have been implemented into several peptides.

Relating hydrogen bonding to binding energy, it was shown that corresponding to the chemical environment the strength of hydrogen bonds can vary from 2 kJ/mol (0.5 kcal/mol) to 15 kJ/mol (3.6 kcal/mol), in extreme cases up to 42 kJ/mol (10 kcal/mol). Hence, an average value may not always be representative, especially in multiple hydrogen bonded systems [Boehm *et al.*, 1996]. The designed peptides are multiple hydrogen-bonded systems of an average of 4-5 hydrogen bonds per peptide receptor molecule. Thus, assuming a number of 4-5 H-bonds should result in a range of average binding energies of 2 to 14.4 kcal/mol for 4 H-bonds and 2.5-18 kcal/mol for 5 H-bonds. The displayed binding energies in Table 5.11 vary between 8 and 18 kcal/mol which is within the theoretical range. Therefore, all of the listed peptide receptors are within the acceptable range of binding energies and can be considered as lead peptide to be synthesized. Considering solubility and ease of synthesis [Patel, 2005] as well as probability of binding interaction in an *in vitro* environment [Tame, 1999], two peptide sequences were chosen for synthesis (Figure 5.8).

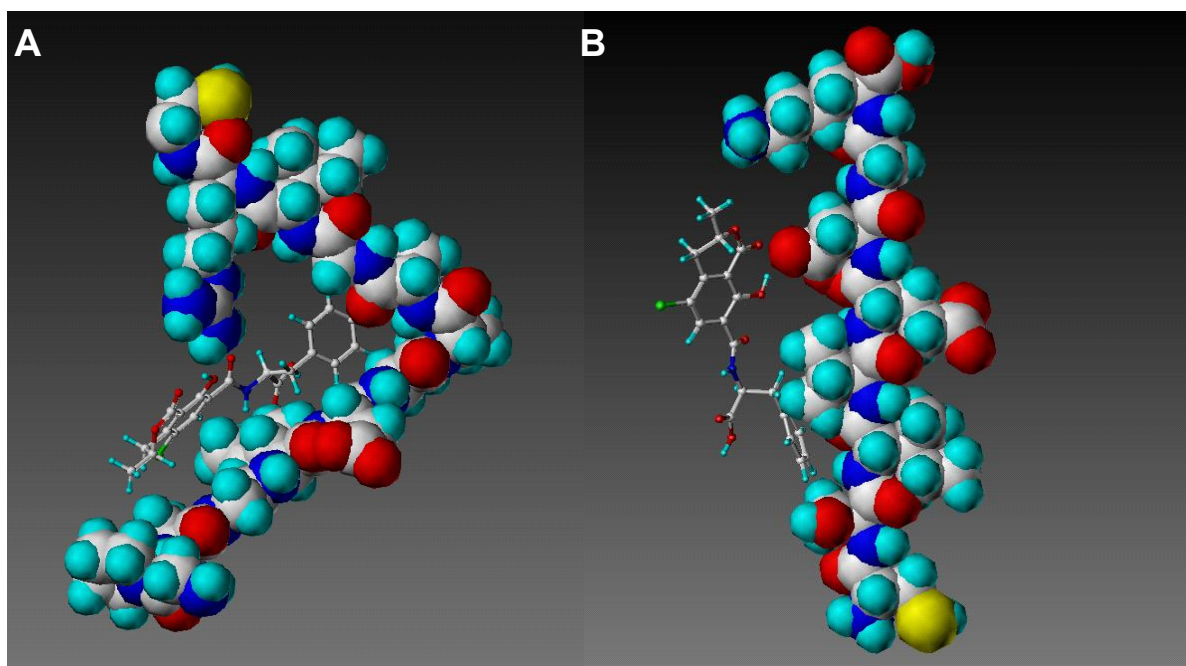


**Figure 5.8:** Final result of de novo designed peptide sequences shown interacting with ochratoxin A. The 13-mer peptide (A, left) and the octapeptide (B, right) sequence are seen as space-filled, ochratoxin A as stick & ball structures.



A 13-mer peptide with the sequence **NH<sub>2</sub>-Gly-Pro-Ala-Gly-Ile-Asp-Gly-Pro-Ala-Gly-Ile-Arg-Cys-COOH** (Figure 5.8, A), which was derived from the basic sequence [PAGI] (Table 5.8), combined into a dimeric molecule that is separated by negatively charged Aspartate and Glycine, where the latter was also incorporated as N-terminal cap. The C-terminal end of the sequence was modified by positively charged Arginine and Cysteine for immobilisation purposes. The second peptide is an octapeptide with the sequence **COOH-Cys-Ser-Ile-Val-Glu-Asp-Gly-Leu-NH<sub>2</sub>** (Figure 5.8, B) with an introduced negatively charged amino acid Aspartate and a C-terminal Cysteine residue. The sequence of the octamer (Table 5.11) was further modified post-simulation by using Leucine instead of Lysine as N-terminal amino acid was chosen with the intent to avoid an accumulation of basic pH at the peptide's N-terminal end. The molecular weight of the peptides was determined by mass spectroscopy. The 13-mer peptide (Appendix 2) has an average molecular mass of 1183.47 and the octapeptide (Appendix 3) of 856.64 m/z.

Table 5.11 also lists a simplified acidity/basic rating, since the pH is an important issue for the charge of the peptide in solution. Changes in the pH value can cause the protonation or deprotonation of the interaction partners and result in different interaction patterns [Krovat *et al.*, 2005]. A rule of thumb in determining peptide pH is the following: Arg, Lys, His and N-terminal -NH<sub>2</sub> all contribute to the basic pH of a peptide. Asp, Glu and a C-terminal COOH-(carboxy) group contribute to the peptide's acidity. Assigning +1 values to basic residues (including CONH<sub>2</sub>) and -1 values to acidic residues (including C-COOH) within the peptide will yield an overall acidic/basic rating [Globalpeptide, 2007]. The overall acidic/basic rating is described in Table 5.11 for all high scoring peptide sequences derived from FlexiDock. One lead sequence selection criteria was to adjust the peptide pH as closely to the sample pH it is destined for. Since the sample matrix is wine in this study, the pH has to be considered. Table wines generally have a pH between 3.3 and 3.7 [Pandell, 1999], therefore, a slightly acidic or neutral peptide structure is favourable since it would be probably more stable in acidic solution.

A critical issue is the multi-factorial dependence of docking results. Much effort has been devoted to investigate how and to what extend, the outcome and accuracy of a

docking approach is influenced by different parameters. Aside from docking simulation algorithm and scoring function, binding-site definitions (electrostatic screening) are decisive [Schulz-Gasch & Stahl, 2005]. Also the nature of the molecular target, the properties of the binding site as well as (bio)-molecule flexibility were found to influence docking reliability [Kontoyianni *et al.*, 2004]. Using FlexiDock tool, to simulate docking of a binding site “around” a ligand as opposed to modeling a ligand “into” a binding pocket, one can only assume that this might have a vast influence on docking results. Furthermore, both the molecular template and receptor structure (i.e. molecular weight) and the manual binding-site definition via the selection of hydrogen-bonds are defining parameters that can influence the outcome of the docking results. Therefore this is a biased docking solution toward formation of hydrogen bonds by marking H-bond donor and acceptor sites on the peptide receptor and ochratoxin A.

As our peptide synthesis facilities were outdated we opted to use outside facilities to synthesise the peptides. The peptide structures were chemically synthesized by The Medical Research Council (MRC) at Imperial College, London. The synthesized peptides were then subjected to *in vitro* affinity characterisation with ochratoxin A to establish the suitability of the peptide sequences as recognition layer in the proposed biosensor application.

## **5.5 Concluding Remarks**

The initial argument of the approach to simulate nature’s evolution to *de novo* design a receptor for a small molecular weight toxin still holds up. The advantages of designing a receptor for ochratoxin A *in silico*, and therefore being able to neither use animal resources nor being directly subjected to ochratoxin A is advantageous. However, one has to review if such an attempt is possible with today’s technology. This work’s results illustrate the design and synthesis of a small peptide receptor for ochratoxin A using *de novo* design software.

In the process, it was confirmed that the *de novo* design tool LeapFrog can be used to produce a virtual library of peptide receptors for ochratoxin A and also screen this library using binding energy algorithms to produce a hit-list of lead peptide sequences.

From the hit-list, a manual selection of a lead sequence was necessary, being subject to correct interpretation of parameters such as H-bonds being part of the interaction. First of all, it has to be mentioned that LeapFrog can be used for the design of relatively small peptide receptors for small molecular weight ligands even though its primary application is the design of molecules into binding pockets of macromolecules like enzymes. However, the lack of background information sources (published literature on the software) supplied with LeapFrog was decimating the possibilities of modifying binding interaction parameters for applications like the peptide receptor design for small molecules. Also, the screening of the LeapFrog-generated library was limited by the lack of structure-activity/ -function simulations.

The applied program FlexiDock, part of the LeapFrog software, can be used for a rough simulation of receptor-ligand docking. However, the application is based on simple parameters and one cannot be sure that it simulates the 'real' nature of the molecular interactions, for example the simulation is subject to selecting the interaction sites for H-bonding manually. In addition to that, the manual extension of the peptide sequence with charged amino acids or with a Cysteine-tag might have an effect on the affinity of the interaction, since it is well known that the interchange of only one charge in an amino acid sequence can have an immense effect on the activity of the molecule, which is not sufficiently characterised using FlexiDock simulations.

Modelling parameters are of critical importance in determining the types of intermolecular forces that underly ligand-receptor interaction. The three major types of parameters that were initially suggested are electronic, hydrophobic, and steric in nature [Hansch *et al.*, 1964 & Hansch, 1969]. Extensive studies using electronic parameters reveal that electronic attributes of molecules are closely related to their chemical reactivities and biological activities.

Thus, molecular interactions have an impact on the receptor-ligand interaction and therefore the affinity of the complex formation and dissociation. It is crucial to determine those parameters carefully to completely understand the extensiveness of molecular interactions and thus being able to simulate the structure-activity function *in silico*. Therefore, one cannot presume a 100% accurate result using FlexiDock. The

binding affinity of the interaction is to be confirmed *in vitro* using solid-state peptide assays and real-time monitoring of the binding interaction with the SPR biosensor Biacore.

Generally, the *de novo* design of biomolecules, particularly receptors for small ligands, using computational modelling is still a sporadic discipline. *De novo* design software problems are approached from different points of view, with different methods and different purposes: such as the optimal estimation of binding energies by either QSAR, empirical energy functions or free energy calculations based on molecular dynamics simulations and relative energies versus absolute enthalpies calculations in the determination of binding affinity.

The specific purpose of the ideal computational model should be a systematic generation and high throughput screen of large molecule libraries for the establishment of inter- and intra-molecular interaction parameters, kinetics and affinity and structure-activity relationships. In the absence of such conglomeration, the state of the art in *de novo* drug design and binding interaction prediction can be summarized by saying that we are still at the stage of exploration and data collection.

So far computer-assisted molecular design (CAMD) cannot substitute for a clear understanding of the biological system being studied. Ideally, one would have 3-dimensional structural information for the peptide receptor and the ochratoxin A-receptor complex from X-ray diffraction or NMR. Ongoing research in receptor design and structure-function studies as well as the introduction of small molecular weight templates are well underway and molecular dynamics simulation techniques will guide computational chemists to real predictions of binding affinities of receptor-ligand interactions without them having to synthesize the molecule.

## CHAPTER 6 : SURFACE PLASMON RESONANCE ANALYSIS OF PEPTIDE RECEPTORS

### 6.1 Introduction

Computational modelling simulates the chemico-physical behaviour of molecular structures using quantum equations and classical physics by generating and representing them numerically. The technique has been successfully used to gain a selection of synthetic receptors based on peptide molecules (Chapter 5). The peptide receptor design for small molecular weight toxins such as ochratoxin A is a completely new approach. To assess the binding interaction of the newly designed peptides with ochratoxin A *in vitro*, binding interaction analysis was performed using solid phase assays and a surface plasmon resonance-based technique (Biacore). Sensors using surface plasmon resonance (SPR) for binding interaction studies have been reviewed by Homola *et al.* [1999]. The SPR biosensor Biacore has been successfully applied for multiple-mycotoxin analysis and was described by van der Gaag *et al.* [2003]. In this work, the peptides were initially characterised on solid phase assays to assess whether they show any binding for ochratoxin A *in vitro*. An extended study was performed using the SPR (Biacore) technique to investigate kinetic and affinity of the binding interaction.

### 6.2 Experimental

The ochratoxin A-BSA conjugate, N-Succinimidyl 3-(2-pyridyldithio) propionate (SPDP) and cysteine was purchased from Sigma Aldrich Ltd. (UK). Acetate buffer and Glycine was from Fluka (UK). The CM5 sensor chips, HEPES buffered saline (HBS-EP), 1M ethanolamine-HCl, EDC (N-(3-dimethylaminopropyl)-N'-ethylcarbodiimide) and NHS (N-hydroxysuccinimide) as well as the BIAcore 3000™ instrument used for the analysis were from BIAcore AB (GE Healthcare, Uppsala, Sweden). The ready-made TMB (3,3',5,5'-tetramethylbenzidine) solution was from Europa Bioproducts Ltd. (UK). Peptides have been synthesized and analysed with mass spectroscopy by the Medical Research Council (MRC) at Imperial College, London.

## 6.3 Methods

### 6.3.1 Solid phase binding assay of peptide-ochratoxin A interaction

This assay formats involve the immobilisation of the peptide receptor molecule. The immobilisation of small molecules, such as the peptide receptors presented here, is more cumbersome since small peptides do not offer as many potential attachment sites. Therefore, the optimal immobilisation technique has to be characterised. Generally, it is recommended to covalently immobilise peptides via reactive amines-, thiol- or carboxyl-groups and using site-directed immobilisation technique is considered to enhance the orientation of peptides [Hermanson, 1992]. Therefore, two immobilisation strategies were employed to test the initial binding of the peptides. One is based on the common amine coupling approach that couples primary and secondary amine groups to carboxy groups. Thiol coupling specifically targets the terminal cysteine-tag (sulfhydryl group) attached to each synthetic peptide and allows site-directed attachment.

The peptide binding assay is performed in a direct binding format; with the peptide being immobilised and using the ochratoxin A-HRP conjugate as label as the peptides are not labelled themselves. The activity of the ochratoxin A-HRP conjugate has been confirmed in Chapter 2 (Section 2.48) and its specificity, even though very low affinity has been shown applying biospecific interaction analysis in Chapter 3 (Section 3.4.3.3). Both peptides were coupled to secondary amine ( $R_2NH$ )-activated polystyrene wells of a micro titre plate. Amine coupling was performed using NHS and EDC as linker and the thiol coupling using SPDP, a heterobifunctional cross-linking reagent with amine and sulfhydryl reactivity. Thiol coupling was used to investigate whether site-directed immobilisation would result in better sensitivity.

Amine coupling was performed by incubating  $100 \mu\text{g ml}^{-1}$  of each peptide solution in 10 mM carbonate buffer pH 9.6 on the NH-plate for 30 minutes. Then, 200 mM EDC and 50 mM NHS was added to the peptide and further incubated for one hour. The plates were washed using PBST and blocked using 0.1 M ethanolamine for 30 minutes. A range of ochratoxin A-HRP dilutions was added to the immobilised peptides and incubated for 2 hours. All incubations were performed at room temperature. The zero

reference was determined with HRP alone. The detection was performed with the chromogen TMB in ready-made solution containing hydrogen peroxide. The absorbance was read after 20 minutes at 450 nm.

Thiol coupling was performed via the immobilisation of 1.5 mg ml<sup>-1</sup> SPDP in phosphate buffer (PBS) pH 7.4 incubated 30 minutes at room temperature. The peptides were added at 100 µg ml<sup>-1</sup> in a phosphate buffer pH 8.0 and incubated for another two hours at room temperature. The plates were washed using PBST and blocked for one hour using 1 mg ml<sup>-1</sup> cysteine in 1 M NaCl and 0.1 M sodium acetate, pH 4.0. The binding was determined by adding varying ochratoxin A-HRP conjugate dilutions in phosphate buffer pH 7.4 to the immobilised peptides and incubate for 1.5 hours. The zero reference was determined with HRP alone. The detection was performed, after washing the microtitre plates using PBST, with the chromogen TMB in ready-made solution containing hydrogenperoxide. The absorbance was read after 20 minutes at 450 nm.

### **6.3.2 Bioanalysis of peptide-ochratoxin A interaction using Biacore**

The binding interaction analysis of the peptide receptor with ochratoxin A was carried out on a CM5 (carboxymethylated dextran) sensor chip at 25 °C. HBS-EP (0.01 M HEPES pH 7.4, 0.15 M NaCl, 3 mM EDTA, 0.005% Surfactant P20) was used as running and dilution buffer. Peptides (100 mg L<sup>-1</sup> in 10 mM acetate buffer, pH 4.5) were immobilised using N-(3-dimethylaminopropyl)-N'-ethylcarbodiimide (EDC) and N-hydroxysuccinimide (NHS), applying amine coupling. The injection volume was 75 µl at a flow rate of 5 µl per minute for 15 minutes. Ochratoxin A-BSA (10 mg L<sup>-1</sup> in 10 mM acetate buffer, pH 4.5) was immobilised using amine coupling at an injection volume of 35 µl at a flow rate of 5 µl per minute. As reference, BSA was immobilised. Every flow cell of a sensor chip was immobilised separately. Non-bound binding sites were subsequently deactivated by injecting 35 µl 1M ethanolamine-HCl, pH 8.5 for 7 minutes. Un-conjugated BSA was injected as zero concentration. Binding interaction analysis was executed at a flow rate of 5 µl min<sup>-1</sup> and an injection volume of 60 µl ochratoxin A-BSA (in HBS-EP, pH 7.4) with an equivalent dissociation time. Dissociation was observed in running buffer without regeneration reagents. The kinetic

parameters of the binding reactions were determined using BIAevaluation 3.2 software [Karlsson *et al.*, 1994].



## 6.4 Results and Discussion

An octapeptide with the sequence CSIVEDGL and a 13-mer peptide with the sequence GPAGIDGPAGIRC have been successfully synthesised. In the following the implementation of the peptides into binding assays is presented.

### 6.4.1 Solid phase binding assay of peptide-ochratoxin A interaction

The peptide binding assay was performed to get a quick yes/no answer whether the peptides bind to ochratoxin A *in vitro*. For that study, both peptides were separately immobilised to the solid-phase support and subjected to varying concentrations of the ochratoxin A-HRP conjugate in a direct (non-competitive) binding format. Two immobilisation techniques were employed to investigate the optimal conditions for peptide immobilisation. Figure 6.1 shows both immobilisation techniques for the octapeptide as a plot of absorbance signal versus ochratoxin A-HRP dilution.

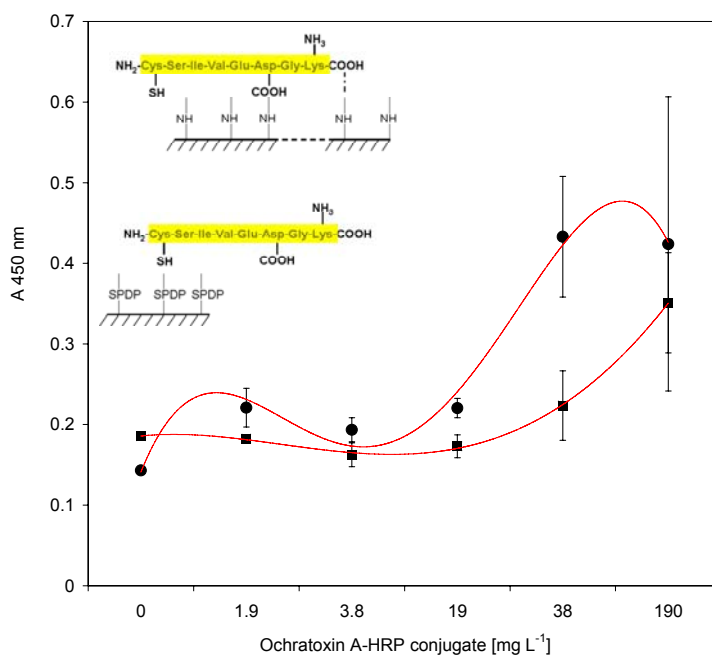


**Figure 6.1:** Plot of absorbance at 450 nm versus ochratoxin A-HRP conjugate (stock concentration of 1.9 mg ml<sup>-1</sup>) using immobilised octapeptide CSIVEDGL via amine coupling (■) and site-directed thiol coupling (●). Standard deviation of the multiple measurements is depicted as error bars. The curves are fitted with a four parameter fit.

As depicted in Figure 6.1, an increase in absorbance with increasing conjugate concentration is observed for both amine and thiol coupling of the octapeptide. It can

also be seen that thiol coupling results in a higher signal when using lower conjugate concentrations, whereby the signal displaying amine coupling is increasing slower but shows a higher signal/noise ratio. At conjugate concentration higher than 1/10 dilution, the resulting signal for both immobilisation techniques is similar and a difference in coupling method is not visible. The same strategy was employed for the 13-mer peptide and the results depicting the immobilisation strategies are shown in Figure 6.2.

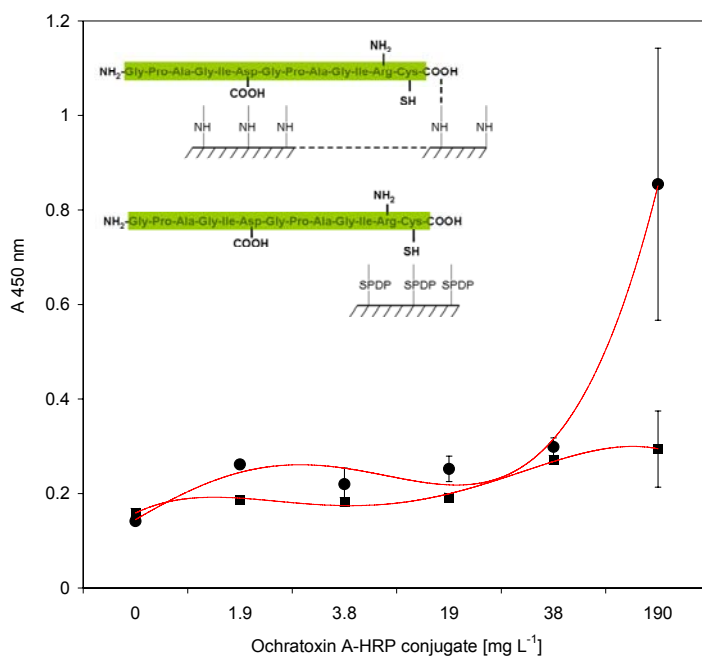


**Figure 6.2:** Plot of absorbance at 450 nm versus ochratoxin A–HRP conjugate (stock concentration of 1.9 mg ml<sup>-1</sup>) using immobilised 13-mer GPAGIDGPAGIRC via amine coupling (■) and site-directed thiol coupling (●). Standard deviation of the multiple measurements is depicted as error bars. The curves are fitted with a four parameter fit.

In Figure 6.2, the thiol-coupled 13-mer peptide demonstrates an increase in signal with increasing conjugate concentration, whereas the amine coupling does not show a significant signal. This might indicate that the amine coupling restricts the binding ability of the 13-mer peptide. The plot also indicates that the binding rate should be lower for the 13-mer peptide than for the octapeptide. Regarding the coupling strategies, for the octapeptide, both coupling strategies seem to work, assuming sufficient flexibility around the peptide's structure to perform a binding event with ochratoxin A. The results in Figure 6.1 and 6.2 suggest that both peptides bind, however with different strength, to ochratoxin A.

### 6.4.2 Peptide immobilisation level on CM5

When having a small ligand immobilised and using a large analyte the amount to be immobilised need to be reduced in order to avoid steric crowding effects on the surface [Biacore Handbook, 2007]. Therefore, the binding level response for small molecular weight peptides, as employed here, is expected to be relatively small. The conformation of the peptides on the CM5 chip will be different to the immobilisation on microtitre plate supports, since covalent attachment to surface carboxy groups will take place through amine and amino groups in different positions on the peptides (Figure 6.3). The ligands and their immobilisation level (RU) are shown in Table 6.1.

**Table 6.1:** Ligands immobilised to CM5 chips and their immobilisation response.

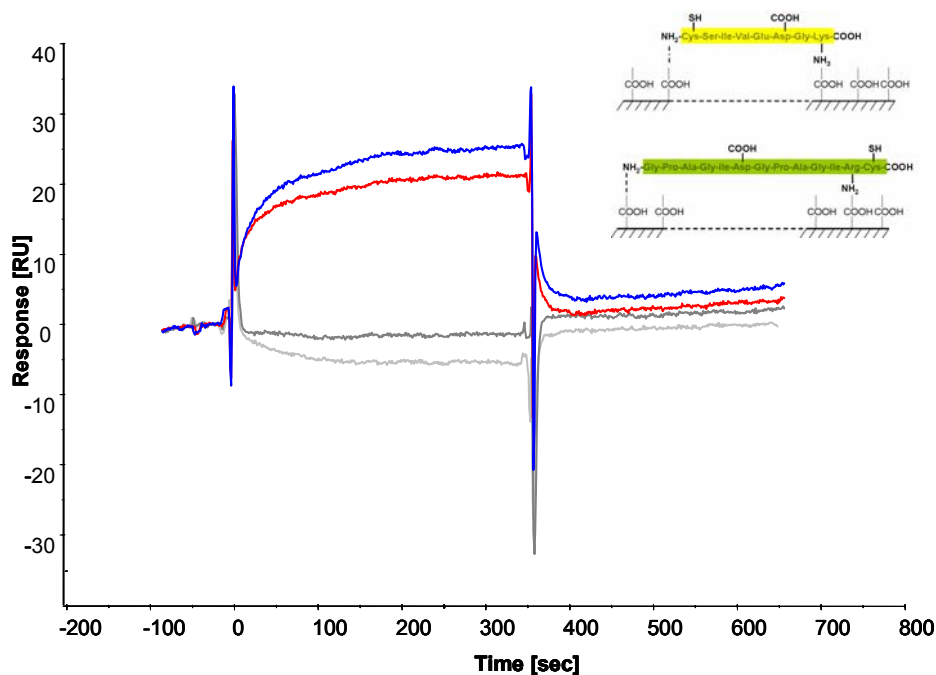
Ligand	Immobilisation level	Analyte
Octapeptide CSIVEDGL	251 RU	Ochratoxin A-BSA
13-mer peptide GPAGIDGPAGIRC	227 RU	Ochratoxin A-BSA

The net surface plasmon resonance signal for immobilised peptides was about 251 RU (octapeptide) and 227 RU (13-mer peptide) after completion of the chip regeneration cycle, which corresponds to 251  $\text{pg}/\text{mm}^2$  (octapeptide) and 227  $\text{pg}/\text{mm}^2$  (13-mer peptide) that is 30 and 19  $\text{fmol}/\text{mm}^2$ , respectively. Even though the immobilisation response was low for both peptides, the calculated immobilisation level is still high in relation to the molecular weight of both peptides.

### 6.4.3 Immobilised peptide interaction with ochratoxin A-BSA

The binding interaction of immobilised peptides with ochratoxin A is studied in a flow system to confirm the results obtained on a static micro titre plate system in Section 6.4.1. For that purpose, both peptides were immobilised onto the sensor chip surface using amine coupling, since the appropriate reagents for sulfhydryl coupling, were at that point of time not available. Using ochratoxin A-BSA as analyte, one has to observe that the binding interaction model does not follow a simple 1:1 stoichiometry, but a 1:3 to 1:6 binding as 3-6 mol ochratoxin A is bound per mol BSA. A saturating concentration of 100  $\text{mg L}^{-1}$  ochratoxin A-BSA conjugate was injected over both

immobilised peptides and the association and dissociation monitored in real-time as seen in Figure 6.3.



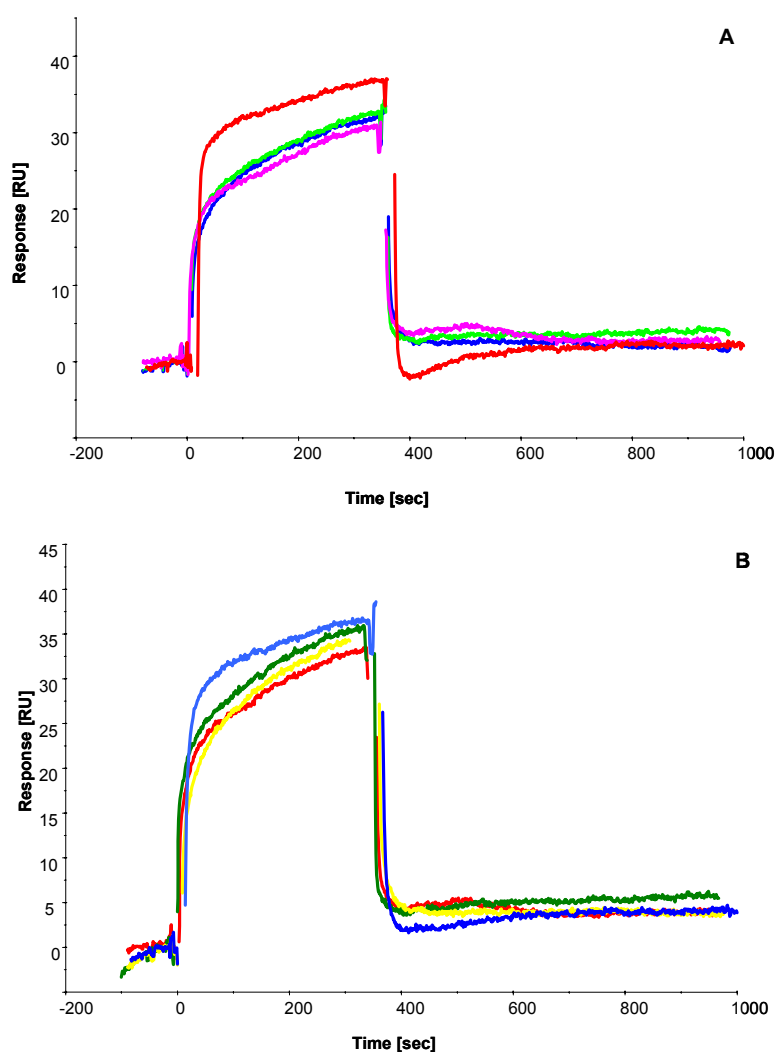
**Figure 6.3:** Sensorgrams displaying  $100 \text{ mg L}^{-1}$  ochratoxin A-BSA binding to immobilised peptides a) 13-mer GPAGIDGPAGIRC in blue and b) CSIVEDGL is shown in red; and  $100 \text{ mg L}^{-1}$  BSA binding to c) 13-mer in dark grey and d) octapeptide in light grey.

Figure 6.3 shows that both 13-mer and octapeptide bind the high concentration of ochratoxin A-BSA conjugate and showed no unspecific binding to the reference analyte BSA. Fast on and off-rates for the both peptides were observed as the baseline was reached almost immediately after the end of analyte injection. Weak affinity can be advantageous as there is the no need for a regeneration step, which improve the stability of the peptides. Weak affinity interactions have been first recognised by Ohlson *et al.* [1988], who defined weak affinity within the range of  $K_A 10^2\text{-}10^4 \text{ M}^{-1}$  (or dissociation constant  $> 10^4 \text{ M}$ ). To establish the maximum response the theoretical binding capacities were calculated according to the equation [Biacore Handbook, 2007]:

$$R_{\max} = (MW_{\text{(analyte)}} / MW_{\text{(ligand)}}) * R_{\text{(ligand)}} * S \quad \text{Equation XV}$$

According to the equation  $R_{\max}$  is the theoretical binding capacity; MW describes the molecular weight of the analyte and ligand, whereas R describes the immobilisation

level of the ligand and  $S$  the stoichiometry of the interaction. Applying equation XV, the theoretical binding capacity was 6742 RU for a 1:3 and 3432 RU for a 1:6 binding model when applying the immobilised octapeptide (CSIVEDGL). The theoretical binding capacity was 4298 RU for a 1:3 and 2188 RU for a 1:6 binding model with the immobilised 13-mer peptide (GPAGIDGPAGIRC). The true binding capacity for the octapeptide was observed at 21 RU and for 13-mer at 25 RU. This could be primarily due to assuming the wrong stoichiometry of the interaction as this can vary in the range of 1:3 - 1:6 molecular ratios. To establish the affinity of the interaction, increasing ochratoxin A-BSA concentrations were injected over both peptide surfaces (Figure 6.4).



**Figure 6.4:** Sensorgrams show the binding interaction of immobilised synthetic octamer CSIVEDGL (A) and 13-mer GPAGIDGPAGIRC (B) peptide with decreasing ochratoxin A-BSA analyte concentration (from top to bottom: 100, 1, 0.1, 0.01 mg L<sup>-1</sup>). The zero reference is shown in grey. The sensorgrams were trimmed by removing the signal spikes occurring at injection start and stop.

It is depicted in Figure 6.4 that the off-rates for both peptides are rapid and baseline was reached almost immediately after the end of analyte injection indicating weak affinity interactions. Also, the sensorgrams for the octapeptide (Figure 6.4, A) and 13-mer peptide (Figure 6.4, B) show quite similar curve shapes and binding response indicating a similar binding stoichiometry. In Figure 6.4 the sensorgrams are showing a bulk refractive index (RI) change of about 20 RU that is probably due to steric hindrance of the ochratoxin A-BSA analyte binding to the peptide layer. The blank sensorgram (un-conjugated BSA) is shown in grey and has been subtracted from the signal curves to eliminate the RI when fitting the curves. Kinetic assessment is not possible for these sensorgrams as  $R_{max}$  (maximum binding capacity) is not reached and the concentration range is too small. Also, the binding stoichiometry is unknown which makes choosing a fitting model more difficult. Preliminary results, fitting the curves with a 1:1 binding fit gives the binding strength of the peptides displayed as equilibrium dissociation constant  $K_D$ . The 13-mer (GPAGIDGPAGIRC) peptide exhibited a binding strength to ochratoxin A with a  $K_A$  of  $6.34 \times 10^4 \text{ M}^{-1}$  and the octapeptide (CSIVEDGL) peptide resulted in a similar  $K_A$  of  $8.45 \times 10^4 \text{ M}^{-1}$ . In contrast, ochratoxin A-specific antibody showed relatively high affinity and slow off-rates indicated by a  $K_D$  of  $3 \times 10^{-6} \text{ M}$  (Biogenesis) and  $K_D$  of  $3.38 \times 10^{-9} \text{ M}$  (Acris) (Chapter 3, Section 3.4.4) when immobilised and subjected to the same ochratoxin A-BSA concentrations.

The resulting affinity of the novel peptide receptors is corresponding to the binding energy calculated by computational modelling. The 13-mer sensorgram indicates faster on and off-rates corresponding to higher binding energy (lower binding score) in comparison to the octapeptide. This was confirmed for both the LeapFrog peptide library design of short peptide sequences and when modelling the dynamics of the binding interaction using FlexiDock. The binding energies for the short peptide sequences as illustrated in Chapter 5 (Table 5.9, No. 4 and 3) correspond to the final sequences as highlighted in Table 5.10 (No. 4 and 9) and to the binding affinities obtained using surface plasmon resonance.

The results strongly suggests that weak affinity interactions are involved in the peptide binding interactions with ochratoxin A as there is the no need for a regeneration step.

The analysis can be performed in an isocratic buffer environment enhancing the stability of the biomolecules and improving the life-time of the receptor surface.

#### 6.4.4 Immobilised ochratoxin A-BSA interaction with peptides

The binding interaction was further characterised by the immobilisation of ochratoxin A-BSA conjugate. This assay format allows both peptide analytes more conformational flexibility when binding immobilised ochratoxin A-BSA. At a MW of 67211-68422 g mol<sup>-1</sup> depending upon the ratio of ochratoxin A (403.81 g mol<sup>-1</sup>) per mol BSA (MW 66000 g mol<sup>-1</sup>), the net surface plasmon resonance signal for immobilised ochratoxin A-BSA, was about 6460 resonance units after completion of the chip regeneration cycle, which corresponds to 6.5 ng/mm<sup>2</sup> (95-96 fmol/mm<sup>2</sup>). Figure 6.5 displays the binding of the octapeptide (CSIVEDGL) analyte to immobilised ochratoxin A-BSA.

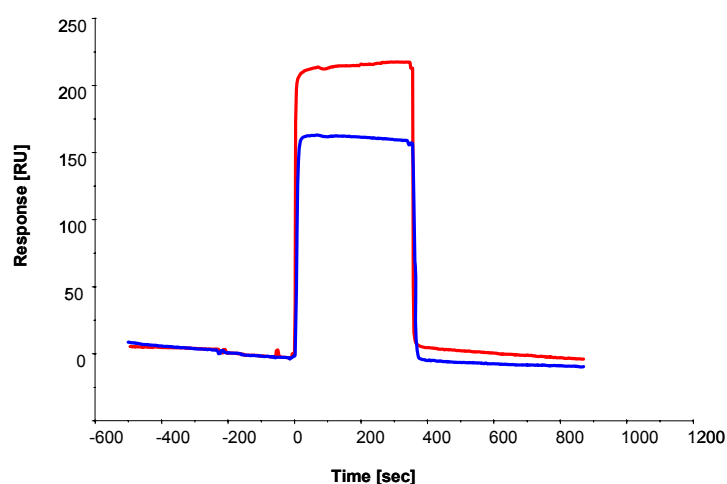


**Figure 6.5:** Sensorgram (resonance units versus time) showing the octapeptide CSIVEDGL (red) binding immobilised ochratoxin A-BSA and the reference BSA (blue).

Figure 6.5 shows a sharp increase in resonance units during the association phase and the distinct dissociation phase compared to the reference cell, it can be assumed that the octapeptide CSIVEDGL (100 mg L<sup>-1</sup>) binds immobilised ochratoxin A-BSA, but not to the BSA reference. The binding response achieved when using the peptide as analyte is much higher than for the immobilised octapeptide, which is a result of the higher flexibility of the octapeptide in solution. The sensorgram also shows high bulk refractive index (RI) indicated by the spike in resonance units at injection start and stop. The RI is about 160 RU for the octapeptide, probably a result of the low flow rate.

Subtracting the RI from the resonance units at the end of association, a binding capacity was 58 RU for the octapeptide. The theoretical maximum binding capacity was calculated at 80 RU. The interaction shows very high on and off-rates for the octapeptide indicating steady state affinity and weak affinity interactions.

The same binding assay was performed using the 13-mer peptide and Figure 6.6 displays the binding of the 13-mer peptide (GPAGIDGPAGIRC) to immobilised ochratoxin A-BSA.

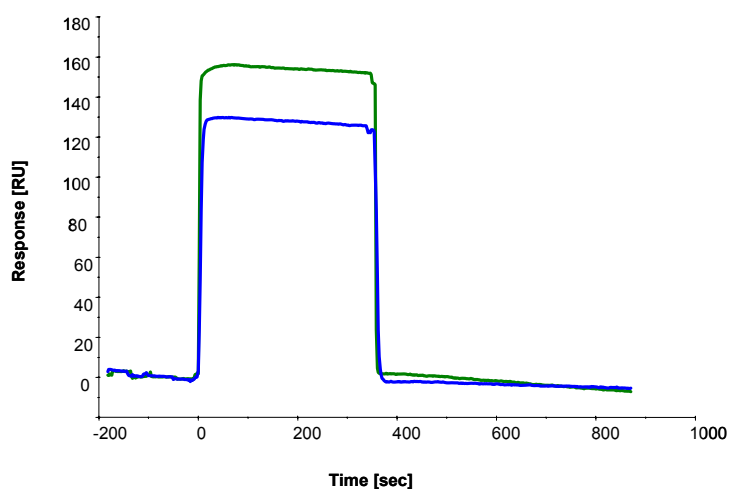


**Figure 6.6:** Sensorgram (resonance units versus time) showing the 13-mer peptide GPAGIDGPAGIRC (green) binding immobilised ochratoxin A-BSA and the reference BSA (blue).

Figure 6.6 shows that the 13-mer peptide binds to immobilised ochratoxin A-BSA in comparison to the reference cell (BSA). The sensorgram also indicates a weaker affinity to ochratoxin A-BSA a higher off-rate than the octapeptide. The bulk refractive index change (RI) is also high at about 125 RU. The binding capacity of  $100 \text{ mg L}^{-1}$  13-mer peptide was calculated at about 27 RU and the theoretical binding capacity was calculated at 113 RU. This shows that it requires much higher concentrations of the 13-mer to reach the maximum binding response than the octapeptide.

Fitting the curves using 1:1 binding stoichiometry resulted kinetic data with a high  $\chi^2$  and were not statistically valid. This indicates that the binding interaction of immobilised ochratoxin A-BSA conjugate with the peptide analytes is more complex



than a simple 1:1 or 1:2 binding event and cannot be fitted using the present kinetic models supplied in the BIAcore software.

However, the interactions of both peptide receptors correlate in their on and off-rates and binding response to the binding energy obtained by computational modelling. The GPAGIDGPAGIRC shows clearly faster on and off-rates, when injected in the flow, which corresponds to less negative binding energy (lower binding score). This confirmed both the computational modelling results shown in Table 5.8 and 5.9 and the results obtained for binding interaction analysis of immobilised peptides (Section 6.4.3).

Van der Gaag and co-workers [2003] describe a competitive binding assay for ochratoxin A using a monoclonal antibody and having an ochratoxin A-derivative immobilised on the sensor surface. The assay results in a sensitivity value of  $0.1 \mu\text{g L}^{-1}$ . The assay described above is non-competitive, however, a binding capacity of 27 RU (13-mer peptide) and 58 RU (octapeptide) at a concentration of  $100 \text{ mg L}^{-1}$  is very low and the sensitivity of the assay is therefore predicted to be much less than the work proposed by van der Gaag *et al.* [2003].

## **6.5 Concluding remarks**

A synthetic peptide receptor for ochratoxin A was designed using an innovative computational approach. The initial argument of the approach to simulate nature's evolution by *de novo* designing a receptor for a small molecular weight toxin was investigated using biospecific interaction analysis. The artificial peptide receptor was binding to ochratoxin A when observing the binding interaction *in vitro* using solid-phase assays and the surface plasmon resonance biosensor. The peptide receptors showed both weak affinity indicated by fast on and off-rates and no need for surface regeneration. The 13-mer showed faster on and off-rates when immobilised and when used as analyte on immobilised ochratoxin A. The sensorgams correlate well with the *in silico* data obtained with both Leapfrog and FlexiDock. It is anticipated that the peptide receptor can be used in receptor binding assays and affinity sensors. Low cost, time-saving and high-throughput screening procedures prior to *in vitro* testing illustrate one major advantage of *de novo* designed peptides towards antibodies.

According to the literature, peptide receptors have been used as receptors and studied by SPR, although in all cases peptide selection was either from a peptide phage library or artificial peptide library using combinatorial analysis. There is no publication record of an artificial peptide that has been custom-designed for a target molecule using computational modelling; hence this work is representing a completely new approach.

Peptides as ochratoxin A receptors have been recently prepared [Giraudi *et al.*, 2007], where a hexapeptide library was produced by combinatorial synthesis. The identification of a suitable peptide sequence binding ochratoxin A has been performed through a displacement assay on peptide-modified microtitre plates by determination of the fluorescence of free ochratoxin A, thereby comparing fluorescence of total to free ochratoxin A and being able to calculate peptide-bound ochratoxin A. Affinity was determined through a Scatchard plot as  $K_A = 3.4 \times 10^4 \text{M}^{-1}$ .

The sequence Ser-Asn-Leu-His-Pro-Lys does not correspond in more than one amino acid each to the peptide sequences for ochratoxin A designed here by computational modelling. The octapeptide (Cys-Ser-Ile-Val-Glu-Asp-Gly-Leu) has serine in common and the 13-mer (Gly-Pro-Ala-Gly-Ile-Asp-Gly-Pro-Ala-Gly-Ile-Arg-Cys) the proline. It is also interesting to see the similarity of the remaining amino acids, where the hexapeptide contains neutral asparagine; both octamer and 13-mer contain aspartate, which is negatively charged. Also, where the hexapeptide contains leucine, both octapeptide and 13-mer contain isoleucine, which are both neutral. So, there are certain similarities in the amino acid sequences.

In this work, the affinity was determined by SPR in a similar format, where the peptides are immobilised and binding directly to ochratoxin A-BSA, however, without the displacement with free ochratoxin A (which would be a useful future experiment). Affinity of the octamer was determined at  $K_A = 8.45 \times 10^4 \text{M}^{-1}$  and of the 13-mer at  $K_A = 6.34 \times 10^4 \text{M}^{-1}$ . Comparing to the hexapeptide obtained from the library, the affinity has the same order of magnitude at about 2-3 fold increased affinity shown by the octapeptide and 13-mer peptide produced in this work. This shows that the computational approach for peptide selection shows corresponding results to

combinatorial selection in terms of affinity of the lead peptide binding to ochratoxin A. By circumventing the effort of preparing a peptide library and the cumbersome and timely process of lead sequence selection, computational modelling has a great advantage towards conventional methods.

Giraudi *et al.* [2007] is using the selected hexapeptide to develop a solid phase extraction method for ochratoxin A in wine and several different wine samples spiked with ochratoxin A at 2 and 4  $\mu\text{g L}^{-1}$  levels showed recovery of 94.7% and 98.4%. Here, the peptide is intended as recognition element in a sensor setting. Detection limits for ochratoxin A in wine were not established yet, but binding of the ochratoxin A conjugate showed that sensitivity could be reached for concentrations around 10  $\mu\text{g L}^{-1}$ . This shows that even if the peptide receptor, upon assay optimisation, should not show the required sensitivity for sensor development, it is comparable in its sensitivity to be used as receptor in solid phase extraction.

Giraudi *et al.* [2007] also cross-referenced a paper by Sbobini *et al.* [2001] that states that a range of affinities between  $10^4$  and  $10^6 \text{ M}^{-1}$  is typical for biomacromolecules binding to coumarinic structures (as in ochratoxin A). However, the developed peptides in this work and Giraudi *et al.* [2007] do not count as macromolecules and therefore show completely different binding properties to ochratoxin A.

Other work involving peptide selection and SPR analysis was done by Gaus and Hall [2003], who selected short peptide sequences from a library to distinguish between normal and oxidised LDL (low density lipoprotein). Here, the peptides were immobilised to a SAM-modified gold surface via carbodiimide coupling as also presented in this work and the binding compared for a number of peptides. This work shows that carbodiimide coupling of peptides can be used in binding analysis and that thiol coupling is not necessary to get sufficient binding for distinguishing affinity.

Also, the use of peptide phage libraries was presented by Soykut *et al.* [2008] for the selection of phage clones displaying peptides that recognize staphylococcal enterotoxin B (SEB). The affinity of the phage clones was determined by SPR where clones were

allowed to bind to the SEB immobilized on the sensor surface. However, the binding constant of the lead peptide was determined at  $K_A = 4.2 \times 10^5 \text{ M}^{-1}$  with isothermal titration calorimetry (ITC).

The affinity of the SEB peptide was in the same range as described by Giraudi *et al.* [2007] for ochratoxin A and the affinities established for the peptides in this work. This might indicate peptide recognition is generally showing weak affinity characteristics, which is also supported by the fact that peptide *in vivo* are predominantly involved in a number of biochemical processes, such as signal transduction (e.g.uropeptides), etabolism (e.g. hormones), cell growth (e.g. Ras-protein, p53), and imune defense (e.g. MHC-receptors) [Schmuck, 2001] often displaying weak affinity characteristics.

## CHAPTER 7 : CONCLUSIONS

This thesis has demonstrated the applicability of screen-printed gold electrodes in the construction of an amperometric affinity sensor for ochratoxin A. The developed and evaluated immunosensor was validated successfully against standard methods used for ochratoxin A analysis in wine samples. All experimental stages of the biosensor development were implemented into the final biosensor demonstrating the capability of sensitive ochratoxin A determination.

- The first stage of the biosensor development involved the characterisation of the antibody recognition elements using enzyme immunoassays (ELISA). Ochratoxin A antibodies were purchased and investigated. This work resulted in the establishment of a limit of detection of  $1 \mu\text{g L}^{-1}$  ochratoxin A.
- Optimal microtitre plate assay parameters were established at a coating concentration of  $750 \mu\text{g L}^{-1}$  ochratoxin A-BSA and an ochratoxin A antibody concentration of  $500 \mu\text{g L}^{-1}$  applying a optimal coating time of ochratoxin A-BSA for 4 hours at room temperature. Casein blocking was used in the coating buffer and an incubation time of ochratoxin A-antibody of 4 hours at an optimal incubation temperature of  $4^{\circ}\text{C}$  was established.
- A preliminary affinity value of the interaction of immobilised ochratoxin A-BSA with a range of antibody concentrations could be established on solid-phase immunoassay (without steady-state equilibrium). The affinity constant  $K_A$  was estimated  $1.66 \times 10^{11} \text{ M}^{-1}$ .
- The results of the enzyme immunoassay work have been compared to another indirect immunoassay for ochratoxin A published by Alarcon *et al.* [2004] using the same BSA-purified ochratoxin A antibody. The results obtained for this thesis show comparably better reproducibility and sensitivity ( $1 \mu\text{g L}^{-1}$ ). A direct immunoassay was presented by Alarcon *et al.* [2004] showing a five times lower LOD as compared to this work.

- Biospecific interaction analysis was used for monitoring binding interaction, kinetic rates and cross-reactivity towards BSA. Affinity data were obtained and compared to the solid phase immunoassay data. The binding interaction analysis resulted in antibody B showing higher affinity for ochratoxin A ( $K_A = 9.84 \times 10^{11} \text{ M}^{-1}$  and  $K_D = 1.02 \times 10^{-12} \text{ M}$ ), whereas antibody A ( $K_A = 2.55 \times 10^{11} \text{ M}^{-1}$  and  $K_D = 3.92 \times 10^{-12}$ ) displayed better sensitivity of the assay and antibody A was chosen as recognition element for the electrochemical immunosensor development. In comparison, the affinity value obtained on the solid-phase immunoassay for antibody B ( $1.66 \times 10^{11} \text{ M}^{-1}$ ) is within the same order of magnitude and suggests that the method to gain the functional affinity analysis, according to Loomans *et al.* [1995] using the Beatty formula [Beatty *et al.*, 1987], is valid.
- Screen-printed gold electrode sensors were mass-produced (200 electrodes per sheet, >20 sheets per batch) by screen-printing applying thick film technology. The screen-printed electrodes provided a cost-effective way to obtain disposable sensor that show good sensitivity.
- The initial immunosensor using ochratoxin A-BSA adsorbed to SPGEs in an indirect immunosensor format showed a detection limit of  $<100 \text{ ng L}^{-1}$ . Further improvement was achieved when covalently immobilising ochratoxin A-BSA by modifying SPGE with CMD thus decreasing the detection limit to  $10 \text{ ng L}^{-1}$ .
- Each measurement took about 200 seconds, where up to three electrodes can be monitored simultaneously. The final construction of each immunoassay-modified electrode takes a minimum of 5 hours (including the covalent surface modification with carboxymethylated dextran).
- The screen-printed immunosensor was optimised for wine analysis in terms of the electrochemical interferences arising from phenolic compounds. This was done by polarising the working electrode at  $-150 \text{ mV}$  versus reference Ag/AgCl.

- The proposed sensor is resulting in a better sensitivity compared to another ochratoxin A immunosensors for wheat analysis [Alarcon *et al.*, 2006]. The group presented an electrochemical biosensor for ochratoxin A in wheat with the lowest detection limit for an indirect assay at  $0.9 (\pm 0.1) \mu\text{g L}^{-1}$ . In this work, detection limits of 9-90 times lower than that using a similar, though improved (CMD-modified SPGE), approach is shown.
- A microelectrode array format as an alternative transducer for the immunosensor was investigated. Preliminary characterisations of the gold microelectrodes prior to microelectrode-immunosensor development were performed and evaluated. The resulting standard curve was inconclusive and a LOD for ochratoxin A on microelectrodes could not be established. It has also been observed that 50 % of the received microelectrodes had faulty connections (as tested with a voltammeter) and as a result did not show a current signal at all. The peculiar shape of the current response upon addition of TMB/H<sub>2</sub>O<sub>2</sub> could be a result of misconnection of the microelectrodes working, counter and reference electrode.
- Furthermore, an initial direct competitive immunosensor format for ochratoxin A showed a detection limit of  $<100 \text{ ng L}^{-1}$  and seems a promising alternative in the development of a BSA-free affinity sensor for ochratoxin A.
- The amperometric screen-printed immunosensor demonstrated good correlation with HPLC results, but less with an immunoassay test kit.
- This work also involved the parallel execution of the computational design of peptide receptors for ochratoxin A and the consecutive characterisation of peptide recognition elements using binding assays as well as their possible implementation into an affinity sensor for ochratoxin A. This work's results illustrate the design and synthesis of a small peptide receptor for ochratoxin A using *de novo* design software.

- It was confirmed that the *de novo* design tool LeapFrog can be used to produce a virtual library of peptide receptors for ochratoxin A and also screen this library using binding energy algorithms to produce a hit-list of lead peptide sequences. The applied program FlexiDock, part of the LeapFrog software, can be used for a rough simulation of receptor-ligand docking. The manual extension of the peptide sequence with charged amino acids or with a Cysteine-tag can not be sufficiently characterised using FlexiDock simulations.
- Two lead peptide sequences were selected from the computational hit list and synthesised. The sequences are a 13-mer (GPAGIDGPAGIRC) and an octapeptide (CSIVEDGL).
- The binding of the peptides to ochratoxin A was confirmed *in vitro* using solid-state peptide assays and real-time monitoring of the binding interaction with the SPR biosensor Biacore. The peptide receptors showed both weak affinity indicated by fast on and off-rates and no need for surface regeneration. The 13-mer showed faster on and off-rates when immobilised and when used as analyte on immobilised ochratoxin A as compared to the octapeptide. Preliminary affinity values indicate a binding strength of the 13-mer (GPAGIDGPAGIRC) peptide to ochratoxin A with a  $K_A$  of  $6.34 \times 10^4 \text{ M}^{-1}$  and the octapeptide (CSIVEDGL) peptide resulted in a similar  $K_A$  of  $8.45 \times 10^4 \text{ M}^{-1}$ . The sensorgrams correlate well with the *in silico* data obtained with both Leapfrog and FlexiDock. It is anticipated that the peptide receptor can be used in receptor binding assays and affinity sensors. Low cost, time-saving and high-throughput screening procedures prior to *in vitro* testing illustrate one major advantage of *de novo* designed peptides towards antibodies.

Conclusively, the thesis reports the development of an affinity sensor that can be applied for ochratoxin A for determination in wine samples. The sensor elements provide sufficient specificity and sensitivity, like the antibody recognition element, while being time and cost-effectiveness through using disposable screen-printed electrodes.



Upon further improvisation in terms of reproducibility and signal variance, the proposed biosensor could be used to monitor ochratoxin A contamination on-site the wine yard and thus prevent wine samples that are above the EC permissible limit to reach the consumer.

## CHAPTER 8 : FUTURE WORK AND ALTERNATIVE APPROACHES

- Enzyme immunoassays for ochratoxin A antibody characterisation could be further improved in its sensitivity by choosing a monoclonal antibody for assay development to increase specificity for ochratoxin A and to avoid cross-interaction with the BSA-conjugate of ochratoxin A. A monoclonal antibody for ochratoxin A can be acquired from Abcam Plc. (UK) since August, 2005. According to the manufacturer, no cross-reactivity towards ochratoxin B or BSA can be observed. The product was not available at the time of this assay development and it was not feasible to implement a novel antibody at such a late stage of the sensor development. The antibody available at that point of time was a polyclonal antibody from Acris GmbH (Germany) that did not use the BSA-conjugate of the toxin as immunogen. Suggested future work involves the analysis of the antibody from Acris GmbH by enzyme immunoassays in the same way as the antibody from Biogenesis Ltd. to compare with the Biacore results.
- Furthermore, the direct competitive enzyme immunoassay format needs to be further explored as it displays a simpler binding interaction approach. Therefore, an ochratoxin A-HRP conjugate needs to be obtained. A conjugate with preferably a 1:1 molar ratio of ochratoxin A to HRP would be optimal, which can be achieved by refining the conjugation method.
- Sample pre-treatment and purification has to be more extensively investigated such as the recovery rates when using immunoaffinity columns for ochratoxin A extraction and furthermore the effect of the wine components and wine pH on the assay performance (also when using diluted samples).
- The binding interaction analysis using Biacore that was performed consecutively of the enzyme immunoassay analysis needs to be improved in its experimental setup to gain accurate kinetic data. For the various binding formats the  $R_{max}$  value (maximum binding capacity) has to be determined by saturating the ligand bound to the sensor surface with higher analyte concentrations. For kinetic

measurements, another chip with low surface capacity should be prepared

- The  $R_{max}$  value is to be compared with the theoretical value to examine whether the stoichiometry is correct. The linked reaction experiment should be performed for all binding interaction formats to confirm the stoichiometry and binding model. The binding analysis should be simplified so that a 1:1 binding can be measured on the sensor surface.
- For the wine analysis using the binding interaction analysis, the competitive assay has to be optimised for a wider range of ochratoxin A standards. The sensitivity and the dynamic range can be positively influenced by using a monoclonal antibody for ochratoxin A. Thus, the competitive assay on the sensor chip can be used for sensitive detection of ochratoxin A.
- The immunosensor in this work could be improved in various ways. Work has been initiated to transfer the immunosensor approach to a handheld device for field-analysis. In this context, the stability of the sensor has to be optimised. It was observed that after several days of storage at 4°C, the ochratoxin A immunosensor showed less bioactivity, being subjected to activity loss of the protein components involved. Consequently, all the measurements with the biosensors were done within a day of the assay construction. Thus, the components of the immunosensor have to be stabilised further. However, the bare screen-printed gold electrodes are stable for several months when storing under dry, inert conditions such as under nitrogen atmosphere. CMD-modified sensors are stable under storage of either  $N_2$  or in phosphate buffer, pH 7.4 at 4°C for several weeks.
- Furthermore, CMD-modified SPGE described in 4.4.16 has to be improved as the carboxymethylated dextran (CMD) is currently adsorbed to the gold surface. By coupling the CMD covalently to the surface, the sensitivity of the assay can be significantly enhanced. This can be achieved by following the protocol of Masson *et al.* [2004], which was derived from the initial protocol for carboxymethylated dextran modification of gold surfaces in SPR measurements

[Lofas & Johnsson, 1990]. The protocol is described in brief: The gold surface is incubated overnight with 0.005 M 11-mercaptoundecanol (80:20 Ethanol:H<sub>2</sub>O) to form a self-assembled monolayer (SAM). The SAM is incubated with 0.6 M epichlorohydrin in 1:1 diglyme and 0.4 M NaOH for 4 hours and then washed with water, ethanol, and water. The surface is then incubated with 0.3 g/ml dextran (500 kDa) in aqueous solution and 0.1 M NaOH. The dextran polymer is then modified to carboxymethylated dextran with bromoacetic acid in 2 M NaOH for another 16 hours and washed again with water, ethanol, and water. To confirm the presence of linked carboxymethylated dextran, the surface can be characterized using FTIR (Fourier Transform Infrared Spectroscopy).

- As the trend in biosensors moves towards homogenous and label-free detection an alternative approach for ochratoxin A detection using screen printed electrodes is suggested as follows. The literature describes the monitoring of ochratoxin A oxidation [Calcutt *et al.*, 2001] which has been performed on glassy carbon electrodes vs Ag/AgCl [Oliviera *et al.*, 2007]. Calcutt *et al.* [2001] monitored the oxidation of ochratoxin A on screen printed gold electrodes versus Ag/AgCl using cyclic voltammetry by observing the oxidation peak with decreasing ochratoxin A concentration. Using the same approach, cyclic voltammograms were obtained in this work illustrating decreasing ochratoxin A concentrations on SPGE. The CV shows a peak on the positive scan at about +1.0 V, but no proportional decrease in peak current or a significant peak shift was observed when varying the ochratoxin A concentration. Since the ochratoxin A oxidation potential is fairly high, a mediator might be introduced into the detection, which would be reduced upon oxidation of ochratoxin A and in turn reduced at the electrode producing a current that can be monitored sensitively via chronoamperometry.
- The development of an ochratoxin A immunosensor on microelectrodes requires further characterisation of the microelectrodes and adaptation of the assay, which involves the optimal coating and binding concentrations of all reagents involved and the reduction of faulty connections of the microelectrode components.

- Computational modelling can be further optimised for instance by the choice of applied force field as well as the simulated solvent environment. In this work the Tripos force field had been selected for molecular modelling. An alternative is the application of protein force fields such as CHARMM22 that has been specifically applied for the modelling of peptides by MacKerell [1998]. As an alternative to LeapFrog, other *de novo* design programs such as LUDI [Böhm, 1992] can be applied for the peptide design task. Another improvement would be the better choice of receptor-ligand interaction simulation software. A suggestion would be either AutoDock 3.0 [Morris *et al.*, 1998] or FlexX/FlexE featured by Tripos Inc., which adds the ability to consider protein structural variability in docking calculations. For refinement one could use a dynamics package like AMBER 7 to refine docked complexes or QSAR, which is a toxicity-modelling algorithm based on Quantitative Structure-Activity Relationships (QSAR), neuronal networks, or artificial intelligence concepts [Selassie, 2003]. A new approach named Quasar (Quasi-atomistic receptor modelling) combines receptor modelling and QSAR technique based on a genetic algorithm by mapping an unknown or hypothetical receptor (such as the peptide receptor) in 3D and quantitatively calculating the affinity of small molecules binding to it [Vedani *et al.*, 2000; Vedani and Dobler, 2002].
- It is known from the literature that small peptides such as trimers or tetramers are very well able of interacting with relatively strong affinity via H-bonds and electrostatic interactions. Smaller peptides have a more defined structure and physicochemical properties. The longer the peptide, the more distinct properties affecting the interaction and thus it occurs that smaller peptides often illustrate higher binding affinities [Schmuck, 2005]. LeapFrog parameters can be manipulated to design small, soluble peptides by choosing only from a set of hydrophilic amino acid monomers for synthetic peptide library construction. In addition to that, using Cysteine as a fixed starting molecule, will introduce it into every peptide sequence, however at random position.
- 3-dimensional structural information for the peptide receptor and the ochratoxin A-receptor complex provided by X-ray diffraction or NMR can give a better

inside into the binding interaction and the complex formation. Ongoing research in receptor design and structure-function studies as well as the introduction of small molecular weight templates are well underway and molecular dynamics simulation techniques will guide computational chemists to real predictions of binding affinities of receptor-ligand interactions without them having to synthesise the molecule.

- The synthesised peptides obtained from LeapFrog were analysed *in vivo* using binding interaction analysis. Further work should examine the suitability of the novel receptors as sensing layer in diagnostic binding assays and sensors. The specificity of the peptide interaction has to be further examined for cross-reactivity towards ochratoxin A derivatives and wine components in general. Also, the peptide receptors have to be validated further against other, random peptide sequences.
- Another approach would be the selection of a peptide sequence from the binding site of a molecule that is known to bind ochratoxin A such as the enzyme t-RNA Synthetase. This, however, is dependent on two issues, 1) if the ochratoxin A binding site on this molecule is of linear or non-linear sequence, hence only a linear sequence can be easily extracted from the binding site and a non-linear one would require more intensive molecular dynamics studies of variants of the non-linear sequence, and 2) if the affinity of the extracted peptide sequence to ochratoxin A is sufficiently high to demonstrate a detectable binding interaction. It is known that ochratoxin A binds to the enzyme t-RNA Synthetase as an inhibitor competing with the enzyme substrate phenylalanine. Thus, ochratoxin A has an effect on protein biosynthesis; one of its bioactive effects on the mammalian system, but is easily replaced when phenylalanine is added. The research group around Qinglai *et al.* [2004] published the development of a tRNA-Synthetase microarray for protein analysis. This paper lead to the hereby suggested idea of applying this sensor for an ochratoxin A inhibition/displacement assay. This would involve the epitope mapping of the t-RNA-Synthetase binding site for ochratoxin A and also computational modelling of the interaction of the enzyme using molecular dynamics studies.

The t-RNA-Synthetase displacement biosensor for ochratoxin A could be used for ochratoxin A analysis in contaminated samples. An advantage of enzymes is that they are more stable in an acidic environment, such as wine, as compared to antibodies. However, this idea has not evolved past the drawing board and can be merely seen as an alternative needing extensive development and optimisation.

**REFERENCES & BIBLIOGRAPHY**

- Aalund, O.K. Brunfeldt, B. Hald, P. Krogh, and Poulsen, K. "A Radioimmunoassay for Ochratoxin A: A Preliminary Investigation." *Acta Pathol. Microbiol. Scand. Sect. C* 83 (1975): 390-392.
- Abcam Plc. Citing internet resource (WWW document): [www.abcam.com](http://www.abcam.com), Accessed 2004 & 2007.
- Adams, M.R. & Moss, M.O. *Food Microbiology*.: The Royal Society of Chemistry, 1995. Reprint, 1997.
- Adgen Ltd. Part of the Neogen Europe group. Citing internet resource: ([www.adgen.co.uk/](http://www.adgen.co.uk/)). Accessed 2004.
- Alarcon, S.H., Micheli, L., Palleschi, G., Compagnone, D. "Development of an Electrochemical Immunosensor for Ochratoxin A." *Anal. Letters* 37 (2004): 1545-1558.
- Alarcon, S.H., Palleschi, G., Campagnone, D., Pascale, M., Visconti, A., Barna-Vetro, I. "Monoclonal Antibody Based Electrochemical Immunosensor for the Determination of Ochratoxin a in Wheat." *Talanta* 69, no. 4 (2006): 1031-1037.
- Albassam, MA., Yong, S.I., Bhatnagar, R., Sharma, A.K. & Prior, M.G. "Histopathological and Electron Microscopic Studies on the Acute Toxicity of Ochratoxin a in Rats." *Vet. Pathol.* 424 (1987): 427-435.
- Alberts, I.L., Todorov, N.P. and Dean, P.M. "Receptor Flexibility in De Novo Ligand Design and Docking." *J. Med. Chem.* 48, no. 21 (2005): 6585-6596.
- Al-Kaissi, E., Mostratos, A. "Assessment of Substrates for Horseradishperoxidase Enzyme Immunoassay." *J. Immunol. Methods* 58 (1983): 1-2.
- Allender, C. "Special Issue on Synthetic Receptors." *Biosensors & Bioelectronics* 22, no. 3 (2006).
- Allinger, N. L., K. Chen, and J-H Lii. "An Improved Force Field (Mm4) for Saturated Hydrocarbons." *J. Comp. Chem.* 17 (1996): 642-668.
- Allinger, N.L. "Conformational Analysis. 130. Mm2. A Hydrocarbon Force Field Utilizing V1 and V2 Torsional Terms." *J. Am. Chem. Soc.* 99 (1977): 8127-8134.
- Allinger, N.L. and Lii, J.H. "Molecular Mechanics. The Mm3 Force Field for Hydrocarbons. 3. The Van Der Waals' Potentials and Crystal Data for Aliphatic and Aromatic Hydrocarbons." *J. Am. Chem. Soc.* 111, no. 23 (1989c): 8576-8592.



- Allinger, N.L., Lii, J.H. "Molecular Mechanics. The Mm3 Force Field for Hydrocarbons. 2. Vibrational Frequencies and Thermodynamics." *J. Am. Chem. Soc.* 111, no. 23 (1989b): 8566-8575.
- Allinger, N.L., Yuh, Y.H., Lii, J.H. "Molecular Mechanics. The Mm3 Force Field for Hydrocarbons." *Journal of the American Chemical Society* 11, no. 23 (1989a): 8551-8566.
- Altieri, A., Bosetti, C., Gallus, S., Franceschi, S., Dal Maso, L., Talamini, R., Levi, F., Negri, E., Rodriguez, T. and La Vecchia, C. "Wine, Beer and Spirits and Risk of Oral and Pharyngeal Cancer: A Case-Control Study from Italy and Switzerland." *Oral Oncology* 40, no. 9 (2004): 904-909.
- Amatore, C. "Physical Electrochemistry: Principles, Methods and Applications." ed. I. Rubenstein, 131. New York: Marcel Dekker, 1995.
- Amit, A., Mariuzza, R., Phillips, S., and Poljak, R. "Three Dimensional Structure of an Antigen-Antibody Complex at 2.8 a Resolution." *Science* 233 (1986): 747-753.
- Ammida, N.H., Micheli, L. and Palleschi, G. "Electrochemical Immunosensor for Determination of Aflatoxin B1 in Barley." *Anal. Chim. Acta* 520 (2004): 159-164.
- Ammida, N.H.S., Micheli, L., Piermarini, S., Moscone, D., Palleschi, G. "Detection of Aflatoxin B1 in Barley: Comparative Study of Immunosensor and Hplc." *Anal. Letters* 39 (2006): 1559-1572.
- Amzel, L.M., Poljak, R.J., Saul, F., Varga, J.M. and Richards, F.F. "The Three-Dimensional Structure of a Crystalline Antibody-Antigen Complex at 3.5 a Resolution." *Proc. Nat. Acad. Sci.* 71 (1974): 1427-1430.
- AOAC International. *Official Methods of Analysis* Citing Internet Resource (Www Document): [Http://Www.Aoac.Org/Testkits/Kits-Toxins.Htm](http://Www.Aoac.Org/Testkits/Kits-Toxins.Htm). Gaithersburg, USA, 2005.
- AOAC International (Association of Official Analytical Chemists). *Test Kits for Toxins*. Citing Internet recourses (WWW document): <http://www.aoac.org/testkits/kits-toxins.HTM>, Accessed 2007.
- Apostolakis, J., Caflisch, A. "Computational Ligand Design." *Comb. Chem. High Throughput Screen.* 2, no. 2 (1999): 91-104.
- Arif, M.; Setford, S.J.; Burton, K.S.; Tothill, I.E. "L-Malic Acid Biosensor for Field-Based Evaluation of Apple, Potato and Tomato Horticultural Produce." *Analyst* 127 (2002): 104-108.
- Arrhenius, S. *Immunochemistry: The Application of the Principles of Physical Chemistry to the Study of Biological Antibodies*. New York: MacMillan, 1907.

- Arrigan, D.W.M. "Voltammetric Determination of Trace Metals and Organics after Accumulation at Modified Electrodes." *The Analyst* 119 (1994): 1953 - 1966.
- Arrigan, D.W.M. "Nanoelectrodes, Nanoelectrode Arrays and Their Applications." *The Analyst* 12, no. 9 (2004): 1157-1165.
- Ash, S., Cline, M.A., Homer, R.W., Hurst, T., Smith, G.B. "Sybyl Line Notation (Sln): A Versatile Language for Chemical Structure Representation." *J. Chem. Inf. Comput. Sci.* 37 (1997): 71-79.
- Atkins, P.W. "Natural Biopolymers - the Primary and Secondary Structure." In *The Elements of Physical Chemistry*, Chapter 10.15, 405: Oxford University Press,, 1996.
- Avramescu, A., Noguer, T., Avramescu, M. and Marty, J.L. "Screen-Printed Biosensors for the Control of Wine Quality Based on Lactate and Acetaldehyde Determination." *Analytica Chimica Acta* 458, no. 1 (2002): 203-213.
- Avramescu, A., Noguer, T., Magearu, V. and Marty, J.L. "Chronoamperometric Determination of Image-Lactate Using Screen-Printed Enzyme Electrodes." *Analytica Chimica Acta*, 433, no. 4 (2001): 81-88.
- Bagirova, N.A., Shekhovtsova, T.N., van Huystee, R.B. "Enzymatic Determination of Phenols Using Peanut Peroxidase." *Talanta* 55, no. 6 (2001): 1151-1164.
- Barbalace, K. *Periodic Table of Elements - Sorted by Electrical Conductivity*. Citing internet resource (WWW document: <http://EnvironmentalChemistry.com/yogi/periodic/electrical.html>, 1995-2007. Accessed 2007.
- Bard, A.J. and Faulkner, L.R. "In: Electrochemical Methods: Fundamentals and Applications." 142-144. New York: Wiley, 1980.
- Barker, S.L.R., Zhao, Y., Marletta, M.A., Kopelman, R., Tsang, A.W., Swanson, J.A. "Cellular Application of a Selective Fibre- Optic Nitric Oxide Based on a Dye-Labelled Heme Domain of Soluble Guanylate Cyclase." *Anal. Chem.* 71 (1999): 2071-2075.
- Baskeyfield, D.E.H. "Development of a Disposable Amperometric Immunosensor for Isoproturon Herbicide Detection in Water and Soil Extracts." PhD thesis, Cranfield University, 2001.
- Baudrimont, I., Betbeder, A.M., Gharbi, A., Pfohl-Leszkowicz, A., Dirheimer, G., Creppy, E.E. "Effect of Superoxide Dismutase and Catalase on the Nephrotoxicity Induced by Subchronical Administration of Ochratoxin a in Rats." *Toxicology* 89, no. 101-111 (1994).
- Beatty, J.D., Beatty, B.G., and Vlahos, W.G. "Measurement of Monoclonal Antibody Affinity by Non-Competitive Enzyme Immunoassay." *J. Immunol. Methods* 100, no. 173 (1987).

- Belli, N., Ramos, A.J., Coronas, L., Sanchis, V., Marin, S. "Aspergillus Carbonarius Growth and Ochratoxin A Production on a Synthetic Grape Medium in Relation to Environmental Factors." *Journal of Applied Microbiology* 98 (2004): 830-844.
- Benedetti, E., Morelli, G., Nemethy, G., Scheraga, H. A. "Statistical and Energetic Analysis of Side-Chain Conformations in Oligopeptides." *Int. J. Peptide Protein Res* 22 (1983): 1-15.
- Beni, V., Berduque, A., Kivlehan, F., Lanyon, Y., Herzog, G., Zazpe, R., Arrigan, D. "Bio-Inspired Electroanalytical Sensing Systems- Chemical Micro Analytics Research at Tyndall." In *Nano2Life Annual Meeting*. Barcelona, Spain, 2006.
- Benitez, L., Martin-Gonzalez, A., Gilardi, P., Soto, T., Rodriguez de Lecea, J. "The Ciliated Protozoa Tetrahymena Thermophila as a Biosensor to Detect Mycotoxins." *Letters in Applied Microbiology* 19, no. 6 (1994): 489-491.
- Benkert, A., Scheller, F.W., Schössler, W., Hentschel, C., Micheel, B., Behrsing, O., Scharte, G., Stöcklein, and Warsinke W., A. "Development of a Creatinine Elisa and an Amperometric Antibody- Based Creatinine Sensor with a Detection Limit in the Nanomolar Range." *Anal. Chem.* 72 (2000): 916-921.
- Berggren, C., Stalhandske, P., Brundell, J., Johansson, G. "A Feasibility Study of a Capacitive Biosensor for Direct Detection of DNA Hybridization." *Electroanalysis* 3 (1999): 156-160.
- Berzofsky, J.A., Schechter, A.N. "The Concepts of Cross-Reactivity and Specificity in Immunology. *Journal of Molecular Immunology.*" *J. Molec. Immunol.* 18 (1981): 751-763.
- Betina, V. "Thin-Layer Chromatography of Mycotoxins." *Journal of Chromatography* 334 (1985): 211-216.
- Bhatnagar, D., Ehrlich, K.C., Chang, P.K. "Mycotoxins." In *Encyclopedia of Life Sciences*: Nature Publishing Group, 2001.
- BIAcore. *Surface Plasmon Resonance*. BIAtechnology Note 107. Citing internet resource: [www.biacore.com](http://www.biacore.com), Accessed 2006.
- Bier, F. F., Jockers, R., Schmid, R.D. "Integrated Optical Immunosensor for S-Triazine Determination, Calibration and Limitations." *The Analyst* 119 (1994): 437-441.
- Bilitewski, U. "Can Affinity Sensors Be Used to Detect Food Contaminants?" *Anal. Chem.* 72 (2000): 692-701.
- Bird, R. B., Stewart, W. E. and Lightfoot, E. N. *Transport Phenomena*. 2nd ed.: Wiley, 2002.
- Blanco, M. "Molecular Silverware. I. General Solutions to Excluded Volume Constrained Problems." *J. Comp. Chem.* 12, no. 2 (1991): 237-247.

- Böhm, H. J., Klebe, G., Kubinyi, H. "Protein-Ligand Wechselwirkungen." In *Wirkstoffdesign*. Heidelberg: Spektrum Akademischer Verlag, 1996.
- Böhm, H.J. "The Computer Program Ludi: A New Method for the De Novo Design of Enzyme Inhibitors." *J. Comp. Aided Molec. Design* 6 (1992a): 61-78.
- Böhm, H.J. "The Development of a Simple Empirical Scoring Function to Estimate the Binding Constant for a Protein-Ligand Complex of Known Three-Dimensional Structure." *J. Comp. Aided Molec. Design* 8, no. 3 (1994): 243.
- Böhm, H.J. "Site-Directed Structure Generation by Fragment-Joining." *Perspectives in Drug Discovery and Design* 3, no. 1 (1995): 21-33.
- Böhm, H.J. "Towards the Automatic Design of Synthetically Accessible Protein Ligands: Peptides, Amides and Peptidomimetics." *J. Comp. Aided Molec. Design* 10, no. 4 (1996): 265-272.
- Böhm, H.J. and Klebe, G. "What Can We Learn from Molecular Recognition in Protein-Ligand Complexes for the Design of New Drugs?" *Angewandte Chemie International Edition in English* 35, no. 22 (1996): 2588-2614.
- Bond, A. M. "Past, Present and Future Contributions of Microelectrodes to Analytical Studies Employing Voltammetric Detection, a Review." *The Analyst* 119 (1994): R1-R21.
- Born, M., Oppenheimer, R. Z. "Zur Quantentheorie Der Molekeln." *Annalen der Physik* 84 (1927): 457-484.
- Bott, A.W. "Practical Problems in Voltammetry 3: Reference Electrodes for Voltammetry." *Current Separations* 14 (1995): 64.
- Boutrif, E. "Mycotoxin Prevention and Control: Fao Programmes." In *Review de Medicine Veterinaire*, ed. Cited in: Foodborne pathogens-Hazards. Risk Analysis and Control, 1998.
- Boyd, S., and Yamazaki, H. "Stability of Polypeptide Immunoreactants and Polyvinyl Alcohol as a Blocking Agent on Polyester Cloth During Dry Storage." *Immunol. Investig.* 24 (1995): 795-803.
- Brett, C.M.A., and Brett, A.M.O. *Electrochemistry: Principles, Methods, and Applications*. Oxford: Oxford Univ. Press, 1993.
- Brooks, B. R., Bruccoleri, R.E., Olafson, B.D., States, D.J., Swaminathan, S., Karplus, M. "Charmm: A Program for Macromolecular Energy, Minimization, and Dynamics Calculations." *Journal of Computational Chemistry* 4, no. 2 (1983): 187-217.
- Burkert, U., Allinger, N.L. "Molecular Mechanics." *ACS Monograph* 117 (1982).

- Butler, D. and Guilbault, G.G. "Disposable Amperometric Immunosensor for the Detection of 17- $\beta$  Estradiol Using Screen-Printed Electrodes." *Actuators Sens. B* 113 (2006): 692.
- Butler, Deidre; Pravda, Miloslav; Guilbault, George G. "Development of a Disposable Amperometric Immunosensor for the Detection of Ecstasy and Its Analogues Using Screen -Printed Electrodes." *Analytica Chimica Acta* 556, no. 2806 (2005): 333-339.
- Butler, J.E., Ni L., Nessler R., Joshi K.S., Suter M., Rosenberg B., Chang, J., Brown W.R. & Cantarero L.A. "The Physical and Functional Behaviour of Capture Antibodies Adsorbed on Polystyrene." *J. Immunol. Methods* 150 (1992): 77-90.
- Butler, John E. "Solid Supports in Enzyme-Linked Immunosorbent Assay and Other Solid Phase Immunoassays." *METHODS* 22 (2000): 4-23.
- Cagnini, A., Palchetti, I., Lioni, I., Mascini, M. and Turner, A.P.F. "Disposable Ruthenized Screen-Printed Biosensors for Pesticides Monitoring." *Sensors and Actuators B: Chemical* 24 (1995): 85-89.
- Calcutt, M.W., Gillman, G.J., Dillon, P.P., Manning, B.M., O'Kennedy, R., Lee, H.A., Morgan, M.R.M. "Electrochemical Oxidation of Ochratoxin A: Correlation with 4-Chlorophenol." *Chemical Research in Toxicology* 14 (2001): 1266-1272.
- Candlish, A. A. G., Samson, W. M. and Smith, J. E. "A Monoclonal Antibody to Ochratoxin A." *Letters in Applied Microbiology* 3 (1986): 9-11.
- Cao, F., Greve, D.W., Oppenheim, I.J. "Development of Microsensors for Chloride Concentration in Concrete." *Sensors IEEE* (2005): 195-198.
- Cao, L. "Immobilized Enzymes: Science or Art?" *Current Opinion in Chemical Biology* 9, no. 2 (2005): 217-226.
- Carter, M.J. "Conjugation of Peptides to Carrier Protein Via Carbodiimide." In *The Protein Protocols Handbook*, ed. J.M. Walker, 693-694. Totowa, New Jersey, USA: Humana Press, 1996.
- Cass, A.E.G., Davis, G., Francis, G.D., Hill, H.A.O., Aston, W.J., Higgins, I.J., Plotkin, E.V., Scott, L.D.L. and Turner, A.P.F. "Ferrocene-Mediated Enzyme Electrode for Amperometric Determination of Glucose." *Anal. Chem.* 56 (1984): 667-671.
- Chaiken, I.M. "Affinity Chromatography in Biology and Biotechnology." In *Handbook of Chromatography*, ed. T. Kline, 63, 219-227: Marcel Dekker, 1993.
- Chaiken, Irwin M. "Analytical High-Performance Affinity Chromatography." *ADVANCES in Chromatography* 27 (1987): Chapter 7.
- Chance, B. "The Properties of the Enzyme-Substrate Compounds of Horse-Radish and Lacto-Peroxidase." *Science* 104 (1949): 204.

- Chemicon. *Monoclonal and Polyclonal Antibodies*. Citing Internet recourses (WWW document):<http://www.chemicon.com/resource/ANT101/a1.asp#MONOCLONAL-POLYCLONAL-ANTIBODIES>, 2004. Accessed.
- Chianella, I. , Lotierzo, M., Piletsky, S.A., Tothill, I.E., Chen, B., Karim, K. and Turner, A.P.F. "Rational Design of a Polymer Specific for Microcystin-Lr Using a Computational Approach." *Anal. Chem.* 74 (2002): 1288-1293.
- Chianella, I., Piletsky, S.A., Tothill, I.E., Chen, B & Turner, A.P.F. "Mip Based Solid Phase Extraction Cartridges Combined with Mip- Based Sensors for the Detection of Microcystin-Lr." *Biosensors & Bioelectronics* 18 (2003): 119-127.
- Chong, X., and Rahimtula, A.D. "Alterations in Atp-Dependent Calcium Uptake by Rat Renal Cortex Microsomes Following Ochratoxin a Administration in Vivo or Addition in Vitro." *Biochem. Pharmacol.* 44, no. 1401-1409 (1992).
- Chothia, C. and Janin, J. "Principles of Protein-Protein Recognition." *Nature* 256 (1975): 705-708.
- Chou, P.Y., and Fasman, G.D. "Prediction of the Secondary Structure of Proteins from Their Amino Acid Sequence." *Adv. Enzymol* 47 (1978): 359-366.
- Chu, F. S. "A Comparative Study of the Interaction of Ochratoxins with Bovine Serum Albumine." *Biochem. Pharmacol.* 23 (1974): 1105-1107.
- Chu, F. S. "Mycotoxins-Occurrence and Toxic Effects." In *Cited In: Encyclopaedia of Food and Nutrition, Food Contaminants*, 858-869. New York: Academic Press, 1998.
- Chu, F.S. "Interaction of Ochratoxin a with Bovine Serum Albumine." *Arch. Biochem. Biophys.* 147 (1971): 359-366.
- Chu, F.S., Chang, F.C., Hinsdill, R.D. "Production of Antibody against Ochratoxin A." *Appl. Environ. Microbiol.* (1976).
- Cinone, N., Hotje, H.D., Carotti, A. "Development of a Unique 3d Interaction Model of Endogenous and Synthetic Peripheral Benzodiazepine Receptor Ligands." *J. Comput. Aided Mol. Des.* 14, no. 8 (2000): 753-768.
- Clark, L. C. and Lyons, C. "Electrode Systems for Continuous Monitoring Cardiovascular Surgery." *Ann.NY Acad.Sci.* 102 (1962): 29-45.
- Clark, M., Cramer, R. D., and van Opdenbosch, N. "Validation of the General Purpose Tripos 5.2 Force Field." *Journal of Computational Chemistry* 10 (1989): 982-1012.
- Coker, R.D. "Mycotoxins and Their Control: Constraints and Opportunities." In *Mycotoxins. Encyclopaedia of Life Sciences*, ed. D. Bhatnagar, Ehrlich, K.C., Chang, P.K.: Nature publishing group, 1997.

- Coker, R.D., Nagler, M.J.H., Blunden, G. Shaskey, A.J., Defize, P.R., Derksen, G.B. and Whitaker, T.B. "Design of Sampling Plans for Mycotoxins in Foods and Feeds." *Natural Toxins* 3 (1995): 257-262.
- Colman, P., Laver, W., Varghese, J., Baker, Tulloch, P., Air, G., and Webster, R. "Three-Dimensional Structure of a Complex of Antibody with Influenza Virus Neuraminidase." *Nature* 326 (1987): 358-363.
- Compagnone, D., Schweicher, P., Kauffman, J. M., and Guilbault, G. G. "Sub-Micromolar Detection of Hydrogen Peroxide at a Peroxidase/Tetramethylbenzidine Solid Carbon Paste Electrode." *Analytical Letters* 31, no. 7 (1998): 1107 - 1120.
- Conneely, G., Aherne, M., Lu, H.H., Guilbault, G.G. "Development of an Immunosensor for the Detection of Testosterone in Bovine Urine." *Anal. Chim. Acta* 583 (2007): 153-160.
- Cornell, W.D., Cieplak, P., Bayly, C.I., Gould, I.R., Merz Jr., K.M., Ferguson, D.M., Spellmeyer, D.C., Fox, T., Caldwell, J.W., Kollman, P.A. "A Second Generation Force Field for the Simulation of Proteins, Nucleic Acids, and Organic Molecules." *J. Am. Chem. Soc.* 117 (1995): 5179-5197.
- Cottrell, F.G. *Z. Physik.Chem.* 42 (1902): 385.
- Cramer, R.D. "Computer Graphics in Drug Design." *Pharmacy International* (1983): 106-107.
- Cramer, R.D., Patterson, D.E., Bunce, J.D. "Comparative Molecular Field Analysis (Comfa): Effect of Shape on Binding of Steroids to Carrier Proteins." *J. Am. Chem. Soc.* 110 (1988): 5959-5967.
- Creppy, E.E., Roseenthaler, R. and Dirheimer, G. "Inhibition of Protein Synthesis in Mice by Ochratoxin a and Its Prevention by Phenylalanine." *Food. Chem. Toxicol.* 22, no. 883-886 (1984).
- Crew, A., Alford, C., Cowell, D.C.C. and Hart, J.P. "Development of a Novel Electrochemical Immuno-Assay Using a Screen Printed Electrode for the Determination of Secretory Immunoglobulin a in Human Sweat." *Electrochimica Acta* 52, no. 16 (2007): 5232-5237.
- Cunningham, A. J. *Introduction to Bioanalytical Sensors*. New York: John Wiley & Sons, Inc., 1998.
- Currie, L.A. "Detection: International Update, and Some Emerging Di-Lemmas Involving Calibration, the Blank, and Multiple Detection Decisions." *Chemometrics and Intelligent Laboratory Systems* 37 (1997): 151-181.
- Dakovic, A., Tomašević-canovic, M., Dondur, V., Rottinghaus, G.E., Medakovic, V. and Zarić, S. "Adsorption of Mycotoxins by Organozeolites." *Colloids and Surfaces B: Biointerfaces* 46, no. 1 (2005): 20-25.

- Daly, S.J., Keating, G.J., Dillon, P.P., Manning, B.M., O'Kennedy, R., Lee, H.A., Morgan, M.R.A. "Development of Surface Plasmon Resonance-Based Immunosensor for Aflatoxin B1." *Journal of Agriculture and Food Chemistry* 48, no. 11 (2000): 5097-5104.
- Danielsson, B. "Enzyme Thermistors for Food Analysis." In *Food Biosensor Analysis*, ed. G. and Guilbault Wagner, G.G., Chapter 8. New York: Marcel Dekker, 1994.
- Danielsson, B. "High- Sensitivity Assay for Pesticide Using a Peroxidase as Chemiluminescent Label." *Analytical Chemistry* 71 (1999): 5258 - 5261.
- Darain, F., Park, S.U. and Shim, Y.B. "Disposable Amperometric Immunosensor System for Rabbit IgG Using a Conducting Polymer Modified Screen-Printed Electrode." *Biosensors & Bioelectronics* 18 (2003): 773-780.
- Day, E.D. *Advanced Immunochemistry*. 2nd ed. New York, USA: John Wiley and Sons, 1990.
- Day, R. "The Development of a Synthetic Receptor Specific to Glycosylated Haemoglobine for Biosensing Application." PhD thesis, Cranfield University, 1999.
- De Groene, E.M., Jahn, A., Horbach, G.J., Fink- Gremmels, J. "Mutagenicity and Genotoxicity of the Mycotoxin Ochratoxin A." *Environmental Toxicology and Pharmacology* 1 (1996): 21-26.
- De La Lastra, J. M. P., Van Den Berg, C. W. , Bullido, R., Almazan, F., Dominguez, J., Llanes, J. D., Morgan, B. P. "Epitope Mapping of 10 Monoclonal Antibodies against the Pig Analogue of Human Membrane Cofactor Protein (Mcp)." *Immunology* 99 (1999): 663-670.
- De Lorimier, A.A. "Alcohol, Wine, and Health." *The American Journal of Surgery* 180, no. 5 (2000): 357-361.
- De Saeger, S., Sibanda, L., Desmet, A., Van Peteghem, C. "A Collaborative Study to Validate Novel Field Immunoassay Kits for Rapid Mycotoxin Detection." *Int J Food Microbiol.* 75, no. 1-2 (2002): 135-142.
- Dietrich, R., Schneider, E., Usleber, E. and Martlbauer, E. "Use of Monoclonal Antibodies for the Analysis of Mycotoxins." *Natural Toxins* 3 (1995): 288-293.
- DiffChamb. Citing internet recourse: [www.diffchamb.com/](http://www.diffchamb.com/), Accessed 2004.
- Dirheimer, G., and Creppy, E.E.,. "Mechanism of Action of Ochratoxin A." *IARC Sci. Publ.* 115 (1991): 171-186.
- Dixon, S., Blaney, J., Weininger, D. "Characterizing and Satisfying the Steric and Chemical Restraints of Binding Sites." In *Presented at the Third York Meeting*, 1993.



- Dominguez Renedo, O., Alonso-Lomillo, M.A., Arcos Martinez, M.J. "Recent Developments in the Field of Screen-Printed Electrodes and Their Related Applications." *Talanta* Article in Press (2007).
- Dong, X., Zhang, Z., Wen, R., Shen, J., Shen, X., and Jiang, H. "Structure-Based De Novo Design, Synthesis, and Biological Evaluation of the Indole-Based Ppar? Ligands (I)." *Bioorganic & Medicinal Chemistry Letters* 16, no. 22 (2006): 5913-5916.
- Donnelly, R.A. "Geometry Optimization by Simulated Annealing." *Chemical Physics Letters* 136, no. 3 (1987): 4.
- Dorrenhaus, A., and Follmann, W. "Effects of Ochratoxin a on DNA Repair in Cultures of Rat Hepatocytes and Porcine Urinary Bladder Epithelial Cells." *Arch. Toxicol.* 71 (1997): 709-7.
- Draisci, R., Quadri, F., Achene, L., Volpe, G., Palleschi, L., Palleschi, G. "A New Electrochemical Enzyme-Linked Immunosorbent Assay for the Screening of Macrolide Antibiotic Residues in Bovine Meat." *The Analyst* 126, no. 1942-1946 (2001).
- Ducey, C. M. and Frank, M. B. *Hybridoma Production*. In: Frank, M. B. ed. *Molecular Biology Protocols*, 1997. Accessed Citing internet reference:<http://omrf.ouhsc.edu/~frank/fill-in.html>.
- Durst, R. A., Baumner, A. J., Murray, R. W., Buck, R. P. and Andrieux, C. P. "Chemically Modified Electrodes: Recommended Terminology and Definitions." *Pure & Appl. Chem.* 69, no. 6 (1997): 1317-1323.
- Durup, J. and Alary, F. "Molecular Dynamics Study of the Dissociation of an Antigen-Antibody Complex in Solution." *Journal of Molecular Engineering* 5, no. 1-3 (1995): 121-134.
- Eden, D.A. "Electrochemical Noise in Uhlig's Corrosion Handbook." ed. R.W. Revie. New York: John Wiley, 2000.
- Eggins, B.R. *Chemical Sensors and Biosensors (Analytical Techniques in the Sciences)*. New York: John Wiley, 2002.
- Einstein, A. "Über Die Von Der Molekularkinetischen Theorie Der Wärme Geforderte Bewegung Von in Ruhenden Flüssigkeiten Suspendierten Teilchen." *Ann. Phys.* 17 (1905): 549.
- EMAN (European Mycotoxin Awareness Network). *Fact Sheet 3. Ochratoxin A*. Citing internet resource (WWW document): <http://193.132.193.215/eman2/fsheet3.asp>, Accessed 2004.
- Engler, E. M., Andose, J.D. and Schleyer, P.v.R. "Critical Evaluation of Molecular Mechanics." *J. Am. Chem. Soc.* 95, no. 8005-5025 (1973).

- Esser, P. "Activity of Adsorbed Antibodies." *Nunc Bulletin No. 11*, no. 2 (1988): 1-6.
- Esser, P. "Principles in Adsorption to Polystyrene." *Nunc Bulletin No. 6* (1988): 1-5.
- Esser, P. "Detergent in Polystyrene Elisa." *Nunc Bulletin No. 8* (1989): 1-8.
- Euro-Diagnostica B.V. *Citing Internet Recourse (Www Document): Www.Eurodiagnostica.Com*. UK distributor: Raisio Diagnostics Ltd., 2004. Accessed 2004.
- European Commission. "Commission Regulation (Ec) No 466/2001." *Official Journal of the European Communities No. L77* (2001): 1-13.
- European Commission. "Commission Regulation (Ec) No 472/2002." *Journal of the European Communities No. L75* (2002): 18-20.
- European Commission. "Corrigendum of 23 March 2002." *Official Journal of the European Communities No. L80* (2002): 42.
- European Commission. "Commission Regulation (Ec) No 123/2005." *Journal of the European Communities L 25* (2005): 3.
- Evans, D. H., O'Connell, K.M., Petersen, R.A., Kelly, M.J. "Cyclic Voltammetry (Soa-Electrochemistry)." *Journal of Chemical Education* 60 (1983): 290.
- Fägerstam, L.G. "Biospecific Interaction Analysis Using Surface Plasmon Resonance Detection Applied to Kinetic, Binding Site and Concentration Analysis." *Journal of Chromatography* 597 (1992): 397-410.
- Fägerstam, L.G. and O'Shannessy, D.J. "Surface Plasmon Resonance Detection in Affinity Technologies." In *In: Handbook of Affinity Chromatography*, ed. T. Kline. New York: Marcel Dekker, 1993.
- FAO (Food and Agriculture Organization). *Regulations for Mycotoxins 1995. A Compendium*. Rome, Italy: Food and Agriculture Organization of the United Nations, 1995.
- FAO (Food and Agriculture Organization). "Worldwide Regulations for Mycotoxins 1995. A Compendium." *FAO Food and Nutrition Paper No. 64* (1997).
- FAO (Food and Agriculture Organization). *Worldwide Regulations for Mycotoxins in Food and Feed in 2003*. Rome, Italy: Food and Agriculture Organization of the United Nations, 2004.
- FEHD (Food and Environmental Hygiene Department). *Risk Assessment Study No. 23. Ochratoxin a in Food. Fehd. Food Consumption Survey.*: Hong Kong Food and Environmental Hygiene Department, 2005.

- Feldman, B.J., Krishnan, R., Plante, P.J., Vivolo, J.A. "Freestyle: A Small (300nl) Volume Electrochemical Glucose Sensor for Home Blood Glucose Testing." In *The Sixth World Congress on Biosensors*. San Diego, USA: Elsevier Science, 2000.
- Fincham, C.I., Horwell, D.C., Ratcliffe, G.S., Rees, D.C. "The Use of a Proline Ring as a Conformational Restraint in Cck-B Receptor "Dipeptoids"." *Bioorg. Med. Chem. Lett.* 2 (1992): 403–406.
- Fletcher, S. and Horne, M.D. "Random Assemblies of Microelectrodes (Ram&Unknown; Electrodes) for Electrochemical Studies." *Electrochemical Communications* 1, no. 10 (1999): 502-512.
- Fletcher, S. and Horne, M.D. "Random Assemblies of Microelectrodes (Ram™ Electrodes) for Electrochemical Studies." *Electrochem. Commun.* 1 (1999): 502-512.
- Forrest, S. "Genetic Algorithm: Principles of Natural Selection Applied to Computation." *Science* 261 (1993): 872-878.
- Forster, R.J. "Microelectrodes: New Dimensions in Electrochemistry." *Chem. Soc. Rev.* 23 (1994): 289-297.
- Francis, F.J. *Wiley Encyclopedia of Food Science and Technology*. Vol. 1-4. 2nd ed., 1999.
- Frenkel, D., Clark, D.E., Li, J., Murray, C.W., Robson, B., Waszkowycz, B. and Westhead, D.R. "Pro\_Ligand: An Approach to De Novo Molecular Design. 4. Application to Design of Peptides." *J. Comput.-Aided Mol.* 9 (1995): 213-225.
- FSA (Food Standards Agency). *Update on Chemical Contaminants Legislation*. 2006.
- Fujii S, Ribeiro RM, Scholz MB, Ono EY, Prete CE, Itano EN, Ueno Y, Kawamura O, Hirooka EY. Reliable indirect competitive ELISA used for a survey of ochratoxin A in green coffee from the North of Paraná State, Brazil. *Food Addit Contam.* (2006), 23(9):902-9.
- Galtier, P., Alvinerie, M. and Charpentreau, J.L. "The Pharmacokinetic Profiles of Ochratoxin a in Pigs, Rabbits and Chickens." *Food Cosmet Toxicol.* 19 (1981): 735-738.
- Gekle, M., Gabner, B., Freudinger, R., Mildenerger, S., Silbernagl, S., Pfaller, W., Schramek, H. "Characterization of an Ochratoxin-a-Dedifferentiated and Cloned Renal Epithelial Cell Line." *Toxicol. Appl. Pharmacol.* 152 (1998): 282-291.
- Geklea, M., Gaßnera, B., Freudingera, R., Mildenergera, S., Silbernagla, S., Pfallerb, W. and Schramek< H. "Characterization of an Ochratoxin-a-Dedifferentiated and Cloned Renal Epithelial Cell Line." *Toxicol. Appl. Pharmacol.* 152 (1998): 282-291.

- Garnier, J., Osguthorpe, D.J. and Robson, B. "Analysis of the Accuracy and Implications of Simple Methods for Predicting the Secondary Structure of Globular Proteins." *J. Mol. Biol.* 120, no. 97–120 (1978).
- Gaus, K. and Hall, E.A.H. Short peptide receptor mimics for atherosclerosis risk assessment of LDL. *Biosensors and Bioelectronics*, 18, (2003):151-164.
- Gilbert, J. "Overview of Mycotoxin Methods, Present Status and Future Needs." *Natural Toxins* 7 (2000): 347-352.
- Gilis, M., Durliat, H., and Comtat, M. "Electrochemical Biosensors for Assays of L-Malic and D-Lactic Acids in Wines." *Am. J. Enol. Vitic.* 47 (1996): 11-16.
- Gilmartin, M.A.T. and Hart, J.P. "Sensing with Chemically and Biologically Modified Carbon Electrodes." *The Analyst* 120 (1995): 1029-1045.
- Gilson, M. K., Given, J. A., Bush, B. L. and McCammon, J. A. "The Statistical & Thermodynamic Basis for Computation of Binding Affinities: A Critical Review." *Biophys. J.* 72 (1997): 1047-1069.
- Giraudi, G., Anfossi, L., Baggiani, C., Giovannoli, C. Tozzi, C. Solid-phase extraction of ochratoxin A from wine based on a binding hexapeptide prepared by combinatorial synthesis. *Journal of Chromatography A*, 1175, 2, (2007):174-180.
- Global Peptide Services. *Peptides*. Citing internet resources (WWW document): <http://www.globalpeptide.com/faq.html>, Accessed 2007.
- Goldblatt, D. "Simple Solid Phase Assays of Avidity." *Immunochemistry* 2 (1997): 31-35.
- González-Peñas, E., Leache, C., Viscarret, M., Pérez de Obanos, A., Araguás, C. and López de Cerain, A. "Determination of Ochratoxin a in Wine Using Liquid-Phase Microextraction Combined with Liquid Chromatography with Fluorescence Detection." *Journal of Chromatography A* 1025, no. 2 (2004): 163-168.
- Goodford, P. J. A. "Computational Procedure for Determining Energetically Favorable Binding Sites on Biologically Important Macromolecules." *J. Med. Chem.* 28 (1985): 849-857.
- Gorton, L. *Electrochemical Biosensors*. Sweden: Chemical Centre at LTH, Lund University, 2003. Seminar as part of a biosensor technology lecture series.
- Goryacheva, I.Y., De Saeger, S., Nesterenko, I.S., Eremin, S.A., Van Peteghem, C. "Rapid All-in-One Three-Step Immunoassay for Non-Instrumental Detection of Ochratoxin a in High-Coloured Herbs and Spices." *Talanta* 72, no. 3 (2007): 1230-1234.

- Goryacheva, I.Y., Basova, E.Y., Van Peteghem, C., Eremin, S.A., Pussemier, L, Motte, J.C., De Saeger, S. "Novel gel-based rapid test for non-instrumental detection of ochratoxin A in beer". *Anal Bioanal Chem.* (2008);390(2):723-7.
- Gronbaek, M. "Type of Alcohol Consumed and Mortality from All Causes, Coronary Heart Disease, and Cancer." *Annals of Internal Medicine* 133 (2000): 411-419.
- Guo, B., Anzai, J., OSA, T. "Adsorption Behaviour of Serum Albumin on Electrodes Surfaces and the Effects of Electrode Potential." *Chem. Pharm. Bull.* 44 (1996): 800-803.
- Gyongyosi-Horvath, A. Barna-Vetro, I. and Solti, L. "A New Monoclonal Antibody Detecting Ochratoxin a at the Picogram Level." *Lett. Appl. Microbiol.* 22, no. 2 (1996): 103-105.
- Hage, D.S. "Immunoassays." *Anal. Chem.* 71 (1999): 294-304.
- Hage, D.S. "Affinity Chromatography: A Review of Clinical Applications." *Clinical Chemistry* 45, no. 5 (1999): 593-615.
- Hage, David S. "Survey of Recent Advances in Analytical Applications of Immunoaffinity Chromatography." *Journal of Chromatography B* 715 (1998): 3-28.
- Hahn, K.W., Klis, W.A., Stewart, J.M. "Design and Synthesis of a Peptide Having Chymotrypsin-Like Esterase Activity." *Science* 248 (1990): 1544-1 547.
- Halgren, T. "Maximally Diagonal Force Constants in Dependent Angle-Bending Coordinates. Ii. Implications for the Design of Empirical Force Fields." *J. Am. Chem. Soc.* 112 (1990): 4710-4723.
- Halgren, T. "Merck Molecular Force Field. I. Basis, Form, Scope, Parameterization, and Performance of Mmff94." *J. Comp. Chem.* 17 (1996): 490-641.
- Halgren, T. "Mmff Vi. Mmff94s Option for Energy Minimization Studies." *J. Comp. Chem.* 20 (1999): 720-748.
- Hansch, C. "Quantitative Approach to Biochemical Structure-Activity Relationships." *Acc. Chem. Res.* 2, no. 8 (1969): 232-239.
- Hansch, C. and Fujita, T. "A Method for the Correlation of Biological Activity and Chemical Structure." *J. Am. Chem. Soc.* 86 (1964): 1616-1626.
- Harris, J.P., Mantle, P.G. "Biosynthesis of Ochratoxins by *Aspergillus Ochraceus*." *Phytochemistry* 58 (2001): 709-716.
- Hart, J. P., Crew, A., Crouch, E., Honeychurch, K. C., Pemberton, R. M. "Some Recent Designs and Developments of Screen-Printed Carbon Electrochemical Sensors/Biosensors for Biomedical, Environmental, and Industrial Analyses." *Anal. Letters* 37, no. 5 (2004): 789-830.

- Hart, J.P., Wring, S.A. "Recent Developments in the Design and Application of Screen-Printed Electrochemical Sensors for Biomedical, Environmental and Industrial Analyses." *Trend. Anal. Chem.* 16, no. 2 (1997): 89-103.
- Haupt, K. "Creating a Good Impression." *Nature Biotechn.* 20 (2002): 884 - 885.
- Haupt, K. and Mosbach, K. "Plastic Antibodies: Developments and Applications." *Trends in Biotechnology* 16, no. 11 (1998): 468-475.
- Haupt, K. and Mosbach, K. "Molecularly Imprinted Polymers and Their Use in Biomimetic Sensors." *Chem. Rev.* 100 (2000): 2495-2504.
- Haupt, K., and Mosbach, K. "Molecular Imprinted Polymers in Chemical and Biological Sensing." *Biochem. Soc. Trans.* 27 (1999): 344-350.
- Haupt, R. and Haupt, S.E. *Practical Genetic Algorithms*: John Wiley & Sons, 1998.
- He, Y.N., Chen, H.Y., Zheng, J.J., Zhang, G.Y., Chen, Z.L. "Differential Pulse Voltammetric Enzyme-Linked Immunoassay for the Determination of Helicobacter Pylori Specific Immunoglobulin G (Igg) Antibody." 44, no. 5 (1997): 823-830.
- He, Y.-N., Chen, H.-Y., Zheng, J.-J., Zhang, G.-Y., and Chen, Z.-L. "Differential Pulse Voltammetric Enzyme-Linked Immunoassay for the Determination of Helicobacter Pylori Specific Immunoglobulin G (Igg) Antibody." *Talanta* 44 (1997): 823-830.
- Helica. Citing Internet recourses (WWW document): [www.accuratechemical.com/](http://www.accuratechemical.com/), Accessed 2004.
- Helrich, K. *Official Methods of Analysis*. 15th ed.: Association of Official Analytical Chemists, 1990.
- Hendrickson, W. A.; Teeter, M. M. "Structure of the Hydrophobic Protein Crambin Determined Directly from the Anomalous Scattering Sulfur Structure of the Hydrophobic Protein Crambin Determined Directly from the Anomalous Scattering of Sulfur." *Nature* 290, no. 5802 (1981): 107-113.
- Hermanson, G.T. *Bioconjugate Techniques*: Academic Press, 1996.
- Hermanson, G.T., Mallia, K.A, Smith, P.K. *Immobilized Affinity Ligand Techniques*. San Diego: Academic Press, 1992.
- Herzog, G. and Arrigan, D.W.M. "Application of Disorganized Monolayer Gold Electrode to Copper Determination in White Wine." *Analytical Letters* 37, no. 4 (2004): 591-602.
- Herzog, G.; Arrigan, D.W.M. "Underpotential Deposition and Stripping of Lead at Disorganized Monolayer-Modified Gold Electrodes." *Electroanalysis* 17, no. 20 (2005): 1816-1821.

- Hickling, J., Goellner, J., Burkert, A. and Heyn, A. "Evaluation of a Round Robin Experiment on Electrochemical Noise, Paper 385." In *Corrosion 98*. Houston: NACE International - Leaders in Corrosion Control Technology, 1998.
- Homola, J., Yee, S.S., Gauglitz, G. "Surface Plasmon Resonance Sensors: Review." *Sensors and Actuators B: Chemical* 54 (1999): 3-15.
- Horányi, G., Rizmayer, E. M. and Joó, P. J. "Radiotracer Study of the Adsorption of Cl<sup>-</sup> and HSO<sub>4</sub><sup>-</sup> Ions on a Porous Gold Electrode and on Underpotential Deposited Metals on Gold." *Electroanal. Chem* 152 (1983): 211-222.
- IARC. *Group 2b: Ochratoxin A*. Lyon, France, 1993.
- IARC (International Agency for Research on Cancer). *Classifications: Group 2b*. Citing internet resource (WWW document) : <http://monographs.iarc.fr/>, 25004. Accessed 2007.
- IARC, International Agency for Research on Cancer, Geneva, 56, 1993, p.26-32. "Monographs on the Evaluation of Carcinogenic Risks to Humans: Some Naturally Occurring Substances, Food Items and Constituents, Heterocyclic Aromatic Amines and Mycotoxins." In *Mycotoxins in the Food Chain: The Role of Ochratoxins*, ed. E. Petzinger, Weidenbach, A, 56, 26-32. Geneva: Livestock Production Science, 1993.
- Il'ichev, Y.V., Perry, J.L. and Simon, J.D. "Interaction of Ochratoxin a with Human Serum Albumin. Preferential Binding of the Dianion and Ph Effects." *J. Phys. Chem. B* 106 (2002): 452-459.
- IUPAC (International Union of Pure and Applied Chemistry). "Recommended Definitions and Classification." *Pure Appl. Chem.* 71, no. 12 (1999): 2333-2348.
- IWSR (International Wine and Spirit Record). *Wine and Spirit Consumption and Export*. Citing internet resource (WWW document): <http://www.iwsr.co.uk> . Accessed 2007.
- Jacobson, M. "Computation of Biological Molecules." *Biophysics* 298 (2003).
- Janeway, C.A., Travers, P., Walport, M. *Immunobiology: The Immune System in Health and Disease*. 6th ed. Chapter 3. US: Garland Publishing Inc, 2004.
- Janin, J. "Elusive Affinities." *Proteins: Struct. Funct. Genet.* 21 (1995): 30-39.
- Janin, J. and Cherfils, J. "Protein Docking Algorithms: Simulating Molecular Recognition." *Curr. Opin. Struct. Biol.* 3 (1993): 265-269.
- Janin, J., Wodak, S., Levitt, M., Maigret, B. "Conformation of Amino Acid Side-Chains in Proteins." *Journal of Molecular Biology* 125 (1978): 357-386+.
- JECFA. *Ochratoxin A*. 47. <http://www.inchem.org/documents/jecfa/jecmono/v47je04.htm>, 2001. Accessed.

- JECFA. "Evaluation of Certain Mycotoxins in Food (56th Report of the Joint Fao/Who Expert Committee on Food Additives)." In *Technical Reports Series No. 906*, 2002.
- Jiao, Kui and Zhang, Shusheng. "A Voltammetric Enzyme-Linked Immunoassay for Southern Bean Mosaic Virus." *Anal. Chem.* 2, no. 11 (2000): 49.
- Jodlbauer, J., Maier, N. M., Lindner, W. "Towards Ochratoxin a Selective Molecularly Imprinted Polymers for Solid Phase Extraction." *Journal of chromatography A* 945 (2002): 45-63.
- Joergensen, J. "Quantum and Statistical Mechanical Studies of Liquids. 10. Transferable Intermolecular Potential Functions for Water, Alcohols, and Ethers. Application to Liquid Water." *J. Am. Chem. Soc.* 103 (1981): 335-340.
- Johnsson, B., Lofas, S., Lindqvist, G. "Immobilization of Proteins to a Carboxymethyl-dextran Modified Gold Surface for Biospecific Interaction Analysis in Surface Plasmon Resonance." *Anal. Biochem.* 198 (1991): 268-277.
- Jones, B.N. "O-Phthalaldehyde Pre-Column Derivatization and R<sub>p</sub> Hplc of Polypeptide Hydrolyses and Physiological Fluids." *Journal of Chromatography B* 266 (1983): 471-482.
- Jones, G. and Willett, P. "Docking Small-Molecule Ligands into Active Sites." *Curr. Opin. Biotechnol.* 6 (1995): 652-656.
- Jones, S. and Thornton, J. M. "Principles of Protein-Protein Interactions." *Proc. Natl. Acad. Sci. USA* 93 (1996): 13-20.
- Jönsson, Ulf. "Real Time Bia-a New Biosensor Based Technology for the Direct Measurement of Biomolecular Interactions." *Biosensoren: Grundlagen, Technologien, Anwendungen* (1991).
- Jordan, D.B., Basarab, G.S., Liao, D.I., Johnson, W.M.P., Winzenberg, K.N. and Winkler, D.A. "Structure-Based Design of Inhibitors of the Rice Blast Fungal Enzyme Trihydroxynaphthalene Reductase." *Journal of Molecular Graphics and Modelling* 19, no. 5 (2001): 434-447.
- Jorgensen, K. "Occurrence of Ochratoxin a in Commodities and Processed Food - a Review of Eu Occurrence Data." *Food Additives and Contaminants* 22, no. 1 (2005): 26-30.
- Jørgensen, W. and Tirado-Rives, J. "The Opls Potential Functions for Proteins. Energy Minimizations for Crystals of Cyclic Peptides and Crambin." *J. Am. Chem. Soc.* 110 (1988): 1657-1666.
- Jørgensen, W., Chandrasekhas, J., Madura, J.D., Impey, R.W., and Klein, M.L. "Comparison of Simple Potential Functions for Simulating Liquid Water." *J. Chem. Phys.* 79 (1983): 926-935.



- Josephy, P.D., Elin, T., and Mason, R.P. "The Horseradish Peroxidase-Catalyzed Oxidation of 3,5,3',5'-Tetramethylbenzidine." *J. Biol. Chem.* 257, no. 7 (1982): 3669-3675.
- Kadara, R.O.; Newman, J.D.; Tothill, I.E. "Stripping Chronopotentiometric Detection of Copper Using Screen-Printed Three-Electrode System- Application to Acetic-Acid Bioavailable Fraction from Soil Samples." *Analytica Chimica Acta* 493 (2003): 95-104.
- Kadara, R.O.; Tothill, I.E. "Resolving the Copper Interference Effect on the Stripping Chronopotentiometric Response of Lead(II) Obtained at Bismuth Film Screen-Printed Electrode." *Talanta* 66 (2005): 1089-1093.
- Karlsson, R., Fägerstam, L., Nilshans, H. and Persson, B. "Analysis of Active Antibody Concentrations. Separation of Affinity and Concentration Parameters." *J. Immunol. Methods* 166 (1993): 74-84.
- Karush, F. "The Affinity of Antibody: Range, Variability, and the Role of Multivalence." *Comprehensive Immunology* 5 (1978): 85-116.
- Kasai, Ken-Ichi. "Frontal Affinity Chromatography: Theory for Its Application to Studies on Specific Interaction of Biomolecules." *Journal of Chromatography B* 376 (1986): 33-47.
- Kato, K. and Shimizu, A. "Highly Sensitive Enzyme Immunoassay for Human Creatine Kinase Mm and Mb Isoenzymes." *Clinical Chimica Acta* 158, no. 1 (1986): 99-108.
- Kennedy, J.F. and Cabral, J.M.S. "Immobilized Enzymes." In *Solid Phase Biochemistry Aspects*, ed. W.H. Scouten. New York: John Wiley & Sons,, 1983.
- Killard, A.J., Zhang, S.Q., Zhao, H.J., John, R., Iwuoha, E.I. and Smyth, M.R. "Development of an Electrochemical Flow Injection Immunoassay (Fiia) for the Realtime Monitoring of Biospecific Interactions." *Anal. Chim. Acta* 400 (1999): 109-119.
- Kilmartin, P.A., Zou, H.L., Waterhouse, A.L. "A Cyclic Voltammetric Method Suitable to Characterise Antioxidant Properties of Wine and Wine Phenolics." *J. Agric. Food. Chem.*, 49 (2001): 1957-1965.
- Kilmartin, P.A., Zou, H.L., Waterhouse, A.L. "Correlation of Wine Phenolic Composition Versus Cyclic Voltammetry Response." *Am. J. Enol. Vitic.* 53 (2002): 294-303.
- Kirkpatrick, S., Gelatt, C.D. and Vecchi, M.P. "Optimization by Simulated Annealing." *Science* 220 (1983): 671-678.
- Kissinger, P.T. and Heineman, W.R. "Cyclic Voltammetry." *J. Chem. Educ.* 60 (1983): 697.

- Kissinger, P.T. and Heinemann, W.R. *Laboratory Techniques in Electroanalytical Chemistry*. 2nd ed. New York: CRC, 1996.
- Koeller, G., Wichmann, G., Rolle-Kampczyk, U., Poppe, P., Herbarth, O. "Comparison of Elisa and Capillary Electrophoresis with Laser-Induced Fluorescence Detection in the Analysis of Ochratoxin a in Low Volumes of Human Blood Serum." *J. Chromatogr. B* 840 (2006): 94-98.
- Kollman, P. "Free Energy Calculations- Applications to Chemical and Biological Phenomena." *Chem. Rev.* 93 (1993): 2395-2417.
- Kong Food and Environmental Hygiene Department. *Food Consumption Survey*. Kong Food and Environmental Hygiene Department, 2005.
- Kontoyianni, M., McClellan, L. M., Sokol, G. S. "Evaluation of Docking Performance: Comparative Data on Docking Algorithms." *J. Med. Chem.* 47 (2004): 558-565.
- Kooyman, R.P.H., Lechuga, L.M. *Handbook of Biosensors and Electronic Noses-Medicine, Food and Environment*. Vol. Chapter 8: CRC Press, 1996.
- Kriz, D., Ramström, O., Svensson, A. and Mosbach, K. "Introducing Biomimetic Sensors Based on Molecularly Imprinted Polymers as Recognition Elements." *Anal. Chem.* 67 (1995): 2142-2144.
- Krovat, E.M., Steindl, T. and Langer, T. "Recent Advances in Docking and Scoring." *Current Computer-Aided Drug Design* 1 (2005): 93-102.
- Labanowski, J., Motoc, I., Naylor, C.B., Mayer, D., Dammkoehler, R.A. "Three-Dimensional Quantitative Structure-Activity Relationships. 2. Conformational Mimicry and Topographical Similarity of Flexible Molecules." *Quantitative Structure-Activity Relationships* 5, no. 4 (1986): 138-152.
- Landsteiner, K. *Specificity of Serological Reactions*. Cambridge, Massachusetts, USA: Harvard University Press, 1945.
- Langman, R.E. "The Specificity of Immunological Reactions." *Mol. Immunol.* 37 (2000): 555-561.
- Lanyon, Y.H., De Marzi, G., Watson, Y.E., Quinn, A.J., Gleeson, J.P., Redmond, G. and Arrigan, D.W.M. "Fabrication of Nanopore Array Electrodes by Focused Ion Beam Milling." *Anal. Chem.* 79 (2007): 3048-3055.
- Larrson, A. "Regression Analysis of Simulated Radio-Ligand Equilibrium Experiments Using Seven Different Mathematical Models." *Journal of Immunological Methods* 206 (1997): 135-142.
- Laschi, S., Palchetti, I., Mascini, M. "Gold-Based Screen-Printed Sensor for Detection of Trace Lead." *Sensors & Actuators B* 114 (2006): 460-465.

- Ledru, S., Ruille, N. and Boujtita, M. "One-Step Screen-Printed Electrode Modified in Its Bulk with Hrp Based on Direct Electron Transfer for Hydrogen Peroxide Detection in Flow Injection Mode." *Biosensors & Bioelectronics* 21, no. 8 (2006): 1591-1598.
- Lee, H.B.; Magan, N. "Impact of Environment and Interspecific Interactions between Spoilage Fungi and *Aspergillus Ochraceus* on Growth and Ochratoxin Production in Maize Grain." *International Journal of Food Microbiology* 61 (2000): 11-16.
- Lee, S. C., and Chu, F. S. "Enzyme-Linked Immunosorbent Assay for Ochratoxin a in Wheat." *J. Assoc. Off. Anal. Chem.* 67, no. 1 (1984): 45-49.
- Leickt, L. and Ohlson, S. "Prediction of Affinity and Kinetics in Biomolecular Interactions by Affinity Chromatography." *Analytical Biochemistry* 291 (2001): 102-108.
- Leitner, A., Zöllner, P., Paolillo, A., Stroka, J., Papadopoulou-Bouraoui, A., Jaborek, S., Anklam, E. and Lindner, W. "Comparison of Methods for the Determination of Ochratoxin a in Wine." *Analytica Chimica Acta* 453, no. 1 (2002): 33-41.
- Leoni, L.A.B., Soares, L.M.V. and Oliveira, P.L.C. "Ochratoxin a in Brazilian Roasted and Instant Coffees." *Food Addit. Contam.* 10 (2000): 867-870.
- Liem, H. H., Cardenas, F., Tavassoli, M., Poh-Fitzpatrick, M. B., and Muller-Eberhard, U. "Quantitative Determination of Hemoglobin and Cytochemical Staining for Peroxidase Using 3,3',5,5'-Tetramethylbenzidine Dihydrochloride, a Safe Substitute for Benzidine." *Analytical Biochemistry* 98, no. 2 (1979): 388-393.
- Lim, V.I. "Structural Principles of the Globular Organization of Protein Chains. A Stereochemical Theory of Globular Protein Secondary Structure." *J. Mol. Biol.* 88 (1974): 857-872.
- Lin, L. "Thin-Layer Chromatography of Mycotoxins and Comparison with Other Chromatographic Methods." *Journal of Chromatography A* 815 (1998): 3-20.
- Lindenmeier, M., Schieberle, P. and Rychlik, M. "Quantification of Ochratoxin a in Foods by a Stable Isotope Dilution Assay Using High-Performance Liquid Chromatography-Tandem Mass Spectrometry." *Journal of Chromatography A* 1023, no. 1 (2004): 57-66.
- Liu, S.Q. and Ju, H.X. "Renewable Reagentless Hydrogen Peroxide Sensor Based on Direct Electron Transfer of Horseradish Peroxidase Immobilized on Colloidal Gold-Modified Electrode." *Anal. Biochem.* 307, no. 1 (2002): 110-116.
- Lofas, S. and Johnsson, B. "A Novel Hydrogel Matrix on Gold Surfaces in Surface Plasmon Resonance Sensors for Fast and Efficient Covalent Immobilization of Ligands." *J. Chem. Soc. Chem. Commun.* 21 (1990): 1526 - 1528.

- Logrieco, A., Arrigan, D.W.M., Brengel-Pesce, K., Siciliano, P., Tothill, I. "Microsystems Technology Solutions for Rapid Detection of Toxigenic Fungi and Mycotoxins." *Food Additives and Contaminants* 22, no. 4 (2004): 335-344.
- Logrieco, A., Arrigan, D.W.M., Brengel-Pesce, K., Siciliano, P. and Tothill, I. "DNA Arrays, Electronic Noses and Tongues, Biosensors and Receptors for Rapid Detection of Toxigenic Fungi and Mycotoxins: A Review." *Food Additiv. Contam.* 22, no. 4 (2005): 335-344.
- Loomans, E.M.G. and Schielen, W.J.G. "Assessment of the Functional Affinity Constant of Monoclonal Antibodies Using an Improved Enzyme-Linked Immunosorbent Assay." *Journal of Immunological Methods* 184 (1995): 207-217.
- Loomans, E.M.G. "The Influence of Binding Capacity and Affinity on the Improved Performance of N-Terminally Extended Hcg Peptides, Determined by Elisa-Based Procedures." *Journal of Immunological Methods* 221 (1998): 119-130.
- Lotierzo, M., Henry, O.Y.F., Piletsky, S., Tothill, I., Cullen, D., Kania, M., Hock B. and A.P.F. Turner. "Surface Plasmon Resonance Biosensor for Domoic Acid Based on Grafted Imprinted Polymers." *Biosensors and Bioelectronics* 20 (2004): 145-152.
- Lu, H., Conneely, G., Pravda, M., Guilbault, G. G. "Screening of Boldenone and Methylboldenone in Bovine Urine Using Disposable Electrochemical Immunosensors." *Steroids* 71 (2006): 760-767.
- Lundström, Ingemar. "Real-Time Biospecific Interaction Analysis." *Biosensors and Bioelectronics* 9 (1994): 725-736.
- Lybrand, T. P. "Ligand-Protein Docking and Rational Drug Design." *Curr. Opin. Struct. Biol.* 5 (1995): 224-228.
- MacKerell, Jr., A.D. "Protein Force Fields." In *Encyclopedia of Computational Chemistry*, ed. P. v.R. Schleyer, Allinger, N.L., Clark, T., Gasteiger, J., Kollman, P.A., Schaefer, H.F., Schreiner, P.R. Chichester: John Wiley & Sons, 1998.
- MacMasters, D.R. und Vedani, A. "Ochratoxin a Binding to Phenylalanyl-Trna Synthetase: A Computational Approach to Ochratoxicosis and Its Antagonism." *J.Med.Chem.* 42, no. 16 (1999): 3075-3086.
- Mahony, J.O., Nolan, K., Smyth, M.R. and Mizaikoff, B. "Molecularly Imprinted Polymers—Potential and Challenges in Analytical Chemistry." *Analytica Chimica Acta* 534, no. 1 (2005): 31-39.
- Maier, N.M., Buttinger, G., Welhartiziki, S., Gaviolo, E., Lindner, W. "Molecularly Imprinted Polymer-Assisted Sample Clean-up of Ochratoxin a from Red Wine: Merits and Limitations." *Journal of Chromatography B* 804, no. 1 (2004): 103-111.

- Malmqvist, M. "Biospecific Interaction Analysis Using Biosensor Technology." *Nature* 361 (1993): 186-187.
- Malmqvist, M. and Karlsson, R. "Biomolecular Interaction Analysis: Affinity Biosensor Technologies for Functional Analysis of Proteins." *Current Opinion in Chemical Biology* 1, no. 3 (1997): 378-383.
- Maragos, C.M., Thompson, V.S. "Fibre-Optic Immunosensor for Mycotoxins." *Natural Toxins* 7 (1999): 371-376.
- Markey, F. "What Is Spr Anyway?" *BIAjournal* 6 (1999): 14-17.
- Mascini, M. "Affinity Electrochemical Biosensors for Pollution Control." *Pure and Applied Chemistry* 73 (2001): 23-30.
- Mascini, M. *New Trends in Nucleic Acid Based Biosensors*. Florence, Italy: Department of Chemistry, University of Florence, 2003.
- Mascini, M., Palchetti, I., Marraza, G. "DNA Electrochemical Biosensors." *Fresenius Journal of Analytical Chemistry* 369 (2001): 15-20.
- McKimm-Breschkin, J.L. "The Use of Tetramethylbenzidine for Solid Phase Immunoassays." *Journal of Immunological Methods* 135, no. 1-2 (1990): 277-280.
- Meusel, Markus Gerdes, Melanie. "Influence of Antibody Valency in a Displacement Immunoassay for the Quantitation of 2,4-Dichlorophenoxyacetic Acid." *Journal of Immunological Methods* 223 (1999): 217-226.
- Micheli, L., Grecco, R., Badea, M., Moscone, D., Palleschi, G. "An Electrochemical Immunosensor for Aflatoxin M1 Determination in Milk Using Screen-Printed Electrodes." *Biosensors and Bioelectronics* 21 (2005): 588-596.
- Micheli, L., Radoi, A., Guarrina, R., Massaud, R., Bala, C., Moscone, D., Palleschi, G. "Disposable Immunosensor for the Determination of Domoic Acid in Shellfish." *Biosensors & Bioelectronics* 20 (2004): 190-196.
- Mitchell, M. *An Introduction to Genetic Algorithms*: MIT Press, 1996.
- Moon, J.B. and Howe, W.J. "Computer Design of Bioactive Molecules: A Method for Receptor-Based De Novo Ligand Design." *Proteins* 11 (1991): 314-328.
- Moore, E. J., Pravda, M., Kreuzer, M. P. and Guilbault, G. G. "Comparative Study of 4-Aminophenyl Phosphate and Ascorbic Acid 2-Phosphate, as Substrates for Alkaline Phosphatase Based Amperometric Immunosensor." *Anal. Letters* 36 (2003): 303-313.
- Morgan, M. R. A., McNenney, R. and Chan, H. W.-S. "Enzyme-Linked Immunosorbent Assay of Ochratoxin a in Barley." *J. Assoc. Off. Anal. Chem.* 66 (1983): 1481-1484.

- Morris, Glenn E. "Treatment of Human Muscle Creatine Kinase with Glutaraldehyde Preferentially Increases the Immunogenicity of the Native Conformation and Permits Production of High Affinity Monoclonal Antibodies Which Recognize Two Distinct Surface Epitopes." *Journal of Immunological Methods* 125 (1989): 251-259.
- Morris, J.R. and Main G.L. "Finishing Agents for Wine." In *14th NM Conference*. New Mexico, 1995.
- Moulton, S.E., Barisci, J.N., Bath, A., Stella, R., Wallace, G.G. "Investigation of Protein Adsorption and Electrochemical Behaviour at a Gold Electrode." *J. Colloid Interface Sci.* 261 (2003): 312-319.
- Muegge, I. and Rarey, M. "Small Molecule Docking and Scoring." *Rev. Comput. Chem.* 17 (2001): 1-60.
- Mukkur, T. K. S. "Thermodynamics of Hapten-Antibody Interactions." *Trends Biochem. Sci.* 5 (1980): 72-74.
- Muller, G., Kielstein, P., Kohler, H., Berndt, A., Rosner, H. "Studies on the Influence of Ochratoxin a on Immune and Defense Reactions in the Mouse Model." *Mycoses* 38 (1995): 85-91.
- Muller, G., Kielstein, P., Rosner, H., Berndt, A., Heller, M., Kohler, H. "Studies on the Influence of Ochratoxin a on Immune and Defense Reactions in Weaners." *Mycoses* 422 (1999): 495-505.
- Murray, R. W., Ewing, A. G. and Durst, R. A. "Chemically Modified Electrodes - Molecular Design for Electroanalysis." *Anal. Chem.* 59 (1987): 379A-385A.
- National Institutes of Health (NIH), CMM (Centre of Molecular Modelling). *Molecular Modelling*. Citing Internet recourses (WWW document): [http://cmm.info.nih.gov/modeling/guide\\_documents/molecular\\_mechanicsdocument.html#mm\\_principles\\_anchor](http://cmm.info.nih.gov/modeling/guide_documents/molecular_mechanicsdocument.html#mm_principles_anchor), Accessed 2005.
- Nemethy, G., Pottle, M.S. and Scheraga, H.A. "Energy Parameters in Polypeptides. 9. Updating of Geometrical Parameters, Nonbonded Interactions, and Hydrogen Bond Interactions for the Naturally Occurring Amino Acids." *J. Phys. Chem.* 87 (1983).
- Neogen. *Citing Internet Recourses (Www Document):* <Http://Www.Neogen.Com/>. Accessed 2004.
- Ngundi, M.M., Qadri, S.A., Wallace, E.V., Moore, M.H., Lassman, M.E., Shriver-Lake, L.C., Ligler, F.S. and Taitt, C.R. *Environ. Sci. Technol.* 40 (2006):2352.
- Ngundi, M.M., Shriver-Lake, L.C., Moore, M.H., Lassman, M.E., Ligler, F.S., and Taitt, C.R. *Anal. Chem.* 77 (2005):148.

- Newman, J., White, S., Tothill, I.E. and Turner, A.P.F. "Catalytic Materials, Membranes and Fabrication Technologies Suitable for the Construction of Amperometric Biosensors." *Analytical Chemistry* 67 (1995): 4594-4599.
- Newman, J.D. and Turner, A.P.F. "Home Blood Glucose Biosensors: A Commercial Perspective." *Biosensors and Bioelectronics* 20, no. 12 (2005): 2435-2453.
- Newman, J.D., Turner, A.P.F. and Marrazza, G. "Ink-Jet Printing for the Fabrication of Amperometric Glucose Biosensors." *Anal. Chim. Acta* 262 (1992): 13-17.
- Nezlin, R. "Immunoglobulin Structure and Function." In *Immunochemistry*, ed. C.J. Van Oss, Van Regenmortel, M.H.V., 3-45. New York: Marcel Dekker, 1994.
- Noh, M., Tothill, I.E. "Development and Characterisation of Disposable Gold Electrodes, and Their Use for Lead (II) Analysis." *Analytical and Bioanalytical Chemistry* 386, no. 7-8 (2006): 2095-2106.
- Nolan, M.A., Tan, S.H., Kounaves, S.P. "Fabrication and Characterization of a Solid State Reference Electrode for Electroanalysis of Natural Waters with Ultramicroelectrodes." *Anal. Chem.* 69 (1997): 1244-1247.
- Norouzi, P., Ganjali, M.R., Alizadeh, T., Daneshgar, P. "Fast Fourier Continuous Cyclic Voltammetry at Gold Ultramicroelectrode in Flowing Solution for Determination of Ultra Trace Amounts of Penicillin G." *Electroanalysis* 18, no. 10 (2006): 947-954.
- Nygren, H., Stenberg, M. "Rate Limitations of Antigen-Antibody Reactions: Theoretical and Practical Aspects." In *Immunochemistry of Solid-Phase Immunoassay*, ed. J.E. Butler, 285. Boca Raton: CRC Press, 1992.
- O'Connor, T., Gosling, J.P. "The Dependence of Radioimmunoassay Detection Limits on Antibody Affinity." *Journal of Immunological Methods* 208 (1997): 181-189.
- Offord, R.E. *Semisynthetic Proteins* Chapter 17: Hydrophobicity Profiles: John Wiley & Sons, 1980.
- Ohlson, S. "Weak-Affinity Chromatography." *Molecular Interactions in Bioseparations* (1993).
- Ohlson, S., Lundblad, A. and Zopf, D. "Novel Approach to Affinity Chromatography Using "Weak" Monoclonal Antibodies." *Analyt. Biochem.* 169 (1988): 204-208.
- Oliveira, S.C.B., Diculescu, V.C., Palleschi, G., Compagnone, D., Oliveira-Brett, A.M. "Electrochemical Oxidation of Ochratoxin a at a Glassy Carbon Electrode and in Situ Evaluation of the Interaction with Deoxyribonucleic Acid Using an Electrochemical Deoxyribonucleic Acid-Biosensor." *Anal. Chim. Acta* 588 (2007): 283-291.
- Oliver, C. "Preparation of Colloidal Gold." *Methods Mol Biol.* 34 (1994): 299-302.

- Olsen, M. *Prevention of Ochratoxin a in Cereals*. EUROPA European Commission Research. Citing internet resource (WWW document): <http://europa.eu.int/comm/research/quality-of-life/ka1/volume1/qlk1-1999-00433.htm>, Accessed 2004.
- Olsson, J., Boerjesson, T., Lundstedt, T., Schnuerer, J. "Detection and Quantification of Ochratoxin a and Deoxynivalenol in Barley Grains by Gc-Ms and Electronic Nose." *International Journal of Food Microbiology* 72 (2001): 203-214.
- Otto, A. "Excitation of Surface Plasma Waves in Silver by the Method of Frustrated Total Reflection." *Z. Physik* 216 (1968): 398-410.
- Palchetti, A. Cagnini, M. Mascini, A.P.F. Turner. "Characterisation of Screen-Printed Electrodes for Detection of Heavy Metals." *Mikrochimica Acta* 131, no. 1-2 (1999): 65-73.
- Pallarola, D., Domenianni, L., Priano, G., Battaglini, F. "A Protein-Resistant Matrix for Electrochemical Based Recognition Assays. Electroanalysis." *Electroanalysis* 19, no. 6 (2007): 690-697.
- Parra, V., Hernando, T., Rodríguez-Méndez, M.L. and de Saja, J.A. "Electrochemical Sensor Array Made from Bisphthalocyanine Modified Carbon Paste Electrodes for Discrimination of Red Wines." *Electrochimica Acta* 49, no. 28 (2004): 5177-5185.
- Patel, G. "Personal Communication: Peptides Synthesis." London: The Medical Research Council (MRC) at Imperial College, 2005.
- Pauling, L. and Corey, R.B. "Specific Hydrogen-Bond Formation between Pyrimidines and Purines in Deoxyribonucleic Acids." *Arch. Biochem. Biophys.* 65 (1956): 164-181.
- Pauling, L., and Corey, R. B. "Two Hydrogen-Bonded Spiral Configurations of the Polypeptide Chain." *J. Am. Chem. Soc.* 72 (1950): 5349.
- Pauling, L., and Corey, R.B. "The Pleated Sheet, a New Layer Configuration of Polypeptide Chains." *Proc. Natl. Acad. Sci. U.S.A.* 37 (1951): 2451-2456.
- Pauling, L., and Corey, R.B. "The Structure of Synthetic Polypeptides." *Proc. Natl. Acad. Sci. U.S.A.* 37 (1951): 241-250.
- Payne, A. W. R., Glen, R. C. "Molecular Recognition Using a Binary Genetic Search Algorithm." *J. Mol. Graph.* 11 (1993): 74.
- Pellequer, J.L, Van Regenmortel, M.H.V. "Measurement of Kinetic Binding Constants of Viral Antibodies Using a New Biosensor Technology." *J. Immunol. Methods* 166 (1993): 133.



- Pemberton, R. M., Hart, J. P. and Mottram, T. T. "An Electrochemical Immunosensor for Milk Progesterone Using a Continuous Flow System." *Sensors and Actuators B: Chemical* 16, no. 9-12 (2001): 715-723.
- Pemberton, R.M., Mottram, T.T. and Hart, J.P. "Development of a Screen-Printed Carbon Electrochemical Immunosensor for Picomolar Concentrations of Estradiol in Human Serum Extracts." *Journal of Biochemical and Biophysical Methods* 63, no. 3 (2005): 201-212.
- Pemberton, R.M., Pittson, R., Biddle, N., Drago, G.A. and Hart, J.P. "Studies Towards the Development of an Electrochemical Immunosensor Array for the Determination of Mycotoxins in Grain: Assay for Aflatoxin B1." *Anal. Letters* 39 (2006): 1573-1586.
- Petska, J.J., Steinert, B.W., and Chu, F.S. "Enzyme-Linked Immunosorbent Assay for Detection of Ochratoxin A." *Appl. Environ. Microbiol.* 41, no. 6 (1981): 1472-1474.
- Petzinger, E., Weidenbach, A. "Mycotoxins in the Food Chain: The Role of Ochratoxins." *Livestock Production Science* 76 (2002): 245-250.
- Pfohl-Leszkowicz, A., Pinelli, E., Bartsch, H., Mohr, U., Castegnaro, M. "Sex- and Strain-Specific Expression of Cytochrome P450s in Ochratoxin a-Induced Genotoxicity and Carcinogenicity in Rats." *Mol. Carcinog.* 23 (1998): 76-85.
- Piermarini, S., Micheli, L., Ammida, N.H.S., Palleschi, G. and Moscone, D. *Biosens. Bioelectron.* 22 (2007):1434.
- Pickering, M., Nerkar, S., Siantar, D., and Ofitserova, M. *Multi-Residue Mycotoxin Analysis - Method Abstract for Post-Column Liquid Chromatography*. Pickering Laboratories. Citing Internet recourses (WWW document): [www.pickeringlabs.com](http://www.pickeringlabs.com), Accessed 2004.
- Piercenet. *Nhs-Esters-Maleimide Crosslinkers*. Accessed 2005 and 2006.
- Piletsky, S.A., Panasyuk, T. L., Piletskaya, E. V., Nicholls, I. A. and Ulbricht, M. "Receptor and Transport Properties of Imprinted Polymer Membranes - a Review." *J. Membr. Sci.* 157 (1999): 263-278.
- Pittet, A. "Natural Occurrence of Mycotoxins in Foods and Feeds - an Updated Review. Cited In: Foodborne Pathogens-Hazards, Risk Analysis and Control © 2001." *Review de Medicine Veterinaire* 149 (1998): 479-492.
- Pittet, A., Royer, D. "Rapid, Low Cost Thin-Layer Chromatographic Screening Method for the Detection of Ochratoxin a in Green Coffee at a Control Level of 10 µG/Kg." *J Agric Food Chem.* 50, no. 2 (2002): 243-247.
- Pliny the Elder. "In Vino Sanitas." (AD 23-79).

- Prasad, K.S., Chen, J.C., Ay, C. and Zen, J.M. "Mediatorless Catalytic Oxidation of Nadh at a Disposable Electrochemical Sensor." (2007).
- Priano, G., Pallarola, D. and Battaglini, F. "Endotoxin Detection in a Competitive Electrochemical Assay: Synthesis of a Suitable Endotoxin Conjugate." *Anal. Biochem.* 362, no. 1 (2007): 108-116.
- Prieto-Simón, B., Noguer, T., Campàs, M. Emerging biotools for assessment of mycotoxins in the past decade. *TrAC Trends in Analytical Chemistry*, 26, 7 (2007): 689-702.
- Pütter, J., and Becker, R. "Peroxidases." In *Methods of Enzymatic Analysis*, ed. Bergmeyer, 3rd. Deerfield Beach, FL: Verlag Chemie, 1983.
- Quinglai, M., Mecklenburg, M., Danielsson, B. and Bin Xie. "Development of a Trna-Synthetase Microarray for Protein Analysis." *Sensors and Materials* 16, no. 8 (2004): 401-412.
- Quirion, R., Björklund, A., Hökfelt, T., ed. *Peptide Receptors Part I and II*, 2000 & 2002.
- Raghuvanshi, R. S., Goyal, S., Singh, O. and Panda, A. K. "Stabilization of Dichloromethane-Induced Protein Denaturation During Microencapsulation." *Pharm. Dev. Technol.* 3 (1998): 269-276.
- Ramstrom, O., Skudar, K., Haines, J., Patel, P., Bruggemann, O. "Food Analyses Using Molecularly Imprinted Polymers." *J. Agric. Food Chem.* 49, no. 5 (2001): 2105-2114.
- Ratcliff, J. "The Role of Mycotoxins in Food and Feed Safety." In *AFMA's symposium*, 2002.
- Ratola, N., Martins, L., and Alves, A. "Ochratoxin a in Wines-Assessing Global Uncertainty Associated with the Results." *Anal. Chim. Acta* 513, no. 1 (2004): 319-324.
- Reinsch, M., Toepfer, V., Lehmann, A., Nehls, I., Panne, U. "Determination of Ochratoxin a in Beer by Lc-Ms/Ms Ion Trap Detection." *Food Chemistry* 100 (2007): 312-317.
- Ricci, F., Amine, A., Palleschi, G. and Moscone, D. "Prussian Blue Based Screen Printed Biosensors with Improved Characteristics of Long-Term Lifetime and Ph Stability." *Biosensors and Bioelectronics* 18, no. 2-3 (2003): 165-174.
- Richon, A.B. "An Introduction to Molecular Modelling." *Mathematech* 1 (1994): 83.
- Rickert, J., Brecht, A. and Göpel, W. "Quartz Crystal Microbalances for Quantitative Biosensing and Characterizing Protein Multilayers." *Biosensors & Bioelectronics* 12, no. 7 (1997): 567-575.

- Ridascreen. *Mycotoxin Kits*. Citing internet reference: [www.r-biopharmrhone.com](http://www.r-biopharmrhone.com), 2004. Accessed.
- Ringot, D., Chango, A., Schneider, Y.J., Larondelle, Y. "Toxicokinetics and Toxicodynamics of Ochratoxin a, an Update." *Chemico-Biological Interactions* 159, no. 1 (2006): 18-46.
- Roach, J.A.G. "Capillary Supercritical Fluid Chromatography/Negative Ion Chemical Ionization Mass Spectrometry of Trichothecenes." *Biomed. Environ.Mass Spec.* 18 (1989): 64-70.
- Rodda, D. J., and Yamazaki, H. "Poly (Vinyl Alcohol) as a Blocking Agent in Enzyme Immunoassays." *Immunol. Investig.* 23 (1994): 421-428.
- Rodriguez, B.B., Bolbot, J.A., Tothill, I.E. "Amperometric Analysis of the Effect of Heavy Metals on the Activity of Isocitric Dehydrogenase." *Analytical Letters* 37, no. 3 (2004): 415-433.
- Rodriguez, B.B., Bolbot, J.A., Tothill, I.E. "Development of Urease and Glutamic Dehydrogenase Amperometric Assay for Heavy Metals Screening in Polluted Samples." *Biosensors and Bioelectronics* 19 (2004): 1157-1167.
- Rogers, K.R., Mascini, M. "Biosensors for Field Analytical Monitoring." *Field Analytical Chemistry and Technology* 2, no. 6 (1998): 317-331.
- Romer Labs Diagnostic GMBH. *Citing Internet Resources (Www Document): Wwww.Romerlabs.Com*. Accessed 2004.
- Romero, J.M.F., Stiene, M., Kast, R., de Castro, M.D.L., Bilitewski, U. "Application of Screen Printed Electrodes as Transducers in Affinity Flow-through Sensor Systems." *Biosensors & Bioelectronics* 13, no. 1107-1115 (1998).
- Rosenfeld, R., Vajda, S., DeLisi, C. "Flexible Docking and Design." *Annu Rev Biophys Biomol Struct.* 24 (1995): 677-700.
- Roterman, I. K., Gibson, K. D., and Scheraga, H. A. "A Comparison of the Charmm, Amber, and Ecepp/2 Potential for Peptides I." *J. Biomol. Struct. and Dynamics* 7 (1989a): 391-419.
- Roterman, I. K., Lambert, M. H., Gibson, K. D., and Scheraga, H. A. "A Comparison of the Charmm, Amber, and Ecepp/2 Potential for Peptides Ii." *J. Biomol. Struct. and Dynamics* 7 (1989): 421-452.
- Rousseau, D. M., Slegers, G. A. and Van Peteghem, C. H. "Radioimmunoassay of Ochratoxin a in Barley." *Appl. Environ. Microbiol.* 50 (1985): 529-531.
- Sáez, J.M., Medina, A., Gimeno-Adelantado, J.V., Mateo, R. and Jiménez, M. "Comparison of Different Sample Treatments for the Analysis of Ochratoxin a in Must, Wine and Beer by Liquid Chromatography." *Journal of Chromatography A* 1029, no. 1-2 (2004): 125-133.

- Saez, J.M., Medina, A., Gimeno-Adelantado, J.V., Mateo, R., Jimenez, M. "Comparison of Different Sample Treatments for the Analysis of Ochratoxin a in Must, Wine and Beer by Liquid Chromatography." *Journal of Chromatography A* 1029 (2004): 125-133.
- Sagawa, T., Azuma, T. and Sasaki, Y.C. "Dynamical Regulations of Protein-Ligand Bindings at Single Molecular Level." *Biochemical and Biophysical Research Communications* 355 (2007): 770-775.
- Saha D, Acharya D, Dhar TK. Method for homogeneous spotting of antibodies on membranes: application to the sensitive detection of ochratoxin A. *Anal Bioanal Chem.* (2006), 385(5): 847-54.
- Saha, D., Acharya, D., Roy, D., Shrestha, D., Dhar, T.K. "Simultaneous Enzyme Immunoassay for the Screening of Aflatoxin B1 and Ochratoxin a in Chili Samples." *Anal. Chim. Acta* 584 (2007): 343-349.
- Sandison, M.E., Anicet, N., Glidle, A., Cooper, J.M. "Optimisation of the Geometry and Porosity of Microelectrode Arrays for Sensor Design." *Anal. Chem.* 74 (2002): 5717-5725.
- Sbobini, J., Mishra, A.K., Sandhya, K. and Chandra, N. Interaction of coumarin derivatives with human serum albumin: investigation by fluorescence spectroscopic technique and modeling studies *Spectrochim. Acta A*, 57 (2001): 1133-1147.
- Scheller, F.S., Warsinke, A., Bier, F.F., Wollenberger, U., Jin, W., Benkert, A. and Pfeiffer, D. "Biosensors and Their Applications." In *TRANSDUCERS '97 International Conference on Solid-state Sensors and Actuators*. Chicago, 1997.
- Scheller, F.W. and Markower, A. "Automated Amplified Flow Immunoassay for Cocaine." *Analytical Chemistry* 70 (1998): 4624-4630.
- Scheller, F.W., Wollenberger, U., Warsinke, A. "Research and Development in Biosensors." *Current opinion in Biotechnology* 12, no. 35-40 (2001).
- Scheper, T., Müller, C., Anders, K. D., Eberhardt, F., Plötz, F., Schelp, C., Thordsen, O. and Schügerl, K. "Optical Sensors for Biotechnological Applications." *Biosensors & Bioelectronics* 9, no. 1 (1994): 73-82.
- Schiller, P.W., Weltrowska, G., Nguyen, T.M.-D., Lemieux, C., Chung, N.N., Marsden, B.J., Wilkes, B.C. "Conformational Restriction of the Phenylalanine Residue in a Cyclic Opioid Peptide Analogue: Effects on Receptor Selectivity and Stereospecificity." *J. Med. Chem.* 34, no. 10 (1991): 3125-3132.

- Schlatter, C.; Studer-Rohr, J.; Rasoyi, T.; Battaglia, R.; Hatzold, T. Kroes, R. "Carcinogenic and Kinetic Aspects of Ochratoxin A." *Food Additives and Contaminants* 13 (1996): 43-44. Cited in: Petzinger, E., and Weidenbach, A. Mycotoxins in the food chain: the role of ochratoxins. *Livestock Production Science*, 76, 2002, p.245-250.
- Schmuck, C. "Von Der Molekularen Erkennung Zum Design Neuer Wirkstoffe." *Chemie in unserer Zeit* 6 (2001): 356-366.
- Schmuck, C. "Personal Communication: On Short Sequence Peptide Receptors." Salzburg, Austria, 2005.
- Schmuck, C., Heil, M., Wich, P., Scheiber, J. and Baumann, K. "Charge Interactions Do the Job: Efficient Binding of Tetrapeptides in Water by Fully Flexible One-Armed Artificial Receptors Identified from Combinatorial Screening." In *Second World Congress on Synthetic Receptors*. Salzburg, Austria: Oral presentation, 2005.
- Schnerr, H., Vogel, R.F., Niessen, L. "A biosensor-based immunoassay for rapid screening of deoxynivalenol contamination in wheat." *Food Agriculture Immunology*. 14, no. 313-321 (2002).
- Schramek, H., Wilflingseder, D., Pollack, V., Freudinger, R., Mildenerger, S., Gekle, M. "Ochratoxin a-Induced Stimulation of Extracellular Signal-Regulated Kinases 1/2 Is Associated with Madin-Darby Canine Kidney-C7 Cell Dedifferentiation." *J. Pharmacol. Exp. Ther.* 283 (1997): 1460-1468.
- Schrödinger, E. "Quantisierung Als Eigenwertproblem." *Ann. Phys.* 79 (1926a): 361.
- Schrödinger, E. "Quantisierung Als Eigenwertproblem II." *Ann. Phys.* 79 (1926b): 489-527.
- Schuller, P.L., Van Egmond, H.P., Stoloff, L. "Limits and Regulations on Mycotoxins." In *Proceedings of the International Symposium on Mycotoxins, 1981*, ed. K. Naguib, Naguib, M.M., Park, D.L. & Pohland, A.E., 111-129. Cairo, Egypt, 1983.
- Schuller, P.L., van Egmond, H.P., Stoloff, L. "Limits and Regulations on Mycotoxins." In *Proc Int Symp on Mycotoxins*, ed. K. Naguib, Naguib, M.M., Park, D.L., and A.E. Pohland, 111-129. Cairo, Egypt, 1983.
- Schulz-Gasch, T. and Stahl, M. "Binding Site Characteristics in Structure-Based Virtual Screening: Evaluation of Current Docking Tools." *J. Mol. Model.* 9 (2003): 47-57.
- Scott, P.M. *Natural Toxins*. Cited in: Cunnif, P. AOAC Official Methods of Analysis. AOAC INTERNATIONAL, 16th ed., Vol.2, 1997, pp.49-1 to 49-51, 1997.
- Scott, P.M. and Trucksess, M.W. "Application of Immunoaffinity Columns to Mycotoxin Analysis." *Journal of AOAC International* 80 (1997): 941-949.

- Selassie, C.D. "History of Quantitative Structure -Activity Relationships." In *Burgers Medicinal Chemistry and Drug Discovery*, ed. D.J. Abraham, 1: John Wiley & Sons, 2003.
- Sharman, M. "Automated Liquid Chromatographic Determination of Ochratoxin a in Cereals and Animal Products Using Immunoaffinity Column Clean-Up." *Journal of Chromatography* 603 (1992): 285-289.
- Siebert, K.J. and Lynn, P.Y. "Mechanisms of Adsorbent Action in Beverage Stabilization." *J. Agric. Food. Chem.* 45, no. 11 (1997): 4275-4280.
- Singh, J., Saldanha, J., Thornton, J.M. "A Novel Method for the Modeling of Peptide Ligands to Their Receptors." *Protein Engineering* 4 (1991): 251-261.
- Singh, U. C., Kollman, P. A. "An Approach to Computing Electrostatic Charges for Molecules." *J. Comp. Chem.* 5 (1984): 129-145.
- Siontorou, C.G., Nikolelis, D.P., Miernik, A. and Krull, U.J. "Rapid Methods for Detection of Aflatoxin M1 Based on Electrochemical Transduction by Self-Assembled Metal-Supported Bilayer Lipid Membranes (S-Blms) and on Interferences with Transduction of DNA Hybridization." *Electrochimica Acta* 43, no. 23 (1998): 3611-3617.
- Skoog, D.A., Leary, J.J. *Principles of Instrumental Analysis*. 4th ed. Orlando, Florida: College Publishing, 1992.
- Smith, J.E. "Mycotoxins." In *In: Food Chemical Safety. Vol. 1-Contaminants. Ch.11*, ed. D.H. Watson: Woodhead Publishing, 2001.
- Smith, J.E. and Henderson, R.S. "Mycotoxins and Animal Foods." In *In: Food Chemical Safety. Vol. 1-Contaminants, 2001, Ch.11*, ed. D.H. Watson: Woodhead Publishing, 1991.
- Solfrizzo, M. Avantiaggiato, G. and A. Visconti, A. "Use of Various Clean-up Procedures for the Analysis of Ochratoxin a in Cereals." *J. Chromatogr. A* 1 (1998): 67-73.
- Soykut, E.A., Dudak, F.C., Boyac, I.H. Selection of staphylococcal enterotoxin B (SEB)-binding peptide using phage display technology. *Biochemical and Biophysical Research Communications*, 370, 1,(2008): 104-108.
- Stander, M.A., Bornscheuer, U.T., Henke, E., Steyn, P.S. "Screening of Commercial Hydrolases for the Degradation of Ochratoxin A." *J. Agric. Food Chem.* 48 (2000): 5736-5739.
- Steinbach, P. *Molecular Modelling*. National Institutes of Health, Division of Computational Bioscience (DCB/CIT), CENTER FOR MOLECULAR MODELING (CMM). Citing internet resource (WWW document): [http://cmm.info.nih.gov/modeling/images/conformation/search\\_grid.gif](http://cmm.info.nih.gov/modeling/images/conformation/search_grid.gif), 1996. Accessed.

- Steinbach, P.J. *Introduction to Macromolecular Simulation*. Center for Molecular Modeling, Center for Information Technology, National Institutes of Health. Citing internet resource (WWW document): <http://cmm.info.nih.gov/modeling/>, 2005. Accessed 2004.
- Steinbach, P.J. and Brooks, B.R. "Protein Simulation Below the Glass-Transition Temperature: Dependence on Cooling Protocol." *Chem. Phys. Letters* 226 (1994): 447.
- Storri, S., Santoni, T., Minunni, M. and Mascini, M. "Surface Modifications for the Development of Piezoimmunosensors." *Biosensors & Bioelectronics* 13, no. 3-4 (1998): 347-357.
- Subrahmanyam, S., Piletsky, S. A., Piletska, E. V., Karim, K., Chen, B., Day, R., Turner, A. P. F. "'Bite-and-Switch' Approach Using Computationally Designed Molecularly Imprinted Polymers for Sensing of Creatinine." *Biosensors & Bioelectronics* 16 (2001): 631-637.
- Surugiu, I., Dey, E.S., Svitel, J., Pirvutoiu, S. and Danielsson, B. "Dextran-Modified Surface for Highly Sensitive Chemiluminescent Elisa." *The Analyst* 126 (2001): 1633-1635.
- Tait, B.D., Hagen, S., Domagala, J., Ellsworth, E.L., Gajda, C., Hamilton, H.W., Vara Prasad, J.V.N., Ferguson, D., Graham, N., Hupe, D., Nouhan, C., Tummino, P.J., Humblet, C., Lunney, E.A., Pavlovsky, A., Rubin, J., Gracheck, S.J., Baldwin, E.T., Bhat, T.N., Erickson, J.W., Gulnik, S.V., and Liu, B. "4-Hydroxy-5,6-Dihydropyrones. 2. Potent Non-Peptide Inhibitors of Hiv Protease." *J. Med. Chem.* 40, no. 23 (1997): 3781 - 3792.
- Tame, J. R. H. "Scoring Functions: A View from the Bench." *J. Comput. Aided Mol. Des.* 13 (1999): 99-108.
- Taub, R., Gould, R. J., Garsky, V. M., Ciccarone, T. M., Hoxie, J., Friedman, P. A., and Shattil, S. J. "A Monoclonal Antibody against the Platelet Fibrinogen Receptor Contains a Sequence That Mimics a Receptor Recognition Domain in Fibrinogen." *Journal of Biological Chemistry* 264 (1989): 259-265.
- Tecna Lab. *Citing Internet Resource (Www Document): Www.Tecna-Lab.Com.* 2004. Accessed 2004.
- Tekeuchi, Toshifumi and Haginaka, Jun. "Separation and Sensing Based on Molecular Recognition Using Molecularly Imprinted Polymers." *Journal of Chromatography B* 728 (1999): 1-20.
- Tepnel BioSystems Ltd. *Citing Internet Resource (Www Document): Www.Tepnel.Com.* Accessed 2004.
- Theegala, C.S.; Suleiman, A.A. "Quantification of Antibody Immobilization Using Peroxidase Enzyme-Substrate Reaction." *Microchemical Journal* 65 (2003): 105-111.

- Thenmozhi, K. and Narayanan, S.S. "Electrochemical Sensor for H<sub>2</sub>O<sub>2</sub> Based on Thionin Immobilized 3-Aminopropyltrimethoxy Silane Derived Sol-Gel Thin Film Electrode." *Sensors and Actuators B: Chemical* 125, no. 1 (2007): 195-201.
- Thermo Electron Corporation. *Microtiter Plate Guide*. Citing internet resource: [www.thermo.com/microtiter](http://www.thermo.com/microtiter), 2004. Accessed.
- Thevenot, D.R., Toth, K., Durst, R.A. and Wilson, G.S. "News and Market Update." *Biosensors & Bioelectronics* 11, no. 4 (1996): i.
- Thevenot, D.R., Toth, K., Durst, R.A., Wilson, G.S. a. "Electrochemical Biosensors: Recommended Definitions and Classification (Technical Report)." *Pure Appl. Chem.* 71, no. 12 (1999): 2333-2348. Citing Internet recourse (WWW document): <http://www.iupac.org/reports/1999/7112thevenot/>.
- Thirumala-Devi, K., Mayo, M.A., Reddy, G., Reddy, S.V., Delfosse, P., Reddy, D.V. "Production of Polyclonal Antibodies against Ochratoxin A and Its Detection in Chilies by Elisa." *J Agric Food Chem.* 48, no. 10 (2000): 5079-82.
- Tingjun, H. and Xiaojie, X. "Recent Development and Application of Virtual Screening in Drug Discovery: An Overview." *Current Pharmaceutical Design* 10, no. 9 (2004): 1011-1033.
- Toko, K. "Biomimetic Sensor Technology." *Meas. Sci. Technol.* 12 (2001).
- Tombelli, S., Mascini, M., Braccini, L., Anichini, M. and Turner, A.P.F.,. "Coupling of a DNA Piezoelectric Biosensor and Polymerase Chain Reaction to Detect Apolipoprotein E Polymorphisms." *Biosensors & Bioelectronics* 15 (2000): 636-370.
- Tombelli, S., Minunni, M. and Mascini, M. "Analytical Applications of Aptamers." *Biosensors and Bioelectronics* 20, no. 12 (2005): 2424-2434.
- Tomera, J.F. "Current Knowledge of the Health Benefits and Disadvantages of Wine Consumption." *Trends in Food Science & Technology* 10 (1999): 129-138.
- Tothill, I.E., ed. *Rapid and on-Line Instrumentation for Food Quality Assurance*: Woodhead Publishing Limited, 2003.
- Tothill, I.E. and Turner, A.P.F. "Biosensors." In *Encyclopaedia of Food Sciences and Nutrition*, ed. L. and Finglas Trugo, P., 489-499: Academic Press, 2003.
- Tothill, I.E., Piletsky, S., Magan, N., and Turner, A.P.F. "New Biosensors." In *Instrumentation and Sensors for the Food Industry*, ed. E. and Brimelow Kress-Rogers, C.J.B., 836: Woodhead Publishing Limited and CRC Press LLC, 2001.
- Tothill, I.E.; Newman, J.; White, S. and Turner, A.P.F. "Monitoring of the Glucose Concentration During Microbial Fermentation Using a Novel Mass-Producible Biosensor Suitable for on-Line Use." *Enzyme and Microbial Technology* 20 (1997): 590-596.



- Toxi-Test. *Citing Internet Recourses (Www Document): Http://Www.Toxi-Test.Com/*. Accessed 2004.
- Tripod bookshelf. *Citing Internet Recourses (Www Document): Www.Tripod.Com*. Accessed 2004.
- Trucksess, M.W. "Methods Used in Testing of Aflatoxins, Don, Ota, and Zearalenone in Grains and Grain Products." In *Food Safety from a Chemistry Perspective, Is There a Role for Haccp?*, ed. J.W. DeVries, J. A. Dudek, M. T. Morrissey and C. S. Keenan. MA, USA: Analytical Progress Press, 1996.
- Trucksess, M.W., Wood, G.E. "Immunochemical Methods for Mycotoxins in Foods." *Food Testing and Analysis* 3 (1997): 24-27.
- Tsai, S.C. *An Introduction to Computational Biochemistry*: John Wiley & Sons, 2002.
- Tudos, A.J., Lucas van de Bos, E.R., Stigter, E.C.A. "Rapid Surface Plasmon Resonance- Based Inhibition Assay of Deoxynivalenol." *J. Agriculture and Food Chemistry* 51 (2003): 5843-5848.
- Turner, A.P.F. "Current Trends in Biosensor Research and Development." *Sensors Actuators* 17 (1989): 433-450.
- Turner, A.P.F. "Biosensors and Bioelectronics 20 Years On." *Biosensors and Bioelectronics* 20, no. 12 (2005): 2387.
- Turner, A.P.F., Karube, I. and Wilson, G.S. *Biosensors: Fundamentals and Applications*. Oxford: Oxford University Press, 1987.
- Turner, N.W., Piletska, E.V., Karim, K., Whitcombe, M.J., Malecha, M.M., Magan, N., Baggiani, C., Piletsky, S.A. Effect of the Solvent on Recognition Properties of Molecularly Imprinted Polymer Specific for Ochratoxin A. *Biosensors & Bioelectronics* 20 (2004): 1060-1067.
- Ueno, Y., Kawamura, O., Sugiura, Y., Horiguchi, K., Nakajima, M., Yamamoto, K., Sato, S. Use of monoclonal antibodies, enzyme-linked immunosorbent assay and immunoaffinity column chromatography to determine ochratoxin A in porcine sera, coffee products and toxin-producing fungi. *IARC Sci Publ.* (1991), 115:71-5.
- Ulbrich, R., Golbik, R. & Schellenberger, A. "Protein Adsorption and Leakage in Carrier-Enzyme Systems." *Biotechnology & Bioengineering* 37 (1991): 280-287.
- Ulmann, A. *Ultrathin Organic Films*: Academic Press, 1991.
- Underberg, W.J.M. "Separation and Detection Techniques for Peptides and Proteins in Stability Research and Bioanalysis." *Journal of Chromatography B* 742 (2000): 401-409.

- Underwood, P.A. "Problems and Pitfalls with Measurement of Antibody Affinity Using Solid-Phase Binding in the Elisa." *J. Immunol. Methods* 164 (1983): 119.
- Underwood, P.A. "Theoretical Considerations of the Ability of Monoclonal Antibodies to Detect Antigenic Differences between Closely Related Variants with Particular Reference to Heterospecific Reactions." *J. Immunol. Methods* 85 (1985): 295-307.
- Updike, S.J., and Hicks, G.P.. "The Enzyme Electrode." *Nature* 214 (1967): 986-988.
- Vagin, M.Y., Karyakina, E.E., Hianik, T., Karyakin, A.A. "Electrochemical Transducers Based on Surfactant Bilayers for the Direct Detection of Affinity Interactions." *Biosensors & Bioelectronics* 18 (2003): 1031-1037.
- Valentini, F., Compagnone, D., Giraudi, G., Palleschi, G. "Electrochemical Elisa for the Screening of Ddt Related Compounds: Analysis in Waste Waters." *Anal. Chim. Acta* 487 (2003): 83-90.
- Van der Gaag, B., Spath, S., Dietrich, H., Stigter, E., Boonzaaijer, G., van Osenbruggen, T., Koopal, K. "Biosensors and Multiple Mycotoxin Analysis." *Food Control* 14 (2002): 251-254.
- Van der Gaag, B., Spath, S., Dietrich, H., Stigter, E., Boonzaaijer, G., van Osenbruggen, T. and Koopal, K. "Biosensors and Multiple Mycotoxin Analysis." *Food Control* 14, no. 4 (2003): 251-254.
- Van der Gaag, B., Stigter, E., van Duijn, G., Bleeker, H., Hofstra, H., Wahlstroem, L. *Application Development on Biacore for the Detection of Mycotoxin in Food and Feed*. Citing Internet recourse (WWW document): [http://www.biacore.com/pdf/food/Mycotoxin\\_2.pdf](http://www.biacore.com/pdf/food/Mycotoxin_2.pdf), Accessed 2004.
- Van der Merwe, K.J., Steyn, P.S., Fourie, L. "Mycotoxins Ii :The Constitution of Ochratoxins a, B, and C, Metabolites of Aspergillus Ochraceus." *J. Chem. Soc.* 1 (1965): 7083-7088.
- Van der Merwe, K.S. Steyn, P.S., Fourie, L., DeScott, B., Theron, J.J. "Ochratoxin a, a Toxic Metabolite Produced by Aspergillus Ochraceus." *Nature* 205 (1965): 1112-1113.
- Van Edgmont, H.P. "Current Situation on Regulations for Mycotoxins. Overview of Tolerances and Status of Standard Methods of Sampling and Analysis." *Food Addit Contam.* 6 (1989): 139-188.
- Van Egmond, H.P., Schothorst, R.C. and Jonker, M. A. "Regulations Relating to Mycotoxins in Food." *Anal. Bioanal. Chem.* 3889 (2007): 147-157.
- Van Gunsteren, W.F., Berendsen, H.J.C. "Computer Simulation of Molecular Dynamics: Methodology, Applications, and Perspectives in Chemistry." *Angewandte Chemie International Edition in English* 29, no. 9 (1990): 992-1023.

- Van Opdenbosch, B. Cramer, R.D., and Giarrusso, F.F. "Sybyl, the Integrated Molecular Modelling System." *Molecular Graphics* 3 (1985): 110-111.
- Van Oss, C.J. "Kinetics and Energetics of Specific Intermolecular Interactions." *J. Molec. Recogn* 10 (1997): 203-216.
- Van Regenmortel, M.H. "Synthetic Peptides Versus Natural Antigens in Immunoassays." *Ann. Biol. Clin.* 51, no. 1 (1993): 39-41.
- Van Regenmortel, M.H.V. "From Absolute to Exquisite Specificity. Reflections on the Fuzzy Nature of Species, Specificity and Antigenic Sites." *J. Immunol. Methods* 216 (1998): 37-48.
- Vedani, A. and Dobler, M. "Internet Laboratory for Predicting Harmful Effects Triggered by Drugs and Chemicals." *ALTEX* 18 (2001): 110-114.
- Vedani, A. and Dobler, M. "5dqsar: The Key for Simulating Induced Fit?" *J. Med. Chem.* 45 (2002): 2139-2149.
- Vedani, A. and Dobler, M. Q. "Quantification of Wide-Range Ligand Binding to the Estrogen Receptor - a Combination of Receptor-MEDIALTED Alignment and 5d Qsar." *Helv. Chim. Acta* 45 (2003): 2139-2149.
- Vedani, A. and Huhta, D. W. "A New Force Field for Modeling Metalloproteins." *J. Am. Chem. Soc.* 112 (1990): 4759-4767.
- Vedani, A., McMasters, D. R. und Dobler, M. "Genetische Algorithmen Im 3d-Qsar: Verwendung Multipler Wirkstofforientierungen Zur Verbesserten Voraussage Der Toxizität." *ALTEX* 16 (1999): 9-14.
- Vicam Corp. *Citing Internet Resource (Www Docuement): Www.Vicam.Com.* Accessed 2004.
- Visconti, A., Pascale, M. and Centonze, G. "Determination of Ochratoxin a in Domestic and Imported Beers in Italy by Immunoaffinity Clean-up and Liquid Chromatography." *J. Chromatogr. A* 888 (2000): 321-326.
- Visconti, A., Pascale, M., and Centonze, G. "Determination of Ochratoxin a in Wine by Means of Immunoaffinity Column Clean-up and High-Performance Liquid Chromatography." *J. Chromatogr. A* 864, no. 1 (1999): 89-101.
- Volpe, G. , Compagnone, D., Draisci, R. and Palleschi, G. "3,3a,5,5a-Tetramethylbenzidine as Electrochemical Substrate for Horseradish Peroxidase Based Enzyme Immunoassays." *The Analyst* 123 (1998): 1303-1307.
- Walker, R. "Mycotoxins of Growing Interest-Ochratoxin." In *In 3rd Joint FAO/WHO/UNEP International Conference on Mycotoxins, 1999.*, 1999.
- Walstra, P. "On the Stability of Casein Micelles." *J. Dairy Sci.* 73 (1990): 1965-1979.

- Wang, J. and Golden, T. "Metalloporphyrin Chemically Modified Glassy Carbon Electrodes as Catalytic Voltammetric Sensors." *Anal. Chim. Acta* 217 (1989): 343-351.
- Wang, X.H., Liu, T., Xu, N., Zhang, Y., Wang, S. "Enzyme-Linked Immunosorbent Assay and Colloidal Gold Immunoassay for Ochratoxin A: Investigation of Analytical Conditions and Sample Matrix on Assay Performance." *Anal. Bioanal. Chem.* 389, no. 3 (2007): 903-911.
- Warsinke, A., Benkert, A., Scheller, F.W. "Electrochemical Immunoassays." *Fresenius J. Anal. Chem.* 366, no. 6-7 (2000).
- Warsinke, A. and Stöcklein, W. and Micheel, B. "Development of a Creatinine Elisa and an Amperometric Antibody-Based Creatinine Sensor with a Detection Limit in the Nanomolar Range." *Analytical Chemistry* 72 (2000): 916-921.
- Weiner, S. J., Kollman, P. A., Nguyen, D. T., Case, D. A. 1986, 7, 230-252. "An All Atom Force Field for Simulations of Proteins and Nucleic Acids." *J. Comp. Chem.* 7 (1986): 230-252.
- Weiner, S.J., Kollman, P.A., Case, D.A., Singh, U.C., Ghio, C., Alagona, G., Profeta, S. Jr. and Weinerl, P. "A New Force Field for Molecular Mechanical Simulation of Nucleic Acids and Proteins." *J. Am. Chem. SOC.* 106 (1984): 765-784.
- Welborn, J.R., Groves, C.E. and Wright, S.H. "Peritubular Transport of Ochratoxin a by Single Rabbit Renal Proximal Tubules." *J. Am. Soc. Nephrol.* 9 (1998): 1973-1982.
- Weller, M.G. "Immuno chromatographic Techniques- a Critical Review." *Fresenius J. Anal. Chem.* 366 (2000): 635-645.
- Whitaker, T.B. "Sampling for Mycotoxins. Chapter 4." In *Mycotoxins in Food*, ed. N. & Olsen Magan, M.: CRC Woodhead Publishing, 2004.
- White, S.F.; Tohill, I.E.; Newman, J.D. and Turner, A.P.F. "Development of a Mass-Produced Glucose Biosensor and Flow-Injection Analysis System: Suitable for on-Line Monitoring During Fermentations." *Analytica Chimica Acta* 321 (1996): 165-172.
- Whitlow, M., and Teeter, M.M. "A Empirical Examination of Potential Energy Minimization Using the Well-Determined Structure of the Protein Crambin." *J. Am. Chem. Soc.* 108 (1986): 7163-7172.
- WHO (World Health Organisation). *Ochratoxin a - Toxicological Evaluation of Certain Food Additives and Contaminants*. WHO Food Additives Ser. 35, 1996.
- Wightman, R.M. and Wipf, D.O. "Electroanalytical Chemistry." ed. A.J. Bard, 15, 267. New York: Marcel Dekker, 1989.

- Wiley Encyclopaedia of Food Science and Technology. *Mycotoxin Analysis*. 2nd ed., 1999.
- Wiley Encyclopaedia of Food Science and Technology. *Natural Contaminants*. 2nd ed., 1999.
- Williams, W., Moss, D., Kieber-Emmons, T., Cohen, J., Myers, J., Weiner, D., and Greene, M. "Development of Biologically Active Peptides Based on Antibody Structure." *Proc. Natl. Acad. Sci. U. S. A.* 86 (1989): 5537-5541.
- Willner, Itamar. "Amperometric Amplification of Antigen-Antibody Association at Monolayer Interfaces: Design of Immunosensor Electrodes." *Journal of Electroanalytical Chemistry* 4, no. 8 (1996): 67-72.
- Wilson, C. and Szostak, J.W. "Solotion of a Fluorophore-Specific DNA Aptamer with Weak Redox Activity." *Chemistry & Biology* 5, no. 11 (1998): 609-617.
- Wilson, I., Stanfield, R. "Antibody-Antigen Interactions." *Curr. Opin. Struct. Biol.* 3 (1993): 113-118.
- Xiao, H., Madhyastha, S., Marquardt, R.R., Vodela, J.K., Frohlich, A.A., Kemppainen, B.W. "Toxicity of Ochratoxin a, Its Opened Lactone Form and Several of Its Analogs: Structure- Activity Relationships." *Toxicology and Applied Pharmacology* 137 (1996): 182-192.
- Xiao, H., Marquardt, R.R., Li, G., Frohlich, A.A. "Isolation, Purification and Identification of Intracellular Protein Targets of Ochratoxin A: Mitochondrial Aldehyde Dehydrogenase Class 2 Is a High- Affinity Ochratoxin a-Binding Protein." *Journal of the Science of Food and Agriculture* 79 (1999): 2099-2104.
- Xu, X.; Liu, S.; Ju, H. "A Novel Hydrogen Peroxide Sensor Via the Direct Electrochemistry of Horseradish Peroxidase Immobilized on Colloidal Gold Modified Screen-Printed Electrode." *Sensors* 3 (2003): 350-360.
- Ya-Min, Z., Shen-Qin, H., Gou-Li, S., Ru-qin, Y. "An Amperometric Immunosensor Based on an Electrochemically Pretreated Carbon-Paraffin Electrode for Complement Iii (C3) Assay." *Biosensors & Bioelectronics* 18 (2003): 473-481.
- Yu, F.Y., Chi, T.F., Liu, B.H., Su, C.C. "Development of a Sensitive Enzyme-Linked Immunosorbent Assay for the Determination of Ochratoxin A." *J. Agric. Food. Chem.* 53, no. 17 (2005): 6947-6953.
- Zanic-Grubisic, T., Zrinski, R., Cepelak, I., Petrik, J., Radic, B., Pepeljnjak, S. "Studies of Ochratoxin a- Induced Inhibition of Phenylalanine Hydroxylase and Its Reversal by Phenylalanine." *Toxicology and Applied Pharmacology* 167, no. 2 (2000): 132-139.
- Zhao, M., Harding, I.S., Hibbert, D.B., Gooding, J.J. "A Portable Fill-and-Flow Channel Biosensor with an Electrode to Predict the Effect of Interferences." *Electroanalysis* 16, no. 15 (2004): 1221-1226.

- Zhihui, H., Ning, G., Wenrui, J. "Determination of Tumor Marker Ca125 by Capillary Electrophoretic Enzyme Immunoassay with Electrochemical Detection." *Anal. Chim. Acta* 497 (2003): 75-81.
- Zhuang, H., Wang, Q., Chen, G., Huang, J., Lin, P. "A New Chemiluminescence Immunoassay Method for the Determination of Cancer Embryo Antigen." *Guang Pu Xue Yu Guang Pu Fen Xi* 20, no. 6 (2000): 889-891.
- Zhuang, H.S., Wang, Q.E., Zhang, F., Huang, Q.J., and Tang, Y.C. "N-(B-Carboxypropionyl)Luminal as a New Chemiluminescence Label in Immunoassays." *Chinese Journal of Chemistry* 15, no. 2 (2000): 123-129.
- Zimmerli, B., Dick, R. "Ochratoxin a in Table Wine and Grape Juice: Occurrence and Risk Assessment." *Food Additives Contam.* 13 (1996): 655-668.
- Zimmerli, R. and Dick, R. "Determination of Ochratoxin a at the Ppt Level in Human Blood, Serum, Milk and Some Foodstuffs by High-Performance Liquid Chromatography with Enhanced Fluorescence Detection and Immunoaffinity Column Cleanup: Methodology and Swiss Data." *J. Chromatogr. B* 666 (1995): 85.
- Zimmerman, S.S., Scheraga, H.A. "Local Interactions in Bends of Proteins." *Proc. Nat. Acad. Sci. U.S.A.* 74: 4126-4129.
- Zimmerman, S.S., Scheraga, H.A. "Influence of Local Interactions on Protein Structure. Conformational Energy Studies of N-Acetyl-N'-Methylamides of Pro-X and X-Pro Dipeptides." *Biopolymers* 16 (1977a): 811-843.
- Zoecklein, B.W. , Fugelsang, K.C., Gump, B.H. and Nury, F.S. "Phenolic Compounds and Wine Color." In *Production Wine Analysis*, 129-168. New York: Van Nostrand Reinhold., 1990.
- Zopf, David and Ohlson, Sten. "Weak Affinity Chromatography." *Nature* 346 (1990): 87-88.
- Zou, H.L., Kilmartin, P.A., Inglis, M.J., Frost, A.,. "Extraction of Phenolic Compounds During Vinification of Pinot Noir Wine Examined by Hplc and Cyclic Voltammetry." *J. Grape Wine Res* 8 (2002): 163-174.

## PUBLICATIONS

### Poster presentation (project meeting)

**Heurich, M.**, Parker, C., Tothill, I.E. (2004). “Food Safety and Quality Monitoring with Microsystems”, GoodFood 6 month meeting, Cork, Ireland.

Lanyon, Y., Watson, Y., Arrigan, D., DeMarzi, G., Quinn, A., **Heurich, M.**, Parker, C., Tothill, I. (2004). “The development of micro-nano-systems for mycotoxins detection”, GOODFOOD 12th month project meeting, Athens, Greece.

**Heurich, M.**, Parker, C., Tothill, I.E., (2005). “The development of sensing receptors for mycotoxins detection”, GOODFOOD Second Review, Montreux, Switzerland.

**Heurich, M.**, Parker, C., Tothill, I.E., (2005). “Microsystems for mycotoxin detection”, GOODFOOD 18th month project meeting, Florence, Italy.

**Heurich, M.**, Parker, C., Tothill, I.E. “Development of Affinity Sensors for Mycotoxins Detection”, GoodFood 24 month review meeting, Milton Keynes, UK.

Tothill, I.E., Parker, C. and **Heurich, M.** (2006). “Micro&Nano technologies for milk and dairy”, GoodFood Second Open Day, Grenoble, France.

Tothill, I.E., **Heurich, M.**, Parker, C., (2007) Development of Sensing Receptors for Mycotoxins Detection, GoodFood 36 month review meeting, Lucerne, Switzerland.

### Poster presentation (Conference)

**Heurich, M.**, Danielsson, B., Tothill, I.E., (2005). “Affinity Sensor for Ochratoxin A using Synthetic Peptide Receptor”, Second world congress on synthetic receptors, Salzburg, Austria (Appendix 4).

**Heurich, M.**, Tothill, I.E., (2005). “Affinity sensor for Ochratoxin A using de novo designed peptide receptors”, Environment Day for Industry, Cranfield University, UK.

**Heurich, M.** and Tothill, I.E. (2006). “Affinity Sensors for Ochratoxin A Detection”, 9th World Congress on Biosensors, Toronto, Canada (Appendix 5).

Tothill, I.E., Parker, C. and **Heurich, M.**, Lanyon, Y.H, Arrigan, D.W. M. (2006). “Microsensors for mycotoxin detection in foods”, Mycoglobe International Conference, Bari, Italy, 26-30 September 2006.

Tothill, I.E., Parker, C. and **Heurich, M.**, Lanyon, Y.H., Arrigan, D.W.M. (2007). “Micro/nanosensor arrays for aflatoxin M1 and ochratoxin A analysis”. XII International IUPAC Symposium on Mycotoxins and Phycotoxins, Istanbul, Turkey.

Tothill, I.E., Parker, C. and **Heurich, M.**, Lanyon, Y.H., Manning, M., and Arrigan, D.W.M. (2008). Microsensor Arrays for Mycotoxin Detection. 10th World Congress on Biosensors, Shanghai, China, 14-16 May 2008 (to be presented).

### **Oral Presentation**

**Heurich, M.** and Tothill, I.E. (2006). “Affinity sensor development for ochratoxin A”. 57th Meeting of the International Society of Electrochemistry, Edinburgh, UK (Oral Presentation)

### **Research Papers**

**Heurich, M.** and Tothill, I.E. “*De novo* designed peptide receptor for ochratoxin A”. *Paper manuscript to be submitted*

**Heurich, M.** and Tothill, I.E. “An electrochemical immunosensor for ochratoxin A in wine using screen-printed gold electrodes”. *Paper manuscript to be submitted*

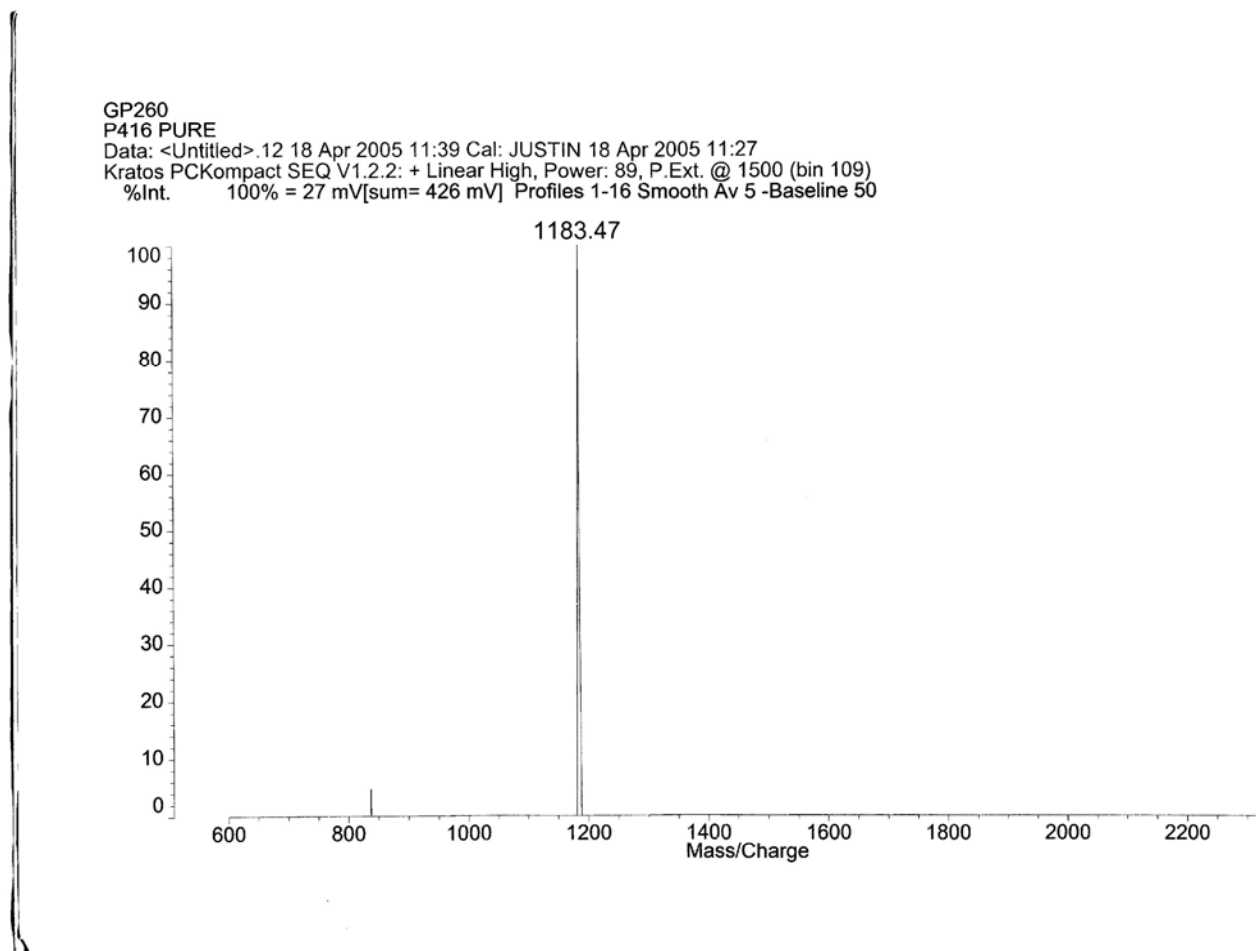


## APPENDICES

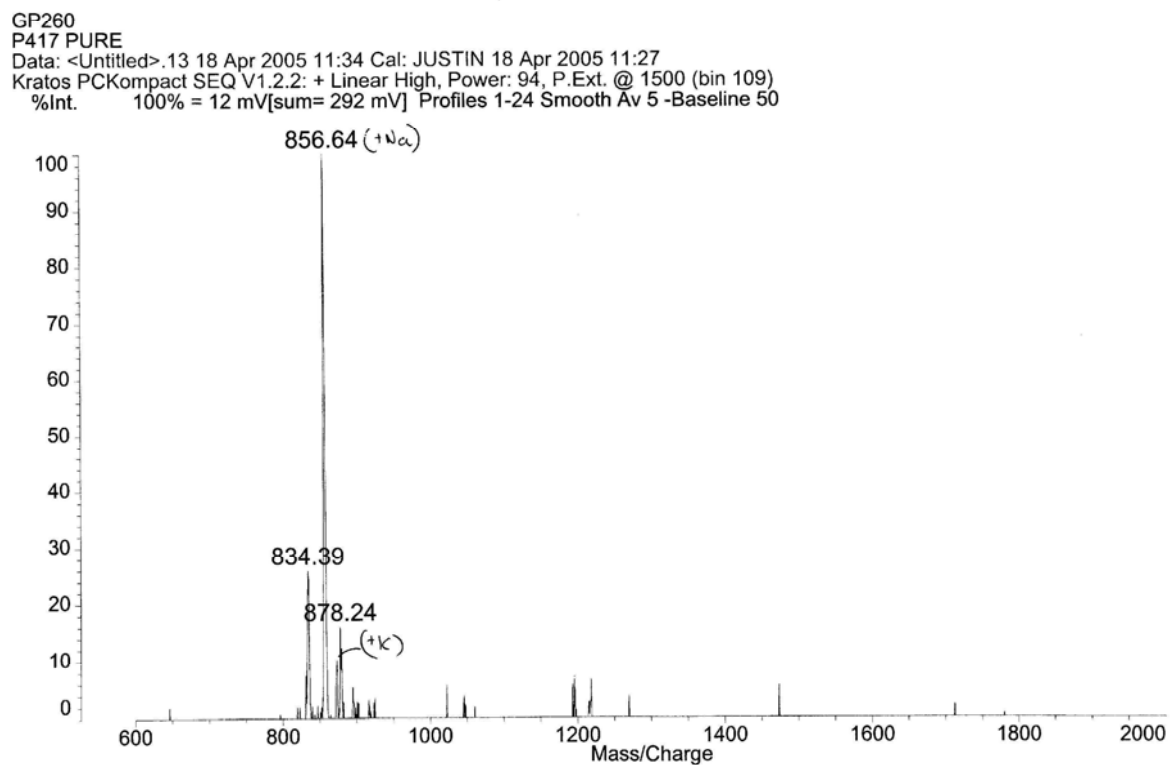
**Appendix A:** Table of synthetic wine compounds and their concentration according to “Estacion Enologica of Rioja” obtained from University of Valladolid, Spain, 2006.

<b>Component</b>	<b>Concentration (mg L<sup>-1</sup>)</b>
Isopenthyl Acetate	0.523
Trans-2- hexenal	0.508
Ethyl Hexanoate	0.523
Hexyl Acetate	0.524
Ethyl Heptanoate	0.521
1-hexanol	0.492
Ethyl Octanoate	0.520
1-heptanol	0.493
Benzaldehyde	0.630
Ethyl Pelargonate	0.520
Linalool	0.517
1-octanol	0.494
Isoamile Lactate	0.517
Phenil Acetate	0.646
Ethyl Decanoate	0.518
Butyrolactone	0.672
Diethyl Succinate	4.156
Terpineol	2.239
Citronellol	2.062
Nellol	3.508
Acetate-2-phenilethyle	2.479
Ethyl Dodecanoate	0.556
Geraniol	3.416
Guayacol	4.516
Bencilic Alcohol	4.200
t-whiskylactone	4.360
2 –Phenilethanol	4.080
wiskylactone	4.360
4-etilguayacol	4.258
2-Ethylphenol	4.148
Eugenol	4.264
4-Ethylphenol	6.080


**Appendix B:** Mass Spectroscopy spectra of the 13-mer peptide with the sequence GPAGIDGPAGIRC. The peptide showed one major signal at  $m/z$  1183.47 (average molecular mass).




**Appendix C:** Mass Spectroscopy spectra of the octapeptide with the sequence CSIVEDGL. The peptide showed a major signal at  $m/z$  856.64 (average molecular mass) and some minor signals at 834.39 and 878.24.



**Appendix 4:** Heurich, M., Danielsson, B., Tothill, I.E., (2005). “Affinity Sensor for Ochratoxin A using Synthetic Peptide Receptor”, *Second world congress on synthetic receptors*, Salzburg, Austria.





## Affinity Sensor for Ochratoxin A using Synthetic Peptide Receptor

M. Heurich\*<sup>1</sup>, B. Danielsson<sup>2</sup> and I. E. Tothill<sup>1</sup>  
<sup>1</sup>Cranfield University, UK; <sup>2</sup>Lund University, Sweden

### Introduction

Mycotoxins are widespread fungal contaminants found in many cereals and other crops. There is a growing concern regarding their potential toxic, mutagenic, carcinogenic, and immunosuppressive effect on human and animals alike.

Ochratoxin A (Figure 1) is produced by several species of *Aspergillus* and *Penicillium* and found in a wide range of foods and also beverages such as wine.

Therefore there is an essential need for sensitive, specific, reusable, rapid and easy-to-perform diagnostic methods for quantitatively detecting ochratoxin A.

### Materials and Methods

Computational modeling was performed on a Silicon Graphics Octane workstation executing Sybyl 6.9. Peptide library design applied molecular modeling software (Figure 2), which uses the ochratoxin A structure as template.

Simulations are based on binding energies for the interaction of amino acid monomers as well as peptide polymers with the ochratoxin A template.

High scoring peptide sequences were screened using a receptor-ligand docking software tool.

Designed sequences were synthesised and screened for their affinity towards ochratoxin A in vitro applying a surface plasmon resonance biosensor (BIAcore 3000) monitoring the binding interaction [1].

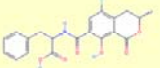


Fig. 1. Ochratoxin A structure.

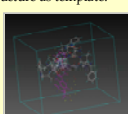


Fig. 2. Electrostatic screening procedure of the ochratoxin A template (purple) with several ligands being tried at distinct positions.

### Results

Peptide libraries were designed by computational modeling (Figure 3) and a list of high scoring peptide sequences produced that were showing high binding interaction with the ochratoxin A template. Selected peptide sequences were further screened using molecular modelling applying docking simulations.

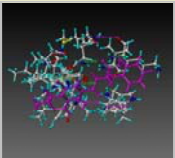
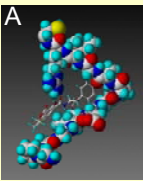
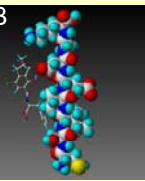


Fig. 3. Computational design result. Ochratoxin template (shown in purple stick & ball) is shown interacting with amino acid monomers (stick & ball).

The final synthetic peptide receptors for ochratoxin A were modified manually resulting in better solubility and applicability in bioassays. The first de novo designed peptide was a 13-mer (Figure 4, A) and the second an octapeptide (Figure 4, B). Both were chemically synthesized for in vitro investigation.

Fig. 4. Final result of de novo designed peptide sequences shown interacting with ochratoxin A. The 13-mer peptide (A, left) and the octapeptide (B, right) sequence are seen as space-filled, ochratoxin A as stick & ball structures.

Both ochratoxin A peptide receptors were characterised in vitro for their affinity and kinetics using a surface plasmon resonance-based biosensor (BIAcore 3000). Two polyclonal ochratoxin A antibodies were compared to the synthetic peptide receptors. Both antibodies showed high affinity and exhibited specific binding to ochratoxin A, with dissociation constants  $K_D$  in the range from 7 nM and 20 nM. Association and dissociation rate constants ( $k_a$  and  $k_d$ ) for the antibodies were slow, showing a need for regeneration of the sensor surface.

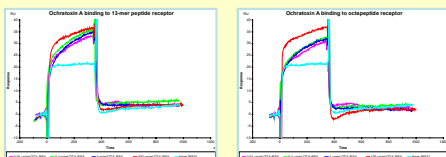


Fig. 5. Sensorgram obtained from BIAcore 3000 showing the binding interaction of immobilized synthetic 13-mer peptide (left) and octapeptide (right) with ochratoxin A (OTA-BSA) at distinct concentrations. The peptide is recognizing ochratoxin A specifically and is showing weak affinity.

Affinity and kinetics evaluation of the two peptides confirmed that the 13-mer peptide (Figure 5, left) exhibited specific binding to ochratoxin A, with dissociation constants  $K_D$  in the range from 0.1-100  $\mu$ M.

The octapeptide (Figure 5, right) also recognized ochratoxin A, with dissociation constants  $K_D$  from 100  $\mu$ M. Association and dissociation rate constants ( $k_a$  and  $k_d$ ) for both peptides were rapid and baseline signal was almost immediately reached after the end of each ochratoxin A injection, hence no need for surface regeneration.

### Conclusions

- Low cost, time-saving and high-throughput screening procedures prior to in vitro testing illustrate the major advantage of de novo designed peptides towards antibodies.
- The work shows the potential of using synthetic peptides as sensitive and specific receptors for detecting ochratoxin A contamination.
- Further work will examine the suitability of the novel receptors as sensing layer in binding assays and electrochemical sensors.

### Bibliography

[1] Van der Gaag *et al.*, Biosensors and multiple mycotoxin analysis. *Food Control*, 2003, 14, p. 251-254.

This work is funded by the GoodFood project (EU 6FP).

**Appendix 5:** Heurich, M. and Tothill, I.E. (2006). "Affinity Sensors for Ochratoxin A Detection", 9<sup>th</sup> World Congress on Biosensors, Toronto, Canada.

Cranfield  
UNIVERSITY

Affinity Sensors for Ochratoxin A Detection

Meike Heurich and Ibtisam E. Tothill

School of Applied Sciences, Cranfield University, Cranfield,  
Bedfordshire, MK43 0AL, UK

---

### Introduction

Mycotoxins are toxic fungal metabolites that occur in food products, such as ochratoxin A which contaminates grapes as a result of mould growth. Ochratoxin A may be transferred to grape containing drinks and wine due to its high chemical stability. There is an increasing concern for human health since ochratoxin A is known to be possibly carcinogenic or can be immunosuppressive for the mammalian system.

Ochratoxin A free beverages are also of economic importance for the wine industry. Therefore, a need exists for a sensitive, selective, rapid and low-cost measurement of ochratoxin A contents that can be implemented on-site in wine yards.

This project focuses on the development of affinity sensors for ochratoxin A. Commercially available natural receptors such as antibodies and specifically designed and synthesised artificial receptors such as peptides are investigated as the sensing layer.

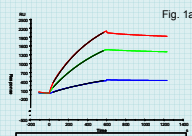
Artificial peptide receptors were designed using a host of computational modeling techniques such as *de novo* design and receptor-ligand dynamic simulations.

Enzyme immunoassays were used as developmental tools prior to transferring the ochratoxin A assay to the sensor surface. The electrochemical immunosensor for ochratoxin A was developed on an Au screen printed electrodes (SPE).

---

### SPR biosensor

Kinetic and affinity data were obtained using a surface plasmon resonance (SPR) biosensor monitoring binding interactions of ochratoxin A with an ochratoxin antibody as seen in the sensorgram in Fig. 1a.



#### Antibody receptor

Plots of resonance units [RU] versus ochratoxin A antibody concentration were obtained from the sensorgrams, illustrating the affinity constants in Fig.1b and 1c respectively. Two different antibodies (A & B) were investigated to select the best antibody. A detection limit of 1 mg L<sup>-1</sup> was monitored for ochratoxin antibody (A), compared to 10 mg L<sup>-1</sup> for antibody (B).

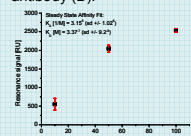


Fig. 1b

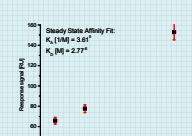


Fig. 1c

#### Peptide Receptor

The peptide receptors were designed using computational modelling.

The final synthetic peptide receptors for ochratoxin A were a 13-peptide (Fig.2a) and an octapeptide (Fig.2b). Both were chemically synthesized for in vitro investigation using a surface plasmon resonance biosensor.

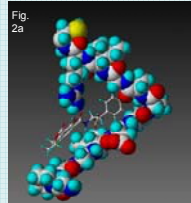


Fig. 2a

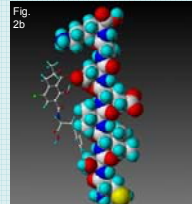
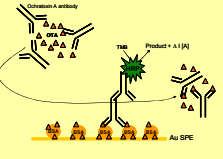


Fig. 2b

Affinity constants determined applying binding interaction analysis for 13-peptide:  
 $K_A [M^{-1}] = 7.40 \times 10^6$ ,  
 $K_D [M] = 1.34 \times 10^{-7}$   
 and for the octapeptide:  
 $K_A [M^{-1}] = 1.49 \times 10^4$ ,  
 $K_D [M] = 6.69 \times 10^{-5}$

### Electrochemical immunosensor

Competitive binding assays for ochratoxin A using ochratoxin antibodies on Au SPE. Amperometric detection is based on a TMB/HRP system.



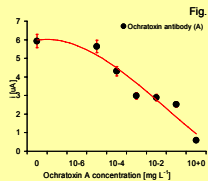


Fig. 3

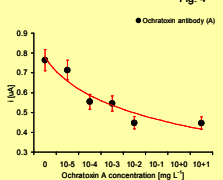


Fig. 4

Ochratoxin A is competing with immobilised ochratoxin A-BSA in an indirect binding assay (Fig. 3) and with ochratoxin A-HRP conjugate in a direct assay format (Fig. 4). The detection limit of the indirect assay resulted in 1 µg L<sup>-1</sup> and for the direct assay format in 0.1 µg L<sup>-1</sup> ochratoxin A.

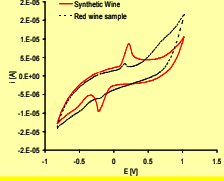


Fig. 5

Electrochemical properties of wine were determined using cyclic voltammetry. CV's were taken of synthetic wine and a random wine sample (Fig. 5). The synthetic wine showed distinctive peaks contrary to the wine sample.

---

### Future Developments

- Sensitivity of the ochratoxin A SPE assay will be optimised for the determination of real wine samples
- The synthesised peptides for ochratoxin A will be investigated as receptors using the Au SPE sensor

The authors thanks the European Union (FP6) GoodFood project for funding this work.